

Yucca Mountain Repository License Application

SAFETY ANALYSIS REPORT

**Chapter 2:
Repository Safety
After Permanent Closure**

This publication was produced by the U.S. Department of Energy
Office of Civilian Radioactive Waste Management.

For further information contact:
U.S. Department of Energy
Office of Civilian Radioactive Waste Management
1551 Hillshire Drive
Las Vegas, Nevada 89134

or call:
Yucca Mountain Information Center
1-800-225-6972

or visit:
Office of Civilian Radioactive Waste Management website
<http://www.ocrwm.doe.gov>

Section 508 Accessibility Elements Included in this Document

The PDF version of this report includes features that address applicable accessibility standards in the 1998 amendment to Section 508 of the Rehabilitation Act. These features include tagged text, which is available to assistive technologies such as screen readers; alternative text (alt text), which complements graphic materials; and bookmarks and hyperlinks, which allow efficient navigation of the report.

If you require an alternative format of this report, or interpretive services, please contact our toll-free information line, at 1-800-225-6972.

CONTENTS

	Page
2. REPOSITORY SAFETY AFTER PERMANENT CLOSURE	2-1
2.1 SYSTEM DESCRIPTION AND DEMONSTRATION OF MULTIPLE BARRIERS.	2.1-1
2.1.1 Identification of Barriers	2.1-3
2.1.1.1 Upper Natural Barrier	2.1-5
2.1.1.2 Engineered Barrier System	2.1-7
2.1.1.3 Lower Natural Barrier	2.1-9
2.1.2 Barrier Capability Description	2.1-10
2.1.2.1 Upper Natural Barrier	2.1-11
2.1.2.2 Engineered Barrier System	2.1-31
2.1.2.3 Lower Natural Barrier	2.1-78
2.1.3 Technical Bases for Barrier Capability	2.1-101
2.1.3.1 Upper Natural Barrier	2.1-102
2.1.3.2 Engineered Barrier System	2.1-103
2.1.3.3 Lower Natural Barrier	2.1-107
2.1.3.4 Technical Basis for Disruptive Events Potentially Affecting Barrier Capability	2.1-108
2.1.3.5 Summary of Technical Bases for Barrier Capability	2.1-109
2.1.4 Summary.	2.1-110
2.1.5 General References.	2.1-112
2.2 SCENARIO ANALYSIS AND EVENT PROBABILITY	2.2-1
2.2.1 Analysis of FEPs and Scenario Classes	2.2-5
2.2.1.1 Identification and Classification of FEPs	2.2-6
2.2.1.2 Screening of FEPs	2.2-16
2.2.1.3 Event Class and Scenario Class Formation	2.2-21
2.2.1.4 Screening of Scenario Classes and Event Classes.	2.2-27
2.2.2 Identification of Events with Probabilities Greater Than 1 Chance in 10,000 of Occurring over 10,000 Years.	2.2-63
2.2.2.1 Seismic Activity	2.2-64
2.2.2.2 Igneous Activity	2.2-90
2.2.2.3 Early Waste Package and Drip Shield Failures	2.2-101
2.2.2.4 Human Intrusion	2.2-102
2.2.3 General References.	2.2-103
2.3 MODEL ABSTRACTION.	2.3-1
2.3.1 Climate and Infiltration	2.3.1-1
2.3.1.1 Summary and Overview	2.3.1-3
2.3.1.2 Climate.	2.3.1-7
2.3.1.3 Infiltration	2.3.1-32

CONTENTS (Continued)

	Page
2.3.1.4	Conclusions 2.3.1-89
2.3.1.5	General References 2.3.1-92
2.3.2	Unsaturated Zone Flow 2.3.2-1
2.3.2.1	Summary and Overview 2.3.2-2
2.3.2.2	Conceptual Description of Unsaturated Zone Flow System 2.3.2-6
2.3.2.3	Data and Data Uncertainty 2.3.2-16
2.3.2.4	Model and Model Uncertainty 2.3.2-39
2.3.2.5	Confidence Building and Model Abstraction 2.3.2-85
2.3.2.6	Conclusions 2.3.2-94
2.3.2.7	General References 2.3.2-99
2.3.3	Water Seeping into Drifts 2.3.3-1
2.3.3.1	Summary and Overview 2.3.3-4
2.3.3.2	Ambient Seepage 2.3.3-9
2.3.3.3	Thermal Seepage 2.3.3-57
2.3.3.4	Total System Performance Assessment Implementation of Drift Seepage 2.3.3-69
2.3.3.5	Analogue Observations 2.3.3-77
2.3.3.6	Conclusions 2.3.3-78
2.3.3.7	General References 2.3.3-81
2.3.4	Mechanical Degradation of the Engineered Barrier System 2.3.4-1
2.3.4.1	Summary and Overview 2.3.4-4
2.3.4.2	System Description and Model Integration 2.3.4-12
2.3.4.3	Ground Motion and Fault Displacement Analyses 2.3.4-16
2.3.4.4	Rockfall Analysis 2.3.4-51
2.3.4.5	Structural Response of EBS Features to Mechanical Degradation 2.3.4-108
2.3.4.6	Computational Algorithm for Seismic Scenario Class 2.3.4-191
2.3.4.7	Evaluation of Material Supporting Mechanical Disruption of the EBS 2.3.4-197
2.3.4.8	Conclusions 2.3.4-197
2.3.4.9	General References 2.3.4-203
2.3.5	In-Drift Physical and Chemical Environment 2.3.5-1
2.3.5.1	Summary and Overview 2.3.5-9
2.3.5.2	Approach to Coupled Processes 2.3.5-13
2.3.5.3	Near-Field Chemistry Model 2.3.5-20
2.3.5.4	In-Drift Thermal-Hydrologic Environment 2.3.5-68
2.3.5.5	In-Drift Chemical Environment Models 2.3.5-115
2.3.5.6	Conclusions 2.3.5-141

CONTENTS (Continued)

	Page
2.3.5.7	General References 2.3.5-146
2.3.6	Waste Package and Drip Shield Corrosion 2.3.6-1
2.3.6.1	Summary and Overview 2.3.6-5
2.3.6.2	Implementation of the Waste Package and Drip Shield Corrosion Models in Total System Performance Assessment 2.3.6-9
2.3.6.3	General Corrosion of the Waste Package Outer Barrier 2.3.6-18
2.3.6.4	Localized Corrosion of Waste Package. 2.3.6-29
2.3.6.5	Stress Corrosion Cracking of the Waste Package Outer Barrier 2.3.6-45
2.3.6.6	Early Failure of Waste Packages. 2.3.6-54
2.3.6.7	Effects of Long-Term Thermal Aging and Phase Stability of Alloy 22 2.3.6-62
2.3.6.8	Drip Shield Degradation 2.3.6-70
2.3.6.9	Conclusions 2.3.6-85
2.3.6.10	General References 2.3.6-92
2.3.7	Waste Form Degradation and Mobilization and Engineered Barrier System Flow and Transport 2.3.7-1
2.3.7.1	Summary and Overview 2.3.7-10
2.3.7.2	Summary of FEPs Evaluated in Waste Form Degradation and In-Drift Radionuclide Transport Models 2.3.7-13
2.3.7.3	Implementation of Conceptual Models 2.3.7-13
2.3.7.4	Radionuclide Inventory 2.3.7-15
2.3.7.5	In-Package Water Chemistry. 2.3.7-25
2.3.7.6	Commercial Spent Nuclear Fuel Cladding Degradation 2.3.7-35
2.3.7.7	Commercial Spent Nuclear Fuel Degradation. 2.3.7-36
2.3.7.8	U. S. Department of Energy Spent Nuclear Fuel Degradation 2.3.7-43
2.3.7.9	High-Level Radioactive Waste Glass Dissolution 2.3.7-45
2.3.7.10	Dissolved Radionuclide Concentration Limits 2.3.7-50
2.3.7.11	Colloidal Radionuclide Availability 2.3.7-59
2.3.7.12	Engineered Barrier System Flow and Transport Model 2.3.7-68
2.3.7.13	Conclusions 2.3.7-87
2.3.7.14	General References 2.3.7-95
2.3.8	Radionuclide Transport in Unsaturated Zone. 2.3.8-1
2.3.8.1	Summary and Overview 2.3.8-2
2.3.8.2	Conceptual Description of Unsaturated Zone Transport Processes 2.3.8-8
2.3.8.3	Data and Data Uncertainty 2.3.8-17

CONTENTS (Continued)

	Page
2.3.8.4 Model Development	2.3.8-34
2.3.8.5 Model Abstraction	2.3.8-56
2.3.8.6 Conclusions	2.3.8-77
2.3.8.7 General References	2.3.8-82
2.3.9 Saturated Zone Flow and Transport	2.3.9-1
2.3.9.1 Summary and Overview	2.3.9-4
2.3.9.2 Saturated Zone Flow System	2.3.9-11
2.3.9.3 Saturated Zone Radionuclide Transport	2.3.9-57
2.3.9.4 Conclusions	2.3.9-105
2.3.9.5 General References	2.3.9-110
2.3.10 Biosphere Transport and Exposure	2.3.10-1
2.3.10.1 Summary and Overview	2.3.10-3
2.3.10.2 Conceptual Model of Biosphere Transport, Receptor, and Receptor Exposure	2.3.10-6
2.3.10.3 Data and Data Uncertainty	2.3.10-28
2.3.10.4 Model Uncertainty	2.3.10-56
2.3.10.5 Abstraction	2.3.10-63
2.3.10.6 Conclusions	2.3.10-75
2.3.10.7 General References	2.3.10-79
2.3.11 Igneous Activity	2.3.11-1
2.3.11.1 Summary and Overview	2.3.11-9
2.3.11.2 System Description and Integration	2.3.11-14
2.3.11.3 Igneous Intrusion Modeling Case	2.3.11-25
2.3.11.4 Volcanic Eruption Modeling Case	2.3.11-47
2.3.11.5 Summary of Igneous Scenario Class Model Abstraction ...	2.3.11-80
2.3.11.6 Conclusions	2.3.11-81
2.3.11.7 General References	2.3.11-86
2.4 DEMONSTRATION OF COMPLIANCE WITH THE POSTCLOSURE PUBLIC HEALTH AND ENVIRONMENTAL STANDARDS	2.4-1
2.4.1 Total System Performance Assessment Model and Summary of Results	2.4-9
2.4.1.1 TSPA Method and Approach	2.4-10
2.4.1.2 Scenario Classes and Modeling Cases	2.4-11
2.4.1.3 TSPA Computational Structure	2.4-19
2.4.1.4 Summary of TSPA Model	2.4-22
2.4.1.5 Summary of TSPA Model Results	2.4-23
2.4.2 Demonstration of Compliance with the Postclosure Individual Protection Standard	2.4-23
2.4.2.1 Scenario Classes and Modeling Cases Used in the Calculation of Annual Dose	2.4-24

CONTENTS (Continued)

	Page
2.4.2.2 Evaluation of Annual Dose to the RMEI with Respect to the Postclosure Individual Protection Standard.	2.4-54
2.4.2.3 Credibility of the TSPA Results	2.4-106
2.4.3 Demonstration of Compliance with the Individual Protection Standard for Human Intrusion	2.4-290
2.4.3.1 TSPA Representation of the Human Intrusion Event	2.4-292
2.4.3.2 Evaluation of the Earliest Occurrence Time of a Human Intrusion Event	2.4-298
2.4.3.3 Evaluation of Human Intrusion Dose to RMEI.	2.4-309
2.4.3.4 Credibility of the Human Intrusion Results.	2.4-319
2.4.4 Analysis of Repository Performance that Demonstrates Compliance with the Separate Standards for the Protection of Groundwater.	2.4-324
2.4.4.1 Demonstration that the Groundwater Radioactivity and Doses at Any Year During the Compliance Period Do Not Exceed the Limits in the Groundwater Protection Standards	2.4-326
2.4.4.2 Evaluation of Total Dissolved Solids in the Aquifer.	2.4-334
2.4.4.3 Physical Dimensions of the Representative Volume of Groundwater	2.4-335
2.4.5 General References.	2.4-338

INTENTIONALLY LEFT BLANK

CHAPTER 2 ACRONYMS

BDCF	biosphere dose conversion factor
BWR	boiling water reactor
DDT	discrete-heat-source, drift-scale, thermal-conduction-radiation [submodel]
DFBA	difluorobenzoic acid
DLL	dynamically linked library
DMTH	discrete-heat-source, mountain-scale, thermal-hydrologic [submodel]
DOE	U.S. Department of Energy
EBS	Engineered Barrier System
ECRB	Enhanced Characterization of the Repository Block
EPA	U.S. Environmental Protection Agency
ERMYN	Environmental Radiation Model for Yucca Mountain Nevada
ESF	Exploratory Studies Facility
FEP	feature, event, or process
HLW	high-level radioactive waste
ITWI	important to waste isolation
LDTH	two-dimensional, line-averaged-heat-source, drift-scale, thermal-hydrologic [submodel]
LMTH	line-source, mountain-scale, thermal-hydrologic [model]
NRC	U.S. Nuclear Regulatory Commission
OIS	oxygen isotope stage
PFBA	pentafluorobenzoic acid
PGV	peak ground velocity
PMA	performance margin analysis
PRCC	partial rank correlation coefficient
PSHA	probabilistic seismic hazard analysis
PVHA	probabilistic volcanic hazard analysis
PWR	pressurized water reactor
RMEI	reasonably maximally exposed individual
RST	residual stress threshold
SAW	simulated acidified water
SCW	simulated concentrated water
SDT	smear-source, drift-scale, thermal-only [submodel]
SDW	simulated dilute water
SMT	smear-source, mountain-scale, thermal-only [submodel]

SNF	spent nuclear fuel
SSW	simulated saturated water
TAD	transportation, aging, and disposal
TSPA	total system performance assessment

CONTENTS

	Page
2. REPOSITORY SAFETY AFTER PERMANENT CLOSURE	2-1

INTENTIONALLY LEFT BLANK

2. REPOSITORY SAFETY AFTER PERMANENT CLOSURE

Introduction—This chapter provides information relating to repository system compliance with postclosure performance objectives, including information relating to performance of the Engineered Barrier System (EBS) and natural barriers consistent with the individual and groundwater protection requirements of proposed 10 CFR 63, Subpart L. As such, [Chapter 2](#) addresses the regulatory requirements of 10 CFR 63.21(c), 10 CFR 63.113, proposed 10 CFR 63.114, 10 CFR 63.115, and proposed 10 CFR 63, Subpart L. The overall organization of [Chapter 2](#), including the correlation between the Safety Analysis Report and the Yucca Mountain Review Plan (NUREG-1804), is described, as is the relationship between the postclosure safety analysis presented in [Chapter 2](#) with [Chapters 3, 4, and 5](#) of the Safety Analysis Report.

The strategy for developing a repository at Yucca Mountain that can safely isolate spent nuclear fuel (SNF) and high-level radioactive waste (HLW) after permanent closure is based on four foundations or principles:

1. A site selected for its ability to safely isolate waste
2. A design intended to complement the characteristics of the site and to enhance its waste isolation capability
3. A comprehensive safety analysis underlain by a sound technical basis
4. Institutional and administrative controls to ensure that the integrity of the repository will not be compromised after closure.

The safety analysis for postclosure (i.e., the collection of evidence that demonstrates that the repository will safely isolate SNF and HLW after closure) is summarized here and is presented in detail in [Chapters 2, 3, 4, and 5](#). [Section 2.1](#) identifies and demonstrates the capability of the multiple natural and engineered barriers that constitute the repository system. The EBS is designed to complement and take advantage of the natural characteristics of the site. [Section 2.2](#) describes the comprehensive set of features, events, and processes (FEPs) that are evaluated in the total system performance assessment (TSPA), which is used to determine compliance with the postclosure repository performance objectives. [Sections 2.3 and 2.4](#) describe the expected behavior of the repository system and present the technical basis for the conceptual and numerical models used to simulate future performance. The technical basis includes data and information collected during the characterization of the Yucca Mountain site as well as other information, such as the use of natural or manmade analogues to the repository that provide insight into how the system will perform. [Chapters 3, 4, and 5](#) include information on institutional and administrative measures and controls that the U.S. Department of Energy (DOE) will implement to assure confidence that the repository will meet its performance objectives and that analyses of the repository system performance are reasonable and defensible. For example, any activities determined to be necessary to resolve safety issues are described in [Chapter 3](#). [Chapter 4](#) describes the Performance Confirmation Program that will determine whether conditions in the repository are consistent with what is anticipated and whether the repository is performing as projected. [Chapter 5](#) describes the management and institutional controls that will be implemented to ensure that the repository is designed, analyzed,

and constructed in accordance with quality assurance requirements, and that appropriate administrative controls are in place to monitor and protect the integrity of the repository after closure.

The postclosure safety analysis demonstrates that a repository at Yucca Mountain can safely isolate SNF and HLW. As more information is acquired through design, construction, and continued testing and performance confirmation, the DOE will update or modify the design and operational concept for the repository system, as necessary, to take advantage of this increased knowledge and improve system safety.

The Multiple Barrier Repository System Concept—The performance of a repository at Yucca Mountain is controlled by the natural and engineered features of the site that act in concert to prevent or reduce the movement of water and/or the transport of radioactive materials to the accessible environment. Multiple natural features of the Yucca Mountain site and engineered features of the repository design combine to form the following three barriers important to waste isolation: the Upper Natural Barrier, the EBS, and the Lower Natural Barrier. The Upper Natural Barrier includes the geologic units from the surface to the repository horizon, including alluvial soils and gravel, the Tiva Canyon welded tuff, the Paintbrush nonwelded tuff, and the Topopah Spring welded tuff. The EBS is composed of the manmade features within the emplacement drifts, including the drip shield, waste package, waste form, and other engineered components. The Lower Natural Barrier includes the unsaturated and saturated volcanic tuff units below the repository and older bedrock units and alluvial deposits below the water table between Yucca Mountain and the accessible environment in Amargosa Valley.

The geologic and hydrologic characteristics of the Yucca Mountain site form effective natural barriers to the flow of water and to the potential movement of radionuclides. The underground environment within the natural setting is conducive to the design and construction of components that prevent or reduce the movement of water or the potential release and transport of radionuclides. The waste isolation capability of the natural setting at the site is a direct function of the favorable intrinsic characteristics of the geologic units and their durability. The capability of the EBS is achieved by designing components specifically to function in the natural setting of the Yucca Mountain repository, particularly its unsaturated rock units. The materials in the EBS have been chosen so that the components perform their intended functions for many thousands of years. The barriers in the repository system work individually and together to prevent or substantially reduce the rate of movement of water, the release rate of radionuclides from the waste, and the rate of movement of radionuclides from the repository to the accessible environment. Analyses of both the natural barriers and the EBS address their effectiveness both during the first 10,000 years after closure and for the period beyond 10,000 years, within the period of geologic stability as prescribed by proposed 10 CFR Part 63.

The data that support the evaluations of the performance of the natural and engineered barriers come from more than 30 years of scientific investigation, including characterization as part of testing programs in Area 25 of the Nevada Test Site, regional screening activities in the 1970s, and a formal program of site characterization conducted under the Nuclear Waste Policy Act. Formal site characterization activities began with the issuance of the Site Characterization Plan in 1988 and concluded with the recommendation of the site for development of a repository in 2002. These site characterization activities have included extensive surface-based and underground geologic

exploration using boreholes and geophysical exploration techniques. This testing has resulted in a wide range of geologic, hydrogeologic, geochemical, and geomechanical data sets that have been used in the development and validation of predictive models used to evaluate the possible range of environments in the emplacement drifts and the performance of the natural and engineered barriers after closure of the repository. This testing has included specific underground testing to evaluate the expected behavior of the repository following construction and emplacement of the waste. This testing has been supplemented by a range of natural and manmade analogue investigations that provide additional lines of evidence related to understanding the processes affecting repository performance. The availability of multiple lines of evidence allows the evaluation of performance from numerous, varying, and complementary perspectives that permit a more complete assessment of the overall safety and risk.

In addition to the site-specific geologic testing and analyses, laboratory testing evaluated the possible degradation, deterioration, and alteration of engineered materials and waste forms under a range of environmental conditions. This testing of features, such as the drip shield, waste package, waste form, and waste package internal materials, all of which contribute to barrier capability, has resulted in data sets that have been used in the development and validation of predictive models used to evaluate the design of the engineered features and the performance of these features after closure of the repository. This testing has included specific laboratory testing of the materials to be used in the construction of the repository, as well as the waste forms to be disposed of in the repository. In addition to laboratory testing of engineered materials, laboratory tests have been conducted to evaluate the characteristics of the rocks and mobility of radionuclides in the groundwater in the vicinity of Yucca Mountain.

Advancing the scientific understanding of the Yucca Mountain site and the associated repository features has involved the following: (1) developing models that can be compared to direct field or laboratory testing; (2) evaluating the uncertainty in these models; (3) conducting additional testing on those aspects of the models that are most significant; (4) subjecting the models and resulting analyses to technical review; and (5) revising the models as additional data are collected or reviews are conducted and comments are received. This iterative process is the basis for developing appropriate technical knowledge and understanding of the different processes and events representing a wide range of scientific disciplines that may potentially affect the features of the natural or engineered barriers. The in situ and laboratory testing programs, natural and man-made analogues, and data and analyses from the technical literature form the technical bases not only for the development but also for the validation of the models used to describe the processes acting on the natural and engineered features. Understanding these processes is the key to simulating the behaviors these processes engendered in the repository system features, which, in turn, is the basis for the TSPA and the analysis of barrier capability.

Notwithstanding the extensive and detailed site characterization program, including the development and validation of models describing the processes relevant to performance assessment, some uncertainty remains in the models and parameters used to evaluate the postclosure performance of the repository system of multiple barriers. This uncertainty includes uncertainty in the spatial and temporal variability in the processes affecting performance and uncertainty in the conceptual model most applicable to the long-term behavior of the repository.

To assess the effects of uncertainty, various approaches have been applied. In many cases, uncertainty in parameters and data have been directly included in the model abstractions, and this uncertainty is propagated to the assessment of repository performance for both the 10,000 year period after closure and for the period beyond 10,000 years within the period of geologic stability as prescribed by proposed 10 CFR Part 63. Except for certain assumptions specified by regulation (such as the average percolation flux rates in the unsaturated zone for the post-10,000 year period), the same FEPs are considered in both the 10,000 year and post-10,000 year calculations. In some cases, conservative modeling approaches have been used which ultimately lead to a higher estimation of the dose to the reasonably maximally exposed individual and radionuclide releases to the accessible environment than would be expected.

Repository performance is evaluated with the TSPA model. The first step in building the model was to identify the relevant FEPs that would or could be important after closure of the repository ([Section 2.2](#)). These FEPs include low probability events such as igneous activity. The FEPs are quantified through the use of models and parameters, which are based on testing and other observations and analogue studies. Uncertainty in these parameters and models is either directly quantified and included in the assessment of postclosure performance or has been conservatively approximated to ensure that predicted dose has not been underestimated. The incorporation of uncertainty into the scenarios analyzed in the TSPA model is described in detail in [Section 2.4](#). Information relevant to the credibility of and confidence in the TSPA results is also presented, including verification and validation of the TSPA model and parameter uncertainty and sensitivity analysis. The validation studies include a performance margin analysis undertaken to assess the extent to which conservative assumptions embedded in the TSPA model affect the results.

DOE selection of the Yucca Mountain site and the design of the EBS and its features to complement the natural characteristics and conditions found at the repository are summarized below and described in detail in [Section 2.1](#). The capability of the barriers to prevent or substantially reduce the rate of movement of water, the release rate of radionuclides from the waste, and the rate of movement of radionuclides from the repository to the accessible environment is also summarized, based on detailed discussions in [Sections 2.1](#) and [2.3](#).

Upper Natural Barrier: Features, Capability, and Technical Basis—The principal barrier function of the Upper Natural Barrier is to prevent or substantially reduce the rate of movement of water from the surface to the repository, thereby reducing the amount of water that can enter the emplacement drifts. Yucca Mountain is in a semiarid region where precipitation and humidity are low, thus promoting high evaporation rates. The topography and surficial soils of Yucca Mountain provide the initial barrier feature that limits the movement of water into the mountain. Runoff, evaporation, and plant transpiration processes combine to divert water and permit only a small fraction of the already low expected precipitation at the site to infiltrate into the mountain. Most of the small amount of infiltration that does occur is associated with low-intensity winter storms that occur at a time when lower evaporation and transpiration rates and slow melting of the snow create conditions in which some limited infiltration can occur. The climate and infiltration analyses for Yucca Mountain demonstrate that only a small percentage of the precipitation actually results in infiltration of water into Yucca Mountain for present and future climates. Precipitation falling on Yucca Mountain is expected to remain low, even for the glacial-transition climates that are forecast for most of the next 10,000 years. The southern Great Basin contains areas, such as Yucca Mountain, that are characterized by great depth to the water table. In the

vicinity of the repository, the water table is currently located approximately 600 m below the ground surface, allowing the repository itself to be located approximately 300 m above the current water table.

Yucca Mountain consists of a series of alternating layers of welded and nonwelded volcanic tuffs with differing hydrologic properties that significantly impact the manner in which water moves through the mountain. The volcanic tuffs in the unsaturated zone above the repository horizon function as a barrier feature to prevent or reduce the movement of water through the unsaturated zone and into the emplacement drifts of the repository. The primary large-scale processes contributing to this capability are evaporation, lateral diversion of percolating water, damping of episodic pulses of precipitation and infiltration, and capillary forces limiting seepage into the emplacement drift. Because of relatively high matrix porosity and permeability and low fracture density, water flow within the nonwelded tuff unit is predominantly in the matrix. Interconnected fracture networks in the nonwelded tuff are rare and are typically associated with faults, so only a small percentage of the water is expected to pass through fractures. Because the flow is matrix-dominated and the rock matrix has a large storage capacity, the nonwelded tuff unit attenuates pulses in flux from the overlying welded unit, and the result is an approximately steady-state flux of water from the nonwelded tuff to the underlying welded tuff unit.

The welded tuff units that comprise the repository host rock have lower matrix porosity and higher fracture frequency than the overlying nonwelded tuff. Unsaturated flow in the welded units is expected to occur primarily through the fractures. The down-to-the-east dip of the units, combined with the effects of the contrast in the hydraulic conductivity and the heterogeneity in the fracture and bulk permeability across the nonwelded–welded interface, results in some lateral diversion of the unsaturated flow.

The rate and distribution of seepage into waste emplacement drifts control the amount of liquid water available to contact the EBS. In the unsaturated zone, seepage into the emplacement drifts is only a few percent of the percolation flux because capillary forces limit the movement of water into the drift openings. Water is retained in the small pores and tight fractures of the low-porosity welded tuff, and a substantial fraction of the flow moves around the drift opening and drains through the rock pillars between the drifts. The effectiveness of capillary forces in limiting water movement into drifts and moving flow around them depends on the characteristics of the fractures, on the connectivity and permeability of the fracture network, and on the characteristics of the drift openings. For a period of time that is dependent on location within the repository, the decay heat of the emplaced waste is great enough to heat the rock near the emplacement drifts. As long as the temperature is above the boiling point of water at the drift wall, liquid water will be vaporized. This thermal effect further limits seepage into the emplacement drifts.

Site data characterizing the features and processes of the unsaturated system at Yucca Mountain have been collected since the late 1970s. The test data are used to develop the numerical models of the processes to which the natural system features are subjected. These process models, in turn, form the basis for the overall model of the repository system, the TSPA. The data are of numerous types, including lithology, rock hydrologic properties, mineralogy, temperature, geochemistry, climate, and infiltration data. The data have been collected from surface based activities, such as geologic mapping and installation of vertical boreholes, as well as from subsurface mapping, sampling, and in situ testing in excavated tunnels. More than 450 boreholes have been drilled as part of the

characterization of the Yucca Mountain site. More than 10 km of tunnel have been constructed to allow scientists the access needed to perform large-scale tests of processes important to understanding the performance of the repository.

Climate studies and infiltration studies are particularly important to understanding how much water could be available and how it would infiltrate. The climate studies include not only local meteorological monitoring stations but also intensive investigations of regional indicators, including paleo-indicators of past climates covering more than several hundred thousands of years of history. The infiltration study used nearly 100 shallow boreholes located on ridge tops, on side slopes, on stream terraces, and in stream channels to measure the changes in water-content profiles in response to precipitation and snowmelt events. Studies of the permeability of the mountain encompass laboratory- to mountain-scale tests. The unique character of the fractured, unsaturated rocks has allowed scientists to test at scales ranging from centimeters to kilometers and to understand the role and effects of the fractures in unsaturated zone flow and transport through Yucca Mountain.

Capillary flow around emplacement drifts has been investigated through a series of tests conducted from the Exploratory Studies Facility (ESF) and the Enhanced Characterization of the Repository Block Cross-Drift. The seepage tests were motivated by the observed absence of seepage in the ESF drifts following their excavation. Seepage into the openings was monitored while pulses of water were applied into the rock above the opening. Staining dyes were used to monitor the presence of seepage and the extent of seepage water movement within fractures and openings. A very large-scale test was also conducted where the upper exploratory tunnel (the Enhanced Characterization of the Repository Block Cross-Drift) crosses over the main tunnel (ESF). These tests indicate that a substantial fraction of the water moving in fractures in the unsaturated zone will be diverted around emplacement drifts.

The ESF was also used to field an ongoing long-term thermal test that involved heating a 50-m-long drift to directly simulate the effects of waste heat in the emplacement drifts in the tuffs at Yucca Mountain. About 6,000 channels of instrumentation yielded data that were used to validate process models, such as the thermal-hydrologic, thermal-mechanical, flow and seepage, and thermal-hydrologic-chemical models. The rock mass heated in this test experienced a thermal environment somewhat hotter than the repository design; temperatures above the boiling point of water were reached in about 20,000 m³ of rock. The test mobilized water held by capillary forces within the rock mass as the boiling front moved into the rock mass. Instrumentation and several types of hydrologic and geophysical probes allowed scientists to track the movement of water and relate this phenomenon to how the repository would perform at Yucca Mountain.

EBS: Features, Capability, and Technical Basis—The EBS is comprised of the emplacement drift, drip shield, waste package, naval SNF structure, waste form and waste package internals (including transportation, aging, and disposal canisters; naval canisters; HLW canisters; and DOE SNF canisters), waste package pallet, and invert features. The principal barrier function of the EBS is to prevent or substantially reduce the release rate of radionuclides from the waste. The capability of the EBS to prevent or limit the movement of water and prevent contact between water and waste depends on the integrity of several features. Although the emplacement drifts are expected to degrade over time, absent disruptive events, engineered features including the drip shield and waste packages are expected to remain largely intact for more than 10,000 years, and

none of the waste forms is expected to be exposed to water during this period. As a result, no release of radionuclides is expected to occur during the first 10,000 years after closure of the repository in the absence of disruptive events. The small possibility of early failure of some waste packages due to fabrication errors or unexpected localized corrosion has been considered in assessing the overall barrier capability. The engineered features that comprise the EBS and a description of their contribution to EBS function are summarized below. The possibility that disruptive seismic and volcanic events may occur has also been considered, as described below.

The emplacement drift feature provides a stable environment for the other engineered features. The mechanical effects of the degradation of the emplacement drifts, such as rockfall and drift collapse, do not significantly affect the performance of the drip shield and waste package except during low probability disruptive seismic and volcanic events. However, during the period beyond 10,000 years, within the period of geologic stability as prescribed by proposed 10 CFR Part 63, all types of engineered features are expected to be degraded by corrosion. The TSPA considers the effects of the degradation of the engineered features over time, including uncertainty with respect to the rate of degradation.

The drip shield is designed to divert seepage away from the waste package. It prevents water from contacting the waste package as long as it remains intact. Similarly, as long as the waste packages are intact, water cannot contact the waste forms. The cladding on SNF also prevents the contact of seepage water with that portion of the SNF that is inside of the cladding as long as it remains intact. However, for the purposes of the TSPA analyses, commercial and DOE SNF cladding are assumed to be instantaneously degraded when the waste packages are breached. The effect of naval SNF structure on radionuclide release is accounted for in the TSPA analyses. The capability of the drip shields, waste packages, and SNF cladding depends on their integrity over time. The degradation rates for general corrosion for titanium are determined to be sufficiently low that none of the drip shields are expected to breach by this mode of corrosion before 10,000 years after closure of the repository. Stress corrosion cracking may occur as a result of rockfall onto the drip shields caused by low probability seismic events. Even with corrosion of the drip shields, the small width of any stress cracks impedes water movement onto the waste packages. For the calculations for the period beyond 10,000 years, within the period of geologic stability as prescribed by proposed 10 CFR Part 63, degradation and failure of the drip shields is expected to occur: the rate and extent of degradation and associated uncertainty are included in the TSPA analyses.

The degradation rates for general corrosion for Alloy 22 (UNS N06022), the material the outer shell of the waste packages is constructed of, are sufficiently low that none of the waste packages are expected to breach as a result of general corrosion mechanisms before 10,000 years after closure of the repository. Stress corrosion cracking may occur in the weld regions of some of the waste packages. Mitigation techniques (e.g., low plasticity burnishing) are employed to reduce residual stresses below the stress corrosion cracking threshold, but there remains the potential for breaches of some waste packages before 10,000 years after closure of the repository. Early failure of a very small fraction (less than 0.01% on average) of waste packages may occur due to flaws that are undetected during fabrication or as a result of damage during handling. The probability for early failure due to manufacturing- or handling-induced defects is small because of the quality control and inspection measures employed, such as nondestructive examination techniques. For the calculation involving the period beyond 10,000 years, within the period of geologic stability as

prescribed by proposed 10 CFR Part 63, degradation of the waste packages is expected to occur. The rate and extent of degradation, and associated uncertainty, are considered in the TSPA analyses.

Even after waste packages are breached, the release rate of radionuclides is limited by the characteristics and behavior of the other features of the EBS. The release of radionuclides is first impeded by the rate of degradation of the waste form. Waste form degradation cannot begin until the waste package is breached, allowing the ingress of air and moisture. Because of the unsaturated environment, the presence of drip shields and waste packages, and the elevated temperatures within waste packages, the amount of water in contact with the waste form is expected to be limited to that which could possibly adsorb on the waste form surface. Release of radionuclides out of the waste package depends on the chemical environment and moisture conditions within the waste package. Release can occur only if radionuclides are dissolved in water or attached to colloids and if there are continuous liquid pathways in the waste package, including thin films of adsorbed water.

Advective transport of radionuclides out of the EBS can occur only if there is a liquid flux of water along these pathways and if breaches are sufficiently open to permit flow. The movement of many dissolved radionuclides, including those that are the greatest contributors to the total inventory, is retarded by sorption on iron corrosion products within the waste package. The retardation depends on the volume of these corrosion products and on the distribution coefficients associated with them. Sorption onto the corrosion products also reduces movement of those radionuclides reversibly attached to colloids in the water. The radionuclide inventory released from the EBS after the waste package is breached is limited so long as the drip shield remains intact or is damaged only by stress corrosion cracking, precluding advective flow out of the waste package and through the invert; in this case, the release is purely diffusive. Both diffusive and advective releases have been considered in the evaluation of radionuclide releases from the EBS.

The EBS prevents, or substantially reduces, the release rate of radionuclides from the waste and prevents, or substantially reduces, the rate of movement of radionuclides from the repository to the accessible environment. It performs these functions by virtue of the materials and design of the individual features of the EBS, which work together to minimize chemical and mechanical degradation and deterioration processes, and to limit or prevent the movement of water and radionuclides out of the repository. In addition, the EBS provides for chemical and thermal-hydrologic environments that lead to low solubilities for most of the radionuclides that comprise the greatest fraction of the inventory activity. Finally, the EBS environments are such that radionuclide transport from the waste to the unsaturated zone is limited to a small fraction of the available inventory (less than $3 \times 10^{-3}\%$ in 10,000 years and 5% in 1 million years), even in the case of seismic-induced mechanical degradation.

Data characterizing the features and processes of the EBS were also collected during site characterization. The test data are used to develop the numerical models of the processes to which the EBS features are subjected. These process models, in turn, form the basis for the overall model of the system: the TSPA. Corrosion tests were conducted on specimens of waste package and drip shield materials, including titanium and Alloy 22. The tests examined many forms of corrosion: pitting, stress corrosion cracking, galvanic corrosion, corrosion in crevices, and general corrosion. The results of the tests were used to develop corrosion models to predict the long-term behavior of the materials in the repository. Test environments for long-term corrosion testing were structured to encompass a range of concentrated geochemical solutions. The samples were exposed in the

aqueous phase, in the vapor phase above the solutions, and at the waterline. Thousands of specimens, including welded samples, have been subjected to multiyear tests under a range of environments. These tests have been supplemented with short-term tests, including tests in more aggressive brines than are anticipated in the repository environment, to evaluate a range of possible degradation processes for the engineered materials.

Models of the behavior of engineered material subjected to heat in an underground environment over the long-term must consider numerous environmental factors. Composition of evaporatively concentrated waters, evolution of the chemical environments, minerals and salts formed by evaporation, the composition of waters in the emplacement drifts, and microbial activity in the emplacement drifts are among the factors that were considered and addressed by the testing programs.

The range of potential types of aqueous solutions that could contact the drip shield and waste package surfaces have been deduced from the range of potential starting water compositions, from knowledge of near-field and in-drift processes that can alter these compositions, and from laboratory experiments and natural analogue observations. From these results, a range of water compositions was developed and used for corrosion testing.

Testing relevant to in-package chemistry has considered the role of heat and the interaction of water chemistry and waste form degradation. Testing has also included the interaction of water with drift gases, waste package materials, and EBS materials. Many tests have been performed to evaluate the mechanism and rate of degradation of commercial SNF under various conditions. These include oxidation tests, batch tests, unsaturated drip tests, vapor phase tests, electrochemical tests, and flow-through tests. These have been supplemented by tests of expected radionuclide mobility once the waste form is altered.

Lower Natural Barrier: Features, Capability, and Technical Basis—The Lower Natural Barrier prevents or substantially reduces the rate of movement of radionuclides from the repository to the accessible environment. The Lower Natural Barrier includes the unsaturated zone below the repository horizon and the saturated zone below the repository and downgradient from the repository to the accessible environment. The sequence of tuffs comprising the unsaturated zone below the repository provides a feature that is currently 300-m thick, on average. The transport of radionuclides through the Lower Natural Barrier is limited by the rate of movement of water down from the repository horizon to the water table. The welded tuff at the repository horizon is characterized by low matrix permeability and well-connected, steeply dipping fracture networks. Below the southern part of the repository, the underlying nonwelded tuff unit is vitric and characterized by relatively high matrix permeability. Fractures are rare to nonexistent in the vitric part of the unit, and flow and transport are predominantly through the rock matrix. Beneath the northern part of the repository, the underlying nonwelded tuff unit is strongly altered to a mixture of minerals, including zeolites and clays. The minerals have precipitated in the pores of the rocks so that the matrix permeability of the zeolitic part of the unit is low. Most of the downward flow that does occur within the zeolitic part of the unit is conservatively assumed to occur in fractures. The fracture network within this unit is poorly developed and not well connected. Below this unit are the devitrified and zeolitized tuffs of the underlying welded tuff unit. These tuffs have lower matrix permeability than the vitric portion of the unit, and flow and transport through them are primarily in fractures. The fracture networks in these nonwelded tuffs are generally not well connected.

Radionuclides that migrate down through the unsaturated zone to the water table must be transported through the saturated zone before they can reach the accessible environment. Groundwater below Yucca Mountain is part of the Alkali Flat–Furnace Creek groundwater subbasin within the Death Valley groundwater system. Present-day flow is to the south and east near Yucca Mountain. The southeasterly flow from the site is incorporated into the stronger southward flow in western Jackass Flats. The saturated zone of the Lower Natural Barrier includes the fractured volcanic rocks from below the repository to approximately 12 to 14 km south of Yucca Mountain and the saturated alluvium to the accessible environment. The movement of radionuclides in the saturated zone is limited first by the velocity of water that transport them. In addition, several processes, such as matrix diffusion and radionuclide sorption, cause the movement of radionuclides to be slower compared to the rate of movement of the water.

Flow in the volcanic aquifers is predominantly in the fractures. Radionuclides can exchange between the fractures and matrix via matrix diffusion. This diffusive exchange results in a slower effective travel velocity for the bulk of the released radionuclides relative to water-flow velocities in the fractures for two reasons. First, the velocity of water in the pores of the matrix is slower than velocities in the fractures. Second, sorption onto mineral surfaces in the matrix pores will result in even slower movement for those sorbing radionuclides that diffuse into the matrix materials.

Because the alluvial materials are a porous medium, water flow and radionuclide transport occur in intergranular pores. The effective porosity of the alluvium is significantly greater than the fracture porosity of the tuffs. Consequently, flow velocities in the alluvium are smaller than those in the fractures of the volcanic aquifers. Although matrix diffusion is not considered to be important in the alluvium, radionuclide movement is slow because of the low water velocity. In addition, sorption onto minerals in the alluvium results in retardation of the radionuclide movement relative to water movement in these sediments.

The Lower Natural Barrier prevents or substantially reduces the rate of movement of radionuclides from the repository to the accessible environment. The key processes associated with the performance of the Lower Natural Barrier include sorption and matrix diffusion. The radionuclides representing the dominant inventory during the first 10,000 years after closure are ^{137}Cs , ^{90}Sr , ^{241}Am , ^{240}Pu , and ^{239}Pu . In the absence of disruptive events, the Lower Natural Barrier reduces activity releases from the EBS by greater than 99.5% (^{240}Pu , ^{239}Pu , ^{241}Am) to 100% (^{137}Cs and ^{90}Sr). Activity releases of the solubility-limited, strongly sorbed, long half-life Pu isotopes (^{239}Pu and ^{242}Pu) are reduced by more than 99%. For radionuclides of low-to-moderate solubility, low sorption, and long half-life (e.g., ^{237}Np and ^{234}U), the Lower Natural Barrier reduces activity releases from the EBS by 78% (^{237}Np) to 89% (^{234}U). Activities associated with radionuclides important to colloid transport and decay chain in-growth (e.g., ^{243}Am , ^{230}Th , and ^{226}Ra) were reduced by the Lower Natural Barrier by more than 99%. The activity of ^{99}Tc , a highly soluble, nonsorbing, long half-life radionuclide, is reduced by the Lower Natural Barrier by about 62% during the first 10,000 years. ^{99}Tc does not represent a significant fraction of initial inventory, but is important to dose projections both before and after 10,000 years.

For the period after 10,000 years, the inventories of ^{137}Cs and ^{90}Sr are depleted by radioactive decay, and the Lower Natural Barrier reduces activity releases of ^{241}Am by 100% and ^{240}Pu by 98%. Activities of the long half-life Pu isotopes are reduced by 90% (^{239}Pu) and 66% (^{242}Pu) respectively. ^{243}Am , ^{230}Th , and ^{226}Ra are reduced by 85% (^{230}Th) to greater than 97% (^{243}Am , ^{226}Ra). The

activities of low-to-moderate solubility, low sorption, long half-life radionuclides are reduced by approximately 23% (^{237}Np) to 32% (^{234}U). Release of the mobile radionuclide, ^{99}Tc , is reduced by about 5% by the Lower Natural Barrier. The nonsorbing nature of this radionuclide causes it to be transported through the EBS and the Lower Natural Barrier at approximately the rate at which the groundwater travels.

In addition to the test programs that address water flow in the unsaturated rock units above the repository, tests were conducted to collect the data necessary to understand the radionuclide transport and retardation phenomena in the unsaturated rock units below the repository horizon. Transport processes in the vitric Calico Hills nonwelded unit were undertaken in the Busted Butte underground facility located approximately 8 km southeast of the repository area. Tracer-injection tests, partial mine-out, and geophysical measurements (e.g., ground-penetrating radar, electrical resistivity tomography, and neutron logging) were performed to map solute migration patterns.

Hydraulic tests in the saturated rocks and alluvium in the vicinity of Yucca Mountain were performed in single-borehole and multiple-borehole tests. Results from large-scale (tens of meters) hydraulic and tracer testing were used to increase confidence in the conceptualization of flow and transport in the fractured tuff. The test results also support the hypothesis that fractures are more important than matrix in controlling hydraulic conductivity of the volcanic rocks in the saturated zone.

Postclosure Performance Assessment: Compliance with Individual and Groundwater Protection Standards—TSPA analyses have been performed to evaluate the performance of the repository for 10,000 years after closure of the repository, as well as for the period beyond 10,000 years, within the period of geologic stability as prescribed by proposed 10 CFR Part 63. The standards for Yucca Mountain embodied in proposed 10 CFR 63, Subpart L, address all potential pathways of radiation exposure. The standards limit an individual's annual radiation exposure from all pathways to no greater than 15 mrem, for 10,000 years after repository closure, and requires that the DOE calculate the dose to which individuals could be exposed for the period beyond 10,000 years, within the period of geologic stability as prescribed by proposed 10 CFR Part 63. To preserve groundwater quality for this and future generations, the U.S. Nuclear Regulatory Commission set a standard to protect the groundwater at and around Yucca Mountain. This standard sets specific limits for the concentration of different types of radioactive particles in the groundwater. The DOE must also assess the likelihood of an inadvertent human intrusion into the repository and, depending on that result, its consequence for a period of 10,000 years after closure, as well as an assessment for human intrusion during the period of geologic stability.

The TSPA is also used to assess the effects of uncertainty in the data and models on the overall results of repository performance assessment. Four scenario classes are considered in the TSPA: (1) the nominal scenario class, which includes all FEPs that are screened in according to the FEPs screening process, except those FEPs related to early waste package and drip shield failure, and igneous or seismic activity; (2) the early failure scenario class, which includes FEPs related to early waste package and drip shield failure due to manufacturing or material defects or to preemplacement operations including improper heat treatment; (3) the igneous scenario class, which is comprised of the igneous intrusion and volcanic eruption modeling cases, both of which are based on unlikely low-probability events; and (4) the seismic scenario class, which is comprised of the seismic ground motion modeling case and the seismic fault displacement modeling case. The

sum of the mean annual dose estimates for the nominal, early failure, igneous, and seismic scenario classes provides an estimate of the mean annual dose for the total system. For the period ending 10,000 years after disposal, the result obtained by adding together the mean annual dose curves for the four scenario classes indicates that the mean annual dose for the total repository system is approximately 0.24 mrem/yr and occurs 10,000 years after repository closure. Even considering the conservative nature of the TSPA model and analyses, this mean annual dose is significantly less than the individual protection standard. This total is most significantly affected by the seismic ground motion modeling case and the igneous intrusion modeling case.

For the period after 10,000 years within the period of geologic stability as prescribed by proposed 10 CFR Part 63, the TSPA projects a peak median annual dose of approximately 0.96 mrem/yr. This total is also most significantly affected by the seismic ground motion modeling case and the igneous intrusion modeling case. The modeled dose is well below the proposed standard of 350 mrem/yr and is a fraction of naturally occurring background radiation.

In addition to the four scenario classes above, there is a separate human intrusion scenario which is a stylized analysis specified in proposed 10 CFR Part 63 that describes performance of the repository system in the event that there is a single human intrusion as a result of exploratory drilling for groundwater.

The earliest time after disposal that the drip shields and waste packages would have degraded sufficiently that a human intrusion could occur without recognition by the drillers is approximately 200,000 years, based on analyses of drip shield and waste package integrity. The estimated annual dose resulting from the stylized human intrusion is approximately 0.01 mrem/yr, well below the regulatory limit of 350 mrem/yr.

Demonstration of the performance of the repository also includes compliance with the separate groundwater protection standards for specific radionuclide concentrations. Radionuclide concentrations are calculated by summing the mass of radionuclides reaching the accessible environment in each year for all likely FEPs and dividing that sum by the representative volume of water to calculate the annual radionuclide concentrations. The groundwater protection standards require calculations of the predicted concentrations of combined ^{226}Ra and ^{228}Ra and gross alpha activity in a representative volume of 3,000 acre-ft of groundwater. The standards also require calculation of the annual dose to the whole body and organs from beta- and photon-emitting radionuclides resulting from drinking 2 L of water per day. The background level of the combined ^{226}Ra and ^{228}Ra concentration in groundwater is about 0.5 pCi/L. This measured background concentration must be added to the calculated concentration of combined ^{226}Ra and ^{228}Ra released from the repository for comparison with the postclosure groundwater protection standard for combined ^{226}Ra and ^{228}Ra . Because the calculated concentration of combined ^{226}Ra and ^{228}Ra released from the repository is less than 10^{-6} pCi/L, the total combined ^{226}Ra and ^{228}Ra concentration is reasonably approximated by the measured background level of about 0.5 pCi/L. This concentration is well below the limit of 5 pCi/L. Thus, the DOE has demonstrated that there is a reasonable expectation that, for 10,000 years of undisturbed performance after closure, releases of ^{226}Ra and ^{228}Ra from waste in the Yucca Mountain repository to the accessible environment will not cause the level of radioactivity in the representative volume of groundwater to exceed the regulatory limits.

The TSPA analyses of gross alpha activity concentrations (excluding radon and uranium) in the representative volume of groundwater due to repository releases are less than 10^{-4} pCi/L. This value is significantly lower than the background concentration of about 0.5 pCi/L, which, in turn, is significantly less than the gross alpha groundwater protection standard of 15 pCi/L.

The TSPA analyses of the mean annual doses associated with beta- and photon-emitting radionuclides in the drinking water indicate a maximum dose of approximately 0.26 mrem for the thyroid. This value is lower than the 4 mrem limit specified in 10 CFR 63.331, Table 1.

Organization of This Chapter—This chapter is organized in a manner generally consistent with Section 2.2.1 of NUREG-1804; each section contains an introduction summarizing information presented in the section and identifying applicable sections of proposed 10 CFR Part 63 and the acceptance criteria of NUREG-1804 addressed by the information in the section. [Section 2.1](#) describes the repository system and the capabilities of its three barriers: the Upper Natural Barrier, the EBS, and the Lower Natural Barrier. The information in [Section 2.1](#) addresses the performance objectives of 10 CFR 63.113(a) and 10 CFR 63.115 regarding the identification of multiple barriers and the demonstration of the ability of such barriers to isolate waste.

[Section 2.2](#) describes the FEPs that are evaluated for incorporation into the models assessing repository performance. The section tabulates the FEPs and indicates whether the FEPs are included or excluded from representation in the TSPA. It also explains how FEPs included for representation in the TSPA are organized into four scenario classes (i.e., nominal, early failure, igneous, and seismic) for assessing compliance with the postclosure performance objectives.

[Section 2.3](#) presents the technical bases for models and model abstractions that are used as a basis for the development of parameter inputs to the TSPA. [Sections 2.3.1](#) to [2.3.11](#) describe the physical setting, coupled processes (i.e., thermal, chemical, mechanical, and hydrologic) in the repository system, processes in the biosphere that determine exposure to radionuclides and resultant doses, and disruptive events. [Sections 2.3.1](#) to [2.3.11](#) cover characterization of the processes, analytical models of the processes, and uncertainty of the characterization of the data and parameters used in the models. In [Section 2.3](#), the order of the presentation of the models generally follows the path of water from the surface of Yucca Mountain down to the repository horizon, through its interaction with the EBS, and then to the accessible environment through the unsaturated and saturated zones. In addition, discussions in [Section 2.3](#) generally mirror the acceptance criteria set forth in NUREG-1804 and appear in the following order:

- Conceptual description of the model (NUREG-1804, Acceptance Criterion 1)
- Data and data uncertainty (NUREG-1804, Acceptance Criteria 2 and 3)
- Model and model uncertainty (NUREG-1804, Acceptance Criterion 4)
- Model abstraction and validation (NUREG-1804, Acceptance Criterion 5).

[Section 2.4](#) presents a discussion of the TSPA model and the analytical results that demonstrate compliance with the performance objectives of 10 CFR 63.113(b), (c), and (d) for individual protection, groundwater protection, and human intrusion, respectively. [Section 2.4.1](#) summarizes the method and approach of the DOE's performance assessment, including the scenario classes, the major components and associated submodels of the TSPA model, and an introduction to the modeling cases used to compute the annual dose. The TSPA computational structure, and the

treatment of aleatory and epistemic uncertainties, is briefly described. [Section 2.4.2](#) shows that the EBS and the natural barriers, working in combination, maintain the mean annual dose to the reasonably maximally exposed individual due to releases from the undisturbed repository system below 0.15 mSv (15 mrem) for the period up to 10,000 years after repository closure. For the period beyond 10,000 years, within the period of geologic stability as prescribed by proposed 10 CFR Part 63, the TSPA projects that the dose will not exceed 3.5 mSv (350 mrem), as set forth in proposed 10 CFR 63.311. [Section 2.4.3](#) provides an evaluation of a potential human intrusion event and demonstrates that intrusion without recognition by drillers will not occur within 10,000 years. [Section 2.4.4](#) describes the location and extent of the representative volume of groundwater used to address repository performance and the results of the assessment. The TSPA shows that there is a reasonable expectation that for 10,000 years of undisturbed performance, any radioactive releases from the repository system into the accessible environment will not cause the level of radioactivity in the representative volume of groundwater to exceed the limits set forth in 10 CFR 63.331, Table 1.

CONTENTS

	Page
2.1 System Description and Demonstration of Multiple Barriers	2.1-1
2.1.1 Identification of Barriers	2.1-3
2.1.1.1 Upper Natural Barrier	2.1-5
2.1.1.2 Engineered Barrier System	2.1-7
2.1.1.3 Lower Natural Barrier	2.1-9
2.1.2 Barrier Capability Description	2.1-10
2.1.2.1 Upper Natural Barrier	2.1-11
2.1.2.2 Engineered Barrier System	2.1-31
2.1.2.3 Lower Natural Barrier	2.1-78
2.1.3 Technical Bases for Barrier Capability	2.1-101
2.1.3.1 Upper Natural Barrier	2.1-102
2.1.3.2 Engineered Barrier System	2.1-103
2.1.3.3 Lower Natural Barrier	2.1-107
2.1.3.4 Technical Basis for Disruptive Events Potentially Affecting Barrier Capability	2.1-108
2.1.3.5 Summary of Technical Bases for Barrier Capability	2.1-109
2.1.4 Summary	2.1-110
2.1.5 General References	2.1-112

INTENTIONALLY LEFT BLANK

TABLES

		Page
2.1-1.	ITWI Features / Components Supporting Each of the Three Barriers	2.1-115
2.1-2.	Summary of Features, Events, and Processes Affecting the Capability of the Upper Natural Barrier	2.1-117
2.1-3.	Summary of Features, Events, and Processes Affecting the Capability of the Engineered Barrier System	2.1-121
2.1-4.	Summary of Features, Events, and Processes Affecting the Capability of the Lower Natural Barrier	2.1-135
2.1-5.	Relationship between Barriers and Total System Performance Assessment Models.	2.1-140
2.1-6.	Seepage Fractions for Codisposal and Commercial SNF Waste Packages for Combined Nominal/Early Failure Modeling Case for Glacial-Transition Climate, 2,000 to 10,000 Years	2.1-141
2.1-7.	Seepage Fractions for Codisposal and Commercial SNF Waste Packages for Combined Nominal/Early Failure Modeling Case for Post-10,000-Year Period.	2.1-141
2.1-8.	Seepage Fractions for Codisposal and Commercial SNF Waste Packages for Seismic Ground Motion Modeling Case for Glacial-Transition Climate, 2,000 to 10,000 Years	2.1-142
2.1-9.	Seepage Fractions for Codisposal and Commercial SNF Waste Packages for Seismic Ground Motion Modeling Case for Post-10,000-year Period	2.1-142
2.1-10.	Drift Wall Condensation for Commercial SNF Waste Packages for Stage 2 and Stage 3 Condensation	2.1-143
2.1-11.	Drift Wall Condensation for Codisposal Waste Packages for Stage 2 and Stage 3 Condensation.	2.1-144
2.1-12.	Mean Seepage Rates for Waste Packages during Stage 2 and Stage 3 Condensation	2.1-145
2.1-13.	Decay of Total Curie Inventory as a Function of Time and Dominant Contributors to Total Curie Inventory	2.1-145

INTENTIONALLY LEFT BLANK

FIGURES

		Page
2.1-1.	Schematic Illustration of the Multiple Barrier Repository System.	2.1-147
2.1-2.	Schematic of the Upper Natural Barrier	2.1-149
2.1-3.	Cross Section of Unsaturated Zone from Surface to Repository Horizon	2.1-151
2.1-4.	Simplified Geologic Map Showing Major Lithostratigraphic Units in the Yucca Mountain Site Area	2.1-153
2.1-5.	Upper Natural Barrier Capability to Prevent or Substantially Reduce the Rate of Water Movement to the Waste for the Mean Spatially-Averaged (a) Annual Precipitation, Net Infiltration, and Post-10,000-Year Percolation and (b) Drift Seepage Fluxes for the Combined Nominal/Early Failure Modeling Case and Seismic Ground Motion Modeling Case—1,000,000 Year Period	2.1-154
2.1-6.	Volume of (a) Lithophysal and (b) Nonlithophysal Rockfall Over 20,000 Years	2.1-155
2.1-7.	Schematic of the Engineered Barrier System	2.1-157
2.1-8.	Probability of Drip Shield Failure by General Corrosion for the Nominal Modeling Case Based on 300 Epistemic Realizations of Drip Shield General Corrosion Rates	2.1-159
2.1-9.	Summary Statistics for Fraction of Waste Packages Breached for (a) Commercial SNF Waste Packages and (b) Codisposal Waste Packages for the Nominal Modeling Case as a Function of Time	2.1-160
2.1-10.	Summary Statistics for Fraction of Commercial SNF Waste Packages (a) Breached by Stress Corrosion Cracking and (b) Breached by General Corrosion Patches for the Nominal Modeling Case as a Function of Time	2.1-161
2.1-11.	Cumulative Distribution Function of Drip Shield Failure Time for (a) Distributions of Failure Time for 300 Epistemic Sample Elements and (b) Distribution of Expected (over Aleatory) Failure Time with Confidence Interval for the Seismic Ground Motion Modeling Case	2.1-162
2.1-12.	Summary Statistics for Expected Fraction of Commercial SNF Waste Packages Breached by (a) Seismic and Nominal Processes and (b) Seismic-Induced Processes only; Codisposal Waste Packages Breached by (c) Seismic and Nominal Processes and (d) Seismic Events Only for the Seismic Ground Motion Modeling Case as a Function of Time (Page 1 of 2).	2.1-163
2.1-12.	Summary Statistics for Expected Fraction of Commercial SNF Waste Packages Breached by (a) Seismic and Nominal Processes and (b) Seismic-Induced Processes only; Codisposal Waste Packages Breached by (c) Seismic and Nominal Processes and (d) Seismic Events Only for the Seismic Ground Motion Modeling Case as a Function of Time (Page 2 of 2)	2.1-164

FIGURES (Continued)

	Page
2.1-13. Summary Statistics for Average Fraction of Commercial SNF Waste Package Surface Breached by Cracks per Breached Waste Package for (a) the Seismic Ground Motion Modeling Case and (b) the Nominal Modeling Case, as a Function of Time	2.1-165
2.1-14. Fraction of Drift Filled with Rubble	2.1-166
2.1-15. Summary Statistics for Fraction of Codisposal Waste Package Surface Breached by Cracks per Breached Waste Package for (a) the Seismic Ground Motion Modeling Case and (b) the Nominal Modeling Case, as a Function of Time	2.1-167
2.1-16. Summary Statistics for Fraction of Commercial SNF Waste Package Surface Breached by Patches per Breached Waste Package for (a) the Seismic Ground Motion Modeling Case and (b) the Nominal Modeling Case, as a Function of Time	2.1-168
2.1-17. Summary Statistics for Expected Fraction of Codisposal Waste Package Surface Breached by Patches per Breached Waste Package for (a) the Seismic Ground Motion Modeling Case and (b) the Nominal Modeling Case, as a Function of Time	2.1-169
2.1-18. Mean Radionuclide Activities in the Nuclear Waste as a Function of Time for (a) 10,000 Years and (b) 1,000,000 Years after Repository Closure	2.1-170
2.1-19. Mean Radionuclide Contributions to Total Inventory as a Function of Time for (a) 10,000 Years and (b) 1,000,000 Years after Repository Closure	2.1-171
2.1-20. Mean Activity Released from the Engineered Barrier System, for the Combined Nominal/Early Failure Modeling Case: (a) 10,000 Years after Repository Closure and (b) Post-10,000 Years after Repository Closure	2.1-172
2.1-21. Uncertainty in Expected Activity of ⁹⁹ Tc Released from the Engineered Barrier System for the Combined Nominal/Early Failure Modeling Case for (a) 10,000 Years and (b) 1,000,000 Years after Repository Closure	2.1-173
2.1-22. Uncertainty in Expected Activity of ²³⁹ Pu Released from the Engineered Barrier System for the Combined Nominal/Early Failure Modeling Case for (a) 10,000 Years and (b) 1,000,000 Years after Repository Closure	2.1-174
2.1-23. Mean Activity Released from the Engineered Barrier System for the Seismic Ground Motion Modeling Case for (a) 10,000 Years and (b) 1,000,000 Years after Repository Closure	2.1-175
2.1-24. Uncertainty in Activity of ⁹⁹ Tc Released from the Engineered Barrier System for the Seismic Ground Motion Modeling Case for (a) 10,000 Years and (b) 1,000,000 Years after Repository Closure	2.1-176
2.1-25. Uncertainty in Activity of ²³⁷ Np Released from the Engineered Barrier System for the Seismic Ground Motion Modeling Case for (a) 10,000 Years and (b) 1,000,000 Years after Repository Closure	2.1-177
2.1-26. Uncertainty in Activity of ²³⁴ U Released from the Engineered Barrier System for the Seismic Ground Motion Modeling Case for (a) 10,000 Years and (b) 1,000,000 Years after Repository Closure	2.1-178

FIGURES (Continued)

	Page
2.1-27. Uncertainty in Activity of ^{226}Ra Released from the Engineered Barrier System for the Seismic Ground Motion Modeling Case for (a) 10,000 Years and (b) 1,000,000 Years after Repository Closure	2.1-179
2.1-28. Uncertainty in Activity of ^{239}Pu Released from the Engineered Barrier System for the Seismic Ground Motion Modeling Case for (a) 10,000 Years and (b) 1,000,000 Years after Repository Closure	2.1-180
2.1-29. Uncertainty in Activity of ^{242}Pu Released from the Engineered Barrier System for the Seismic Ground Motion Modeling Case for (a) 10,000 Years and (b) 1,000,000 Years after Repository Closure	2.1-181
2.1-30. Schematic of Lower Natural Barrier	2.1-183
2.1-31. Conceptualized Water Flow Behavior in the Different Hydrogeologic Units Below the Repository	2.1-185
2.1-32. Cross Section of the Saturated Zone Downgradient from the Repository	2.1-187
2.1-33. Satellite Image and Superimposed Generalized Geologic Map of Areas of Exposed Bedrock, Showing the Location of the Cross Section in Figure 2.1-32	2.1-189
2.1-34. Mean Activity Released from the (a) Saturated Zone and (b) Engineered Barrier System, for the Combined Nominal/Early Failure Modeling Case for 10,000 Years after Repository Closure	2.1-190
2.1-35. Mean Activity Released from the (a) Saturated Zone and (b) Engineered Barrier System, for the Combined Nominal/Early Failure Modeling Case for 1,000,000 years after Repository Closure	2.1-191
2.1-36. Mean Activity Released from the (a) Saturated Zone and (b) Engineered Barrier System, for the Seismic Ground Motion Modeling Case for 10,000 Years after Repository Closure	2.1-192
2.1-37. Mean Activity Released from the (a) Saturated Zone and (b) Engineered Barrier System, for the Seismic Ground Motion Modeling Case and 1,000,000 Years after Repository Closure	2.1-193
2.1-38. Uncertainty in Activity of ^{99}Tc Released from the Saturated Zone for the Seismic Ground Motion Modeling Case for (a) 10,000 Years and (b) 1,000,000 Years after Repository Closure	2.1-194
2.1-39. Uncertainty in Activity of ^{237}Np Released from the Saturated Zone for the Seismic Ground Motion Modeling Case for (a) 10,000 Years and (b) 1,000,000 Years after Repository Closure	2.1-195
2.1-40. Uncertainty in Activity of ^{234}U Released from the Saturated Zone for the Seismic Ground Motion Modeling Case for (a) 10,000 Years and (b) 1,000,000 Years after Repository Closure	2.1-196
2.1-41. Uncertainty in Activity of ^{226}Ra Released from the Saturated Zone for the Seismic Ground Motion Modeling Case for (a) 10,000 Years and (b) 1,000,000 Years after Repository Closure	2.1-197
2.1-42. Uncertainty in Activity of ^{239}Pu Released from the Saturated Zone for the Seismic Ground Motion Modeling Case for (a) 10,000 Years and (b) 1,000,000 Years after Repository Closure	2.1-198

FIGURES (Continued)

	Page
2.1-43. Uncertainty in Activity of ²⁴² Pu Released from the Saturated Zone for the Seismic Ground Motion Modeling Case for (a) 10,000 Years and (b) 1,000,000 Years after Repository Closure	2.1-199

2.1 SYSTEM DESCRIPTION AND DEMONSTRATION OF MULTIPLE BARRIERS

[NUREG-1804, Section 2.2.1.1.3: AC 1, AC 2, AC 3]

A critical element for repository safety is a site and system that provide multiple barriers to the movement of water and radionuclides. A barrier is defined in 10 CFR 63.2 as any material, structure, or feature that prevents or substantially reduces the rate of movement of water or radionuclides from the Yucca Mountain repository to the accessible environment, or prevents the release or substantially reduces the release rate of radionuclides from the waste. The barrier capability analyses were conducted for two time periods: the 10,000-year period after closure, and the post-10,000-year period after closure through the period of geologic stability (defined to end at 1,000,000 years) (proposed 10 CFR 63.302 (70 FR 53313)).

The repository system is composed of natural and engineered features that function together as two natural barriers, and an engineered barrier, designated as the Upper Natural Barrier, the Lower Natural Barrier, and the Engineered Barrier System (EBS). These three barriers provide the following principal barrier functions:

- The Upper Natural Barrier, by preventing or substantially reducing the rate of movement of water into the repository, prevents or substantially reduces the rate of movement of radionuclides from the repository to the accessible environment.
- The EBS prevents or substantially reduces the rate of movement of water to the waste, prevents or substantially reduces the release rate of radionuclides from the waste, and prevents or substantially reduces the rate of movement of radionuclides from the repository to the accessible environment.
- The Lower Natural Barrier prevents or substantially reduces the rate of movement of radionuclides from the repository to the accessible environment.

As defined by 10 CFR 63.302, the accessible environment means any point outside of the controlled area, including: (1) the atmosphere (including the atmosphere above the surface area of the controlled area); (2) land surfaces; (3) surface waters; (4) oceans; and (5) the lithosphere. For the purposes of the total system performance assessment (TSPA), the reasonably maximally exposed individual (RMEI) is to be located in the accessible environment, designated as 18 km south of the repository in the Amargosa Valley (GI Section 5.2.6.1 and GI Figure 1-4).

The three repository system barriers are important to waste isolation (ITWI), and function in a manner to provide a reasonable expectation that spent nuclear fuel (SNF) and high-level radioactive waste (HLW) can be disposed of without exceeding the release limit and exposure limit requirements of 10 CFR 63.113(b) and (c). The specification of these barriers as ITWI is a result of an analysis conducted and documented in *Postclosure Nuclear Safety Design Bases* (SNL 2008a). The understanding of the barriers gained through characterization of the site and repository system permits a demonstration that the barriers work together to perform their postclosure functions. This demonstration is presented in this section, and is outlined as follows.

[Section 2.1.1](#) identifies the features of the natural barriers and the EBS that contribute to barrier performance. This section also identifies the relationships between the three barriers and the models utilized in the TSPA.

Events and processes act upon the natural and engineered features (SNL 2008a). The primary analytical bases for inclusion and exclusion of events and processes in the postclosure performance assessment are summarized in [Section 2.2](#) and are documented in *Features, Events, and Processes for the Total System Performance Assessment: Analyses* (SNL 2008b, Section 6.2). [Section 2.3](#) describes the models that implement the included events and processes. For completeness, some models related to excluded processes are also discussed in [Section 2.3](#).

[Section 2.1.2](#) describes the capability of the barriers to perform one or more barrier functions and considers the impacts of likely and unlikely events. This section also demonstrates that the EBS and the two natural barriers, working in combination, result in a repository system with multiple barriers. [Section 2.1.2](#) includes an evaluation of (1) the time period over which the barriers function; and (2) the uncertainty associated with analyses of barrier capability. The demonstration of barrier capability considers both qualitative and quantitative information. Qualitative information includes a summary of the events and processes acting on each barrier feature that contribute to barrier capability. Quantitative information supporting barrier capability is developed using the TSPA model, and is presented both for the time period up to 10,000 years after repository closure and for the post-10,000-year period (i.e., after 10,000 years but through the period of geologic stability ending at 1,000,000 years).

Barrier capabilities determined to be important are included in the TSPA model. Potential barrier capabilities related to excluded features, events, and processes (FEPs) are not included in the TSPA model (SNL 2008a, Section 6.2). Reasonably conservative model assumptions are sometimes made in the TSPA that result in the tendency of the TSPA model to overestimate release and subsequent dose. Such assumptions are made to reduce model complexity or data needs, or to account for uncertainty in processes. An example discussed in [Section 2.1.1.2](#) is cladding. Although it is recognized that cladding on commercial SNF may contribute to barrier capability, no credit is taken for its potential performance in the TSPA model. The rationale for this assumption is described in [Section 2.3.7.6](#). The technical basis for the barrier capabilities discussed in [Section 2.1.2](#) is consistent with the technical basis for the TSPA, and is commensurate with the importance of each barrier's capability.

[Section 2.1.3](#) summarizes and cross-references the technical basis for the models that are used to evaluate barrier performance and capability, and which are abstracted for use in the TSPA to demonstrate compliance with the performance objectives of 10 CFR 63.113(b) and (c). [Section 2.1.4](#) integrates the content of [Section 2.1.1](#) through [2.1.3](#) into a brief overview.

The demonstration of barrier capability presented in [Section 2.1](#) is based on data and analyses described in [Section 2.3](#). These data and analyses are the same as those used to support the TSPA model and analyses presented in [Section 2.4](#). More detailed discussion of the implementation of these data, models, and analyses in the TSPA is presented in [Section 2.4](#).

The information presented in the table below summarizes the content of this section, the corresponding regulatory requirements, and the applicable acceptance criteria from NUREG-1804:

SAR Section	Information Category	Proposed 10 CFR Part 63 Reference	NUREG-1804 Reference
2.1	System Description and Demonstration of Multiple Barriers	63.21(c)(9) ^a 63.21(c)(14) ^a 63.113(a) ^a 63.115(b) ^a 63.115(c) ^a	Section 2.2.1.1.3: Acceptance Criterion 1 Acceptance Criterion 2 Acceptance Criterion 3
2.1.1	Identification of Barriers	63.21(c)(9) ^a 63.21(c)(14) ^a 63.113(a) ^a 63.115(a) ^a	Section 2.2.1.1.3: Acceptance Criterion 1
2.1.2	Barrier Capability Description	63.21(c)(9) ^a 63.21(c)(14) ^a 63.113(a) ^a 63.115(b) ^a	Section 2.2.1.1.3: Acceptance Criterion 2
2.1.3	Technical Bases for Barrier Capability	63.115(c) ^a	Section 2.2.1.1.3: Acceptance Criterion 3
2.1.4	Summary	Not applicable	Not applicable

NOTE: ^aNot changed by the proposed rule.

2.1.1 Identification of Barriers

[NUREG-1804, Section 2.2.1.1.3: AC 1]

The repository system is composed of three barriers: the Upper Natural Barrier, the EBS, and the Lower Natural Barrier (SNL 2008a). These three barriers are ITWI. The specification of these barriers as ITWI is a result of an analysis conducted and documented in *Postclosure Nuclear Safety Design Bases* (SNL 2008a, Section 6). Table 2.1-1 identifies the features that comprise each barrier, their contribution to barrier function, and their safety classification (SNL 2008a).

As defined by 10 CFR 63.2, ITWI—with reference to design of the EBS and characterization of natural barriers—means those engineered and natural barriers whose function is to provide a reasonable expectation that SNF and HLW can be disposed of without exceeding the requirements of 10 CFR 63.113(b) and (c). For the purposes of this section, the term barrier is used in the context of the three defined barriers described above. A barrier's features may contribute to the barrier's capability. Therefore, ITWI is a classification assigned to a barrier or a barrier's feature, based on its capability of preventing or substantially reducing the rate of movement of water or radionuclides from the Yucca Mountain repository to the accessible environment, or preventing the release or substantially reducing the release rate of radionuclides from the waste (SNL 2008a, Section 6.1.1). A barrier's feature is classified as ITWI if it meets two conditions: (1) the feature is associated with

one or more processes or characteristics (SNL 2008a) classified as important to barrier capability; and (2) the feature is a significant contributor to the barrier capability relative to the other features of the barrier. In addition, a feature is classified as ITWI if it is one of the engineered features of the geologic repository whose function is to prevent or mitigate the consequences of potential disruptive events (e.g., criticality) per 10 CFR 63.142(a).

The association of FEPs with features of barriers and the identification of FEPs that are important contributors to barrier capability (SNL 2008a) are presented for the Upper Natural Barrier, EBS, and Lower Natural Barrier in [Tables 2.1-2](#), [2.1-3](#), and [2.1-4](#), respectively. To ensure that the TSPA is representative of repository postclosure performance, it is necessary that the features, together with the geologic conditions relied upon in the TSPA, are within analyzed conditions at the time the repository is closed. [Table 1.9-9](#) contains a summary of the parameters that require controls to ensure that the postclosure performance assessment analytical bases are established during design, preclosure construction, procurement, operations, and closure.

[Figure 2.1-1](#) is a schematic representation of the repository system that shows the three barriers and the features making up each barrier. The geologic and hydrologic features and characteristics of the Yucca Mountain site form effective natural barriers to the flow of water and to the potential movement of radionuclides. The underground environment within the natural setting is conducive to the design and construction of EBS features that prevent or substantially reduce the potential release of radionuclides from the waste. [Table 2.1-5](#) shows the relationships among the three barriers and the models utilized in the TSPA. These models are the same as those used for the analysis of barrier capability that is presented in [Section 2.1.2](#).

The barrier capability discussion that follows is organized by barrier and by the features of each barrier. The features of the Upper Natural Barrier are evaluated with respect to how they prevent or substantially reduce the rate and amount of water that may seep into the repository drifts and, in turn, reduce the quantity of water potentially contacting the waste form. The features of the EBS are evaluated with respect to how they prevent or substantially reduce the release rate of radionuclides from the waste, and how they prevent or substantially reduce the rate of movement of radionuclides from the repository to the accessible environment. The features of the Lower Natural Barrier are evaluated with respect to how they prevent or substantially reduce the rate of movement of radionuclides from the repository to the accessible environment.

Features have various processes acting on them that contribute to the ability of the feature to perform one or more functions related to barrier capability. To evaluate the capability of the barriers, the contribution of different processes acting on the features that make up each barrier is assessed. For example, matrix diffusion and radionuclide sorption are processes acting within both features of the Lower Natural Barrier (i.e., the unsaturated zone below the repository and the saturated zone) that contribute to preventing or substantially reducing the rate of movement of radionuclides away from the repository. It is, therefore, appropriate to evaluate the capability of barriers in the context of the processes that act within the features.

Features also have various events acting on them that may affect their barrier function and capability. The evaluation of barrier capability provides information on the time period over which each barrier and feature performs its function, including the potential effects associated with events that are expected to occur. For example, the potential effect of seismic events on the capability of

the EBS is considered in the evaluation of the EBS barrier capability. The impacts of seismic events on the EBS and its barrier function during the period of geologic stability (1,000,000 years) are potentially more significant than impacts during the 10,000 years following repository closure. This result is based primarily on the fact that corrosion processes acting over long periods of time will degrade the EBS features and reduce their structural integrity, thereby making them more susceptible to damage induced by vibratory ground motion. Igneous intrusion events are addressed only qualitatively in the barrier capability analysis, because they are unlikely to occur. Volcanic eruption events are not considered in the barrier capability analysis, because they are very unlikely to occur.

In the following discussion, all physical attributes of the repository system, whether natural or engineered, are called features. This allows a direct comparison and mapping to the features identified in [Section 2.2](#) as relevant to postclosure performance. The processes that act on the natural features, which allow the natural barriers to perform the functions of preventing or substantially reducing the rate of movement of water or radionuclides, are generally hydrologic and thermal-hydrologic processes or transport processes. The processes that act on the engineered features, which allow the EBS to perform the function of preventing or substantially reducing the release rate of radionuclides from the waste and the repository, are generally hydrologic and thermal-hydrologic, chemical and thermal-chemical, mechanical and thermal-mechanical, and transport processes. These include the degradation, deterioration, or alteration processes (evaluated in accordance with proposed 10 CFR 63.114(a)(6)) that can affect the integrity of the EBS.

2.1.1.1 Upper Natural Barrier

The Upper Natural Barrier consists of (1) surface topography and surficial soils, and (2) the unsaturated zone above the repository. Both of these features are ITWI (see [Table 2.1-1](#)). Surface topography and surficial soils act to limit infiltration into the unsaturated zone through a combination of evaporation, transpiration, and runoff ([Section 2.3.1.1](#)). The unsaturated zone above the repository horizon prevents or limits seepage into emplacement drifts by attenuating episodic flow, and by diverting flow around the drift opening through a combination of capillarity and thermal processes ([Section 2.3.2.2](#)).

The location and elevation of the repository take advantage of the characteristics of the geologic and hydrogeologic setting of Yucca Mountain. These characteristics include the following:

- An arid climate with limited precipitation and significant evapotranspiration
- A thickness of rock and soil above the repository everywhere greater than 200 m, and up to more than 400 m
- Geologic, geochemical, and geomechanical characteristics compatible with the design and construction of an effective EBS
- Geomechanical and thermal characteristics that provide a stable facility with adequate capacity for waste disposal.

At Yucca Mountain, the majority of precipitation does not infiltrate into the unsaturated zone because of surface runoff, evaporation, and transpiration. On the basis of the values in [Tables 2.3.1-17](#), [2.3.1-18](#), and [2.3.1-19](#), the infiltration on average ranges up to about only 10% of the precipitation expected over the repository area, even for future wetter climates. This small fraction of total precipitation that infiltrates through the surficial soils moves into the bedrock and flows downward by gravity and capillary forces. This water then flows through the series of welded and nonwelded tuff units and percolates downward as percolation flux, driven by gravity and capillary forces, through layers of welded and nonwelded tuff units. The major hydrogeologic units within the Upper Natural Barrier include the Tiva Canyon welded (TCw) and the Paintbrush nonwelded (PTn) units located above the repository, and the Topopah Spring welded (TSw) unit that hosts the repository ([Figure 2.1-2](#)).

As water percolates downward through the unsaturated zone, it is redistributed between fractures and matrix, and by lateral flow along layer interfaces to faults ([Section 2.3.2.2](#)). For the entire unsaturated zone flow model domain, a substantial portion of flow is laterally diverted into faults, where fault flow increases from 1% to 2% at the top of the PTn to 12% to 32% at the repository level. However, at the repository horizon, fault flow only accounts for about 1% of the total percolation flux within the repository footprint ([Section 2.3.2.4.1.2.4.6](#); [Table 2.3.2-7](#)). The PTn unit has high matrix permeability and high matrix porosity with low fracture density, and its matrix system has a large capacity for storing groundwater. The relatively high matrix permeability and porosity, and the low fracture density of the PTn unit, convert the predominant fracture flow in the TCw unit above the PTn to dominant matrix flow within the PTn unit, thus damping flow through the unsaturated zone ([Section 2.3.2.2.1.2](#)). In contrast, water flow in the fractured welded tuffs that host the repository (i.e., the TSw hydrogeologic unit) occurs primarily in widely distributed fractures ([Section 2.3.2.2.1.3](#)).

The location of repository excavations in the unsaturated zone also limits the seepage of water as a result of capillary processes. Water moving through the rock matrix or in fractures in the unsaturated zone tends not to flow into large openings, such as drifts, but tends to continue to flow in the matrix and fractures in the rock around openings. This process diverts percolating water around the emplacement drifts and into the rock pillars between the drifts ([Section 2.3.3.2](#)). Seismic events ([Section 2.3.4](#)) and igneous intrusion events ([Section 2.3.11](#)) would tend to decrease the water flow diversion effect of drifts ([Section 2.3.3.2](#)). Emplacement drifts degrade with time as a result of seismic activity, potentially leading to changes in drift shape and size and the filling of drift openings with rubble rock material. Igneous intrusion events potentially lead to magma-filled drifts. The impact of changes in shape or size or filling the drifts in both of these events would be to decrease the water flow diversion effect of drifts.

The design of the repository system also takes advantage of the heat generated by emplaced waste to increase the diversion of percolating water away from and around the emplacement drifts ([Section 2.3.3.3](#)). As long as the drift-wall temperature in the emplacement drifts exceeds the boiling point of water, no liquid water will be available to flow into emplacement drifts. Above-boiling temperatures will generally persist for several hundred to more than 1,000 years following closure ([Section 2.3.5.6](#)), particularly in the drifts near the center of the repository footprint ([Section 2.3.3.3.1](#)).

The models that represent the physical processes of the Upper Natural Barrier are described in [Sections 2.3.1 to 2.3.3](#).

2.1.1.2 Engineered Barrier System

The basic objective of the EBS is to provide long-term containment of the radionuclides contained in the waste forms to be disposed at Yucca Mountain. The EBS achieves this objective by ensuring three important barrier functions: (1) preventing or substantially reducing the amount of seepage water and drift wall condensation that contacts the waste; (2) preventing or substantially reducing the rate of release of radionuclides from the waste; and (3) preventing or substantially reducing the rate of release of radionuclides from the EBS to the Lower Natural Barrier. The features of the EBS, their contributions to barrier function, and their safety classification are provided in [Table 2.1-1](#) and illustrated in [Figure 2.1-1](#). [Table 1.9-8](#) also provides further details with respect to the structures, systems, or components that comprise each engineered feature.

The characteristics of the EBS include the following:

- A thermal, mechanical, hydrologic (including isolation of waste from moisture), and chemical environment favorable to waste isolation and affected principally by the thermal effects of radioactive decay and possible seismic events
- Corrosion-resistant metals that are designed to perform and function in the thermal, mechanical, hydrologic, and chemical environments expected in the emplacement drifts
- Drip shield, waste package, and cladding materials with designs and fabrication methods that reduce the potential effects of stress corrosion cracking, creep, and other physical-chemical degradation processes
- Generally low solubility and high sorption capacity of radionuclides, thus delaying or preventing their release in the event that waste packages are breached
- Delayed transport of radionuclides through the EBS due to insignificant advection through the EBS features for several hundreds of thousands of years and the slow diffusion of radionuclides through any continuous water film.

Emplacement drifts provide the thermal, mechanical, hydrologic, and chemical environment in which the rest of the EBS features function ([Sections 2.3.4 and 2.3.5](#)). These environments are affected by the heat caused by the decay of radioactive materials in the waste—in particular, in the commercial SNF waste form that makes up the bulk of the repository waste and therefore generates the most heat. Although these environments are expected to change with time, in the absence of low-probability events (such as seismic or igneous events), the rate of change is very slow.

The drip shield ([Section 2.3.6.1](#)) is ITWI (SNL 2008a, Section 6.2.1.2). The drip shield, which will be placed over the waste packages, is fabricated from Titanium Grade 7 (UNS R52400), which is a commercially available, nearly pure titanium alloy containing a small addition of palladium to provide a higher degree of corrosion resistance. The structural components of the drip shield will be constructed using the higher-strength titanium alloy Titanium Grade 29 (UNS R56404), which has

alloying elements aluminum and vanadium to provide the required strength, and ruthenium to provide corrosion resistance. This titanium alloy is also highly corrosion resistant in a wide variety of chemical environments. The design and fabrication of the drip shield are described in [Section 1.3.4](#).

The waste package ([Section 2.3.6](#)), including the waste package outer barrier and the inner vessel, is ITWI (SNL 2008a, Section 6.2.1.2). Commercial SNF waste packages, which constitute approximately 70% of the waste packages that will be emplaced in the repository, contain a transportation, aging, and disposal (TAD) canister. The naval SNF waste packages that will be emplaced are treated in the TSPA as commercial SNF waste packages ([Section 2.3.7.3](#)). The waste package consists of two concentric cylinders: (1) an inner vessel of Stainless Steel Type 316 (UNS S31600, with further compositional restrictions as described in [Section 1.5.2.7](#)) designed for structural support; and (2) a corrosion-resistant outer shell made of Alloy 22 (UNS N06022, a nickel-chromium-molybdenum alloy with further compositional restrictions as described in [Section 2.3.6.7](#)). The design and fabrication of the waste package is described in [Section 1.5.2](#).

Components of waste package internals that are ITWI ([Table 2.1-1](#)) include the TAD canister, naval canister, naval SNF canister system components, and the TAD canister and DOE SNF canister internals. Information regarding the design and performance of naval SNF and the naval SNF canister system components is provided in [Section 1.5.1.4](#). The TAD canister internals, DOE SNF canister internals, and naval SNF canister system are ITWI because they include features that reduce the probability of criticality ([Table 1.9-8](#)). The TAD canister is constructed of Type 300-series stainless steel (such as Stainless Steel Type 316) that fits within the inner vessel of the waste package (SNL 2007a).

The types of waste to be placed in the repository ([Section 1.5.1](#)) include commercial SNF, DOE SNF (including naval SNF), and HLW. The waste forms that are ITWI include commercial SNF, naval SNF, and HLW. DOE SNF, except for naval SNF, is not classified as ITWI (SNL 2008a, Table 7-1). A description of key characteristics associated with performance of naval SNF assemblies in the repository are provided in Section 1.5.1.4 of the Naval Nuclear Propulsion Program Technical Support Document. Commercial SNF is primarily composed of uranium dioxide pellets that oxidize and hydrate. DOE SNF is composed of uranium metal (N Reactor) fuel and other DOE SNF waste forms. These fuel types decompose by several processes, including dissolution, phase separation, selective leaching, and oxidation. HLW is composed of a borosilicate glass waste form that reacts with water and forms clays, zeolites, and oxides. The waste packages that contain canisters of naval SNF will contain only that waste form. Codisposal waste packages, which constitute approximately 30% of the waste packages in the repository, contain both HLW canisters and DOE SNF canisters (except for HLW packages that are loaded in the Initial Handling Facility, which contain only HLW canisters). These two canister types are not ITWI (SNL 2008a, Table 7-1).

As discussed above, the naval SNF waste-package content (that is, the naval waste form and canister system) have features that contribute to EBS barrier capability. [Section 2.4.2.3.2.2.4](#) discusses TSPA analyses that utilize these features to compare naval and commercial waste-package contributions to dose. These analyses demonstrate that naval SNF waste packages can be represented by commercial SNF waste packages in the TSPA (SNL 2008a, Section 6.2.1.2, and

table 7-1). Therefore, naval SNF waste packages that will be emplaced are treated in the TSPA as commercial SNF waste packages.

Commercial cladding provides protection for commercial SNF from the surrounding environment as long as it is intact. Commercial SNF cladding will fail by mechanical action from seismic or igneous activity, and/or by long-term chemical degradation (Section 2.3.7.6). Commercial SNF cladding is modeled in the TSPA as being failed upon emplacement of the waste packages in the repository. Thus, no credit is taken for any barrier capability of the commercial SNF and DOE SNF (except for naval SNF) cladding. Note that naval SNF structure (including cladding) is credited as contributing to barrier capability.

The waste package pallet (Section 2.3.4.5) and the emplacement drift invert (Section 2.3.7.12) are two features of the EBS that are not ITWI (SNL 2008a, Table 7-1). The emplacement pallet rests on the invert and is a platform that supports the waste package. The pallet is constructed of Alloy 22 end support piers and Stainless Steel Type 316 connector tubes (Section 1.3.4.6). The emplacement drift invert is composed of two parts: a mild steel framework and ballast (or fill). The ballast material is crushed, graded, and compacted tuff derived from tunneling operations (BSC 2004a, Section 8.2).

The characterization of physical-chemical processes occurring in the EBS, and models that represent those processes, are described in Sections 2.3.4 to 2.3.7.

2.1.1.3 Lower Natural Barrier

The Lower Natural Barrier consists of two natural features: (1) the unsaturated zone below the repository horizon; and (2) the saturated zone beneath the repository and extending to the accessible environment. Both of these features are ITWI (Table 2.1-1). The characteristics of the Lower Natural Barrier include the following:

- Depth to groundwater below repository emplacement drifts ranges from about 200 m to nearly 400 m for the present-day climate (estimated to decrease on average by up to 120 m during future climate states)
- Long transport distance from the repository to the accessible environment
- Hydrogeologic and geochemical characteristics that limit radionuclide movement.

The Lower Natural Barrier below the repository horizon prevents or substantially reduces the rate of radionuclide movement to the accessible environment through a variety of natural processes and characteristics. In the unsaturated zone, these processes and characteristics include low percolation water flow rates, matrix diffusion, and sorption of radionuclides onto mineral surfaces. Perched water bodies are found primarily below the northern part of the repository block, where low-permeability, sparsely fractured zeolitic rock units predominate. Perched water zones may laterally divert a considerable amount of flow to major faults, which are conservatively treated as localized fast flow paths that may focus flow downward to the water table. Vitric zones are located in the southern half of the area below the repository. These vitric layers have relatively high matrix porosity and permeability, and matrix flow dominates. Transport in the vitric layers is slower than

through fractures in the zeolitic rock because matrix flow dominates. The relatively fast flow down faults below the northern half of the repository block result in faster mean transport times than in the southern half of the repository area.

The Lower Natural Barrier includes the volcanic rock (devitrified and zeolitic tuff) and alluvium in the saturated zone below the water table ([Section 2.3.9.2.2](#)). Saturated zone processes and characteristics that limit the movement of radionuclides include low groundwater flow rates, matrix diffusion, sorption, and filtration of colloids that could potentially transport radionuclides.

Certain aspects of the performance of the Lower Natural Barrier are radionuclide specific. Matrix diffusion and sorption within the Lower Natural Barrier cause a delay between release of the radionuclides from the EBS and arrival at the accessible environment. In addition, radioactive decay reduces the radioactivity of short-lived radionuclides to negligible levels.

The models that represent the physical-chemical processes occurring in the Lower Natural Barrier are described in [Sections 2.3.8](#) and [2.3.9](#).

2.1.2 Barrier Capability Description

[NUREG-1804, Section 2.2.1.1.3: AC 2]

This section describes the capability of the barriers identified in [Section 2.1.1](#), and presents an analysis supporting this description. The description includes information on the time period over which each barrier performs. Uncertainties associated with each barrier's capability are also described and appropriately addressed in the analysis.

The analysis supporting barrier capability is developed using the TSPA model, and is presented in [Sections 2.1.2.1.6](#), [2.1.2.2.6](#), and [2.1.2.3.6](#), for the Upper Natural Barrier, EBS, and Lower Natural Barrier, respectively. Information is presented for the time period up to 10,000 years after repository closure, and for the post-10,000-year period (i.e., after 10,000 years but through the period of geologic stability ending at 1,000,000 years). This information was developed from, and is consistent with, the TSPA calculations used for the compliance demonstrations described in [Section 2.4](#).

In [Section 2.4](#), TSPA calculations are developed for four scenario classes that describe the possible ways in which the repository system can evolve in the future. Section 2.2 describes the identification, classification, screening, and construction of these scenario classes from the FEPs considered at the Yucca Mountain site. These scenario classes are as follows: (1) the early failure scenario class, which accounts for all possible futures in which one or more early failures of drip shields or waste packages occur; (2) the igneous scenario class, which accounts for all possible futures in which one or more igneous events occur; (3) the seismic scenario class, which accounts for all possible futures in which seismic events occur; (4) and the nominal scenario class, which accounts for all possible futures in which no early failures, igneous, or seismic events occur.

Each scenario class is implemented in the TSPA model by one or more modeling cases ([Section 2.4.2.1.5](#)). The early failure scenario class is implemented in two modeling cases: (1) the waste package early failure modeling case; and (2) the drip shield early failure modeling case. Similarly, the seismic scenario class is implemented in two modeling cases: one accounting for

damage due to ground motion; and a second accounting for damage due to fault displacement. The igneous scenario class is also comprised of two modeling cases: one for igneous intrusion, and one for volcanic eruption. The nominal scenario class is implemented in one modeling case that represents those waste packages that fail because of nominal corrosion processes (e.g., general corrosion, stress corrosion cracking, or localized corrosion). This modeling case is referred to as the nominal modeling case.

For the purposes of quantifying barrier capability, two demonstration modeling cases are evaluated in [Sections 2.1.2.1.6](#), [2.1.2.2.6](#), and [2.1.2.3.6](#), for the Upper Natural Barrier, EBS, and Lower Natural Barrier, respectively. These demonstration modeling cases are (1) the combined nominal/early failure modeling case (the drip shield and waste package early failure modeling cases and the nominal modeling case are combined into one modeling case); and (2) the seismic ground motion modeling case (representative of the presence of disruptive events). The first demonstration modeling case is a representation of repository futures in which disruptive events do not occur, and drip shield and waste package early failures are included. This case was selected for the EBS barrier capability demonstration because it provides a projection of a reference capability. In addition, the case is useful in that it facilitates the examination of individual waste package breach modes. The seismic ground motion modeling case addresses postclosure performance of the EBS as a function of disruptive conditions caused by vibratory ground motion, as well as degradation by nominal corrosion processes. This modeling case was selected because it has been shown to be important to demonstration of compliance with the regulatory standards ([Section 2.4.2.2](#)). In particular, the seismic ground motion modeling case dominates the mean annual dose for the first 10,000 years after permanent closure, whereas for the post-10,000-year period, the igneous intrusion modeling case and seismic ground motion modeling case provide approximately equal contributions to the total mean annual dose to the RMEI for the last 300,000 years of the time period ([Section 2.4.2.2.1.1.2](#)).

In the following sections, barriers are discussed and evaluated in the sequence that water flowing through the repository system encounters them: the Upper Natural Barrier, the EBS, and the Lower Natural Barrier.

2.1.2.1 Upper Natural Barrier

The Upper Natural Barrier is composed of two natural features: (1) the topography and surficial soils; and (2) the unsaturated zone above the repository. Both of these features are ITWI ([Table 2.1-1](#)). The topography and surficial soils substantially reduce the amount of precipitation that can infiltrate into and percolate through the underlying unsaturated zone. In addition, free drainage characteristics and capillary retention behavior of the unsaturated zone prevent water from entering the emplacement drifts over about 30% to 70% of the repository during the 10,000-year and post-10,000-year periods after closure ([Section 2.1.2.1.6](#)). These features and characteristics contribute to the barrier's capability to prevent or substantially reduce the amount and rate of water seeping into the drifts, and therefore prevent or substantially reduce the rate of movement of water from the repository to the accessible environment.

The unsaturated zone above the repository is composed of three types of hydrogeologic units with distinct properties that play important roles in limiting the flow of water: the TCw, the PTn, and the TSw units ([Section 2.3.2.2](#) and [Table 2.3.2-2](#)). These hydrostratigraphic units are illustrated in

Figure 2.1-2. As discussed below, these hydrostratigraphic units have various processes and characteristics that influence the ability of the Upper Natural Barrier to prevent or substantially reduce the rate of movement of water into the repository. The hydrologic processes that affect the rate of water movement to the repository for both the topography and surficial soils feature and the unsaturated zone above the repository feature are tabulated in [Table 2.1-2](#). The basis for determining which of the processes listed in [Table 2.1-2](#) significantly affect the capability of the Upper Natural Barrier to provide its barrier function is presented in *Postclosure Nuclear Safety Design Bases* (SNL 2008a).

Several climatic and hydrologic processes are important contributors to the overall capability of the Upper Natural Barrier to prevent or substantially reduce the rate of water movement into the repository. In the evaluation of the important processes related to the capability of the Upper Natural Barrier, consideration is given to both the beneficial as well as the potentially deleterious processes that act on each of the features of the barrier. Beneficial processes generally result in (1) reducing the amount of water from precipitation that is available for infiltration (e.g., runoff and evapotranspiration); (2) preventing the movement of water; or (3) substantially reducing the rate of movement of water from the surface to the repository, therefore preventing the movement of water or substantially reducing the rate of movement of water that could transport radionuclides from the repository to the accessible environment. The presence of a potentially deleterious process, on the other hand, could result in an increase in the rate of movement of water. The evaluation of both beneficial and potentially deleterious processes that could affect the movement of water enhances understanding of the barrier capability.

A few examples illustrate both beneficial and potentially deleterious processes and their effect on the Upper Natural Barrier. Flow diversion around repository drifts is a beneficial attribute of the unsaturated zone flow system that decreases the amount of water that can seep into emplacement drifts. Climate change is a potentially deleterious process that could increase precipitation and, thus, could reduce the effectiveness of the Upper Natural Barrier by increasing the rate of water movement.

Topography and Surficial Soils—The following processes and characteristics of topography and surficial soils are important to the capability of the Upper Natural Barrier:

- **Climate Change**—Long-term climate change processes can significantly affect the amount of precipitation that falls in any year, as well as (1) the timing of when that precipitation is expected to occur; (2) the air temperature and other conditions that affect evapotranspiration; and (3) the amount and type of vegetation expected to be present in the surficial soils. As a result, the climate state affects the amount of water available and several of the key processes that are expected to affect the amount of water that can infiltrate into the surficial soils and percolate through the unsaturated zone (SNL 2008a, Section 6.2.2.1). The effects of climate change have been included in the assessment of net infiltration and the variation of the net infiltration for 10,000 years after closure ([Section 2.3.1](#)). After 10,000 years, the rate of percolation at the repository horizon is specified by proposed 10 CFR 63.342(c)(2) (70 FR 53313). The proposed rule requires that DOE represent the effects of climate change after 10,000 years by assigning percolation rates at the repository horizon that vary between 13 to 64 mm/yr.

- **Climate Modification Increases Recharge**—Future climate change may significantly affect temperature and the amount and timing of precipitation, which in turn affect net infiltration into surficial soils. The net effect of climate change in the 10,000 years after closure is to increase the amount of water that precipitates and can infiltrate and eventually percolate through the unsaturated zone. This increased recharge is calculated by the infiltration model that is presented in [Section 2.3.1](#). The climate effect on net infiltration has been directly included in the TSPA by developing infiltration scenarios for each of three climates for the first 10,000 years after closure: present-day, monsoon, and glacial-transition. After the first 10,000 years, and through the period of geologic stability, the effect of climate modification on percolation is incorporated into the performance assessment using the distribution of deep percolation rates specified in proposed 10 CFR 63.342(c)(2) (70 FR 53313). Percolation through the unsaturated zone is described in the site-scale unsaturated zone flow model in [Section 2.3.2](#).
- **Precipitation**—Precipitation processes are important in the evaluation of net infiltration into the bedrock below the surficial soils. The temporal and spatial distribution of precipitation affects the amount of water available to potentially run off, evaporate, transpire, or infiltrate. Given the arid climate at Yucca Mountain, precipitation events are intermittent and result in long periods of time when there is a net evapotranspiration from the surficial soils, interrupted by short-duration precipitation events that can result in some infiltration. Net infiltration during current and future climate states is calculated in the infiltration model that is presented in [Section 2.3.1](#). For the period after 10,000 years of disposal and through the period of geologic stability, the precipitation effect is implicitly incorporated into the TSPA by using the distribution of deep percolation rates specified in proposed 10 CFR 63.342(c)(2) (70 FR 53313).
- **Topography and Morphology**—The topography and morphology of the ground surface above the repository are such that a portion of the precipitation that falls at Yucca Mountain is unavailable for infiltration due to surface runoff. Generally, the steeper slopes have more runoff and less infiltration than the more gentle slopes. The effects of variability in topography on surface runoff have been included in the assessment of net infiltration presented in [Section 2.3.1](#).
- **Rock Properties of Host Rock and Other Units**—The hydrologic characteristics of the surficial soils and shallow bedrock above the repository significantly affect the amount of net infiltration following a precipitation event. The characteristics of the surficial soils and shallow bedrock also affect the soil retention and the time infiltrating water takes to pass below the root zone to become net infiltration (i.e., where it is not subject to further evapotranspiration processes). The hydrologic characteristics of the surficial soils at Yucca Mountain, including associated uncertainty (most notably, the permeability) are included in the assessment of net infiltration presented in [Section 2.3.1](#).
- **Infiltration and Recharge**—Infiltration is the net result of all surficial processes related to the availability of water. These processes include the effects of seasonal and climate variations, climate change, surface water runoff, evapotranspiration, and site topography (such as hillslopes and washes). The processes result in a significant reduction in the amount of water available to infiltrate into the unsaturated zone beneath the surficial soils.

Uncertainty in infiltration is a result of uncertainty in soil and rock characteristics, precipitation, and surface topography. The rate of net infiltration and its associated uncertainty are assessed for the first 10,000 years following repository closure using the net infiltration model presented in [Section 2.3.1](#). For the post-10,000-year period, the effects of infiltration are implicitly included in the TSPA by using the distribution of deep percolation rates specified in proposed 10 CFR 63.342(c)(2) (70 FR 53313). Recharge is the percolation flux through the unsaturated zone that reaches the water table ([Section 2.3.2](#)).

- **Surface Runoff and Evapotranspiration**—Surface runoff affects the redistribution of precipitation to areas away from the repository footprint, where it may infiltrate. Runoff is significant in moving precipitation water from where it intersects the surface to alluvial materials in washes, where flooding may allow storage and transpiration or infiltration below the root zone. Evapotranspiration potentially removes a significant fraction of water from soil by evaporation and transpiration via plant root water uptake, and results in a reduction in the amount of water available to infiltrate into the unsaturated zone beneath the surficial soils. Both of these processes are included in the infiltration model for the first 10,000 years following repository closure ([Section 2.3.1](#)).
- **Fractures**—Open fractures in the bedrock will tend to increase the bedrock effective hydraulic conductivity and result in an increased rate of net infiltration into the subsurface. However, a lower effective conductivity of the bedrock will tend to increase water storage in the surficial soil and increase the effectiveness of runoff and evapotranspiration, thereby reducing the rate of net infiltration into the subsurface. For example, fractures at or near the surface may be partially or completely filled, which could substantially reduce infiltration. The bedrock effective hydraulic conductivity is an important parameter, and an appropriate range of uncertainty has been included in the infiltration model ([Section 2.3.1](#)).
- **Fracture Flow in the Unsaturated Zone**—Fracture flow in the bedrock beneath the surficial soil affects the rate of water movement below the soil–bedrock contact, especially in areas of thin soils ([Section 2.3.1](#)). The rate of water flow in fractures at the soil–bedrock interface is influenced by such fracture properties as fracture frequency and permeability. As the magnitudes of these properties increase, the effective conductivity of the bedrock will also increase and result in an increased rate of net infiltration into the subsurface. Uncertainty in the effective hydraulic conductivity has been included in the infiltration model ([Section 2.3.1](#)).

Unsaturated Zone above the Repository—The following processes and characteristics of the unsaturated zone above the repository are important to the capability of the Upper Natural Barrier:

- **Climate Change**—Future climate change causes several responses in the unsaturated zone, including changes in percolation flux through the unsaturated zone, seepage into the repository emplacement drifts, water table rise, and recharge to the saturated zone. Precipitation and net infiltration into the unsaturated zone tend to increase with future climate change, causing an increase in these responses. The effects of future climate change on groundwater flow in the unsaturated zone above the repository are

incorporated into the TSPA using time-dependent infiltration rates as boundary conditions for the site-scale unsaturated zone flow model (Section 2.3.2) for the first 10,000 years, and for the post 10,000-year period using the distribution of deep percolation rates specified in proposed 10 CFR 63.342(c)(2) (70 FR 53313). The response of seepage to climate change is discussed in Section 2.3.3.

- **Climate Modification Increases Recharge**—The percolation flux in the host rock above the emplacement drifts is significantly affected by the change in recharge and infiltration associated with the projected future climate changes in the 10,000 years, after closure. The increased infiltration and percolation significantly increase both the amount of water potentially available to seep into the drifts and the amount of water that is projected to seep. The effects of current and future climate states on the amount of water percolating through the unsaturated zone are included in the site-scale unsaturated zone flow model that is presented in Section 2.3.2. After 10,000 years and through the period of geologic stability, the effect of climate modification on percolation and recharge is incorporated into the site-scale unsaturated zone flow model using the distribution of deep percolation rates specified in proposed 10 CFR 63.342(c)(2) (70 FR 53313).
- **Stratigraphy**—The stratigraphic sequence of unsaturated strata defines the hydrologic characteristics through which percolating water flows between the surface and the repository horizon. This sequence of both welded and nonwelded tuffs affects the transient propagation of infiltration pulses and tends to spatially redistribute the percolation rates. Stratigraphy has been directly included in the site-scale unsaturated zone flow model (Section 2.3.2).
- **Rock Properties of Host Rock and Other Units**—Rock properties, such as fracture capillarity and permeability, significantly affect the distribution of percolation flux in the unsaturated zone and the amount of flow diversion for a given percolation flux around emplacement drifts. Layer-specific rock properties and fault properties represent large-scale heterogeneity and have a significant effect on site-scale flow processes. Small-scale heterogeneity within hydrogeologic units has much less of an effect on site-scale flow processes. In addition, the degree of flow focusing is related to the local heterogeneity of the permeability distribution of the host rock. Properties of rock units and associated uncertainties are included in the unsaturated zone flow models presented in Sections 2.3.2 and 2.3.3.
- **Fractures**—Fractures are the main conduits for flow in most of the hydrogeologic units in the unsaturated zone above the repository. Fractures account for 87% to 98% of the total water flux at the repository horizon within the repository footprint (Section 2.3.2.4.1.2.4.6 and Table 2.3.2-7). Fractures and their properties are included in the unsaturated zone flow models presented in Section 2.3.2.
- **Fracture Flow in the Unsaturated Zone**—Above the repository, the net infiltration into the unsaturated zone flows principally by gravity through a network of fractures in the TCw, PTn, and TSw units. Fracture flow is the dominant flow mechanism in the welded units, which have a high density of interconnected fractures. In the nonwelded PTn unit, with relatively high matrix permeability and porosity and relatively low fracture density,

the predominantly fracture flow in the overlying TCw is converted to predominantly matrix flow. In the TSw unit below the PTn unit, fracture flow again dominates over matrix flow. As noted above, fractures account for 87% or more of total water flux at the repository horizon within the repository footprint ([Section 2.3.2.4.1.2.4.6](#) and [Table 2.3.2-7](#)).

- **Unsaturated Groundwater Flow in the Geosphere**—Unsaturated groundwater flow defines the distribution of percolation flux in the unsaturated zone as a function of time, and is the primary mechanism for radionuclide transport below the repository. Although the flow rate in the unsaturated zone defines the amount of fracture flow, the fracture characteristics are also significant in determining the rate of radionuclide movement in the unsaturated zone ([Section 2.3.8](#)).
- **Flow Diversion around Repository Drifts**—Above the emplacement drifts, a portion of the percolating unsaturated flow is diverted around the repository drifts. This diversion prevents or substantially reduces the rate of movement of liquid water to the emplacement drifts. The amount of water flow diversion is a function of (1) the percolation in the unsaturated zone above the emplacement drifts; (2) hydrologic properties around the emplacement drifts, notably the permeability and capillarity of the fractured rock mass; and (3) the geometry of the emplacement drift and drift-wall properties. The assessment of the distribution of seepage into the emplacement drifts, including the associated uncertainties, is presented in [Section 2.3.3](#).
- **Water Influx at the Repository**—Water influx into repository drifts is related to the flow diversion processes described above. Water that is not diverted around the emplacement drifts will flow into the emplacement drifts as seepage. Assessment of the distribution of seepage into the emplacement drifts, and the associated uncertainties, is presented in [Section 2.3.3](#).

The process models relevant to the Upper Natural Barrier and their abstraction for use in the TSPA are described in more detail in [Sections 2.3.1](#) to [2.3.3](#). The process models and their abstractions are founded on physical principles and extensive tests and observations from Yucca Mountain and appropriate analogue sites. The capability of the Upper Natural Barrier is analyzed using models that simulate the flow of water (i.e., infiltration, percolation, and seepage) through the topography and surficial soils and the unsaturated zone above the repository. These models consider 12 infiltration scenarios, resulting in sets of four maps representing the 10th, 30th, 50th, and 90th percentile infiltration rates for each of the three climate states (i.e., present-day, monsoon, and glacial-transition) estimated for the Yucca Mountain site, and also for the post-10,000-year representation of climate change specified in proposed 10 CFR 63.342(c)(2) (70 FR 153313) as a log-uniform distribution for deep percolation rates. These infiltration maps, used as upper boundary conditions for the unsaturated zone flow model, represent uncertainty in infiltration. For the post-10,000-year period, the site-scale unsaturated zone flow model uses a surface water flux boundary condition developed to provide the average percolation flux distribution at the repository footprint that is specified in proposed 10 CFR 63.342(c)(2) (70 FR 53313) to produce an additional four steady-state percolation flow fields. These flow fields incorporate a range of variability and uncertainty based on the calibrated unsaturated zone flow models for the site. For a given climate state, the relative importance of a selected infiltration map and corresponding flow field is

represented by a weighting factor. The weighting factors are determined through comparison with measured data from the unsaturated zone (e.g., distributions of temperature and chloride) using a generalized likelihood uncertainty estimation method. Weighting factors of 61.9%, 15.7%, 16.5%, and 6.0% were determined for the 10th, 30th, 50th, and 90th percentile infiltration maps, respectively (Section 2.3.2.4.1.2.4.5.5). These same weighting factors are used for the monsoon, glacial-transition climates, and the post-10,000-year period. As noted earlier, the post-10,000-year deep percolation representation of climate change is also implemented as a distribution of deep percolation rates in accordance with proposed 10 CFR 63.342(c)(2) (70 FR 53313). The post-10,000-year climate change representation extends the simulations from 10,000 years to 1,000,000 years. This post-10,000-year representation of climate change contains four uncertainty cases (31st, 70th, 86th, and 97th percentile cases (Section 2.3.2.4)), based on the prescribed percolation flux distribution through the repository footprint in accordance with proposed 10 CFR 63.342(c)(2) (70 FR 53313). The percentiles are the midpoints of the probability ranges as a cumulative value; e.g., the 31st percentile is the midpoint of 0.619, and the 70th percentile is 0.619 plus one-half of 0.157, and so on (Section 2.3.2.4.1.2.4.5.5).

2.1.2.1.1 Capability of the Topography and Surficial Soils to Prevent or Substantially Reduce Infiltration

Yucca Mountain is in an arid region where precipitation and humidity are low, thus promoting high potential evaporation rates. The topography and surficial soils feature significantly reduces the movement of water into the unsaturated zone. Runoff, evaporation, and plant transpiration combine to divert water and permit only a small fraction of the expected low precipitation at the site to infiltrate into the unsaturated zone. Abstraction models that include these processes are presented in Section 2.3.1.

The capability of the Upper Natural Barrier to prevent or substantially reduce infiltration into Yucca Mountain is due to the geographic and geologic setting of the site. Yucca Mountain is located in the Great Basin of the arid desert southwest. The Sierra Nevada Mountains serve as a physiographic barrier to the eastward migration of moisture from weather systems originating in the Pacific Ocean. As a result, average precipitation in the Yucca Mountain area is low throughout the year. The characteristics of topography and surficial soils and the processes acting on them—including the effects of evapotranspiration and runoff—combine to result in infiltration into Yucca Mountain that is significantly less than the already low incident precipitation. During the warmer months, precipitation occurs intermittently, usually as isolated storms in the spring or late summer. Infiltration during these events is limited because of the high runoff associated with the topography and because of the high evaporation and transpiration rates associated with warm temperatures. Most of the small amount of infiltration that does occur is associated with low-intensity winter storms when lower evaporation and transpiration rates and the slow melting of snow create conditions favoring limited infiltration. The arid climate and the topography and surficial soils portion of the Upper Natural Barrier also contribute to favorable site characteristics, such as the low rates of water flow in the unsaturated zone and the great depth of the water table (Sections 2.3.1, 2.3.2, and 2.3.9).

Determination of net infiltration rates take into account processes important to infiltration, including run-on and runoff, evaporation and transpiration, soil and bedrock hydraulic properties and their spatial distribution, as well as topographic and climatic influences. The effect of climate

variability (i.e., variations in precipitation, temperature, and humidity) on infiltration rates is also incorporated into the model for both present-day and potential future climates. The infiltration model is described in [Section 2.3.1](#).

The precipitation and infiltration that influence potential seepage rates into the emplacement drifts are assessed for three climate states representing the climate conditions forecast to exist in the 10,000 years after closure ([Section 2.3.1.2.3.1](#)):

- Present-day climate state, representing conditions forecast to prevail for approximately the next 600 years
- Monsoon climate state, representing conditions forecast to prevail for approximately 1,400 years after the present-day climate conditions (i.e., 600 to 2,000 years)
- Glacial-transition climate state, representing conditions that are forecast to prevail over 8,000 years following the monsoon climate conditions (i.e., 2,000 to 10,000 years).

In proposed 10 CFR 63.342(c)(2) (70 FR 53313), the NRC has specified that long-term climate, after 10,000 years following disposal, be represented by a probabilistic distribution for a constant-in-time, but uncertain long-term average climate for Yucca Mountain.

For each climate state, four infiltration scenarios are evaluated: the 10th, 30th, 50th and 90th percentile scenarios. On average, the 10th percentile infiltration scenario for each climate state during the post-10,000-year period represents relatively dry conditions, whereas the 30th, 50th, and 90th percentile scenarios generally represent increasingly wetter conditions ([Tables 2.3.1-2](#), [2.3.1-3](#), and [2.3.1-4](#)). The climate analysis and infiltration model for Yucca Mountain demonstrate that limited infiltration of water into Yucca Mountain is expected for present-day and future climates. Precipitation falling on Yucca Mountain is low, even for the glacial-transition climates forecast for most of the first 10,000 years after closure. For example, annual precipitation rates for the glacial-transition climate at the 50th percentile are expected to be 223 mm/yr to 287 mm/yr for the 90th percentile ([Table 2.3.1-4](#)). About 87% or more of the water falling on Yucca Mountain as precipitation during the glacial-transition climate state is expected to be diverted by runoff or returned to the atmosphere by evapotranspiration, whereas about 90% is diverted or returned to the atmosphere during present day and monsoon climate states ([Section 2.3.1.3.3.1.2](#)).

Estimated average present-day net infiltration ranges from less than 3% of precipitation for the drier 10th percentile climate scenario to about 13% of precipitation for the 90th percentile climate scenario, with a median 50th percentile infiltration of about 7% of the average present-day precipitation ([Table 2.3.1-2](#)). The average net infiltration rates for the 10th to 90th percentile present-day climate scenarios vary from about 4 to 27 mm/yr, with a 50th percentile of about 13 mm/yr ([Table 2.3.1-2](#)). For the monsoon climate scenarios, average net infiltration rate estimates for the 10th to 90th percentile climate scenarios range from about 3% to 17% of precipitation, with a range from about 6 to 53 mm/yr ([Table 2.3.1-3](#)). For the glacial-transition climate scenarios, the average net infiltration rate estimates for the 10th to 90th percentile climate scenarios range from about 5% to 16% of precipitation, with a range from about 13 to 47 mm/yr ([Table 2.3.1-4](#), [Section 2.3.1](#)).

2.1.2.1.2 Capability of the Unsaturated Zone above the Repository to Prevent or Substantially Reduce Seepage

The unsaturated zone above the repository horizon prevents or substantially reduces the movement of water through the unsaturated zone and into the emplacement drifts of the repository. There are two primary large-scale processes contributing to this capability:

- Damping of episodic pulses of precipitation and infiltration
- Capillary forces limiting seepage into the emplacement drift.

Analyses of the effectiveness of the unsaturated zone above the repository horizon to prevent or substantially reduce water movement are described in [Sections 2.3.2](#) and [2.3.3](#). The site-scale unsaturated zone flow model is based on field and laboratory testing, and is calibrated to match data and observations from pneumatic testing, water content (saturation) data, hydraulic-potential data, and geochemical and isotopic data.

A cross section of the unsaturated zone down to the repository horizon is shown in [Figure 2.1-3](#). This figure shows the major hydrostratigraphic units, including subunits broken down by distinct mineralogic characteristics (e.g., crystal-rich and crystal-poor members). The location of this cross section is shown in [Figure 2.1-4](#). From the surface to the repository horizon, the unsaturated zone includes the TCw unit, the PTn unit (indicated as nonwelded bedded tuffs in the figure), and the upper part of the TSw unit. The TCw and TSw units are composed of moderately to densely welded, highly fractured tuff deposits. The high density of interconnected fractures and the low matrix permeability of the welded tuffs result in a majority of the water flow occurring in the fractures. Episodic infiltration pulses resulting from precipitation at the surface, less the effects of runoff, evaporation, and transpiration, are expected to move through the fractured TCw unit into the underlying PTn unit with little additional attenuation ([Section 2.3.2](#)).

The high density of interconnected fractures and low permeability of the matrix in the TCw unit ([Section 2.3.2.2.1.1](#)) are conceptualized as giving rise to significant water flow in fractures and limited matrix imbibition (water flow from fractures to the matrix) within the TCw. Thus, episodic infiltration pulses are expected to move rapidly through fracture networks in this unit, with little attenuation by the matrix within the TCw. The relatively high matrix permeability and porosities and low fracture densities in the underlying PTn unit ([Section 2.3.2.2.1.2](#)) convert the predominant fracture flow in the TCw to dominant matrix flow within the PTn. The dominance of matrix flow in the PTn, and the relatively large storage capacity of the matrix, resulting from its high porosity and typically low saturation, give the PTn significant capacity to attenuate infiltration pulses. Faults (or geologic structures) may cut through the entire PTn unit at some locations, leading to fast flow paths if the local PTn tuff matrix is not able to convert all of the fault flow into matrix flow. In addition, some lateral diversion of water occurs in the PTn unit owing to the capillary barrier effects and the slope of the stratigraphic units ([Section 2.3.2.2.1.2](#)). The PTn unit as a whole exhibits very different hydrogeologic properties from the TCw and TSw units that bound it above and below.

The TSw unit has lower matrix porosity and higher fracture frequency than the overlying nonwelded tuff (PTn). The low matrix porosity in the TSw causes increased saturation above the interface and results in fracture flow into the TSw unit. The matrix hydraulic conductivity of the

welded tuff is less than the estimated average water flux. Therefore, unsaturated flow is primarily through the fractures within the TSw unit (Section 2.3.2).

A primary effect of the unsaturated zone above the repository horizon is the damping of the pulses of flow down through the unsaturated zone within the PTn. Net infiltration at the surface of Yucca Mountain is variable in space and time. Significant pulses of infiltration occur only once every few years, and infiltration varies spatially depending on the degree of focusing by surficial processes. Pulses of moisture may also percolate rapidly through the fractured tuffs of the TCw unit, as indicated by the potential bomb-pulse ^{36}Cl signatures in the TSw unit. However, geologic and geochemical evidence indicates that percolation rates are comparatively homogeneous (Section 2.3.2.2.3). The change from fracture-dominated to matrix-dominated flow at the contact of the TCw and the PTn units significantly attenuates the episodic infiltration flux, effectively smoothing the temporal variability in percolation flux rates. Evenly distributed chloride mass-balance data and estimates of mineral accumulation rates in fractures and lithophysae indicate that percolation rates are relatively homogeneous, except for some focused flow in fault zones outside of the repository footprint (Section 2.3.2.4.2.1.2).

As noted at the end of Section 2.1.2.1, 16 unsaturated zone flow fields were generated for four infiltration scenarios (10th, 30th, 50th, and 90th-percentile scenarios) for each of three climate states (present-day, monsoon, glacial-transition) and for the post-10,000-year period. Analysis of these flow fields indicates that percolation fluxes at the repository horizon are very different from surface infiltration patterns, mainly in the north of the model domain (Section 2.3.2.5.2). However, the percolation flux values within the repository footprint are similar to surface infiltration values and only differ by a few percent. Under a steady-state flow condition, percolation flux and its distribution along any horizon of the model domain would be the same or very similar if there were no lateral flow. The major differences in percolation flux at the repository level (Figure 2.3.2-52) from the surface infiltration maps (Figure 2.3.2-38) are (1) flow diverted through faults in the very northern part of the model domain; and (2) flow diverted into or near faults located in the rest of the model domain. However, it should be emphasized that within the repository footprint, fault flow is about 1% of the total at the top of the PTn and at the repository horizon, indicating less significant lateral flow in the PTn for this smaller area (Section 2.3.2.4.1.2.4.6).

The flow field analysis also indicates that fracture flow is dominant in the TCw along the top of the PTn unit and the repository horizon (Section 2.3.2.2.1.2). At the repository level, fracture flow consists of about 60% to 80% of the total percolation flux over the entire model layer, and is generally greater than 90% within the repository footprint (Table 2.3.2-7). On the other hand, the flow of water in larger fault zones increases with depth. Over the entire model layer, fault flow at the TCw–PTn interface is about 1% to 2% of the total flux over the entire model domain, and increases to 12% to 32% of the total flux over the entire model domain at the repository horizon (Section 2.3.2.4.2.1.1; Table 2.3.2-7).

The rate and distribution of seepage control the amount of water available to contact the EBS (Section 2.3.3.2.1.2). In the unsaturated zone, seepage into the emplacement drifts is less than the percolation flux because capillary forces limit the movement of water into the drift openings. Water is retained in the small pores and tight fractures of the low-porosity welded tuff, and a substantial fraction of the flow moves around the drift opening and drains through the rock pillars between the drifts. The effectiveness of capillary forces in limiting water movement into drifts and moving flow

around them depends on the characteristics of the rock matrix and fractures, and on the connectivity and permeability of the fracture network. In addition, seepage rates are affected by the characteristics of the drift openings (e.g., asperities on the drift walls and flow in fractures that may have modified hydrologic properties in the disturbed zone created by drift excavation or heat from emplacement waste). For a period of time, the decay heat of the emplaced waste is great enough to heat the rock near the emplacement drifts above boiling. As long as the temperature is above the boiling point of water at the drift wall, the water vapor will be driven away from the emplacement drift wall surfaces. This thermal effect, combined with the capillary effects, further prevents or substantially reduces seepage into the emplacement drifts.

The model that simulates seepage into the emplacement drifts under both the ambient and thermally perturbed conditions is described in [Section 2.3.3](#). The drift seepage model considers the matrix and fracture hydrologic properties of the TSw unit and the design of the emplacement drifts. The drift seepage model and analysis supporting the development of the abstraction of drift seepage model described in [Section 2.3.3](#) uses a continuum fracture model, and samples the uncertain stochastic distributions for the fracture permeability and capillary strength parameters to estimate the probability and amount of seepage. For the modeled future glacial-transition climate, on average, only about 30% of the drip shield locations are expected to experience any seepage in the 10,000 years after closure.

The following summary illustrates the barrier capability in the fractured rock at and above the repository horizon. The results of the probabilistic seepage analysis for intact drifts are described in terms of the mean seepage rate, the mean seepage percentage (i.e., ratio of mean seepage rate to mean percolation flux), and the seepage fraction (i.e., fraction of waste packages in a percolation region experiencing seepage), during the present-day, the monsoon, and the glacial transition climate states ([Section 2.3.3.4.2](#)). The four unsaturated zone flow fields corresponding to the 10th, 30th, 50th and 90th percentile infiltration scenarios arrive at four different sets of seepage results. For the flow field based on the 10th percentile infiltration scenario—the most likely flow field with a relative probability of approximately 62%—seepage is expected to occur at about 8% of all waste packages during the present-day climate, rising to about 13% of waste packages during the monsoon climate, and to about 17% during the glacial-transition climate ([Section 2.3.3.4.2](#); [Figure 2.3.3-49](#)). On average over all waste packages, the amount of seeping water is 1.2, 4.6, and 14.4 kg/yr per waste package for the present-day, monsoon, and glacial-transition climate states, respectively ([Section 2.3.3.4.2](#); [Figure 2.3.3-47](#)). This translates to mean seepage percentages of 1.1%, 2.2%, and 4.7% ([Section 2.3.3.4.2](#); [Figure 2.3.3-48](#)). In other words, during the present-day climate, on average about 99% of the percolation flux would be diverted around intact drifts in the TtpII unit ([Section 2.3.3.4.2](#)). For the wetter climate stages of the monsoon and the glacial-transition period, the mean percentage of diverted flux would be smaller, but still at about 98% and 95%, respectively ([Section 2.3.3.4.2](#)).

The higher infiltration scenarios would result in more seepage, as described in [Section 2.3.3.4.2](#) and shown in [Figures 2.3.3-47](#) through [2.3.3-49](#). For the 30th percentile infiltration scenario, the seepage fraction varies from 16.7% for the present-day climate, to 22.8% during the monsoon period, to 29.5% during the glacial-transition climate. The respective mean seepage percentages are 3.0%, 4.9%, and 8.0%. Most seepage is seen for the 90th percentile infiltration scenario, with the seepage fraction as high as 52.6% during the monsoon climate. The mean seepage percentage during this climate state is 19.5%. Thus, even for the least likely of the four unsaturated zone flow

fields, with a relative probability of 6% and comparably strong downward percolation, the diversion capacity of the unsaturated rock is about 81% overall. However, more than half of all waste packages are expected to experience some amount of seepage in this case (Section 2.3.3.4.2). Overall, the observed seepage percentages demonstrate the important barrier capability of the unsaturated flow processes in the fractured rock at and above the repository horizon.

2.1.2.1.3 Time Period over Which the Upper Natural Barrier Functions

The topography and surficial soils and the unsaturated zone above the repository horizon are durable features of the geologic environment at Yucca Mountain. The characteristics and properties of these features are not expected to change in the 10,000 years after closure. Geomorphologic studies of the landforms at Yucca Mountain indicate that the basic configuration of topography, soil depth and characteristics, and stream channel locations has been consistent for at least hundreds of thousands of years (YMP 1993, Section 3.4). Minor changes in the precise location of stream channels may occur, and erosion and sediment accumulation will continue at low rates, but the changes to the parameters describing these features (e.g., soil depth and slope aspect) are expected to be less than the variability explicitly accounted for in the infiltration model.

With the exception of the very minor effects caused by the construction of the repository, the basic geologic features of the site are not expected to change in any significant way in the 10,000 years after closure. However, climate is expected to vary in the future. This variability has been incorporated into performance models by forecasting climate states—the present-day, monsoon, and glacial-transition climates—and by using the regulatory specification for deep percolation changes after 10,000 years.

Wetter, cooler conditions are expected to result in changes to vegetation that could affect transpiration rates, thereby affecting net infiltration rates. The infiltration model includes parameter adjustments to address increases in plant height, root zone depth, and vegetation cover and changes in vegetation type (Section 2.3.1.3.2).

The effectiveness of the Upper Natural Barrier is expected to change in the 10,000 years after closure and during the post-10,000-year period because of changes in the infiltration flux. Climate changes that result in increased net infiltration are propagated through the unsaturated zone, which result in increased percolation at the repository horizon. This type of change in barrier effectiveness is taken into account in the unsaturated zone flow and seepage models (Sections 2.3.2 and 2.3.3).

The long-term effects of heat generated by the emplaced waste on the properties of the Upper Natural Barrier, including changes to rock hydrologic properties due to mineral dissolution or precipitation and mechanical changes in the rock, have been investigated. The analyses indicate that the magnitudes of changes attributable to coupled thermal-hydrologic-chemical-mechanical processes do not affect the barrier capability (Section 2.3.3.3.4). On the basis of these analyses, changes in drift-scale hydrologic properties induced by thermal effects are concluded to have no significant impact on seepage (SNL 2008b, Section 6.2, excluded FEPs 2.1.09.12.0A, Rind (chemically altered zone) forms in the near-field; 2.2.01.02.0A, Thermally-induced stress changes in the near-field; and 2.2.10.04.0A, Thermo-mechanical stresses alter characteristics of fractures near repository) (Section 2.3.3.3.4). Although excluded from the TSPA, the permeability of rock in the mechanically disturbed zone around the emplacement drifts is expected to be higher than that

of the undisturbed rock, and this is effectively accounted for in the test analyses used to support the development and validation of the seepage calibration model presented in [Section 2.3.3](#).

Drift collapse can lead to seepage behavior that is much different from that in intact drifts ([Section 2.3.3.4](#)). The larger size and possibly different shape of a collapsed drift tends to reduce the potential for flow diversion. In addition, the capillary barrier behavior at the drift wall can be affected by the rubble rock blocks filling the opening, as the capillary strength inside the opening is different from the zero-capillary-strength condition in the initially open drift ([Section 2.3.3.2.1.4](#)). In the case of full drift collapse in the lithophysal unit, when the original openings have filled with rubble rock material, capillary effects are still expected to cause some flow diversion at the interface between the solid rock and the rubble-filled drift. In the nonlithophysal units, partial drift collapse can result in the loss of capillary diversion. These effects are included in the drift seepage model ([Section 2.3.3.2.3.4.2](#)).

2.1.2.1.4 Uncertainties Associated with Upper Natural Barrier Capability

Uncertainties associated with the capability of the Upper Natural Barrier are derived both from the models used to simulate important processes and from uncertainty and variability in the data and parameters used to represent the characteristics of the natural system. The uncertainties associated with data and models that are important to barrier capability are described in [Sections 2.3.1.2](#), [2.3.1.3](#), [2.3.2.3](#), [2.3.2.4](#), [2.3.3.2](#), and [2.3.3.3](#).

Uncertainty in the climate analysis is considered in the development of the range of possible future climate states used in the barrier capability analysis ([Section 2.3.1.2.3](#)). These uncertainties are principally related to (1) uncertainty in the Owens Lake paleoclimate record and its extrapolation to mean annual precipitation and mean annual temperature; (2) uncertainty in the average sediment accumulation rate used to project the duration of the present-day and monsoon climate states; (3) decade- to century-scale variability in the climate proxy records; and (4) the selection of analogue meteorological stations to represent future climate conditions.

Uncertainty is also accounted for in the numerical model for net infiltration ([Sections 2.3.1.3.2](#) and [2.3.1.3.3](#)). The boundary conditions for the model include uncertainty in the annual precipitation estimates. In addition, the model includes uncertainty in infiltration, evaporation, and transpiration processes evaluated in the model. The model includes uncertainty distributions for parameters describing precipitation, evapotranspiration, soil depth, potential evapotranspiration, bedrock saturated hydraulic conductivity, soil water holding capacity, and bare-soil evaporation ([Tables 2.3.1-22](#), [2.3.1-23](#), and [2.3.1-24](#)).

The performance of the Upper Natural Barrier is also subject to uncertainty that is a function of (1) the applicability of the conceptual and numerical models used to describe unsaturated zone flow; and (2) the degree of knowledge of the characteristics of the Yucca Mountain site. To accommodate both variability and uncertainty in the description of the site conditions, the unsaturated zone flow model captures the range of variation and resulting uncertainty in surface infiltration and calibrated properties through the use of four infiltration scenarios for the present-day, monsoon, glacial-transition climates, and the post-10,000-year period and four sets of calibrated parameters for the 10th, 30th, 50th, and 90th percentile infiltration maps for each of the climate infiltration scenarios, and 31st, 70th, 86th, and 97th percentile infiltration maps

(Section 2.3.2.4) for the post-10,000-year period. These uncertainties are propagated through the TSPA by use of the 16 unsaturated zone flow fields (Section 2.3.2.1). The model projections for flow have been calibrated and compared to hydrogeologic data to ensure that results are consistent with the characteristics of the unsaturated zone flow system in the vicinity of Yucca Mountain. Uncertainties in the percolation flux due to flow focusing are addressed in site-scale unsaturated zone flow through the parameters of the active fracture model, and in drift seepage through both the parameters for the active fracture model and a flow focusing factor (Section 2.3.3.3.3.1). These parameters are adjusted to provide consistency with measurements that implicitly take flow focusing into account (Sections 2.3.3.2.3.5 and 2.3.3.2.3.6.3).

The effectiveness of the capillary diversion around the emplacement drifts is dependent on the percolation flux, the spatial variability of the hydrologic properties of the lithophysal and nonlithophysal repository host rock units, the initial geometry of the emplacement drift opening and subsequent geometry resulting from drift collapse, the properties of the emplacement drift wall, and the in-drift conditions determining the evaporation potential. In addition, a vaporization effect develops when the emplacement drifts are ventilated or are heated to above the boiling temperature of water. The key hydrologic properties are the capillary strength parameter and the fracture permeability (Section 2.3.3.2.3). Distributions representing these input uncertainties are developed as part of the seepage abstraction, and are implemented by a probabilistic treatment of seepage in the TSPA. The capillary strength parameter is uncertain due to uncertainty in the seepage-rate data and uncertainty in the seepage calibration model. The capillary strength parameter is also variable in space because different locations in the repository have different rock property characteristics and different capillary barrier behavior. Uncertainties in permeability values stem from uncertainties in the measured airflow rate and pressure data from the air injection testing and the analytical method used to derive the permeability values from these data. There are several sources of uncertainty related to the percolation flux estimates provided by the site-scale unsaturated zone flow model, including uncertainty related to the future climates and infiltration.

2.1.2.1.5 Impact of Disruptive Events on the Upper Natural Barrier

The Upper Natural Barrier may be affected by disruptive events. For seismic activity, it is expected that the general configuration of the geologic units will be unchanged. However, at the interface between the Upper Natural Barrier and the EBS, there may be changes in the shape of the drift opening caused by drift collapse. Drift collapse can lead to seepage behavior that is much different from that in intact drifts (Section 2.3.3.2.1.4). The larger size and possibly different shape of a collapsed drift may impact flow diversion. In addition, the capillary barrier behavior at the drift wall can be affected by the rubble rock blocks filling the opening, as the capillary strength inside the opening is different from the zero-capillary-strength condition in the initially open drift (Section 2.3.3.2.1.4).

In the case of full drift collapse in the lithophysal rock units, when the original openings have filled with rubble rock material, capillary effects are still expected to cause some flow diversion at the interface between the solid rock and the rubble-filled drift. Analyses indicate that in the lithophysal rock units (comprising more than 85% of the repository horizon (Section 2.3.3.2.3.2)), peak ground velocities (PGV) of about 2 m/s or greater are required for full drift collapse, but that multiple lower velocity events are assumed to result in accumulation of rockfall rubble and have the same net effect

(Section 2.3.3.2.4.2.2). Velocities on the order of 2 m/s are only expected for events with annual exceedance probabilities of about one chance in 1,000,000 (Section 2.3.4.3.2.4).

Model results for rubble accumulation in the lithophysal zone indicate that individual seismic events with PGV greater than about 2 m/s would completely fill the drifts with rockfall, while individual seismic events with PGV between 1 m/s and 2 m/s would fill a substantial fraction of the free space in a drift, covering the sides of the drip shield to approximately the height of the drip shield, and possibly covering the top of the drip shield (Section 2.3.4.4.8.3.1 and SNL 2008a, Section 6.2.2.1.5). The rockfall volume in the nonlithophysal zones is significantly less than in the lithophysal zones at the same PGV level (Section 2.3.4.4.8.3.2). Drift collapse and its effect on seepage is included in the quantification of the capability of the Upper Natural Barrier presented in Section 2.1.2.1.6. Such changes in barrier performance are considered in the model abstractions used in the TSPA (Section 2.3.4) and in the assessment of barrier capability (Section 2.1.2.1.6). Other potential effects of seismic events on the hydrology and hydrogeologic characteristics (e.g., porosity and permeability) of the features within the unsaturated zone above the repository have insignificant effects on the performance of the repository, and are excluded from assessments of the Upper Natural Barrier capability (SNL 2008b, Section 6.2); see Table 2.1-2 for pertinent excluded seismic FEPs, for example, FEP 1.2.10.01.0A, Hydrologic response to seismic activity, and FEP 2.2.06.01.0A, Seismic activity changes porosity and permeability of rock.

If an igneous intrusion into the repository occurs, the affected drifts are assumed to fill with magma; however, the general configuration of the Upper Natural Barrier will not change. As presented in Section 2.3.11.3, seepage into the emplacement drifts is expected to change as a result of igneous intrusion and is treated in the TSPA as equivalent to the percolation flux in the vicinity of the igneous intrusion. Other potential effects of igneous intrusion on the hydrology and rock properties do not significantly affect the performance of the repository, and are excluded from assessments of the Upper Natural Barrier capability (SNL 2008b, Section 6.2); see Table 2.1-2 for pertinent excluded igneous FEPs, such as FEP 1.2.04.02.0A, Igneous activity changes rock properties.

2.1.2.1.6 Quantification of the Upper Natural Barrier Capability

The topography and surficial soils and the unsaturated zone above the repository horizon combine to substantially reduce the movement of water from the surface of Yucca Mountain into the emplacement drifts. The combination of reduced infiltration into Yucca Mountain, in addition to limited and attenuated percolation down to the repository, and capillary effects in the host rock, results in a seepage flux into the repository that is substantially reduced from the precipitation flux at the surface. The integrated effects of precipitation, infiltration, percolation, and seepage are included in the models used to evaluate the rate of water movement through the Upper Natural Barrier.

The effectiveness of the upper natural barrier is described using the following relative metrics:

1. Net infiltration into the bedrock as a percentage of precipitation rate for the 10,000-year period
2. Spatially averaged drift seepage rate as a percentage of percolation flux for the 10,000-year and post 10,000-year periods
3. Seepage fraction for each percolation subregion (defined in [Section 2.4.1.2.1](#) and [Figure 2.4-3](#)) for the 10,000-year and post-10,000-year periods.

The first barrier capability metric provides a quantitative demonstration of the effectiveness of the topography and surficial soils. The second and third metrics focus on the effectiveness of the unsaturated zone tuff units above (and inclusive of) the repository horizon. The quantification of these relative metrics is presented for each of the three climate states of the 10,000-year period, namely (1) present-day (from 0 to 600 years); (2) monsoon (from 600 to 2,000 years); and (3) glacial-transition (from 2,000 to 10,000 years). For the post-10,000-year period, net infiltration and precipitation are not used because the percolation rates are prescribed in proposed 10 CFR 63.342(c)(2) (70 FR 53313).

As discussed in [Section 2.1.2](#), two demonstration modeling cases—nominal/early failure and seismic ground motion—are evaluated to demonstrate barrier capability. In the case of the first metric, net infiltration is the same for the nominal/early failure and seismic ground motion modeling cases, because the barrier function of surficial soils is independent of the repository conditions. In contrast, drift seepage (i.e., volume of liquid water flowing into a drift per unit time per waste package) and seepage fractions (i.e., ratio of waste packages experiencing seepage to all waste packages in a percolation subregion) are direct functions of hydrologic, thermal, and drift degradation conditions. Thus, these two metrics will have different values for nominal/early failure and seismic ground motion modeling cases. The quantification of these relative metrics is presented for each of the three climate states of the first 10,000-year period, namely: (1) present-day (prevailing to 600 years); (2) monsoon (from 600 to 2,000 years); and (3) glacial-transition (from 2,000 to 10,000 years). For the post 10,000-year period, net infiltration and precipitation are not used because deep percolation fluxes are prescribed in proposed 10 CFR 63.342(c)(2) (70 FR 53313).

2.1.2.1.6.1 Topography and Surficial Soils

Net infiltration as a percentage of climate-induced annual precipitation is a useful metric to provide insights into the effectiveness of the surficial soils and topography to prevent or reduce the rate of water flow into the unsaturated zone. In addition, examining the partitioning of precipitation rate into the various water balance components (e.g., change in water storage in soil, runoff, evapotranspiration, and sublimation) is also useful in explaining the factors controlling the

reduction in net infiltration. Estimates of the mean net infiltration rate as a percentage of the mean precipitation rate are as follows (Section 2.3.1.1; SNL 2008c, Tables 6.5.7.4-1 through 6.5.7.4-3):

- Present-day climate: 8.02%
- Monsoon climate: 8.69%
- Glacial-transition climate: 10.38%.

Ranges of net infiltration for the four infiltration scenarios (defined by the 10th, 30th, 50th, and 90th percentiles) can be summarized as follows. Estimated average present-day net infiltration ranges from less than 3% of precipitation for the drier 10th percentile infiltration scenario to about 13% of precipitation for the 90th percentile infiltration scenario (SNL 2008c, Table 6.5.7.1-3). For the monsoon climate, average net infiltration rate estimates for the 10th to 90th percentile infiltration scenarios range from about 3% to 17% of precipitation (SNL 2008c, Table 6.5.7.2-3). For the glacial-transition climate, the average net infiltration rate estimates for the 10th to 90th percentile infiltration scenarios range from about 5% to 16% of precipitation (SNL 2008c, Table 6.5.7.3-3).

Climate analysis and infiltration modeling (Section 2.3.1.1; SNL 2008c, Tables 6.5.7.4-1 through 6.5.7.4-3) show that the process of evapotranspiration (i.e., transfer of moisture from soil to the atmosphere by evaporation and transpiration from plants) alone accounts for most of the reduction in net infiltration. This is predicted to account for 87.7%, 84.9%, and 86.2% of mean precipitation rate during the present-day, monsoon, and glacial-transition climates, respectively. The remainder of the reduction is accounted for by the change in moisture storage in the soil and surface runoff. The infiltration study contains comparisons with published estimates for other Nevada hydrographic areas/subareas (Section 2.3.1.3.4.2.2; Figure 2.3.1-48).

It is important to clarify that the TSPA model does not directly use the spatially averaged net infiltration rates cited above. The infiltration study provided maps of mean annual net infiltration that were used as boundary conditions for the site-scale unsaturated zone flow model (Section 2.3.2). In turn, that flow model was used to develop percolation flux fields for direct input to the TSPA model.

2.1.2.1.6.2 Unsaturated Tuff Units and Repository Horizon

To describe the combined barrier effectiveness of the tuff units and repository horizon, two metrics were used: (1) seepage rate as a percentage of percolation; and (2) seepage fraction for each of the five percolation subregions (Section 2.3.5.4.1.4). Seepage rate is defined as the water flow rate through a unit cross-sectional area. The seepage fraction is the ratio of waste packages experiencing seepage to the total waste packages in a percolation subregion; seepage fractions apply to codisposal and commercial SNF waste packages. To calculate these metrics, the TSPA model integrates the coupled effects of climate changes, net infiltration, and deep percolation through the unsaturated zone, and computes percolation flow to and around the repository drifts. Projections for the combined nominal/early failure and seismic ground motion demonstration modeling cases are presented here.

Seepage Rate as Percentage of Local Percolation Rate—Water entering the unsaturated zone as net infiltration from precipitation at the land surface affects the overall hydrologic and thermal-hydrologic conditions within the Yucca Mountain unsaturated zone. Net infiltration is the

ultimate source of percolation through the unsaturated zone. Water percolating downward through the unsaturated zone is the source for seepage into the drifts. Multidimensional modeling of water flow in the unsaturated zone rock layers indicates that average percolation flux flowing to the repository is within a few percent of the net infiltration rate (Section 2.3.2.4.1.2.4.6). In addition, of the water flow (percolation) arriving at the repository horizon, only a small portion results in drift seepage. The reduction from percolation to seepage is the result of two natural processes that divert flow around and away from the emplacement drift. These processes are referred to as (1) the vaporization barrier effect during the thermal period (Section 2.3.3.3); and (2) the capillary barrier effect after the thermal period (Section 2.3.3.2). While the vaporization barrier effect persists for a short time relative to the compliance periods, the capillary barrier effect in the lithophysal unit persists through the period of geologic stability.

The combination of reduced infiltration into Yucca Mountain, and the vaporization and capillary barrier effects in the TSw unit, result in a seepage flux that will be substantially reduced from the precipitation flux at the surface. The magnitude of this reduction is shown in Figure 2.1-5. The top figure (a) illustrates the effectiveness of surficial soils and topography in preventing or reducing the rate of water flow into the unsaturated zone. The bottom figure (b) illustrates the effectiveness of vaporization and capillary diversion in limiting water movement into the drifts. In Figure 2.1-5(a), the mean spatially-averaged annual precipitation and net infiltration rates are plotted for each of the three climates in the 10,000-year period. Net infiltration rates are shown to range from approximately 5% of precipitation during the present-day climate to over 7% of precipitation during the glacial-transition climate (SNL 2008d, Section 8.3.3.1.1[a]). For the post-10,000-year period, the effects of infiltration are implicitly included in the TSPA model by using the distribution for deep percolation rate as specified in proposed 10 CFR 63.342(c)(2) (70 FR 53313); namely, a log-uniform distribution with a range of 13 to 64 mm/yr. The mean value of deep percolation from this distribution, 32 mm/yr, is shown in Figure 2.1-5(a).

The values for annual precipitation and net infiltration used in Figure 2.1-5(a) were derived as follows. The net infiltration and mean annual precipitation rates for the 10th-, 30th-, 50th-, and 90th-percentile infiltration maps were taken from *Simulation of Net Infiltration for Present-Day and Potential Future Climates* (SNL 2008c, Tables 6.5.7.1-3, 6.5.7.2-3 and 6.5.7.3-3) for the present-day, monsoon, and glacial transition climates, respectively. These values are based on spatial averaging over the infiltration model. For each climate state, the averaged precipitation and net infiltration rates were then generated by taking the sum of the products of the rates and the unsaturated zone flow field weighting factors (0.6191, 0.1568, 0.1645, and 0.0596) for the 10th-, 30th-, 50th, and 90th-percentile values (Section 2.3.2.2.1). This approach of using mean infiltration values for the infiltration modeling domain, rather than over the repository footprint, tends to underestimate the percolation flux that occurs within the repository footprint as compared to the unsaturated zone flow fields implemented in the TSPA. For example, compare the mean infiltration modeling domain (30mm/yr) and the repository footprint (38.7 mm/yr) for glacial transition climate (SNL 2008c, Table 6.5.7.3-2). Therefore, since the TSPA calculated seepage rates presented in Figure 2.1-5(b) are based on higher percolation fluxes, the results summarized here for seepage diversion are slightly underestimated.

Three mean spatially-averaged drift seepage rate curves are shown in Figure 2.1-5(b). The top curve denoted by the dashed line represents an ambient seepage rate that would result if capillary and thermal effects at the drift wall were neglected. This volumetric seepage rate is obtained by applying

the average net infiltration flux to the projected area of an intact emplacement drift segment that is 5.1 m long by 5.5 m wide. This ambient seepage rate is compared to the TSPA-calculated seepage rates for the two demonstration modeling cases (i.e., the combined nominal/early failure modeling case and the seismic ground motion modeling case) to illustrate the effectiveness of the unsaturated zone barrier in limiting the movement of water into the drifts. Note that the average net infiltration flux and, thus, the ambient seepage rate used here, is based on a spatial averaging over the entire infiltration model domain. Therefore, the ambient seepage rate is only a representative approximation of the average flux that would occur within the repository footprint. In contrast, the TSPA-calculated seepage fluxes are based on the percolation flux within the repository footprint.

The nominal seepage rate curve in [Figure 2.1-5\(b\)](#) shows that seepage varies in the early part of the thermal period, when temperatures above 100°C are achieved. As temperatures gradually decrease to lower values, seepage rates into the drift increase. The estimate shows that, for the 10,000-year period, on average, 2% to 11% of the ambient seepage rate occurs as seepage into the drifts. The mean seepage rate for the post-10,000-year period is about 0.095 m³/yr, or about 11% of the ambient seepage rate.

The seepage curve for the seismic ground motion modeling case shown in [Figure 2.1-5\(b\)](#) is discussed next. For the 10,000-year period following repository closure, the mean seepage flux curve is almost identical to the mean curve for the nominal and early failure modeling cases. This similarity occurs because (1) for the most part, low-magnitude seismic events are projected to predominate in this time period; and, as a result, (2) relatively little drift degradation (i.e., damage to the drift openings) is projected to occur. The observation of low-magnitude seismic events is based on the mean seismic hazard curve, which shows that exceedance frequencies on the order of 10⁻⁴/yr correspond to relatively small-amplitude vibratory ground motions (SNL 2008d, [Figure 6.6-6](#)). Drift degradation, quantified in terms of mean rubble volume per meter of drift length (i.e., by seismic-induced rockfall), is less than 5 m³/m and 0.5 m³/m for the lithophysal and nonlithophysal rock zones, respectively, for the first 10,000 years after repository closure ([Figure 2.1-6](#)). It is important to note that the curves for the 5th percentile and median are absent from [Figure 2.1-6](#); this result is because of the large number of realizations with very little or no drift degradation. The lithophysal rock zones encompass approximately 85% of the emplacement drifts in the repository ([Section 2.3.3.2.3.2](#)). A mean rubble volume of less than or equal to the 5 m³/m of drift length for lithophysal rock zone, or 0.5 m³/m for nonlithophysal rock zone, indicates that the emplacement drifts are essentially intact and, thus, the seepage fluxes correspond to the ambient percolation fluxes and nominal flow processes in the repository horizon ([Section 2.3.3](#)). Therefore, the values of the seepage/precipitation metric would be about the same as those given previously for the nominal and early failure modeling cases.

For the post-10,000-year time period, the seismic ground motion modeling case seepage rates in [Figure 2.1-5\(b\)](#) are significantly different from the seepage rates for the combined nominal/early failure modeling case. This difference is due to a greater degree of drift degradation and, at late times, to drift collapse in lithophysal rock. In nonlithophysal rock, once rockfall has accumulated to an amount of 0.5 m³/m, capillary diversion is no longer considered, and the seepage rate is set to the percolation rate in the TSPA model. The spatially averaged mean seepage rates for the seismic ground motion modeling case increase with time and are larger than those for the combined nominal/early failure modeling case. The mean drift seepage rates for the seismic ground motion modeling case range from 0.109 m³/yr, just after 10,000 years, to 0.434 m³/yr at 1,000,000 years.

For these same two times, the seepage rates, as a percentage of the mean zero diversion seepage rate calculated using the NRC prescribed local percolation rate, are about 12% and 48%, respectively (SNL 2008d, Section 8.3.3.1.1[a]). Although the effectiveness of capillary diversion is reduced from that of the combined nominal/early failure modeling case, it is still substantial in the seismic ground motion modeling case.

Seepage Fractions for Percolation Regions—Drift seepage rates are expected to vary spatially over the length of emplacement drifts. Thus, emplacement drifts can exhibit both seeping (with seepage) and non-seeping (no seepage) environments. In the TSPA model, this spatial variability is quantified by the seepage fraction. The seepage fraction is the ratio of the number of waste packages experiencing seepage to the total number of waste packages in a percolation subregion. Separate values are computed for codisposal and commercial SNF waste packages. Distributions of seepage fraction have been computed for each climate and for the five percolation subregions that represent the repository footprint. The calculations were performed using the drift seepage abstraction model (Section 2.3.3.2.4). Implementation of the abstraction in the TSPA model is summarized in Section 2.4.2.3.2.1.3. Unlike seepage rates, which vary with time, seepage fractions are constant values that are based on the percolation flux at the end of the simulation period (either 10,000 years or 1,000,000 years).

For the combined nominal/early failure modeling case, statistics for distribution of seepage fraction are tabulated in Table 2.1-6 for glacial-transition climate (2,000 to 10,000 years), and in Table 2.1-7 for post-10,000-year deep percolation rates. The post-10,000-years statistics are summarized here. The statistics consist of mean, 5th, and 95th percentiles for each waste package type (i.e., codisposal and commercial SNF). In Percolation Subregion 3, the mean seepage fraction is about 0.44 (SNL 2008d, Table 8.3-3[a]) for the codisposal and commercial SNF waste package locations (SNL 2008d, Section 8.3.3.1.1[a]). Percolation Subregion 5, which represents about 5% of the repository footprint (SNL 2008d, Section 6.3.2.2.1), has the highest mean seepage fraction of about 0.49 for both codisposal and commercial SNF waste packages (SNL 2008d, Section 8.3.3.1.1[a]). Averaging over the entire repository footprint, the mean seepage fractions for both codisposal and commercial SNF waste packages are about 0.4. This indicates that, on average, about 60% of the emplacement locations in the repository have nonseep environments for the nominal and early failure modeling cases.

For the seismic ground motion modeling case, the seepage fraction statistics are tabulated in Table 2.1-8 for glacial-transition climate (Section 2.3.8.4.1) and Table 2.1-9 for post-10,000-year deep percolation rates. As can be noted from Table 2.1-9 for the post-10,000-year period, the mean seepage fraction in Percolation Subregion 3 is about 0.72 for both codisposal and commercial SNF waste packages. Percolation Subregion 5, which represents about 5% of the repository footprint, has the highest mean seepage fractions of about 0.75 for both the codisposal and commercial SNF waste package locations. The mean seepage fraction for the overall repository footprint is about 0.7 for both codisposal and commercial SNF waste package locations. These results indicate that about 30% of the emplacement locations in the repository are in nonseeping environments for the seismic ground motion modeling case. It is important to note that the calculations of mean seepage fractions for the seismic ground motion modeling case account for effects of drift degradation and collapse, which reduce the flow diversion by the capillary barrier (Section 2.3.3.2.4). This is the reason that the seepage fractions are higher than those for the combined nominal/early failure modeling case.

Summary of Upper Natural Barrier Capability—The barrier capability analyses presented above demonstrate that topography and surficial soils substantially reduce the net infiltration into the underlying unsaturated zone rock layers above the repository. For climate states projected for the first 10,000 years after closure, the topography and surficial soils prevent (on average) about 90% or more of the precipitation from entering the underlying unsaturated zone rock layers. More specifically, the mean net infiltration rate as a percentage of mean precipitation rate for each climate state is estimated to be approximately (1) 8% for present-day climate; (2) 9% for monsoon climate; and (3) 10% for glacial transition climate.

Of the water ultimately reaching the repository horizon (i.e., Topopah Spring welded [TSw]), only a fraction of the local percolation would enter the emplacement drifts as a result of the capillary barrier effect. This capillary barrier effect diverts ambient water flow around the emplacement drifts. Taking this effect into account, the mean drift seepage is less than 11% of mean annual percolation rate for intact drifts, and is less than 12% to 48% for degraded drifts, varying with the extent of drift degradation.

These seepage rate reductions indicate that very small fractions of the precipitation and ensuing net infiltration would enter the emplacement drifts.

2.1.2.2 Engineered Barrier System

As described in [Section 2.1.1.2](#) and illustrated in [Figure 2.1-7](#), EBS features that are ITWI ([Table 2.1-1](#)) and that contribute to barrier capability are (1) emplacement drift ([Section 1.3.4](#)); (2) drip shield ([Section 1.3.4](#)); (3) waste package including waste package outer barrier and inner vessel ([Section 1.5.2](#)); and (4) waste form and waste package internals including commercial SNF ([Section 1.5.1.1](#)) and HLW ([Section 1.5.1.2](#)), the TAD canister ([Section 1.5.1.1](#)), naval canister ([Section 1.5.1.4](#)), naval SNF canister system components ([Section 1.5.1.4](#)), naval SNF ([Section 1.5.1.4](#)), TAD canister internals ([Section 1.5.1.1](#)), and DOE SNF canister internals ([Section 1.5.1.3](#)). EBS features/components that are non-ITWI are (1) commercial SNF cladding ([Section 1.5.1.1](#)); (2) DOE SNF ([Section 1.5.1.3](#)); (3) the waste package emplacement pallet ([Section 1.3.4](#)); and (4) invert ([Section 1.3.4](#)). [Table 1.9-8](#) provides further detail with respect to the structures, systems, or components that comprise each engineered feature.

Commercial SNF waste packages are used to represent the naval SNF waste packages in the TSPA as discussed in [Section 2.3.7.3](#). Note that TAD canister internals, DOE SNF canister internals, and the naval SNF canister system components are classified as ITWI because these components provide criticality control in the waste packages (see [Table 1.9-8](#)).

As discussed in [Section 2.1.1.2](#), the features of the EBS have processes and characteristics that influence the capability of these features to prevent or substantially reduce the release of radionuclides from the waste. These processes include chemical and thermal-chemical processes, mechanical and thermal-mechanical processes, hydrologic and thermal-hydrologic processes, and transport processes, as identified in [Table 2.1-3](#) (SNL 2008a). This table also indicates those processes and characteristics relevant to each feature that are important contributors to barrier capability.

In the evaluation of the important processes and events related to the capability of the EBS, consideration is given to both the beneficial as well as the potentially deleterious processes and events that act on each of the features of the barrier. The presence of a beneficial process generally results in either (1) preventing the release or substantially reducing the release rate of radionuclides from the waste; or (2) preventing the movement of radionuclides or substantially reducing the rate of movement of radionuclides from the repository to the accessible environment. Similarly, the absence or slow rate of a potentially deleterious process generally results in preventing or substantially reducing the release of radionuclides from the waste. The presence of a potentially deleterious process could result in an increase in the release rate or rate of movement of radionuclides. Both beneficial and potentially deleterious processes have been identified as important contributors to the EBS capability.

A few examples illustrate beneficial and potentially deleterious processes and their effects on the EBS. General corrosion of the waste package (Section 2.3.6.3) is a potentially deleterious process. However, a beneficial attribute of the waste package is that general corrosion rates for Alloy 22 are so slow and spatially variable under repository-relevant conditions that degradation and breaching of waste packages will be distributed over hundreds of thousands of years. Sorption of dissolved radionuclides on corrosion products in the waste package and on the invert ballast material (crushed tuff) in the EBS (Section 2.3.7.12) is a beneficial process of the EBS when the waste packages are breached. Seismic ground motion is a potentially deleterious process that can diminish the performance of the EBS (Section 2.3.4.5) by inducing both dynamic and static loads on the waste packages. In turn, these loads could cause stress corrosion cracking of the outer corrosion barrier and allow moisture to enter the waste package and degrade the waste form.

The features of the EBS that are ITWI and the processes and characteristics that contribute significantly to their barrier capability are summarized below.

Emplacement Drift—The following processes and characteristics are important contributors to the barrier capability of the emplacement drifts and EBS:

- **Unsaturated Flow in the EBS**—The repository and emplacement drifts are located above the water table and saturated zone. Therefore, water saturations in the EBS tend to be low, thus reducing the effective diffusivity and mobility of radionuclides in a breached waste package and in the invert (Section 2.3.2).
- **Chemical Characteristics of Water in Drifts**—The chemical characteristics of water in the drift are affected by the incoming water chemistry (due to seepage, condensation, or capillary flow), evaporation, and other thermal-chemical processes in the drift that are a function of the thermal-hydrologic environment (Sections 2.3.5.1 and 2.3.5.5). These chemical characteristics affect the likelihood of potential localized corrosion of the waste package outer barrier (Section 2.3.6.4), as well as the transport characteristics of any radionuclides released from the waste package to the invert. Sections 2.3.7.10, 2.3.7.11, and 2.3.7.12 discuss the transport characteristics affected by the range of in-drift water chemical characteristics, notably radionuclide solubility and colloid stability.
- **Seismic Induced Drift Collapse Damages EBS Components**—Vibratory ground motions associated with seismic activity could cause failure of the host rock around the

emplacement drifts. The resulting drift degradation could cause damage to the drip shields as a result of the static load from the rock rubble amplified by the dynamic load associated with vibratory ground motion. Such mechanisms may result in damaged areas on the drip shield plates and stress corrosion cracking. However, stress corrosion cracking would not compromise the barrier capability of the drip shield because crack openings would be very small and tight, so effective water flow rates would be too low to affect the performance of the drip shield in preventing or substantially reducing the amount of water that could directly contact the waste package, and is excluded from the TSPA (SNL 2008b, FEP 2.1.03.02.0B, Stress corrosion cracking of drip shields, and FEP 2.1.03.10.0B, Advection of liquids and solids through cracks in the drip shield). Accumulated rubble on the drip shield can also cause failure (rather than just damaged areas) of the drip shield during a seismic event. Two failure modes of the drip shield could occur: (1) rupture or tearing of the drip shield plates; and (2) buckling or collapse of the sidewalls of the drip shield (Section 2.3.4.5). In addition, this drift collapse may have a very significant effect on waste package degradation. This effect manifests itself by significantly reduced waste package damage (i.e., improved performance and enhanced barrier capability) if the rubble surrounds the waste package in the absence of a drip shield. The effects of drift collapse tend to degrade the performance of the drip shield while improving the performance of the waste package if the waste package is surrounded by rubble at late times (about 200,000 years) (SNL 2008a, Section 6.2.2.2).

- **Heat Generation in the EBS**—The heat generated by radioactive decay has multiple effects on repository-relevant processes, including degradation, deterioration, and alteration of the EBS. Heat generation in the emplacement drifts affects the timing of the onset of seepage processes, as discussed in Sections 2.3.5.3 and 2.3.5.4, as well as the distribution of in-drift convection and condensation (as discussed in Section 2.3.5.4). The heat generation and resultant temperature also affect the chemical evolution of water in the rock and emplacement drifts, as presented in Sections 2.3.5.3 and 2.3.5.5, respectively.
- **Thermal Effects on Chemistry and Microbial Activity in the EBS**—As noted above, thermal effects strongly influence the evolution of the water chemistry in the rock and emplacement drifts. The chemistry of the water in the emplacement drift determines the potential for localized corrosion of the waste package outer barrier and, in the event of waste package failure, can affect the stability of radionuclide-bearing colloids and radionuclide solubility in the invert (Section 2.3.5.5). Microbial effects will not significantly affect the in-drift chemical environment, including water chemistry (Section 2.3.6.3.2).
- **Chemistry of Water Flowing into the Drift**—As seepage waters percolate into the drift, their chemical compositions change by dilution or by evaporation and mineral precipitation. Evaporation causes dissolved aqueous species concentrations to increase, minerals to precipitate, and the most soluble components to become concentrated in the resulting solution, ultimately leading to the formation of potentially deleterious brine. Dilution generally has the opposite effect. The chemical composition of the seepage water on the waste package surface determines the potential for localized corrosion of the waste package outer barrier. The chemical composition of seepage in the invert affects

radionuclide solubility and colloid stability in the invert, which in turn affect the mobile radionuclide source term for transport. The range of expected water chemistries, as well as their variation in time due to the heat generated in the EBS, is presented in [Section 2.3.5.3](#).

- **Seismic Ground Motion Damages EBS Components**—Vibratory ground motion has the potential to cause seismically-induced rockfall that changes the cross-sectional shape and volume of the emplacement drifts ([Section 2.3.4.4](#)) and changes the configuration of the EBS components within the emplacement drifts ([Section 2.3.4.5](#)). A change in the cross section of the emplacement drifts and the presence of rockfall and/or rubble about the drip shield can alter the seepage into the drifts, flow pathways within the drift, condensation within the EBS, and the mechanical response and temperature-time history of the EBS components ([Sections 2.3.4.1](#) and [2.3.4.5.6](#)).
- **Seismic-Induced Rockfall Damages EBS Components**—Seismic activity could produce jointed-rock motion and/or changes in rock stress, leading to rockfall that could impact drip shields, waste packages, or other EBS components. Rockfall refers to rock blocks that fall from the roof or sides of a drift in the nonlithophysal zones of the repository during a seismic event, rather than complete or partial collapse of the emplacement drift, which may cover the drip shield with rubble and cause a sustained, static loading to the structure. Damage to the drip shields and waste packages as a result of seismic-induced rockfall from jointed-rock motion in nonlithophysal units is excluded from the TSPA model, as documented by the analysis in *Features, Events, and Processes for the Total System Performance Assessment: Analyses* (SNL 2008b, FEP 1.2.03.02.0B, Seismic-induced rockfall damages EBS components). Note that the effects of seismic-induced drift collapse in the lithophysal units of the repository are included in TSPA, as discussed above (in Seismic Induced Drift Collapse Damages EBS Components).
- **Seismic Induced Drift Collapse Alters In-Drift Thermal Hydrology**—Seismic activity could produce jointed-rock motion and/or changes in rock stress, leading to enhanced drift collapse and/or rubble infill throughout part or all of the emplacement drifts ([Sections 2.3.4.1](#) and [2.3.4.8.1](#)). Drift collapse could impact flow pathways and condensation within the EBS, mechanisms for water contact with EBS components, and temperature-time history within the EBS ([Section 2.3.4.1](#)).

Drip Shield—The following processes and characteristics are important contributors to the barrier capability of the drip shield and the EBS:

- **Physical Form of Drip Shield**—The physical characteristics of the drip shield, consistent with the design of this feature, have been included in the analyses and models of drip shield degradation ([Section 2.3.6.8](#)), EBS flow and transport ([Section 2.3.7.12](#)), and EBS environments ([Sections 2.3.5.4](#) and [2.3.5.5](#)). These characteristics are significant contributors to the capability of the drip shield to limit the flow of water and release of radionuclides. The assessment of barrier capability and performance accounts for design features, material characteristics, and the ways in which the design influences the evolution of the in-drift environment. Administrative controls for repository

construction and operations will be developed to assure that drip shields are manufactured in accordance with design specifications and are emplaced properly (Table 1.9-9).

- **General Corrosion of Drip Shield**—General corrosion rates of titanium alloys in a range of expected environmental conditions in the emplacement drifts are sufficiently low that this process does not cause a through-wall penetration of the drip shield until about two to three hundred thousand years after repository closure (Section 2.1.2.2.6). General corrosion is also an important process affecting drip shield structural integrity, because general corrosion weakens the drip shields over long time periods by gradually thinning the drip shield plates and framework. Thinning makes these components more susceptible to damage by vibratory ground motion. The slow degradation rate of the titanium drip shield is an important beneficial characteristic of the drip shield feature.
- **Localized Corrosion of Drip Shields**—Titanium alloys are extremely resistant to localized corrosion, due to their very passive film. Localized corrosion of these alloys will not occur in repository environments and is excluded from the TSPA (SNL 2008b, Section 6.2; FEP 2.1.03.03.0B, Localized corrosion of drip shields). The model for drip shield localized corrosion is presented in Section 2.3.6.8.
- **Stress Corrosion Cracking of Drip Shields**—In the presence of residual stresses or sustained loading, titanium is potentially susceptible to stress corrosion cracking. Residual stresses and sustained loading are possible as a result of rockfall or seismically induced damage. Uncertainty exists in the stress state and threshold stress required for a stress corrosion crack to be initiated, and other uncertainties exist regarding the degree of propagation of any stress-induced crack of titanium. Due to the long time frames, stress corrosion cracking is modeled to be independent of the environment, although the environments needed to support stress corrosion may not occur within the repository as explained in Section 2.3.6.8. Although stress corrosion cracking is modeled to occur in the drip shield, the presence of cracks is an insufficient condition to affect the performance of the drip shield in preventing or substantially reducing the amount of water that could directly contact the waste package, as discussed in Sections 2.3.6.8 and 2.2, and water flow through stress corrosion cracks is therefore excluded from the TSPA (SNL 2008b, Section 6.2, FEP 2.1.03.02.0B, Stress corrosion cracking of drip shields).
- **Effects of Drip Shield on Flow**—The drip shield prevents seepage water from contacting the waste package. Thus, the drip shield reduces the rate of movement of water that may contact the waste, as well as preventing potentially deleterious brines from contacting the waste package surface during the period when the waste package may be susceptible to localized corrosion (Section 2.3.6.8).
- **Advection of Liquids and Solids through Cracks in the Drip Shield**—Any cracks that extend through the drip shield are expected to be of insufficient size and morphology to allow the advective flow of water through them. The process of formation and the physical characteristics of stress corrosion cracks resulting from denting of the drip shield by seismic-induced rockfall or drift collapse is summarized in Section 2.3.4.5.2.2. The advection of liquids through seismic-induced stress corrosion cracks in the drip shield is excluded from the TSPA based on low consequence as a result of a number of factors,

including (1) the small aperture width (narrow opening and tight cracks) and the presence of capillary forces within the stress corrosion cracks; and (2) the potential for plugging of the cracks due to mineral deposits. In response to stresses induced by rockfall deformations, stress relief via creep mechanisms or stress corrosion cracking of the drip shield may occur. Such cracks in passive alloys, such as Titanium Grade 7, are tight (e.g., small crack-opening displacement) and are expected to be plugged by corrosion products and precipitates (SNL 2008b, FEP 2.1.03.10.0B, Advection of liquids and solids through cracks in the drip shield). The lack of significant advection through cracks in the drip shield is an important beneficial characteristic of the drip shield.

- **Localized Corrosion on Drip Shield Surface Due to Deliquescence**—The potential for salts to deliquesce on the drip shield surface has been evaluated. Although the potential for salts to deliquesce exists, the effects of such deliquescence have been determined to be insignificant to performance because localized corrosion processes are not expected to be initiated. Even if localized corrosion were initiated, due to the limited volumes of brine caused by deliquescence, it is expected that the process would not propagate through the drip shield surface. As a result, this process is excluded from the performance assessment (SNL 2008b, FEP 2.1.09.28.0B, Localized corrosion on drip shield surfaces due to deliquescence). The lack of significant drip shield degradation by this process is a beneficial characteristic of the drip shield.
- **Early Failure of Drip Shields**—During fabrication and emplacement, a range of undetected and unmitigated errors could result in a drip shield being emplaced that has the potential for a drip shield failure (Section 2.3.6.8). This possibility has been included in abstraction models used in the early failure scenario class of the TSPA, as presented in Section 2.4.2.1.
- **Creep of Metallic Materials in the Drip Shield**—Titanium Grade 7, used for the drip shield plates, may undergo creep deformation at temperatures as low as room temperature when subjected to tensile stresses exceeding approximately 50% of the yield strength (Section 2.3.6.1.1). Titanium Grade 29, used for the drip shield structural supports, has significantly higher creep resistance than Titanium Grade 7 (SNL 2007b, Section 6.8.3). When the drip shield deforms through long-term creep, a confinement caused by the rubble is developed which tends to inhibit further creep deformation. Creep of titanium resulting in instability (collapse) of the drip shield has been excluded from the performance assessment (SNL 2008b, Section 6.2; FEP 2.1.07.05.0B, Creep of metallic materials in the drip shield). Although not credited in the treatment of stress corrosion cracking of the drip shield titanium alloys, creep following any stress corrosion cracking has the beneficial effect of decreasing crack propagation.
- **Seismic Induced Drift Collapse Damages EBS Components**—Vibratory ground motions associated with seismic activity could cause failure of the host rock around emplacement drifts. The resulting drift degradation could cause damage to the drip shields as a result of the static load from the rock rubble amplified by the dynamic load associated with vibratory ground motion. Such mechanisms may result in damaged areas on the drip shield plates and stress corrosion cracking. However, stress corrosion cracking would not compromise the barrier capability of the drip shield because crack openings

would be very small and tight, so effective water flow rates would be too low to affect the performance of the drip shield in preventing or substantially reducing the amount of water that could directly contact the waste package, and is excluded from the TSPA, as discussed in *Features, Events, and Processes for the Total System Performance Assessment: Analyses* (SNL 2008b, FEPs 2.1.03.02.0B, Stress corrosion cracking of drip shields, and 2.1.03.10.0B, Advection of liquids and solids through cracks in the drip shield). Accumulated rubble on the drip shield can also cause failure (rather than just damaged areas) of the drip shield during a seismic event. Two failure modes of the drip shield could occur: (1) rupture or tearing of the drip shield plates; and (2) buckling or collapse of the sidewalls of the drip shield (Section 2.3.4).

Waste Package (Including Waste Package Outer Barrier and Inner Vessel)—The following processes and characteristics are important contributors to the barrier capability of the waste package and the EBS:

- **Physical Form of the Waste Package**—The physical characteristics of the waste package, consistent with the design of this feature, have been included in the analyses and models of waste package degradation. These characteristics are significant contributors to the capability of the waste package to reduce the release rate of radionuclides from the waste. The assessment of barrier capability accounts for design features, material characteristics, and the ways in which the design influences the evolution of the in-drift environment. Administrative controls for repository construction and operations will be developed to assure that waste packages are manufactured in accordance with design specifications and are emplaced properly (Table 1.9-9).
- **General Corrosion of Waste Packages**—General corrosion rates of Alloy 22 in a range of expected environmental conditions are sufficiently low that this process is projected to cause a through-wall penetration in only 9% (based on the mean curve) of the waste packages by 1,000,000 years (Section 2.1.2.2.6) (SNL 2008d, Figure 8.3-6[a]). General corrosion is an important process affecting waste package structural integrity, because general corrosion thins and weakens the waste packages over long time periods by gradually thinning the outer corrosion-resistant Alloy 22 barrier, which makes the waste package more susceptible to being damaged by vibratory ground motion. Although the stainless steel inner vessel of the waste package and the TAD canister shell for the commercial SNF waste package will reduce the rate of movement of water that may contact the waste for tens of thousands of years after the Alloy 22 outer corrosion barrier is breached, this beneficial characteristic is not included in the performance assessment. The stainless steel inner vessel and TAD canister will provide additional structural resistance to vibratory ground-motion-induced damage to the waste packages. This beneficial characteristic is also incorporated into the performance assessment (Section 2.3.4), but is not included in the performance assessment after the waste package Alloy 22 outer corrosion barrier has been breached.
- **Stress Corrosion Cracking of Waste Packages**—Stress corrosion cracking is the process by which cracks initiate in a material under stress in the presence of a corrosive environment (Section 2.3.6.5). Stress corrosion cracking may affect the time to waste package breach. Stress corrosion cracks would allow diffusive transport of radionuclides

from the waste package, and therefore could compromise the barrier capability of the waste package. Alloy 22, the material used for the waste package outer corrosion barrier, is highly resistant to stress corrosion cracking, but may be susceptible to cracking in the Yucca Mountain environment and the stress conditions described in [Section 2.3.6.5.1](#). Stress corrosion cracking breaches can occur via three possible modes: (1) through-wall propagation of fabrication flaws (other than in the outer corrosion barrier weld region) in the waste packages ([Section 2.3.6.6](#)) that result in early waste package failure; (2) through-wall propagation of incipient cracks that can occur on the waste package outer corrosion barrier closure weld regions; (3) damage to the waste package induced by seismic events, as discussed in [Section 2.3.4.5](#).

- **Localized Corrosion of Waste Packages**—Localized corrosion is a phenomenon in which corrosion progresses at discrete sites or in a nonuniform manner ([Section 2.3.6.4](#)). At least upon initiation, the propagation rate of localized corrosion is faster than that of general corrosion. Localized corrosion mechanisms on the waste package surface are dependent on the thermal-hydrologic and thermal-chemical environment on the waste package surface. The initiation of localized corrosion is possible in those cases where the drip shield has degraded sufficiently that incoming seepage is allowed to contact the waste package during the early part of the thermal period. In most cases, the drip shield will be intact during this period, protecting the waste package from seepage water contact. Should the drip shield fail to perform its function, such as in the unlikely event of drip shield failure due to fault displacement in the first 12,000 years, seepage waters may form concentrated aggressive solutions on the waste package (SNL 2008d, Volume 1, [Section 6.3.5.2](#)). In this case, waste packages that are susceptible to localized corrosion are expected to have already experienced substantial mechanical damage failure, and any additional damage caused by localized corrosion would not significantly impact radionuclide release from already damaged waste packages ([Section 2.4.2.3.2.1.5](#)). The possibility of localized corrosion also requires aggressive environmental exposure conditions ([Section 2.3.6.4.1](#)) that are generally not present (SNL 2008d, Volume 3, Appendix O). The model of localized corrosion of the waste package used in the performance assessment is presented in [Section 2.3.6.4](#). The expected absence of the conditions necessary to initiate localized corrosion is an important beneficial characteristic of the waste package feature.
- **Early Failure of Waste Packages**—During fabrication, waste loading, and emplacement, a range of undetected and unmitigated errors could result in a waste package being emplaced that has the potential for an early waste package failure ([Section 2.3.6.6](#)). This possibility has been included in abstraction models used in the early failure scenario class of the TSPA, as presented in [Section 2.4.2.1](#).
- **Advection of Liquids and Solids through Cracks in the Waste Package**—Similar to cracks in the drip shield, cracks in the waste package are expected to be of insufficient size and morphology to allow for the advection of water into the waste package. As a result, as discussed in *Features, Events, and Processes for the Total System Performance Assessment: Analyses* (SNL 2008b), advective release from the waste package ([Section 2.3.7.12](#)) is only possible when the degradation mode causing breach is general ([Section 2.3.6.3](#)) or localized corrosion ([Section 2.3.6.4](#)), when manufacturing defects

result in early failure of waste packages (Section 2.3.6.6), or when waste packages rupture due to stresses in the outer barrier exceeding the residual stress threshold as result of seismic vibratory ground motion or fault displacement.

- **Localized Corrosion on Waste Package Outer Surface Due to Deliquescence**—Dust will be deposited on the surfaces of waste packages in emplacement drifts primarily during the operational and the preclosure ventilation periods. After emplacement, there is a period up to approximately 1,000 years in which no seepage is possible because the drift wall temperature is above boiling (Section 2.3.5). During this interval, and for as long as the drip shields perform their function, the only aqueous phase that could potentially contact the waste package is brine that originates by deliquescence of soluble salts in dust residing on the waste package. The potential for brines formed by dust deliquescence to initiate and sustain localized corrosion resulting in breach of the waste package outer corrosion barrier has been evaluated and excluded from the TSPA (SNL 2008b, Section 6.2, FEP 2.1.09.28.0A, Localized corrosion on waste package outer surface due to deliquescence).
- **Seismic Ground Motion Damages EBS Components**—Ground motion associated with seismic activity has the potential to disrupt the integrity of the waste package and other EBS components, which could lead to impaired waste package performance and/or breaching, with subsequent radionuclide release. Seismic-induced deformation of the waste package could result in plastic yielding or even breach of the waste package. If the residual stress on a plastically deformed waste package exceeds a threshold value (Section 2.3.4.1), then stress corrosion cracking may result in the formation of diffusive transport pathways for radionuclides. Additional structural failures corresponding to the tearing or rupture of the waste package could also occur. A rupture or tear may occur if the local strain exceeds the ultimate tensile strain (Section 2.3.4.1), and may partly or completely negate the effectiveness of the waste package in preventing the inflow of seepage water or the outward transport of radionuclides.
- **Seismic Induced Drift Collapse Damages EBS Components**—Vibratory ground motions associated with seismic activity could cause failure of the host rock around emplacement drifts. Drift collapse enhances the barrier capability of the EBS, specifically the waste package, by surrounding the waste package with rubble that shields the waste package from potentially damaging rockfall after the drip shield plate has failed, especially at late times when the walls of the waste package are thinned and weakened by general corrosion. Rubble surrounding the waste package also helps to reduce seismic-induced kinematic damage to the waste package by confining the waste package and dampening the effect of ground motion.

Waste Form and Waste Package Internals (Including the TAD Canister, Naval Canister, TAD and DOE SNF Canister Internals, and Naval SNF Canister System Components)—The following processes and characteristics of the waste form and waste package internals are

important contributors to the barrier capability of the waste form and waste package internals and EBS:

- **Seismic Ground Motion Damages EBS Components**—Vibratory ground motion has the potential to damage the waste package outer corrosion barrier as a result of waste package-to-waste package impacts and waste package-to-pallet impacts that may occur during a seismic event. This damage may result in residual stresses that exceed a tensile threshold for initiation and growth of stress corrosion cracks. The TAD and naval canisters enhance the structural stability of the waste packages prior to waste package breach. Once the outer corrosion barrier is breached by a crack network, corrosion of the waste package internals (specifically TAD and naval canisters) will compromise their capacity to support structural loads and to isolate the waste form during vibratory ground motion.
- **Commercial SNF Degradation (Alteration, Dissolution, and Radionuclide Release)**—The availability of individual radionuclides for dissolution, once a commercial SNF waste package and fuel cladding are breached, is limited by the structure, microstructure, and physiochemical properties of the irradiated fuel, as well as by the distribution of radionuclides in the fuel rods. The part of the radionuclide inventory present, either as a solid solution in the fuel matrix or embedded as discrete phases in the fuel grains, is not available for dissolution until the fuel matrix is dissolved or degraded. The rate of dissolution or degradation will influence the rate at which soluble radionuclides can enter solution (Section 2.3.7). The commercial SNF degradation rate is the product of the fuel surface area and the surface area-normalized dissolution rate. The latter depends on pH, carbonate levels, and the oxygen partial pressure (Section 2.3.7.7.3.2).
- **Naval SNF (Naval SNF Structure (Including Cladding))**—Refer to naval SNF cladding FEP. In the modeled repository, there are 8,213 waste packages modeled as commercial SNF, of which 417 represent naval SNF (SNL 2008d, Table 6.3.7-1). Waste packages containing naval SNF are conservatively modeled in the TSPA as commercial SNF waste packages (SNL 2008b, FEP 2.1.02.25.0B, Naval SNF cladding).
- **HLW Glass Degradation (Alteration, Dissolution, and Radionuclide Release)**—The availability of individual radionuclides for transport and release once a codisposal waste package is breached is determined by the rate at which radionuclides leave the HLW glass and enter solution. The rate at which radionuclides enter a solution is controlled either by the dissolution rate of the waste form or by the solubility limit of the constituent elements. A few soluble radionuclides, such as ⁹⁹Tc, will enter solution at the same rate glass dissolves, so the waste form dissolution rate determines their rate of release. ⁹⁹Tc from HLW is a key contributor to the annual dose to the RMEI in the first 10,000 year period (Section 2.1.2.2.6). HLW glass degradation depends upon the glass surface area and the surface area-normalized glass dissolution rate. The dissolution rate varies as a function of pH, being lowest at about pH 9 (Section 2.3.7.5.2). Many radionuclides, however, quickly saturate the solution, so the solubility limits of these radionuclides determine their rate of release.

- **Chemical Characteristics of Water in Waste Package**—The chemical characteristics of the water in contact with the waste package internals, including void spaces, and the waste form affect the degradation characteristics of the waste form, the solubility of radionuclides in the dissolved phase, and the stability of colloidal particles. These chemical effects are significant in affecting the release of low-solubility radionuclides (e.g., ^{90}Sr , ^{237}Np , ^{239}Pu , ^{240}Pu , ^{241}Am , and ^{243}Am) and radionuclides that may be released attached to colloidal particles (e.g., ^{239}Pu , ^{240}Pu , ^{241}Am , and ^{243}Am). Uncertainty in the in-package chemistry, in particular the ionic strength and pH that have the most significant effect on these coupled processes, has been considered in the in-package chemistry abstraction model used in the TSPA ([Section 2.3.7.5](#)).
- **Chemical Interaction with Corrosion Products**—The corrosion products of the steel and aluminum alloys in the waste package, and their control on the concentration of aqueous species, are of primary importance in determining the pH and ionic strength of the solution, which impact the alteration rates of the different waste forms, the solubility of radionuclides ([Section 2.3.7.12](#)), and the colloid concentration and stability in the waste package ([Section 2.3.7.11](#)). In addition, sorption of radionuclides onto waste package corrosion products will occur and can significantly slow the release of radionuclides from the waste package ([Section 2.3.7.12](#)). As discussed in *EBS Radionuclide Transport Abstraction* (SNL 2007c, Section 6.3.4.2), retardation of radionuclides will occur in the waste package corrosion products.
- **Radionuclide Solubility, Solubility Limits, and Speciation in the Waste Form and EBS**—Solubility limits of low-solubility dissolved radionuclides (e.g., ^{90}Sr , ^{237}Np , ^{239}Pu , ^{240}Pu , ^{241}Am , and ^{243}Am) significantly affect the amount of these radionuclides that may be released from the waste form through the other EBS features. Solubility models are presented in [Section 2.3.7.10](#). The more soluble the radionuclide, generally the greater mass flux of that radionuclide that will be released by diffusive or advective release mechanisms from the waste form. As presented in [Section 2.4.2.2.1.1.3](#), the radionuclides most significant to dose that are released by diffusion are highly soluble ^{99}Tc and ^{129}I .
- **Sorption of Dissolved Radionuclides in the EBS**—The degradation of the waste package inner vessel and internals (such as the TAD canister) results in a significant quantity of iron/chromium/nickel oxide materials. These materials have a significant amount of retardation potential, due to sorption, for a number of radionuclides that are potentially significant for the release from the waste form, including ^{90}Sr , ^{137}Cs , ^{237}Np , ^{239}Pu , ^{240}Pu , ^{241}Am , and ^{243}Am . This sorption significantly reduces the release of these radionuclides from the waste in the event that a breach in the waste package has occurred. The models used to evaluate radionuclide sorption are presented in [Section 2.3.7.12](#).
- **Reaction Kinetics in Waste Package**—Chemical reactions, such as radionuclide dissolution/precipitation reactions and reactions controlling the reduction–oxidation state, may not be at equilibrium within the waste package and may influence the in-package solution chemistry ([Section 2.3.7.5](#)), the solubility of radionuclides ([Section 2.3.7.10](#)), the degradation rate of HLW glass ([Section 2.3.7.9](#)), and radionuclide sorption onto corrosion products ([Section 2.3.7.12](#)). The effects of reaction kinetics on these processes and radionuclide releases from the waste package are included in the TSPA.

- **Diffusion of Dissolved Radionuclides in the EBS**—Diffusion is an important mechanism that transports dissolved radionuclides from the waste form surface to the waste package internals and then through the degraded waste package to the invert. Diffusion is controlled by the degree of degradation of the waste package and the hydrologic characteristics within the waste package, which, in turn, are a function of the type of waste ([Section 2.3.7.12](#)). The model presented in [Section 2.3.7.12](#) assumes there is a continuous water film if the relative humidity is greater than 95% and the temperature is less than 100°C through which radionuclides can diffuse.
- **Advection of Dissolved Radionuclides in EBS**—Once the drip shields fail and patch breaches in the waste package form, water may enter the waste package, dissolve radionuclides, and flow out, thereby generating advective releases of radionuclides. Patch breaches may form due to manufacturing defects (early failure), general corrosion, or seismic-induced rupture or puncture. When advective transport occurs, advective release rates of radionuclides from the waste package are typically greater than diffusive release rates, particularly for solubility-limited radionuclides (e.g., ^{90}Sr , ^{237}Np , ^{239}Pu , ^{240}Pu , ^{241}Am , and ^{243}Am) and radionuclides that may be released attached to colloidal particles (e.g., ^{239}Pu , ^{240}Pu , ^{241}Am , and ^{243}Am). Models used for the advective transport processes are presented in [Section 2.3.7.12](#).
- **Chemical Effects of Void Space in Waste Package**—Upon waste package breach, the inert gas initially present escapes and is replaced by humid air. The reaction of this air with waste package internals and the resulting changes in water chemistry influence the solubility characteristics of radionuclides, the degradation of waste package internals and the waste form, and the transport behavior of radionuclides released from the waste form. Chemical effects induced by the presence of voids in the waste package internals are included in models of in-package water chemistry ([Section 2.3.7.5](#)).
- **In-Package Criticality (Intact Configurations, Degraded Configurations Resulting from a Seismic Event (Intact and Degraded Configurations), and Resulting from Rockfall (Intact and Degraded Configurations))**—For a criticality event to occur, the appropriate combination of materials (e.g., neutron moderators, neutron absorbers, fissile materials, or isotopes) and geometric configurations favorable to criticality must exist. As documented in [Section 2.2.1.4.1](#) (SNL 2008b, FEPs 2.1.14.15.0A, In-package criticality (intact configuration); 2.1.14.16.0A, In-package criticality (degraded configurations); 2.1.14.18.0A, In-package criticality resulting from a seismic event (intact configuration); 2.1.14.19.0A, In-package criticality resulting from a seismic event (degraded configurations); 2.1.14.21.0A, In-package criticality resulting from rockfall (intact configuration); and 2.1.14.22.0A, In-package criticality resulting from rockfall (degraded configurations)) the probability of criticality for the in-package location is less than 1 chance in 10,000 of occurrence within 10,000 years after disposal. Therefore, in-package criticality is excluded from the performance assessment. Finally, although the criticality FEPs listed here are not identified as significant contributors to barrier capability in [Table 2.1-3](#), they are noted here because they do contribute to the reduction in probability of criticality.

- **DOE SNF Degradation (Alteration, Dissolution, and Radionuclide Release)**— Varying quality-level data exist on the DOE SNF fuel, so a bounding approach is used to account for uncertainty in the characteristics of the DOE SNF fuel, and the degradation rate of all DOE SNF (except naval waste packages) is bounded in the TSPA as instantaneous (SNL 2008a, Section 6.2.2.2). The degradation of DOE SNF waste strongly influences the pH of the water chemistry within the codisposal waste packages by buffering pH in the near-neutral range and therefore impacts radionuclide solubilities, colloid stability, and radionuclide mobility ([Section 2.3.7.5](#)).

Waste Package Pallet—The following process involving the waste package pallet is an important contributor to the capability of the EBS:

- **Seismic Ground Motion Damages EBS Components**—The waste package emplacement pallet provides mechanical stability for the waste package during a potential seismic event. A seismic damage abstraction model was not developed explicitly for the waste package pallet because it will not form new pathways for transport and release of radionuclides after strong vibratory ground motion events ([Section 2.3.4.5](#)). However, the effect of this EBS component on damage to, or failure of, the waste package is included in the waste package damage abstractions in that the mechanical effects of the pallet have been included in the structural calculations described in [Sections 2.3.4.5.2](#), [2.3.4.5.3](#), and [2.3.4.5.4](#).

As noted in [Table 2.1-1](#), the waste package pallet and emplacement drift invert are two features of the EBS that are not ITWI. However, they do contribute to the barrier capability of the EBS. The presence of the pallet can delay diffusive releases of radionuclides from the waste package to the invert, as long as the cradles remain intact and can support the waste package above the invert (SNL 2008a, Section 6.2.2.2). To simplify the modeling required, the EBS flow and transport model ([Section 2.3.7.12](#)) does not include this beneficial characteristic of the pallet and assumes that the waste package is in direct contact with the invert. The emplacement drift invert is composed of two parts: a steel invert structure and ballast (or crushed tuff). The invert provides a stable mechanical foundation for the waste package pallet and drip shield (SNL 2008a, Section 6.2.2.2). In the unsaturated repository environment, the crushed tuff in the invert sorbs radionuclides and slows the diffusive movement of radionuclides into the Lower Natural Barrier ([Section 2.3.7.12](#)).

The significant processes described above determine the manner in which the features of the EBS work together to prevent or substantially reduce the release of radionuclides from the waste and prevent or substantially reduce the rate of movement of radionuclides from the repository to the accessible environment. These processes and their effects on the EBS can be summarized as (1) chemical, thermal, and mechanical processes that affect the degradation of the drip shield and waste package; (2) thermal-hydrologic processes that affect the potential for liquid flow through cracks in degraded drip shields and waste packages; and (3) thermal and chemical processes that affect alteration of the waste form and waste package internals and transport from the waste form to the edge of the EBS. The most significant drip shield and waste package degradation processes are related to mechanical degradation processes associated with likely and unlikely seismic events that cause through-wall stress corrosion cracks ([Section 2.3.4.5](#) and [2.4.2.2](#)). The most significant thermal-hydrologic processes are related to water entering the waste package. However, tight flow paths through potential cracks prevent liquid flow into the waste package and limit the radionuclide

release process to follow a diffusive path through the waste package (Section 2.3.7.12). The most significant thermal and chemical processes are related to waste form degradation, corrosion of internal materials, and diffusive transport processes limited by the low solubility of the radionuclides that are a significant fraction of the total inventory (notably ^{90}Sr , ^{239}Pu , ^{240}Pu , ^{241}Am , and ^{243}Am), as well as the sorption of these radionuclides onto iron oxide and other degradation products in the waste package (Section 2.3.7.12).

The models developed to represent the physical and chemical environment in the emplacement drift are described in Section 2.3.5. The drip shield and waste package degradation models are described in Section 2.3.6. Models for mechanical degradation of the drip shield and waste package due to seismic effects are described in Section 2.3.4. The TSPA model integrates the models of degradation processes with models used to describe the environment within the emplacement drift. The discussion of drip shield and waste package performance in Section 2.1.2.2.1 is based on projections produced using the TSPA model.

The waste form degradation models, as well as the in-package chemistry and radionuclide solubility models described in Section 2.3.7, are implemented in the TSPA model. Similarly, the model for EBS transport that is described in Section 2.3.7.12, which simulates the mobilization and movement of radionuclides from inside the waste package to and through the invert, is implemented in the TSPA model. The TSPA model integrates the degradation, mobilization, and transport models with other components, such as those used to describe the chemical and physical environment within the emplacement drift (Section 2.3.5). The radionuclide release curves presented in Section 2.1.2.2.6 to describe the capability of the EBS to prevent or substantially reduce radionuclide movement are produced using the TSPA model.

2.1.2.2.1 Capability of the Engineered Barrier System to Prevent or Substantially Reduce the Contact of Seepage with the Waste Form

The capability of the EBS to prevent or limit the movement of water and prevent contact between water and waste depends on the integrity of the drip shields and waste packages. Should the majority of waste packages remain intact for hundreds of thousands of years, as expected, only a limited number of the waste forms will be exposed to water during this period. The data and analyses used to assess waste form degradation are discussed in detail in Sections 2.3.7.6 to 2.3.7.9. The possibility of early failure of some waste packages due to fabrication errors, as well as the effects of seismic-induced mechanical damage, have been considered in evaluating the overall barrier capability.

The drip shield (Section 1.3.4) is designed to divert seepage away from the waste package. It prevents water from contacting the waste package as long as it remains intact. The waste packages prevent water from contacting the waste forms. As long as the waste packages are intact, moisture cannot contact the waste forms. The Zircaloy cladding that encases much of the commercial SNF would also prevent the contact of seepage with the waste form as long as it remains intact. This capability is not considered in the TSPA, or in the quantitative analysis of barrier capability presented in Section 2.1.2.2.6. A detailed description of the testing data, geochemical constraints, and models of drip shield, waste package, and cladding integrity is presented in Sections 2.3.6 and 2.3.7.

The degradation rates for general corrosion of Titanium Grade 7 are sufficiently low so that even the highest measured rates would not lead to failure of the drip shield for over 150,000 years (Section 2.3.6.2.3). Seismic-induced stress corrosion cracking is not expected to have significant consequences to drip shield performance, and is excluded from the TSPA (SNL 2008b, FEP 2.1.03.02.0B, Stress corrosion cracking of drip shields). Localized corrosion that is induced by seepage or by deliquescence will not occur in repository environments and is excluded from TSPA (SNL 2008b, FEPs 2.1.03.03.0B, Localized corrosion of drip shields, and 2.1.09.28.0B, Localized corrosion on drip shield surfaces due to deliquescence). Early failure of a very small number of drip shields potentially may occur due to flaws that are undetected during fabrication and handling (SNL 2008d, Section 6.4.1). These types of flaws would diminish the drip shield's ability to withstand dynamic and static loads caused by seismic activity. However, they are treated in the TSPA model as an immediate and complete failure, which means loss of protection of the waste package from seepage or drift degradation at the time of repository closure (Section 2.4.2.2.1).

The degradation rates for general corrosion of Alloy 22 are sufficiently low that mean breach time of the waste packages due to general corrosion will be distributed over many hundreds of thousands of years, beginning at about 600,000 years from the 95th percentile curve value (Section 2.1.2.2.6). Although stress corrosion cracking may occur in the closure-lid weld regions of some of the waste packages, mitigation techniques are employed to reduce residual stresses below the stress corrosion cracking initiation threshold (Section 2.3.6.5). However, stress corrosion cracking can eventually initiate—beginning after about 100,000 years (Section 2.1.2.2.6)—as general corrosion removes the stress-mitigated layer. Stress corrosion cracking of Alloy 22 may also occur as a result of residual stresses caused by mechanical impacts during seismic events. Such stress cracks are small and tight and limit the movement of water that could potentially contact the waste form and reduce the release rate of radionuclides from the waste packages (Section 2.3.6.1). Localized corrosion is only possible in those cases where the drip shield fails to perform its function and certain aggressive incoming seepage potentially contacts the waste package (Section 2.3.6.1.1). This condition may occur in the unlikely case where seismic ground motion is accompanied by fault displacement, as described in Section 2.3.4, or in the case of early drip shield failure. Early failure of a small number of waste packages potentially may occur due to flaws that are undetected during fabrication and handling, as discussed in Section 2.3.6.6.

No performance credit is taken for the ability of the stainless-steel inner vessel or TAD canister to preclude or limit water influx into the waste package once the Alloy 22 outer corrosion barrier is breached (Section 2.3.6.2.2). However, performance credit is applied in the TSPA for the increase in waste package structural strength and accompanying resistance to seismic damage due to the inclusion of the inner vessel and the TAD and naval canisters.

Credit is taken for naval SNF structure, including cladding. Although no credit is taken for the contribution of commercial SNF cladding to barrier performance, it is expected that cladding will be largely intact in the repository environment (Section 2.3.7.6), except after being subjected to seismic-initiated events, and therefore will provide some capability to prevent or delay radionuclide releases from the waste form.

2.1.2.2.2 Capability of the Engineered Barrier System to Prevent the Release or Substantially Reduce the Release Rate of Radionuclides from the Waste and Transport to the Lower Natural Barrier

In the event that waste packages are breached, the release rate of radionuclides is limited by the characteristics and behavior of the EBS. The release of radionuclides is first impeded by the rate of degradation of the waste form. Waste form degradation cannot begin until the waste package is breached, allowing the ingress of air and water. Because of the unsaturated environment, the elevated temperatures within waste packages, and the presence of drip shields and waste packages, the amount of water in contact with the waste form is expected to be limited as long as decay heat exists. The data and analyses used to assess waste form degradation are discussed in detail in [Sections 2.3.7.6 to 2.3.7.9](#).

Release of radionuclides out of the waste package depends on the chemical environment within the waste package and on moisture conditions within the waste package. Release can only occur if radionuclides are dissolved in water and/or attached to colloids, and if there are continuous liquid pathways in the waste package, including thin films of adsorbed water. Slow diffusive transport of radionuclides can occur in these thin films. Advective transport of radionuclides out of the waste package and EBS can occur only if breaches are sufficiently open to permit flow and there is a liquid flux of water through the waste package and invert. Waste heat and evaporation from hot surfaces within the waste package will prevent moisture from entering the waste package and subsequently forming continuous liquid pathways for diffusive transport. Continuous liquid pathways will form only when the waste cools and relative humidity in the waste package increases sufficiently ([Section 2.3.7](#)). Continuous pathways may not form in the hotter commercial SNF waste packages for several thousand years ([Section 2.4.2.2.1.2.4.2](#)).

The transport of many dissolved radionuclides, including those that are the greatest contributors to the total inventory activity, such as ^{90}Sr , ^{137}Cs , ^{239}Pu , ^{240}Pu , ^{241}Am , and ^{243}Am , is retarded by sorption on iron corrosion products within the waste package (SNL 2008a, [Section 6.2.2.2](#)). The retardation depends on the volume of these corrosion products and on the distribution coefficients associated with them. Sorption onto the corrosion products also reduces movement of those radionuclides reversibly attached to colloids in the water. The mobilization and transport of radionuclides out of breached waste packages and through the invert in the EBS are described in [Sections 2.3.7.10, 2.3.7.11, and 2.3.7.12](#). The radionuclide inventory released from the EBS would be limited by diffusive transport if (1) the drip shield remains intact; or (2) the waste package breach is a stress-induced crack. Although advective transport is not expected from the waste package for hundreds of thousands of years after closure, both diffusive and advective transport are considered in the calculation of radionuclide releases from the invert feature of the EBS, starting at the time of repository closure, as presented in [Section 2.3.7.12](#).

2.1.2.2.3 Time Period over Which the Engineered Barrier System Functions

The EBS consists of features that are designed, fabricated, and constructed to perform their functions for well beyond 10,000 years. Through the appropriate use of thick, diverse, corrosion-resistant materials, the drip shields and the waste packages are expected to remain intact for tens to hundreds of thousands of years. The EBS features will gradually degrade during the 1,000,000-year period of geologic stability. This process will result in the slow release of

radionuclides over extended periods of time. Some components, such as the waste packages, are expected to contribute substantially to barrier performance up to and beyond 1,000,000 years.

The capability of the drip shield and the waste package to prevent or reduce the movement of water and radionuclides is not impacted until sufficient corrosion has occurred to cause through-wall breaches in the waste packages. General corrosion and stress corrosion cracking, along with seismic-initiated mechanical damage, will cause through-wall breaches in the waste package. Detailed discussion of the models for degradation of the drip shields and waste packages can be found in [Section 2.3.6](#), and the changes in repository conditions over time under nominal conditions can be found in [Section 2.3.5](#). Detailed discussion of models for seismic-induced mechanical damage to the waste package and drip shield can be found in [Section 2.3.4](#). A summary discussion of the thermal environment within the emplacement drift, and how it evolves in time with respect to corrosion and condensation, is presented below followed by a summary of TSPA drip shield and waste package performance projections. These projections are presented first for nominal degradation processes, and then for seismic-induced mechanical damage. A more complete description of drip shield and waste package performance is presented in [Section 2.1.2.2.6](#).

The environment within the emplacement drift evolves through three main stages. The initial stage includes the heat-up after closure, with the drift wall and waste package surface temperatures increasing above the boiling point of water, then reaching their peak temperatures. This is followed by a subsequent cool down period in which the drift wall and waste package surface temperatures continue to be above the boiling point of water. No seepage is expected during this period due to vaporization ([Section 2.3.3.3](#)) and capillary diversion effects ([Section 2.3.3.2](#)). Any water vapor that flows from the host rock into the drift will be transported axially toward unheated regions at either end ([Section 2.3.5.4.2.1](#)). The unheated regions are cooler so that condensation is possible (SNL 2007d, Section 6.3.3.1). Deliquescent brine films may form from salts or moisture in the air if the temperature is below the deliquescence point. Given the low volumes and high nitrate concentrations of such brines, even if they were to form and be stable, localized corrosion is not expected to occur under these films (SNL 2008b, Excluded FEPs 2.1.09.28.0A, Localized corrosion on waste package outer surface due to deliquescence; and 2.1.09.28.0B, Localized corrosion on drip shield surfaces due to deliquescence). This dryout period is expected to last for several hundred to more than 1,000 years, depending on the location in the repository. Elevated temperatures would persist longer near the center of the repository and would dissipate more quickly at the edges of the repository (SNL 2008e, Section 6.1.4 and Figure 7.8-10[b] through 7.8-17[b]).

The second stage is the transition period, during which drift wall temperatures drop below the boiling point of water and the waste package surface temperature is near the boiling point of water and localized corrosion on the waste package surface is possible under certain geochemical conditions. The emplacement drifts will enter this stage at the edges of the repository first, where heat dissipates more quickly. It is during this transition period when drift wall temperatures are above and below the boiling point of water in different parts of the repository that water evaporated from the emplacement drift walls and is transported primarily by natural convection from warmer to cooler areas, where it condenses on cooler surfaces. In those regions where drift wall temperatures are below the boiling point of water and waste package surface temperatures are near 100°C, waters from the rock (seepage) and condensation can fall onto hot metal surfaces. Evaporative concentration of seepage may produce aggressive chemistry that is more conducive to localized corrosion for Alloy 22 ([Section 2.3.6.4](#); SNL 2008d, Section 6.3.3, and Appendix O).

Condensation that forms on the drip shield or waste package surface, or that occurs in the absence of seepage, is assumed to have a benign composition with respect to the corrosion environment because it is dilute (SNL 2008b, FEP 2.1.08.14.0A, Condensation on underside of drip shield). Should the drip shield fail to perform its function, these seepage and condensation waters may fall on the waste package. However, given the absence of drip shield failure during this transition period, except in the rare case of early drip shield failure and the unlikely occurrence of a damaging fault displacement event, localized corrosion is not expected to be initiated in environmental conditions relevant to the repository (SNL 2008d, Section 6.3.5.2.3). In the rare case of early drip shield failure, it was assumed in the TSPA that a waste package under an early failed drip shield would fail completely due to localized corrosion if the drip shield is being seeped on (SNL 2008d, Section 6.4.1.3). This assumption is conservative with respect to barrier capability because a smaller failure would reduce the release rate of radionuclides from the waste and waste package. In addition, for the case where drip shields and waste packages are damaged by a fault displacement event, analyses show that any additional damage caused by localized corrosion would not significantly impact radionuclide release from already damaged waste packages (SNL 2008d, Section 6.3.5.2.3).

The third stage is the period in which drift wall and waste package surface temperatures have further decreased, and the likelihood of localized corrosion on the waste package surface progressively decreases until it reaches the point, after about 12,000 years, when it will no longer occur (SNL 2008d, Volume 3, Appendix O). During this stage the relative humidity within the drift increases. At the locations of cooler waste packages, especially in the outer portions of the drift, relative humidity may achieve 100% so that condensation occurs. At the hotter locations (the central portion of the drift and hotter waste packages in the outer portions of the drift), the relative humidity remains below 100%, evaporation in the host rock continues, and condensation does not occur. TSPA projections indicate that condensation will cease throughout the repository by approximately 2,000 years (Section 2.1.2.2.6). This period lasts for the remainder of the regulatory period of geologic stability. General corrosion and stress corrosion cracking, along with seismic-initiated mechanical damage, may still occur. Detailed discussion of the degradation of the drip shields and waste packages and the changes in repository conditions over time can be found in Sections 2.3.6 and 2.3.5, respectively. The TSPA models presented in Section 2.3.6 for nominal waste package degradation processes show that drip shield failures by general corrosion are not expected to occur until after about 270,000 years, and most of the drip shields would fail by 340,000 years (Section 2.1.2.2.6). Waste packages, on average, are not expected to begin to fail until after 100,000 years, with breaches caused by through-wall stress corrosion cracks in the weld of the outer closure-lid. About 54% of the waste packages are estimated to fail by stress corrosion cracking by 1,000,000 years (Section 2.1.2.2.6). General corrosion failures would start, on average, at approximately 600,000 years (from the 95th percentile value) and about 9% of the waste packages would experience a general corrosion breach in 1,000,000 years (also the time of general corrosion failure is the same for both commercial SNF and codisposal waste packages). Diffusion is the only transport mechanism acting to release radionuclides from a waste package when cracks are the only penetration through the waste package.

As the emplacement drift environment evolves (as described above) the mechanical state of the EBS components evolves as well. Manufacturing and handling defects may result in the early failure of drip shields (Section 2.3.6.8) and waste packages (Section 2.3.6.6). The types of manufacturing and handling defects are discussed in detail in Section 2.3.6.6. Within the TSPA model, early failure of

a defective drip shield and waste package is conservatively modeled to occur at the time of repository closure. As noted above, under nominal conditions, drip shields are expected to remain intact for several hundred thousand years. Also, under nominal conditions, the waste packages are expected to fail by general corrosion at much later times than the drip shields. For example, a propagation rate of 7.5 nm/yr, which is the mean corrosion rate for creviced Alloy 22 samples at 60°C, is equivalent to more than 130,000 years per millimeter of passive metal loss (Section 2.3.6.3). Over time earthquakes are expected to occur with a shaking intensity at the repository horizon described by the bounded hazard curve (Section 2.3.4.3). The mechanical consequence of this seismic shaking on the EBS components depends not only on the intensity of the seismic event, but also on the condition of the EBS components. The EBS components will thin over long time periods as a result of nominal corrosion processes. The drift, itself, will undergo degradation over time as it is subjected to repetitive seismic events. The analyses presented in Section 2.3.4.4.3 show that the drifts are expected to be stable with minimal rockfall during the thermal loading phase of the repository. Time-dependent (non-seismic) failure of the rock mass around the emplacement drifts has been excluded from the TSPA because it will have a minor impact on drift degradation (FEP 2.1.07.02A, Drift collapse (SNL 2008b, Section 6.2)). However, seismic events have the potential to result in rockfall from the drift roof and walls, with partial to complete filling of the emplacement drift with rock rubble over longer times. While the drip shields remain intact, the waste packages and pallets beneath them are free to translate in response to seismic shaking. In this configuration, the primary mechanism for mechanical damage to the waste package and drip shield is from plastic deformation (and potential stress corrosion cracking) resulting from impacts from seismic shaking (Section 2.3.4.5). As time evolves in the range of hundreds of thousands of years, general corrosion of the drip shield—coupled with static and dynamically-amplified rubble loads from repetitive seismic events—are expected to buckle the drip shield framework and, eventually, lead to the rupture of the drip shield plates. Failure of the drip shield leads to two distinct waste package configurations (Section 2.3.4.5). These configurations are referred to as damage for a waste package beneath (loaded by) a buckled drip shield, and damage for a waste package surrounded by rubble, respectively.

The different waste form types (commercial SNF, DOE SNF, and HLW glass) degrade at different rates once they are exposed to the humid air and oxidizing conditions following a breach of the waste package. These rates, and their dependency on the environment, are presented in Sections 2.3.7.7, 2.3.7.8, and 2.3.7.9, respectively.

Degradation of the materials used in the pallet supporting the waste package may occur by mechanical or chemical degradation processes. Mechanical processes have been determined not to result in a significant adverse change in the magnitude or timing of radionuclide releases to the accessible environment and are excluded (SNL 2008b, FEPs 2.1.06.05.0A, Mechanical degradation of emplacement pallet, and 2.1.06.05.0C). However, thinning of the waste package emplacement pallet due to chemical degradation is included in seismic analyses, and may affect the long-term performance of the EBS (SNL 2008b, FEP 2.1.06.05.0C, Chemical degradation of emplacement pallet).

The invert is anticipated to provide a stable mechanical foundation for the waste package pallet and drip shield for at least 10,000 years after closure. Although chemical and mechanical changes may occur in the invert, these changes do not significantly affect the transport characteristics of the invert (SNL 2008b, Section 6.2, FEPs 2.1.06.05.0D, Chemical degradation of invert, and 2.1.06.05.0B,

Mechanical degradation of invert). The transport characteristics of the invert that affect radionuclide release from the EBS are presented in [Sections 2.3.7.12](#) and [2.4.2.3.2.1.7](#).

2.1.2.2.4 Uncertainties Associated with Engineered Barrier System Capability

Uncertainty in the representation of the capability of the EBS arises primarily from uncertainties in environmental conditions (e.g., thermal and chemical conditions) and from uncertainties in the various degradation processes. These uncertainties are described in detail in [Sections 2.3.5](#) and [2.3.6](#). These include uncertainties in the data from tests measuring the various degradation processes, and uncertainties in the models used to analyze both environmental conditions and degradation processes. These uncertainties are incorporated probabilistically in the models for thermal-hydrologic conditions, waste form degradation, radionuclide transport, radionuclide solubility, and radionuclide sorption by sampling across uncertainty ranges in the inputs to these models. Similarly, uncertainty in corrosion or degradation processes is also represented by sampling degradation parameters across their uncertainty ranges. These uncertainties are analyzed directly in the TSPA model with multiple realizations. For each realization, input and parameter values are sampled and a complete simulation of the EBS thermal and chemical environment is performed that includes the resulting drip shield and waste package degradation, waste form degradation, and radionuclide mobilization. Accordingly, multiple realizations represent the range of uncertainty in the EBS capability, as modeled. Uncertainties in the environmental conditions affecting the degradation of the waste package (Alloy 22) and the drip shield (Titanium Grade 7), including general corrosion, microbially influenced corrosion, stress corrosion cracking, and localized corrosion, are summarized below. Note that model uncertainty has been assessed by comparison with alternative conceptual models of EBS processes. [Sections 2.3.6](#) and [2.3.7](#) describe the alternative conceptual models considered for the various EBS processes, and provide the rationale for selection of the preferred models for implementation in the TSPA. In general, alternative conceptual models were not incorporated directly into the probabilistic analysis of uncertainty; rather, the conceptual models implemented in the TSPA were selected because they provide a conservative yet reasonable assessment of performance, and preclude the need for detailed treatment of uncertainty as a consequence of the approach taken and assumptions made in modeling of the system.

A source of uncertainty in the Alloy 22 general corrosion model is a potential temperature dependence of the general corrosion rate. The use of a temperature dependence term is appropriate because the general corrosion (passive dissolution) of highly corrosion-resistant alloys (such as Alloy 22) is governed by the transport properties of reacting species in the passive film and the rate of activation-controlled ion transfer at the film–solution interface, both of which are thermally activated processes ([Section 2.3.6.3.2.2](#)). Data from short-term polarization-resistance data for Alloy 22 samples tested for a range of sample configurations, metallurgical conditions, and exposure conditions (temperature and water chemistry) indicate a temperature dependence. Accordingly, the general corrosion model addresses temperature dependence and uncertainty in the temperature dependence data consistent with the short-term polarization-resistance tests ([Section 2.3.6.3.2.2](#)). Uncertainty associated with projection of Alloy 22 general corrosion rates, based on the five-year test data to the 10,000 years after closure, is bound in the TSPA by applying time-independent, constant general corrosion rates. As discussed in [Section 2.3.6.3.2](#), the general corrosion rates of metals and alloys decrease with time.

Nickel-based alloys, such as Alloy 22, are resistant to microbially influenced corrosion. Microbially influenced corrosion is represented within the TSPA as a rate multiplier on the general corrosion rate of Alloy 22, with a uniform distribution between 1 and 2. Titanium Grade 7 is shown not to be susceptible to microbially influenced corrosion, and, therefore, no multiplier is applied to this material. A detailed discussion of the effects of microbially influenced corrosion on these materials is provided in [Section 2.3.6](#).

Stress corrosion cracking may occur and contribute to the degradation of Alloy 22 and Titanium Grades 7 and 29. The sources of uncertainty in the stress corrosion cracking model have been considered in analyses of waste package degradation. These analyses consider an expanded range of parameter values for the residual stress profile in closure-lid weld regions of waste packages, the threshold stress for stress corrosion crack initiation, and the orientation of the weld flaws. The modeling of stress corrosion cracking for Alloy 22 and Titanium Grades 7 and 29 is discussed in [Section 2.3.6.5](#) and [2.3.6.8](#), respectively. The effects of seismic-induced motion and rockfall on stress corrosion cracking are discussed in [Section 2.3.4.5](#).

Uncertainty in the possible initiation and propagation of localized crevice corrosion is a function of the chemical environment on the waste package surface, as well as the uncertainty in the functional dependency of the corrosion potential and critical potential to the thermal-chemical environment. Uncertainty in the chemical environment for both aqueous and salt-deliqescence conditions has been included in the models presented in [Section 2.3.5](#). Uncertainty in the data used to develop the functional dependence, in particular the effect of variable chloride, nitrate, and chloride-to-nitrate ratios, has been included in the localized corrosion model described in [Section 2.3.6](#).

Uncertainty in the characterization of the degradation of the waste form and in the mobilization and transport of radionuclides through the EBS arises primarily from uncertainties in the inputs for the models of the various degradation and transport processes. These uncertainties are described in [Section 2.3.7](#). These uncertainties include, for example, the initial mass of each radionuclide per waste package, in-package pH and ionic strength, porosity of the commercial SNF, gap and grain boundary inventories, fuel specific surface area, HLW glass degradation rate and surface area exposure coefficients, equilibrium constants used to predict radionuclide solubilities, sorption coefficients and sorption rate constants for radionuclide sorption in the waste package and invert, and corrosion rates for waste package internals (such as the inner vessel and the TAD canister). These uncertainties are incorporated probabilistically in TSPA by using ranges of parameter values in the models for the chemical and physical environments and for the rates of the various degradation and transport processes, as well as dissolved concentration limits. The ranges of parameters and process rates used in the performance model are based on the results of testing and analysis, as well as on the fundamental physical principles that apply.

2.1.2.2.5 Impact of Disruptive Events on the Engineered Barrier System

Disruptive events may significantly impact the features of the EBS ([Sections 2.3.4.5](#) and [2.4.1](#)); however, as discussed in [Sections 2.1.2.1.5](#) and [2.1.2.3.5](#), the natural barrier features remain generally intact and continue to prevent or substantially reduce the rate of movement of water or radionuclides from the repository to the accessible environment following the occurrence of a disruptive event.

Seismic activity may cause sufficiently high levels of ground motion to result in mechanical interactions between waste packages, or between a waste package and the waste package pallet, which may, in turn, cause waste packages to develop small stress corrosion cracks. In addition, the accumulation of rubble as well as drift collapse caused waste package damage and failure. Lithophysal rubble is selected for the calculation of load on waste packages (Section 2.4.2.3.2.1.12.3). However, seismic events are not expected to significantly affect the performance of the drip shield with respect to its function of protecting the waste package from the potential effects of seeping water or rockfall for about the first 240,000 years after repository closure. Should the degraded EBS lose its ability to prevent or substantially reduce the release rate of radionuclides from the waste, the Lower Natural Barrier remains intact to prevent or substantially reduce the rate of movement of radionuclides to the accessible environment. A complete discussion of the effects of seismic activity on the EBS is provided in Section 2.3.4. The effect of seismic events on the capability of the EBS was summarized in Section 2.1.2.2.3 and is evaluated in Section 2.1.2.2.6.

Should an unlikely igneous event occur, it is estimated that the EBS would be subjected to significant damage. There are two components of an unlikely igneous event: an eruptive component and an intrusive component (Sections 2.3.11 and 2.4.1). In the eruptive component of an igneous event, the rising magma conduit interacts with an uncertain small number of waste packages (i.e., a maximum of seven waste packages), destroying the waste packages and releasing the contained radionuclides in the erupting material.

In the intrusive component of an unlikely igneous event, the rising magma is assumed to interact with the entire inventory in the repository. Although complete destruction of the affected waste packages is not expected, the ability of the EBS to prevent water from contacting the waste is assumed to be completely compromised. The general performance of the natural barriers continues once the drifts return to temperatures less than the boiling point of water (Section 2.3.11.3.1). A discussion of the effects of igneous activity on the EBS is provided in Section 2.3.11.3.

2.1.2.2.6 Quantification of the Engineered Barrier System Capability

This section evaluates the capability of the EBS to provide the principal barrier functions of (1) preventing or substantially reducing the rate of movement of water to the waste; (2) preventing or substantially reducing the rate of release of radionuclides from the waste; and (3) preventing or substantially reducing the rate of movement of radionuclides from the repository to the accessible environment. The first barrier function is provided by the emplacement drift, drip shield, and waste package outer barrier (Figure 2.1-7), whereas the second and third functions are provided by the waste forms and waste package internals and the waste package. As described in Section 2.1.2, EBS capability is evaluated first for future repository conditions in the absence of disruptive events by discussing TSPA model results for a combined nominal/early failure demonstration modeling. TSPA model results for the seismic ground motion modeling case are also included in the evaluation of EBS barrier capability to assess the significance of degradation and alteration of EBS features following seismic events.

To develop a basis for assessing the capability of the EBS to achieve the first barrier function, projections for three barrier capability metrics were developed for the drip shield and waste package. The first metric is the failure time profile; this metric is quantified in terms of a cumulative

probability distribution function for failure time of the drip shield plates (Titanium Grade 7). Drip shield failure is defined as a hole or opening through the 15-mm-thick drip shield plate. Breach of the plate by stress corrosion cracking is not considered as a drip shield failure because a crack-damaged drip shield will still perform the drip diversion function and, thus, prevent seepage water from contacting the underlying waste package (SNL 2008d, Section 8.3.3.2[a]). The second capability metric is the waste package breach time profile; in this metric, a breach is defined as a penetration of the outer barrier, by either cracks or patch openings. In the combined nominal and early failure modeling case, waste package breaches include crack breaches due to stress corrosion cracking of the closure-lid welds, and patch breaches of the waste package outer barrier due to general corrosion penetrations. In the seismic ground motion modeling case, crack breaches include seismically-induced stress corrosion cracking of the waste package outer barrier as well as stress corrosion cracking of the closure-lid welds. Patch breaches include seismically-induced rupture and puncture, in addition to general corrosion penetrations. In addition, a third metric, the capability of the EBS to retain radionuclides, is developed to evaluate the second barrier function and is discussed later in this section.

Insights into potential waste package breach modes were developed by examining the breach characteristics of the individual modeling cases. For the combined nominal and early failure modeling case, two waste package breach characteristics were calculated and are presented here:

1. Fraction of waste packages breached by general corrosion (i.e., patch penetration) as a function of time
2. Fraction of waste packages breached by cracks (i.e., nominal process stress corrosion cracking in closure welds) as a function of time.

The following three waste package breach characteristics (SNL 2008d, Section 8.3.3.2[a]) for the seismic ground motion modeling case are presented and discussed:

1. Fraction of waste packages breached by nominal and seismic ground-motion induced processes as a function of time
2. Fraction of waste package surface area breached by nominal and seismic ground-motion induced stress corrosion cracks per breached waste package as a function of time
3. Fraction of waste package surface area breached by patches resulting from general corrosion, and seismic induced puncture and rupture failure mechanisms per breached waste package as a function of time.

The degradation of the waste package by general corrosion is modeled by subdividing the outer barrier surface into subareas referred to as patches, which are used to simulate the variability of general corrosion across the waste package surface. The general corrosion model is applied at the patch level, such that each patch might have a different general corrosion rate (Section 2.3.6.3.4.1). When one or more patches are penetrated, the waste package is considered to be breached. In the case of the codisposal waste packages, the outer surface area is divided into 1,430 patches; the commercial SNF waste package is divided into 1,408 patches (SNL 2008d, Section 6.3.5.1.2). In

the case of seismic-induced stress corrosion cracking of the waste package outer barrier, the damaged area is conceptualized as a tightly spaced network of cracks (SNL 2008d, Section 6.6.1.1.2).

In the following discussion, waste package performance is generally presented in terms of mean barrier capability metrics and breach characteristics. To illustrate uncertainty in these metrics and characteristics, quantiles (median, 5th, and 95th percentiles) are also shown. It is important to note that the TSPA model computes waste package degradation metrics and breach characteristics for each of five percolation subregions that represent the repository footprint. The graphical results presented in the following sections for the waste packages were computed as a weighted average combining all of the five percolation regions to arrive at a representation for the entire repository.

An assessment of the EBS capability was developed based on probabilistic projections of mean radionuclide activity (in curies) released from the EBS as a function of time. This barrier capability metric is calculated using the inventory balance equation:

$$\bar{R}_{EBS,k}(\tau|\mathbf{e}) = \bar{A}_{T,k}(\tau|\mathbf{e}) - (\bar{A}_{WP,k}(\tau|\mathbf{e}) + \bar{A}_{I,k}(\tau|\mathbf{e})) \quad (\text{Eq. 2.1-1})$$

where $\bar{R}_{EBS,k}(\tau|\mathbf{e})$ is the expected (average over aleatory uncertainty) activity (Ci) of radionuclide k released from the EBS; $\bar{A}_{T,k}(\tau|\mathbf{e})$ is the expected activity (Ci) of radionuclide k in the inventory disposed in the geologic repository (initial inventory decayed through time); $\bar{A}_{WP,k}(\tau|\mathbf{e})$ is the expected activity (Ci) of radionuclide k retained in the waste packages (including the activity still in undegraded waste forms); and $\bar{A}_{I,k}(\tau|\mathbf{e})$ is the expected activity (Ci) of radionuclide k retained in the invert. The term τ is time, and \mathbf{e} is the set of epistemically uncertain parameters, which are sampled in the Monte Carlo simulation (Section 2.4.2.3.3) (SNL 2008d, Section 8.3.3.2[a]). The activity quantities, $\bar{A}_{T,k}(\tau|\mathbf{e})$, $\bar{A}_{WP,k}(\tau|\mathbf{e})$, and $\bar{A}_{I,k}(\tau|\mathbf{e})$, are obtained from the Monte Carlo simulation performed with the TSPA model.

As noted above, radionuclide releases from the EBS are presented in units of activity (i.e., curies). A curie is the original unit used to describe the intensity of radioactivity in a sample of material. One curie equals 37 billion disintegrations per second, or approximately the radioactivity of 1 g of radium. This unit is not part of the International System (SI) of Units. The SI unit is the becquerel (Bq), which equals one disintegration per second (1 Bq = 27 pCi). Activity was used as the metric of significance from a barrier capability perspective because activity is most closely related to the radiological hazard (i.e., the greater the activity, the greater the affect of the radioactivity on the human tissues and organs). Mass is used in Section 2.4.1 because radioelement solubility constraints and retardation characteristics are provided in mass units. The relationship between radionuclide mass and radionuclide activity is dependent on the radionuclide and is presented in Table 2.3.7-5.

Basis for EBS Barrier Capability Projections—The conceptual models and mathematical basis for drip shield and waste package degradation can be found in Section 2.3.6. An important aspect to note is that the drip shield degradation abstraction does not implement spatial variability for general corrosion rates. This means that in a given epistemic realization of the Monte Carlo simulation process, the sampled drip shield failure time applies to all drip shields in the repository

(i.e., the drip shields fail in unison at the sampled failure time by general corrosion). The stochastic model parameters for drip shield general corrosion are derived from laboratory data for general corrosion of the Titanium Grade 7 samples ([Section 2.3.6.8](#)). Similarly, the experimental basis for the waste package degradation models and parameters can be found in [Section 2.3.6.3](#).

Probabilistic projections for drip shield and waste package breach time profiles were developed to provide insight into barrier capability. These projections (SNL 2008d, Sections 8.3.3.2[a] and 8.3.3.2.1[a]) used an optimized version of the TSPA model to efficiently calculate drip shield and waste package performance under nominal and seismic conditions. The optimized version of the TSPA model uses the same Monte Carlo simulation approach as the full TSPA model, which incorporates aleatory and epistemic uncertainties into the projections in two separate computational loops:

1. An outer calculational loop that samples probability distributions for model parameters with epistemic uncertainty using the Latin hypercube sampling technique (Helton and Davis 2002)
2. An inner loop that samples, for each epistemic set, values from probability distributions of parameters describing aleatory uncertainty (i.e., randomness) in the occurrence of events.

The optimized version of the TSPA model uses the same samples for aleatory and epistemic uncertainty that are used to produce the TSPA model results shown in [Section 2.4](#).

For the combined nominal/early failure demonstration modeling case, the probabilistic analysis of drip shield capability included general corrosion of the drip shield plates. Other drip shield corrosion mechanisms such as stress corrosion cracking and localized corrosion have been screened out ([Table 2.2-5](#)). As described in [Section 2.3.6.2](#), the degradation of the topside of the drip shield plate is based on a corrosion rate model for an aggressive water chemistry environment, whereas the underside surface degradation is based on a corrosion rate model for water chemistry that is representative of a benign environment. For the waste packages, the probabilistic analysis included general corrosion, microbially influenced corrosion, and stress corrosion cracking in the closure-lid weld region ([Section 2.3.6.2](#)).

As described in [Section 2.4.2.2.1](#), drip shield and waste package early failure mechanisms are represented by conservative assumptions. The early failure modeling cases assume (1) a through-wall penetration of a waste package or drip shield caused by manufacturing or handling-induced defects; and (2) penetration occurring at the time of repository closure. In the case of the early drip shield failure, the penetration of the Titanium Grade 7 plate is assumed to represent complete failure of the drip shield. In addition, if an early failed drip shield is located in a seeping environment, it is assumed that the surface of the underlying waste package is completely degraded by localized corrosion processes. In the case of early waste package failure, it is assumed that the entire surface of the waste package is completely degraded. The numbers of drip shield and waste package early failures are simulated in the TSPA model as random Poisson processes ([Section 2.4.2.2.1](#)).

For the seismic ground motion modeling case (Section 2.4.2.2.1), analysis of the seismic impacts to the drip shield and waste package degradation was performed by first applying WAPDEG (Section 2.4.2.3.2.1.5) to simulate the nominal corrosion processes, then transferring the calculational results to GoldSim to evaluate damage and breaches caused by vibratory ground motion. Details of the associated model implementation are discussed in Sections 6.6.1.3 and 6.6.2.3 of the TSPA (SNL 2008d). Localized corrosion of the waste packages was analyzed with a standalone model, and was shown not to impact the seismic ground motion modeling case (SNL 2008d, Section 6.3.5.2.3).

EBS Capability to Prevent or Reduce Movement of Water to the Waste—The drip shields serve as the first engineered feature that prevents seepage water and drift-wall condensation water from contacting the waste package and thereby the waste forms. The drip shields would maintain this barrier function until the 15-mm-thick Titanium Grade 7 drip shield plates are fully penetrated by general corrosion or ruptured as a result of seismic events. The drip shield capability to achieve the first barrier function is demonstrated considering both nominal general corrosion of the plate (topside and underside surfaces) and seismic induced loading (dynamic and static) causing plate failure (rupture).

The waste packages serve as the second feature that prevents seepage water from contacting the waste forms. The codisposal and commercial SNF waste packages maintain this function until the Alloy 22 outer barrier is breached by general corrosion, ruptured, or punctured. These three breach modes are modeled as patch breach. The waste package barrier capability is demonstrated considering breaches attributed to the following:

- Nominal corrosion degradation conditions: Stress corrosion cracking of the closure-lid weld region (Section 2.3.6.5.4) and general corrosion of the waste package outer barrier (Section 2.3.6.3).
- Seismic ground motion conditions: Seismic-induced stress corrosion cracking of the outer barrier, rupture, and puncture of the waste package outer barrier. The seismic-induced stress corrosion cracking of the waste package outer barrier is attributed to a local residual stress field exceeding a tensile stress threshold for stress corrosion cracking initiation, and is conceptualized as a tightly spaced network of stress corrosion cracks (SNL 2008d, Section 6.6.1.1.2). Note that the drip shield and waste package capability analysis results for these conditions also include degradation by the nominal corrosion mechanisms.

The following sections present results for each performance metric for the EBS capability to prevent or reduce movement of water to the waste, as well as characteristics for breaches of waste packages, including the following:

- Drip shield failure time for nominal conditions
- Waste package breach time for nominal conditions
- Waste package breach characteristics for nominal conditions
- Drip shield failure time for seismic ground motion conditions
- Waste package breach time for seismic ground motion conditions
- Waste package breach characteristics for seismic ground motion conditions.

It is important to note that the process of liquid water flow through the stress corrosion cracks in the waste package outer barrier has been screened out (Table 2.2-5; SNL 2008b, FEP 2.1.03.10.0A, Advection of liquids and solids through cracks in the waste package). Consequently, liquid seepage water would not contact the waste form until a breach opening, modeled as a patch penetration, develops in the Alloy 22 outer barrier.

Drip Shield Failure Time Profile for Nominal Conditions—A failure time profile for the drip shield was developed through a probabilistic projection of the general corrosion degradation of the Titanium Grade 7 plates as a function of time. For this performance metric, drip shield plate failure for nominal conditions is defined as complete penetration of the Titanium Grade 7 plate by general corrosion (Section 2.3.6.8). Degradation of the drip shield Titanium Grade 29 framework is also considered and used in the seismic damage calculations (Section 2.3.4). However, drip shield framework failure does not alter the capability of the drip shield plate to deflect seepage away from the waste packages (Section 2.3.4).

One noteworthy aspect about the basis for the probabilistic projections for drip shield plate failure times under nominal conditions is that spatial variability in drip shield general corrosion rates is not accounted for in the TSPA model (Section 2.3.6.8). This aspect is important because it means that the failure profile simplifies to a single cumulative probability distribution curve, which is computed directly from the epistemic realizations. This means that the cumulative probability distribution curve is a representation of failure times for all the drip shields in the geologic repository for a given realization. To calculate the cumulative probability distribution curve for drip shield plate failure times, the WAPDEG software was run with a total of 300 epistemic realizations. Each realization is based on one general corrosion rate for each of the topside and underside plate surfaces sampled from their respective probabilistic general corrosion models (Section 2.3.6.8).

The epistemic uncertainty in the general corrosion rates for the topside and underside surfaces are represented by cumulative distribution functions developed from laboratory data (Section 2.3.6.8.1). The corrosion rate cumulative distribution function for the topside is for aggressive corrosion conditions, while the cumulative distribution function for the underside is for benign corrosion conditions. The distribution of drip shield plate failure times is shown in Figure 2.1-8. Uncertainty in failure time is dominated by the uncertainty in the general corrosion rate for the topside because the corrosion rate on the topside of the drip shield is much greater than that on the underside. The cumulative distribution function for drip shield plate failure times has a median value of approximately 290,000 years, with drip shield plate failure times ranging from about 270,000 to 340,000 years, respectively (SNL 2008d, Section 8.3.3.2.1[a]).

Waste Package Breach Time Profiles for Nominal Conditions—Breach time profiles for the waste packages for the nominal modeling case were developed using a probabilistic projection of the breaches consisting of cracks in the closure lid-weld region of the Alloy 22 outer barrier (SNL 2008d, Section 6.3.5.1.1) and corrosion patch penetrations of the Alloy 22 outer barrier (SNL 2008d, Section 6.3.5.1.1). Projections were made for both the codisposal and commercial SNF waste packages in the entire repository. To calculate the breach time profile as a function of time, a total of 300 epistemic realizations were run. Spatial variability in the degradation processes is accounted for in the projections by the aleatory uncertain parameters of the corrosion models. Temporal variability in the degradation processes is represented by the temperature-dependent general corrosion rate of the outer barrier (SNL 2008d, Section 6.3.5.1.2). Plots of the breach time

profiles for both types of waste packages are shown on [Figure 2.1-9](#). These plots show breach time curves corresponding to the mean, median, and 5th and 95th percentiles.

Comparing the plots on [Figure 2.1-9\(a\)](#) and [2.1-9\(b\)](#), it is evident that the codisposal and commercial SNF waste package breach time profiles for nominal conditions are very similar. This similarity is explained by the fact that the two waste package types have common design characteristics (e.g., outer barrier material (Alloy 22), outer barrier thickness (25 mm), and closure-lid weld stress mitigation method (i.e., low plasticity burnishing) for the closure-lid weld surface) ([Section 2.3.6.5](#)). A small difference in breach time profiles is expected because the two waste package types have different temperature histories (i.e., commercial SNF waste packages have higher thermal output and, therefore, a hotter outer surface than the codisposal waste packages), which affect general corrosion rates during the thermal period ([Section 2.3.6.3](#)). In addition, because the commercial SNF waste package and codisposal waste packages have different nominal diameters and therefore different closure-lid-weld volumes, different values for the associated stress corrosion crack-model parameters for the closure-lid weld region are expected to introduce small differences in the stress corrosion crack breach time profiles for the waste packages. Based on the 95th percentile curves, breaches in codisposal and commercial SNF waste packages are likely to begin occurring after approximately 170,000 years. The mean breach time curves for both waste packages also show that 54% of the waste packages could be breached at 1,000,000 years, as a result of stress corrosion crack penetration and general corrosion patch penetration (SNL 2008d, Section 8.3.3.2.1[a]).

Waste Package Breach Characteristics for Nominal Conditions—To better understand the degradation behavior of the waste packages under nominal corrosion conditions in the repository, the breach time profiles for the codisposal and commercial SNF waste packages were further analyzed to quantify the fraction of waste packages (1) breached by stress corrosion cracking as a function of time; and (2) breached by general corrosion patches as a function of time. Under nominal conditions, stress corrosion cracking occurs in the closure-lid weld region of the waste package outer barrier, and general corrosion occurs in the entire waste package outer barrier surface, including the closure-lid weld region. Because the breach profiles for codisposal and commercial SNF waste packages are very similar, only the breach characteristics for the commercial SNF waste package are discussed here. The summary statistic plots on [Figure 2.1-10](#) show the projected fraction of commercial SNF waste packages breached as a function of time, which clearly show the dominance and timing of the two breach modes.

From the 95th percentile curve on [Figure 2.1-10\(a\)](#), breach of a commercial SNF waste package by stress corrosion cracking becomes more likely to occur after 170,000 years. At the end of the 1,000,000-year period, the mean fraction of the waste packages with at least one stress corrosion crack breach would be 0.54, or 54% of the commercial SNF waste packages in the repository. This result also means that almost half of the commercial SNF waste packages in the repository would not be breached by stress corrosion cracks by 1,000,000 years. Comparing these results with those for the first breach time profile of commercial SNF waste packages ([Figure 2.1-9](#)) confirms that the initial breach of the waste packages would be by stress corrosion cracking. It is important to reiterate that the cracks induced by stress corrosion cracking are highly tortuous, tight hairline cracks. Because of these typical tight hairline crack properties, plus sealing of the cracks by corrosion products and mineral precipitates, no seepage water in liquid phase would flow into the waste

package and contact the waste form. However, diffusion of water vapor through cracks and into the waste packages is accounted for in the TSPA model.

Based on the 95th percentile curve in [Figure 2.1-10\(b\)](#), commercial SNF waste package is not likely to be breached by general corrosion patch penetration until after 560,000 years. By 1,000,000 years, the mean fraction of the commercial SNF waste packages with at least one patch breach would be 0.09 or 9%. This suggests that about 90% of the commercial SNF waste packages would not exhibit general corrosion patch penetrations by 1,000,000 years. Note that the sampling of general corrosion rates uses the corrosion rate distribution presented in [Figure 2.3.6-9](#). Considering that sampling occurs over the entire waste package surface of about 1400 patches (SNL 2008d, Section 6.3.5.1.2), the extremes of the sampled distribution of corrosion rates (equivalent to the 99.9th percentile value) will be sampled for at least one patch on each waste package. It is these maximum or near maximum values of corrosion rates, when combined with the thermal dependency of the corrosion rate, the microbially influenced corrosion enhancement factor, and the thermal history that waste packages experience, that determine the time of first general corrosion patch penetration through the outer corrosion barrier, as presented in [Figure 2.1-10\(b\)](#). It is also important to note that the curves for the 5th percentile and median are absent from [Figure 2.1-10\(b\)](#); this result is because of the large number of realizations with no patch penetration by general corrosion (i.e., zero occurrences) within 1,000,000 years (SNL 2008d, Section 8.3.3.2.1[a]).

Drip Shield Failure Time Profile for Seismic Ground Motion Conditions—The mechanical strength properties of the drip shield plate (i.e., Titanium Grade 7) and framework (i.e., Titanium Grade 29) were specifically selected to perform their barrier function in the seismic environment of the Yucca Mountain site. However, over a very long time period of 1,000,000 years, the combination of dynamic loads induced by vibratory ground motion, static loads associated with drift degradation and rubble accumulation, and plate thinning due to general corrosion would ultimately cause failures of the drip shields. As outlined in [Section 2.3.4.5](#), vibratory ground motion can cause drip shield plates to (1) rupture when the local strain exceeds the ultimate tensile strain; and (2) degrade by induced high residual tensile stress, resulting in stress corrosion crack breach.

Drip shield plate failure by large rock block impact in the nonlithophysal zones has been screened out based on low consequence (SNL 2008b, FEP 1.2.03.02.0B, Seismic-induced rockfall damages EBS components, and [Table 2.2-5](#)). In the lithophysal units, the accumulation of rubble from multiple seismic events and ground motion during a seismic event can create damaged areas on drip shields. Because advective flow through stress corrosion cracks in the drip shield has been screened out (SNL 2008b, FEP 2.1.03.10.0B, Advection of liquids and solids through cracks in the drip shield, and [Table 2.2-5](#)), the drip shield damage due to stress corrosion cracks is not included in the TSPA. In addition to being affected by dynamic and static loads, the drip shield plate is subjected to degradation by general corrosion. Failure of the drip shield framework occurs as result of buckling that would be caused by the combined processes of general corrosion of the framework and seismic-induced loads. Buckling of the framework does not alter the capability of the drip shield plate to divert seepage away from the waste packages ([Section 2.3.4.5](#)). However, framework failure may affect the susceptibility of the underlying waste package to seismic damage from subsequent ground motion events because the combination of rubble accumulation and a collapsed drip shield plate can inhibit the free motion of the underlying waste package and its emplacement pallet.

The drip shield plate failure time profile for seismic ground motion conditions was computed using a total of 300 epistemic realizations, with 30 aleatory realizations to represent future random sequences of future seismic events for each epistemic realization. Plate rupture failure is a function of rubble accumulation and thinning of the plate by general corrosion. The epistemic and aleatory sampled elements are the same as those used to generate results for the seismic ground motion modeling case for post-10,000 years (Section 2.4.2.1). The failure (rupture) time profile for the drip shield plate is described by the cumulative probability distribution function presented on Figure 2.1-11. The plot in Figure 2.1-11(a) shows three types of curves: (1) the “best estimate” cumulative distribution function for drip shield failure time; (2) the set of cumulative probability distribution functions constructed from the 30 aleatory realizations for each of the 300 epistemic realizations; and (3) the expected (averaged over epistemic uncertainty) cumulative probability distribution function of drip shield plate failure times. The second plot in Figure 2.1-11(b) shows the cumulative probability distribution function of expected (averaged over aleatory uncertainty) time of drip shield failure, along with the 95th percentile confidence interval.

As used here, the best estimate CDF is defined as an unbiased estimate of the CDF based on all the simulation outcomes for the drip shield plate failure times. Based on this definition, the cumulative distribution function is constructed directly from the 9,000 realizations (300 epistemic and 30 aleatory) simulated by the TSPA model; this cumulative distribution function includes both aleatory uncertainty and epistemic uncertainty. The best estimate cumulative distribution function has the following statistics: (1) median of about 255,000 years; (2) 5th percentile of 191,000 years; and (3) 95th percentile of about 280,000 years (SNL 2008d, Section 8.3.3.2.1[a]). The long leading tail of the cumulative probability distribution function indicates that very few drip shield failures occur before 100,000 years. In fact, only about 50 out of the 9,000 realizations exhibit drip shield failures before 100,000 years. This means that there is approximately a 0.55% chance of drip shield failure occurring on or before 100,000 years by seismic events (SNL 2008d, Section 8.3.3.2.1[a]). Drip shield failures before 100,000 years are the result of low-cumulative-probability, high-magnitude events. The probability of drip shield failures after 100,000 years increases gradually, as thinning of the drip shield plate progresses by general corrosion (SNL 2008d, Section 8.3.3.2.1[a]). At about 200,000 years, the titanium drip shield plate is projected to have thinned to about one-third of its original thickness, or about 5 mm, making it much more susceptible to failure. From the best estimate cumulative probability distribution function, the average probability of drip shield failure on or before 200,000 years is approximately 6%; after about 300,000 years, the probability of drip shield failures is effectively one (SNL 2008d, Section 8.3.3.2.1[a]).

The set of 300 probability distribution functions in Figure 2.1-11(a) is presented to illustrate the range of uncertainty about the best estimate cumulative distribution function. Each cumulative distribution function represents the uncertainty introduced by parameters with aleatory uncertainty (e.g., timing of seismic event), and is conditional on the set of drip shield parameter values (e.g., residual stress threshold, general corrosion rate) sampled for the given epistemic realization. The spread among the cumulative probability distribution functions gives an estimate of uncertainty in drip shield failures associated with epistemically uncertain parameters. The expected cumulative distribution function highlights the influence of aleatory uncertainties. The expected cumulative distribution function, which is computed by averaging over the epistemic uncertainty, represents what should be, on average, the randomness in the time of drip shield failure. As demonstrated by

the plot, the expected cumulative probability distribution function is very close to the best-estimate cumulative distribution function except in the tail of the distribution.

The influence of epistemic uncertainty on drip shield failure times is highlighted by the cumulative distribution function of expected drip shield failure time, which is shown in [Figure 2.1-11\(b\)](#). In this case, the cumulative probability distribution function was constructed by averaging over the aleatory uncertainty to obtain an expected drip shield plate failure time for each epistemic realization, then ranking the 300 expected drip shield plate failure times as a cumulative distribution function. Recognizing that the accuracy of the cumulative probability distribution function is limited by using only 30 aleatory realizations, the 0.95 confidence interval was computed and plotted in [Figure 2.1-11\(b\)](#). This confidence interval provides an estimate of the reliability of the cumulative probability distribution function of expected drip shield failure times.

Waste Package Breach Time Profile for Seismic Ground Motion Conditions—The mechanical design of the codisposal and commercial SNF waste packages, as well as the corrosion properties of the outer barrier material (i.e., Alloy 22), were specifically selected so the waste package would perform its barrier function for a wide range of seismic events and corrosion conditions at the Yucca Mountain site. However, over very long time periods, the combination of dynamic and static loads induced by vibratory ground motion would ultimately cause breaches in the waste package outer barrier. As outlined in [Section 2.3.4.3](#), vibratory ground motion can potentially cause waste package damage and breaches of the following types:

1. Breaches of the outer barrier caused by stress corrosion cracking (crack penetration)
2. Rupture of the outer barrier occurs when the local strain exceeds the ultimate tensile strain (note that rupture can only occur after the waste package internals have degraded following an earlier breach in the outer barrier)
3. Puncture of the outer barrier by a combination of static load due to rubble accumulation, and sharp corners or edges from degraded waste package internals.

With regard to the latter two breach modes, rupture can occur while the drip shields are intact; puncture can occur after drip shield failure. In the seismic ground motion damage submodel (SNL 2008d, Section 6.6.1), it is assumed that the waste package internals degrade as structural elements when the outer corrosion barrier is breached (typically by stress corrosion cracks). This degradation of internals has the effect of making the waste packages more susceptible to seismic damage by subsequent events. The cumulative effects from multiple seismic events are analyzed for time frames up to 1,000,000 years.

The statistics on the expected fraction of breached commercial SNF waste packages as a function of time are shown in [Figure 2.1-12\(a\)](#) for the nominal processes and seismic events combined, and in [Figure 2.1-12\(b\)](#) for the seismic events only. The same statistics for breached codisposal waste packages are shown in [Figure 2.1-12\(c\)](#) and [Figure 2.1-12\(d\)](#) for the nominal and seismic events combined and the seismic events only. The mean of the expected fraction of waste packages breached under seismic conditions at 200,000 years is projected to be approximately 0.7% for the commercial SNF waste packages ([Figure 2.1-12\(a\)](#)) and 37% for the codisposal waste packages ([Figure 2.1-12\(c\)](#)) (SNL 2008d, Section 8.3.3.2.1[a]).

Prior to about 200,000 years after repository closure, the breach behavior of the waste packages is primarily due to seismic events only. Therefore, the expected fraction can be interpreted as a probability that a damaging seismic event has occurred. As shown in Figure 2.1-12(b), the 95th percentile transitions from an expected fraction of 0 to 3.3% (which is 1/30) at approximately 61,000 years for commercial SNF waste packages. That is, for 5% of the (300 epistemic) realizations, the probability of failure due to seismic events only before 61,000 years is at least 1/30. For 95% of the realizations, this probability is lower than 1/30 (note that the probability of 1/30 is linked to the fact that there are 30 futures for representing aleatory uncertainty). This same level of confidence is reached for codisposal waste package as early as 500 years, indicating that codisposal waste packages are much less resistant to seismic damage and that damage is likely to occur much earlier.

As can be noted by comparing Figure 2.1-12(b) and Figure 2.1-12(d), the commercial SNF waste packages are far less likely to be breached by seismic events than the codisposal waste packages. The higher resistance to seismic damage of the commercial SNF waste package than the codisposal waste package is explained by the enhanced structural response capability (i.e., damping) contributed by the massive TAD canister (SNL 2007a) in the commercial SNF waste packages (SNL 2008d, Section 8.3.3.2.1[a]). For both the codisposal and commercial SNF waste packages, however, the initial breaches consist of stress corrosion cracking or rupture induced by seismic damage while breaches at very late times are dominated by nominal general corrosion processes. For purposes of comparison, note that for nominal conditions, the initial breaches of the commercial SNF and codisposal waste packages from the 95th percentile curves occurred at about 170,000 years (Figure 2.1-9(a) and Figure 2.1-9(b)). These breaches, however, were due to nominal process stress corrosion cracks in the closure-lid weld region.

Waste Package Breach Characteristics for Seismic Ground Motion Conditions—To develop a quantitative description of the extent of seismic damage to the codisposal and commercial SNF waste packages, probabilistic projections for two breach characteristics were developed: (1) the fraction of the outer barrier surface area breached by stress corrosion cracks, and (2) the fraction of outer barrier surface area breached by patches. To provide a comparative basis, these two breach area fractions were also computed for the nominal conditions (i.e., in the absence of disruptive events).

The fraction of surface area breached by stress corrosion cracks (i.e., crack area fraction) per breached (crack or patch) commercial SNF package is shown in Figure 2.1-13. The statistics for the seismic ground motion modeling case are shown in Figure 2.1-13(a), and for the nominal modeling case in Figure 2.1-13(b). Focusing on the seismic modeling case plot (Figure 2.1-13(a)), the initial slope of the mean curve indicates that the seismic-induced stress corrosion cracks would predominately occur within the first 250,000 years (SNL 2008d, Section 8.3.3.2.1[a]). After 250,000 years, the slope of the mean curve is much smaller, due to a significant reduction in the probability of further seismic damage. This decrease in the probability of further seismic damage is attributed to the failure of drip shield plates by general corrosion and accompanying seismic induced drift degradation, which progressively fills the emplacement drift with rubble (as shown in Figure 2.1-14). This figure shows that over 60% of the drift is filled with rubble by 250,000 years. The accumulation of rubble around the waste packages after drip shield failure, in turn, reduces the probability of damage by dynamic impacts (e.g., waste package to pallet impacts).

In terms of the mean crack-breach characteristic for seismic conditions, the peak mean crack area fraction for the commercial SNF waste package occurs at 1,000,000 years and is approximately 4.4×10^{-5} . In contrast, the peak mean crack-area fraction for nominal conditions at 1,000,000 years, from [Figure 2.1-13\(b\)](#), is 6.5×10^{-6} . The slope of the mean curve in [Figure 2.1-13\(b\)](#) indicates a steady but gradual progression of additional crack breaches in the closure-lid weld region of the outer barrier. In the closure-lid weld region, additional stress corrosion cracking cracks can initiate over time as general corrosion removes the stress-mitigated layer of the outer barrier ([Section 2.3.6.5](#)).

The average crack-breach area fraction per breached waste package for the codisposal waste package is presented in [Figure 2.1-15](#). The statistics on the expected fraction for the seismic ground motion modeling case are shown in [Figure 2.1-15\(a\)](#), and for the nominal modeling case in [Figure 2.1-15\(b\)](#). The mean curve for the seismic ground motion modeling case shows a very rapid rise in the crack-breach area fraction in the first 50,000 years, then gradually transitions to a near-horizontal line after about 250,000 years (SNL 2008d, Section 8.3.3.2.1[a]). The near horizontal line is again reflecting a sharp decrease in the rate of crack breaches. The timing of this decrease corresponds to the time frame when drip shields fail ([Figure 2.1-11\(a\)](#)) and emplacement drifts are being filled by rubble ([Figure 2.1-14](#)). The peak mean crack breach area fraction estimated from [Figure 2.1-15\(a\)](#) occurs at 1,000,000 years, and is approximately 2.1×10^{-4} . This estimate of a codisposal waste package crack-breach open area is almost five times greater than for the commercial SNF waste package. The greater crack-breach open area for codisposal waste packages reflects a greater accumulation of seismic damage, due to the lower resistance to seismic damage for the codisposal waste packages. Focusing on the peak mean crack breach area fraction for nominal conditions ([Figure 2.1-15\(b\)](#)), the largest mean value is 7.1×10^{-6} (SNL 2008d, Section 8.3.3.2.1[a]).

The average fraction of surface area breached by patches (i.e., patch area fraction) per breached (crack or patch) commercial SNF waste package is shown in [Figure 2.1-16](#) for the seismic ground motion modeling case and the nominal modeling case. It is important to clarify that patch breaches include general corrosion penetrations, ruptures, and punctures (modeled as patch breaches) of the waste package outer barrier, whereas the patch breaches in the nominal modeling case ([Figure 2.1-16\(b\)](#)) include only general corrosion penetrations. The statistics on the expected fraction for the seismic ground motion modeling case are shown in [Figure 2.1-16\(a\)](#), and for the nominal modeling case in [Figure 2.1-16\(b\)](#). Comparison of the mean curves for breaches by cracks ([Figure 2.1-13](#)) and by patches ([Figure 2.1-16](#)) shows that breaches by cracks are much more likely to occur than patch breaches. The 5th percentile and median are absent from [Figure 2.1-16](#) because of the large number of realizations with no patch breaches.

As can be noted from [Figure 2.1-16\(a\)](#), the mean curve for the outer barrier average patch-breach area fraction begins abruptly at approximately 240,000 years. The 5th percentile and median are absent from the plots because of the large number of realizations with no patch breaches (i.e., zero occurrences). This abrupt increase results from the first occurrence of rupture or puncture in the waste package outer barrier. Due to the low probability of seismic events that cause crack damage to commercial SNF waste packages, which is a prerequisite for rupture of a commercial SNF waste package, as well as the low probability of seismic events that induce ruptures or punctures in the waste package outer barrier, ruptures and punctures occur in only a few realizations. Accordingly, until about 480,000 years, the mean curve remains relatively flat, because it is determined by the few

realizations in which ruptures or punctures occur. After 480,000 years, the mean curve then ascends gradually, corresponding to an increasing likelihood that general corrosion penetrations have occurred. The timing of the initiation of the general corrosion patch penetrations is consistent with the mean curve for the nominal conditions shown on [Figure 2.1-16\(b\)](#). At the end of 1,000,000 years, the patch-breach area fraction attributed to seismic conditions is about 0.26%, whereas for nominal conditions, shown in [Figure 2.1-16\(b\)](#), it is about 0.24%. This small difference between seismic and nominal patch-breach area fractions means that the fraction of surface area breached by patch penetrations on the commercial SNF waste package outer barrier is dominated by the general corrosion degradation.

Summary statistics for the average fraction of codisposal waste package surface area breached by patches (i.e., patch area fraction) per breached (crack or patch) codisposal waste package is shown in [Figure 2.1-17](#). The projection for the seismic ground motion modeling case is shown in [Figure 2.1-17\(a\)](#), and for the nominal modeling case in [Figure 2.1-17\(b\)](#). The mean curve for the average patch-breach area fraction for the seismic ground motion case shows a sharp increase beginning at about 14,000 years, which then gradually increases until about 480,000 years. Similar to the results for commercial SNF waste packages, this part of the mean curve is determined by a few realizations in which ruptures and/or punctures occur. Because codisposal waste packages are more likely to be damaged by seismic events ([Figure 2.1-12\(c\)](#)), it is also more likely that codisposal waste packages could be ruptured, as is evident in the earlier occurrence of patch breaches for codisposal waste packages ([Figure 2.1-17\(a\)](#)) as compared to commercial SNF waste packages ([Figure 2.1-16\(a\)](#)). At about 480,000 years, general corrosion begins to penetrate the codisposal waste package outer barrier ([Figure 2.1-17\(b\)](#)). At the end of 1,000,000 years, the patch-breach area fraction attributed to seismic conditions is about 0.45%, whereas for nominal conditions, shown in [Figure 2.1-17\(b\)](#), it is about 0.24% (SNL 2008d, Section 8.3.3.2.1[a]). The larger patch-breach area fraction for codisposal waste packages for seismic conditions (as compared to nominal conditions) results because codisposal waste packages are relatively likely to be damaged by seismic events ([Figure 2.1-12\(d\)](#)). When stress corrosion cracking occurs, the waste package outer barrier begins to corrode from the inside out ([Section 2.3.6.3](#)), effectively doubling the rate of thinning of the waste package outer barrier, and thus increasing the likelihood of general corrosion patch penetrations before 1,000,000 years. In addition, the waste package internals degrade after seismic damage, and thus the early occurrence of stress corrosion cracking increases the probability that ruptures may occur.

Summary of the Capability of the EBS to Prevent or Substantially Reduce Water Contacting the Waste—The capability of the EBS to prevent or limit the movement of water and prevent contact between water and waste depends on the integrity of the drip shields and waste packages. The performance demonstration for the EBS indicates that the drip shields will remain intact for hundreds of thousands of years and protect the waste packages from seepage. Moreover, the majority of waste packages will remain intact for tens of thousands to hundreds of thousands of years. Thus, only a fraction of the emplaced waste will be exposed to water during this period.

For the combined nominal/early failure demonstration modeling case, with early-failed drip shields notwithstanding, the performance demonstration projects a distribution of drip shields plate failure times ([Figure 2.1-8](#)) with a median of approximately 290,000 years, with drip shield plate failure times generally ranging from 270,000 to 340,000 years ([Figure 2.1-8](#)). For the seismic ground motion modeling case, the best estimate distribution of drip shield failure times ([Figure 2.1-11\(a\)](#))

has a median of about 255,000 years, with the average probability of drip shield failure at or before 200,000 years being approximately 0.06.

With regard to waste package performance capability, the projected distributions for the mean fraction of waste packages (codisposal or commercial SNF) breached ([Figure 2.1-9](#)) for the nominal modeling case show that at 500,000 years, about 15% of waste packages would have breaches and at 1,000,000 years about 54% of waste packages would be breached. For the seismic ground motion modeling case, the mean of the expected fraction of waste packages breached at 200,000 years is projected to be approximately 0.7% for the commercial SNF waste packages ([Figure 2.1-12\(a\)](#)) and 37% for the codisposal waste packages ([Figure 2.1-12\(c\)](#)). After 200,000 years, nominal corrosion processes start to dominate the expected fraction of breached waste packages for the seismic ground motion modeling case. These performance metrics show that the drip shields and waste packages together substantially reduce the contact of water with the emplaced waste for hundreds of thousands of years.

EBS Capability to Prevent or Reduce the Rate of Radionuclide Releases—The EBS prevents or substantially reduces the release rate of radionuclides from the waste and prevents or substantially reduces the rate of movement of radionuclides from the repository to the accessible environment. The EBS performs these functions by (1) preventing or substantially reducing the contact of water with the waste; (2) reducing the rate of release due to the slow alteration of the waste and low solubility of many radionuclides; and (3) reducing the rate of radionuclide transport from the waste form to the Lower Natural Barrier. This section summarizes how the different processes contribute to the EBS functions, then presents results demonstrating the EBS capability to prevent or reduce radionuclide releases for the combined nominal/early failure modeling case and seismic ground motion modeling case.

To provide a metric for a demonstration of EBS barrier capability, the activity (in curies) of each radionuclide released from EBS as a function of time was computed using the TSPA model. This metric provides a direct measure of EBS performance by permitting a comparison between activity released from the EBS to the initial inventory activity emplaced as it decays in time. In addition, information concerning the behavior of radionuclide release rates and barrier function can be inferred from this metric by examining the shape of the activity release curve. The variation in shape with time provides insights into the capability of the EBS to prevent or reduce the rate of movement of radionuclides from the repository to the unsaturated zone. The activity release curve for a given radionuclide typically starts with a positive slope that gradually decreases to zero prior to becoming negative. This shape is attributed to the interplay of the release rate of a radionuclide from the EBS (or mass retention rate in the EBS) compared to its effective radioactive decay rate. As shown in [Equation 2.1-1](#), the activity release of a given radionuclide from the EBS is computed by taking the difference between the activity of the emplaced inventory and that retained in the EBS. The positive slope in the activity release curve typically indicates that the rate of mass release from the EBS is greater than the effective rate of decay of the emplaced mass, where the effective rate of decay accounts for any ingrowth from decay of a parent radionuclide. A positive slope typically occurs when the release rate out of the EBS is non-zero (a small positive slope can occur due to ingrowth). When the slope is zero, the release rate from the EBS is the same as the effective decay rate. A negative slope occurs when mass is released from the EBS slower than the effective rate of decay. This latter condition is typically the case when the EBS release rate becomes negligible and the

slope of the activity release curve approaches the rate of change corresponding to the effective decay rate.

Waste packages can be breached through general corrosion, through stress corrosion cracking, through seismic damage, or by early failure. In the latter case, the waste package is assumed to provide no protection from the drift environment starting at the time of repository closure. After waste packages are breached, SNF assemblies and HLW canisters will be exposed to the drift environment including air, water vapor, and possibly dripping seepage water. The waste package exterior will be subjected to advective seepage flow only if seepage is dripping at the waste package location and the drip shield fails—possibly due to early failure, seismic ground motion, or general corrosion. Seismic-induced rupture of the package, as well as general corrosion, can provide pathways for advective fluxes of water into a breached waste package. Stress corrosion cracks will not permit advective flux of water through them; they will, however, permit the transfer of oxygen and water vapor by diffusion into the waste packages.

Radionuclide transport out of the EBS and into the unsaturated zone is dependent on several processes. The processes discussed below are described in detail in [Section 2.3.7](#). After a waste package is breached, radionuclides are not available for release and transport until the following processes have occurred:

- Oxygen, liquid water, or water vapor enters the waste package, enabling degradation of the waste form and formation of a liquid pathway for radionuclide transport. At and above the boiling point of water in the repository, a liquid pathway is assumed not to exist, and no transport of radionuclides takes place. When only water vapor enters a waste package, no transport takes place until a continuous water film is formed on the internal components. This condition occurs when the waste package temperature falls below 100°C and the relative humidity interior to these packages reaches 95% (the relative humidity in the waste package interior is assumed to be equal to the relative humidity at the exterior of the waste package).
- The fuel cladding or canisters (HLW, TAD, DOE SNF, and naval) degrade and fail and allow water to contact the waste. (Note: with the exception of naval SNF structure (including cladding), the barrier capability to prevent water from contacting the waste provided by the SNF cladding and by all canisters is not accounted for in the TSPA.)
- The solid waste form degrades. This process provides the rate at which the radionuclides are made available for mobilization and release.
- Radionuclides are mobilized into aqueous solution, aqueous colloidal suspension, or gaseous phase. (Note: gaseous transport is not included in the TSPA because it is not a significant release mode (SNL 2008d, Section 8.3.3.2.2[a]).)

Once water and oxygen are available within a breached waste package, corrosion products from degradation of steel internal components would form. In commercial SNF waste packages, these steel components include the fuel basket guides, the TAD canister, and the inner vessel. In codisposal waste packages, these steel components include the central support tube, divider assembly, the inner vessel, and HLW and DOE SNF canister steel. The TAD canister shield plug

(15 in. thick) in commercial SNF waste packages and the inner lid (9 in. thick) in codisposal waste packages are not included as contributing to corrosion products available for sorption, because the large mass of these components is localized at one end of the waste package, and will not appreciably affect transport throughout the rest of the waste package (SNL 2007c, Section 6.3.1.1).

Mobile radionuclides are transported out of the degraded waste package and through the EBS to the unsaturated zone. Transport out of the waste package can occur by advection when there is a liquid flux through the waste package, and by diffusion through continuous liquid pathways in the waste package, including thin films of adsorbed water. As noted above, a continuous thin film cannot form until the waste package temperature falls below 100°C and the relative humidity exterior to these packages reaches 95% (the interior relative humidity is assumed to be same as the exterior relative humidity). Diffusive transport through waste package corrosion products depends on the water saturation, porosity, temperature, and relative humidity in the waste package. In the TSPA model, it is assumed that temperature and relative humidity in the waste package are equal to the temperature and relative humidity on the waste package outer surface (SNL 2008d, Section 8.3.3.2.2[a]). The two transport processes (diffusion and advection) are each a function of the type of penetrations through the drip shield and waste package and the local seepage conditions. Diffusion can occur through stress corrosion cracks or through general corrosion patches in the waste package, both with and without liquid flux through the waste package. Advection is not considered through stress corrosion cracks or through corrosion patches in the absence of seepage flux.

The corrosion products from the waste package internal components have the potential to be strong sorbers for the actinides (SNL 2008d, Section 8.3.3.2.2[a]). The process of radionuclide sorption onto the waste package corrosion products and invert ballast material (crushed tuff) is beneficial to performance because this process can retain radionuclides in the EBS and delay release to the unsaturated zone. Because the waste package corrosion products are in intimate contact or are directly in the flow or diffusion path of the radionuclide source inside the waste package, retardation by corrosion products inside the waste package will occur. However, note that because corrosion products in the invert formed by its structural steel members are more localized and not necessarily in any flow path from the waste package, sorption onto corrosion products in the invert is excluded in the TSPA model (SNL 2008d, Section 8.3.3.2.2[a]).

Within the emplacement drifts, water evaporated from the emplacement drift walls and invert is transported primarily by natural convection from warmer to cooler areas, where it condenses on cooler surfaces (such as the drift wall). The rates of evaporation and condensation, as well as the rate of water vapor transport in the emplacement drift, determine the extent of condensation. In-drift condensation is evaluated with the in-drift condensation model (Section 2.3.5.4.2). This model provides the TSPA model with both the probability and magnitude of condensation on the drift wall during cooldown. The TSPA treats the flow of drift wall condensation as a source of liquid water to be added to the liquid water entering the drift as seepage. The TSPA uses this combined liquid-water source term in the EBS flow and chemical environment calculations (SNL 2008d, Section 8.3.3.2.2[a]).

The in-drift condensation model defines three stages for the occurrence of condensation. Stage 1 is when the drift wall temperature is above the boiling temperature of water at all locations in the drift. No condensation occurs during Stage 1. Stage 2 is for times between when the first location in a drift

drops below the boiling temperature and the last location drops below the boiling temperature. Stage 3 occurs after all waste packages (and thus the drift wall) drop below the boiling temperature. Drift wall condensation results are presented in [Tables 2.1-10](#) and [2.1-11](#). Results in [Table 2.1-10](#) show that drift wall condensation does not occur in the presence of the commercial SNF waste packages during Stage 2, and that there is a small probability that a negligible condensation rate will occur during Stage 3 on a very small fraction of commercial SNF waste packages. Results in [Table 2.1-11](#) show that a significant drift wall condensation rate (approximately $0.5 \text{ m}^3/\text{yr}$) will occur in the presence of the codisposal waste packages (probability of one and mean waste package fraction of one) during Stage 2 for approximately 1,000 years (SNL 2008d, Section 8.3.3.2.2[a]). For comparison, mean seepage rates at 1,500 years are presented in [Table 2.1-12](#). During Stage 3, which lasts about 2,000 years after closure, the probability of condensation decreases dramatically, and the condensation rates are negligible (SNL 2008d, Section 6.3.3.2.2 and 8.3.3.2.2[a]).

The impact of condensation water on the barrier capability of codisposal waste packages is not significant, because drip shields do not fail to perform their water diversion function during the time condensation will occur. Thus, in the TSPA model, condensation water is diverted around the codisposal waste packages except possibly in the case of a very small number of early failure drip shields or in the unlikely event of drip shield failure by fault displacement.

Radionuclides Selected to Demonstrate Multiple Barrier Capability—One of the basic functions of the multiple barriers is to prevent or substantially reduce the rate of radionuclide movement from the repository to the accessible environment. To demonstrate the capability of the EBS (and the Lower Natural Barrier) for a range of releases and yet limit the number of calculations, a small subset of 12 radionuclides was selected for the barrier performance demonstrations. That subset was selected from two lists: (1) radionuclides identified as dominating the mean annual doses to the RMEI for the 10,000-year and post-10,000-year time periods; and (2) radionuclides identified as dominating the curie inventory for the 10,000-year and post 10,000-year time periods. The first list of important radionuclides was developed directly from the probabilistic projections of mean annual dose ([Section 2.4.2](#)). The second list was compiled by examining the inventory decay histories, which are discussed here.

Calculations of inventory decay histories for the 12 radionuclides are shown in [Figure 2.1-18](#) for the two periods of 10,000 years and post-10,000 years (i.e., after 10,000 years but within 1,000,000 years). The time-dependent behavior of individual radionuclides is the result of simple radioactive decay and, in some cases, decay chain in-growth. From the curves on these plots, one can note that, in the first 100 years, two fission products— ^{90}Sr (half life of 28.8 years) and ^{137}Cs (half-life of 30 years)—dominate the inventory. Thereafter, the actinide radionuclide ^{241}Am (half-life of 432.7 years) dominates to about 1,000 years, ^{240}Pu (half life of 6,560 years) dominates to about 7,000 years, and ^{239}Pu (half life of 2.41×10^4 years) dominates to about 115,000 years. Dominance then shifts to the fission product ^{99}Tc (half-life of 2.13×10^5 years) for the majority of time in the 1,000,000-year time period.

More refined insights into inventory dominance can be gained by examining plots of the fraction of total activity, at time τ , for each radionuclide. Two plots are shown on [Figure 2.1-19](#) for 10,000

years and 1,000,000 years. From these plots, it is evident that the dominant radionuclides in the curie inventory from the subset of 12 radionuclides, grouped by compliance period, are as follows:

1. For 10,000 years: ^{137}Cs and ^{90}Sr , ^{241}Am , ^{240}Pu and ^{239}Pu
2. For post-10,000 years: ^{239}Pu , ^{99}Tc , ^{237}Np , ^{233}U , and ^{229}Th .

At closure, the three radionuclides— ^{137}Cs , ^{90}Sr , and ^{241}Am —collectively represent about 85% of the total curie inventory, with ^{137}Cs representing about 46%, ^{90}Sr about 29%, and ^{241}Am about 10%. From [Figure 2.1-19\(a\)](#), it can be clearly seen that ^{241}Am dominates the curie inventory in the interval from 100 to 1,000 years. Dominance shifts to ^{240}Pu and ^{239}Pu from 1,000 years to 10,000 years, with these two actinides alone representing more than 90% of the inventory at the end of 10,000 years. As shown in [Figure 2.1-19\(b\)](#), ^{239}Pu dominance peaks at about 50,000 years. From roughly 100,000 years to 1,000,000 years, the inventory dominance shifts to ^{99}Tc (half-life of 2.13×10^5 years) until roughly 850,000 years, then transitions to dominance by three actinides: ^{237}Np (half-life of 2.14×10^6 years); ^{233}U (half life of 1.59×10^5 years), and ^{229}Th (half-life of 7.3×10^3 years). The curves for ^{233}U and ^{229}Th overlay due to secular equilibrium. The latter three actinides are members of a decay chain in the neptunium series. A summary of the decay history of the total curie inventory and the major contributors is presented in [Table 2.1-13](#); the percentages shown in the table were calculated directly from the data files used to create [Figure 2.1-18](#).

Comparing the above radionuclides that dominate the inventory with the radionuclides identified as important to mean annual doses to the RMEI (namely, for the 10,000-year compliance period: ^{99}Tc , ^{14}C , ^{129}I , ^{239}Pu , ^{36}Cl , ^{79}Se , and ^{240}Pu ; and for the post-10,000-year compliance period: ^{226}Ra , ^{242}Pu , ^{237}Np , ^{129}I , ^{233}U , ^{135}Cs , ^{230}Th , ^{99}Tc , ^{229}Th , and ^{231}Pa), it can be noted that the radionuclides that dominate the inventory also appear in the list of radionuclides important to dose, with the exception of the short-lived ^{137}Cs , ^{90}Sr , and ^{241}Am .

Based on the above considerations, the following subset of radionuclides was selected for use in describing barrier capabilities with regard to preventing or substantially reducing the rate of radionuclide movement.

These radionuclides represent a broad range of nuclear properties, geochemical behavior, and transport characteristics including the following:

- Large initial inventory and short half-life: ^{137}Cs , ^{90}Sr , ^{241}Am , ^{240}Pu
- Highly soluble, nonsorbing, long half-life and major contributor to dose: ^{99}Tc
- Solubility limited, strongly sorbed, long half-life, transported in dissolved and colloidal phases, and important contributor to dose: ^{239}Pu and ^{242}Pu
- Moderately soluble, low sorbing, very long half-life, and transported in dissolved phase: ^{237}Np and ^{234}U
- Strongly sorbed, and contributes to or is produced by decay chain in-growth: ^{243}Am , ^{230}Th , and ^{226}Ra .

These 12 radionuclides represent a broad range of radioactive decay properties, geochemical behaviors, biosphere dose conversion factors, and transport characteristics in geologic media. Because of these diverse properties, these 12 radionuclides provide a means of examining the performance characteristics of the natural and engineered barriers.

Activity Releases from the EBS for Combined Early Drip Shield Failure, Early Waste Package Failure, and Nominal Processes—The aspects of EBS performance that determine the release of radionuclides, as modeled in the TSPA for the combined nominal/early failure modeling case, can be summarized as follows:

- Nominal processes cause only a single waste package failure within the 0 to 10,000-year time interval over all the epistemic samples (SNL 2008d, Section 8.3.3.2.2[a]).
- Prior to 170,000 years, radionuclide release rates and releases from the EBS are determined by events related to early drip shield failure and early waste package failure.
- After 170,000 years, radionuclide release rates and releases from the EBS are determined primarily by processes related to the failure of waste packages from nominal processes.
- Drip shield failure for nominal conditions is defined as complete penetration of the Titanium Grade 7 plate by general corrosion. Drip shield failure times are distributed between 270,000 and 340,000 years (Figure 2.1-8)
- The expected number of early failed waste packages is 1.09 (SNL 2008d, Section 8.3.3.2.2[a]). The probability of one or more early failed (i.e., breaches of closure-lid welds) waste packages is 0.442 (Section 2.4.2.3.2.1.12.1). The expected number of waste package early failures, given that an early failure occurs, is approximately 2.5 (Section 2.4.2.3.2.1.12.1).
- The expected number of early failed drip shields is 0.018 (Section 2.4.2.3.2.1.12.1). The probability of one or more early failed drip shields is 0.017 (Section 2.4.2.3.2.1.12.1). The expected number of drip shield early failures, given an early failure occurs, is approximately 1.1 (Section 2.4.2.3.2.1.12.1).
- Early drip shield breach is assumed to result in waste package failure only if the breached drip shield is in a seeping environment; otherwise, there is no waste package failure and, hence, no radionuclide release. Water flows into the failed waste package as soon as the waste package temperature falls below 100°C, and advective transport occurs immediately (SNL 2008d, Section 6.4.1.3).
- The present-day climate persists from the time of repository closure to 600 years from the present. At 2,000 years, the climate changes from monsoon to glacial-transition and percolation rates generally increase (Section 2.3.2.4.1.2.4.2), which in turn increases seepage and the release rate of radionuclides from waste packages underneath early failed drip shields.

- At 10,000 years, the percolation rates at the repository change, generally increasing in accordance with proposed 10 CFR 63.342(c)(2) (70 FR 53313). In addition, seepage fractions range from about 12% to 40% for both commercial SNF and codisposal waste packages.
- Prior to drip shield failure, early waste package failure results in diffusive releases of radionuclides. After drip shield failure, advective transport and an increase in release rates can occur if the waste package is experiencing dripping conditions and has been breached by general corrosion.
- By about 340,000 years, all drip shields have failed (SNL 2008d, Section 8.2.1) and the number of failed waste packages steadily increases (Figure 2.1-9). As a result, radionuclide release rates and releases also tend to increase with time.
- The TSPA model represents 11,629 waste packages (8,213 commercial SNF and naval SNF waste packages, and 3,416 codisposal waste packages) (Section 2.3.7.4.1.2). HLW contains almost all of the ^{99}Tc in codisposal waste packages, with a nominal initial inventory of 1.01×10^3 g (17.2 Ci) per codisposal waste package. In contrast, the DOE SNF component of waste in codisposal waste packages contains 1.58×10^2 g (2.69 Ci) of ^{99}Tc . The amount of ^{99}Tc contained in the commercial SNF waste is substantially greater, at 7.55×10^3 g (128 Ci) per commercial SNF waste package (Table 2.3.7-3).
- At 10,000 years, there is a sharp increase in radionuclide release rates and releases, resulting from early failed commercial SNF waste packages. Commercial SNF waste packages are hotter than codisposal waste packages, with the result that releases from commercial SNF waste packages are delayed until both the waste package temperature falls below 100°C and the relative humidity interior to these packages reaches 95%, at which time a continuous thin film of adsorbed water required for diffusive radionuclide transport begins (SNL 2008d, Section 8.3.3.2.2.[a]).
- Most commercial SNF waste packages begin diffusive transport between 9,000 years and 14,000 years, whereas codisposal waste packages begin diffusive transport between 500 years and 3,000 years (SNL 2008d, Section 8.3.3.2.2[a]).
- Because infiltration rates and temperatures vary across the repository footprint (Section 2.3.5), the time at which a continuous thin film of adsorbed water required for diffusive transport begins also varies.
- Because ^{99}Tc is assumed to have no solubility limit and is non-sorbing in the invert (or anywhere else in the disposal system), released technetium moves rapidly from the EBS to the unsaturated zone (SNL 2008d, Section 6.3.7.5). The EBS release characteristics of ^{99}Tc are representative of other highly soluble and non-sorbing radionuclides, such as ^{129}I .
- ^{239}Pu is not an important contributor to expected dose in the first few thousand years for the combined nominal/early failure modeling case (SNL 2008d, Figure 8.2.6[a]). Much of the mobilized plutonium sorbs onto stationary corrosion products, and its subsequent

release rate depends on the rates of desorption (SNL 2008d, Section 8.3.3.2.2.[a]), which results in the slow but steady release of ^{239}Pu from the waste package.

- The initial release of ^{239}Pu is primarily from DOE SNF waste forms, which are conservatively assumed to immediately degrade when a codisposal waste package is breached (Section 2.3.7.8). The release rate and releases of ^{239}Pu later in the first 10,000 years are primarily from HLW, which degrades relatively slowly over time. Releases of ^{239}Pu from commercial SNF waste packages are delayed until diffusive transport begins after about 9,000 years.

Figure 2.1-20 compares the mean total activity of all radionuclides remaining after decay of the initial inventory to the mean total activity of all radionuclides released from the EBS for the combined nominal/early failure demonstration modeling case for both compliance periods. This figure indicates that, under the combined nominal and early failure scenario classes, only a small fraction of the total initial radionuclide inventory would be released from the EBS in the first 10,000 years (less than 3.9×10^{-7}). The mean total release in 10,000 years is equivalent to less than 1/300th of the inventory of one of the 11,629 waste packages in the repository. After 1,000,000 years, the mean total release would be about 7% of the inventory at that time (SNL 2008d, Section 8.3.3.2.2[a]).

Figure 2.1-20 indicates that, for both compliance periods, the most significant radionuclide with respect to activity release from the EBS is ^{99}Tc . The contribution for the other radionuclides selected is much less. In the case of plutonium species, the plots in Figure 2.1-20 show the activity of radionuclides transported irreversibly sorbed to colloids (designated by the superscript I) and the total activity of the mass in dissolved phase, and reversibly and irreversibly associated with colloids (designated by the superscript T). For americium, only the total activity is plotted because the colloidal phase is small compared to the dissolved phase.

The release of ^{99}Tc during the first 10,000 years (Figure 2.1-20(a)) is primarily due to diffusive releases from early failure of waste packages and, to a lesser extent, advective releases from early drip shield failure and concomitant waste package failure (SNL 2008d, Section 8.3.3.2.2[a]). Nominal waste package degradation processes do not cause waste package failures, on average, prior to about 170,000 years after closure (Figure 2.1-9). As a result, average release rates and releases from the EBS during this period are determined by processes related to the combined early drip shield failure and early waste package failure. This result is primarily due to the fact that the expected number of early failure waste packages is about 60 times greater than the number of expected early failure drip shields. In addition, early drip shield failure is assumed to result in waste package failure only if the early failed drip shield is experiencing seeping conditions. Otherwise, there is no waste package failure and, hence, no radionuclide release. Under nominal conditions approximately 70% of the waste package locations in the repository have non-seeping conditions (Table 2.1-6). Thus, on average, the number of early failure waste packages is about 100 times greater than the number of failed waste packages associated with early failure drip shields. Hence, releases from early waste package failure tend to be substantially greater than releases from early drip shield failure.

Furthermore, of those waste packages that become breached, radionuclide releases during the first 10,000 years are primarily from the cooler codisposal waste packages. As noted above, commercial

SNF waste packages are hotter than the codisposal waste packages (SNL 2008d, Section 8.3.3.2.1[a]), with the result that releases from commercial SNF waste packages are delayed, on average, until after 9,000 years, whereas releases from codisposal waste packages are delayed until after 500 years, until such time as a continuous thin film of adsorbed water required for diffusive radionuclide transport begins (SNL 2008d, Section 6.3.8.1). In addition, the infiltration and percolation fluxes at the repository increase at 10,000 years, thus increasing the seepage fluxes and seepage fraction. The impact of the change in infiltration and transport from commercial SNF waste packages on release rates and releases from the EBS is illustrated in Figure 2.1-20(b) by the sharp increase in radionuclide release rates and releases just before and after 10,000 years.

Figure 2.1-18 indicates that radionuclides such as ^{90}Sr , ^{137}Cs , and ^{241}Am dominate the total inventory activity at the earliest times (SNL 2008d, Section 8.3.3.2.2[a]). Figure 2.1-20(a) shows that these radionuclides are released from the EBS in small amounts of activity immediately from early failure of codisposal waste packages and/or drip shields, and experience only moderate sorption and negligible delay during transport out of the EBS (SNL 2008d, Sections 6.3.7 and 6.3.8). Note that these early releases of ^{90}Sr and ^{137}Cs are from cooler codisposal waste packages. Releases from hotter commercial SNF waste packages would be delayed for several thousand years, until the RH in the waste package exceeds 95%. These radionuclides have short half-lives and decay to negligible levels in a few hundred years. Because of the longer half-life of ^{241}Am , this radionuclide is a secondary contributor to the mean total activity releases until about 2,000 years. A second peak in activity releases of ^{241}Am occurs just after 10,000 years, and is caused by releases from early failed commercial SNF waste packages. At 10,000 years, the activity releases of ^{239}Pu and ^{240}Pu are small, but still the 2nd and 3rd most important contributors to total activity released (SNL 2008d, Section 8.3.3.2.2[a]). These two radionuclides dominate the total inventory activity at 10,000 years, with ^{239}Pu and ^{240}Pu contributing 52% and 40% of the fraction of total activity, respectively. ^{237}Np represents the less-mobile solutes whose mobilization is generally limited by their solubility. Other radionuclides in this category include ^{226}Ra and ^{234}U . ^{239}Pu and ^{242}Pu represent less-mobile solutes that can be irreversibly strongly sorbed to corrosion product solid phases in the waste packages. The activity releases of ^{239}Pu and ^{242}Pu are shown as total concentrations denoted by $^{239}\text{Pu}^{\text{T}}$ and $^{242}\text{Pu}^{\text{T}}$, and as irreversibly sorbed on colloids denoted by $^{239}\text{Pu}^{\text{I}}$ and $^{242}\text{Pu}^{\text{I}}$. Total concentrations include both dissolved and colloiddally associated activity. Other radionuclides in this latter category include ^{240}Pu , ^{241}Am , and ^{243}Am .

The relatively small value of mean total activity released from the EBS after 10,000 years, and prior to 170,000 years (Figure 2.1-20(b)) in the combined nominal and early failure scenario classes, is a result of the absence of drip shield failures and the limited number of waste package failures prior to 170,000 years. As noted above, drip shield failure times range from 270,000 to 340,000 years. In addition, stress corrosion crack penetrations of the waste package closure-lid welds begin at around 170,000 years (as shown by the 95th percentile curves on Figure 2.1-13(b) and Figure 2.1-15(b)). As stress corrosion cracking penetrations occur, the release rates from the waste packages and EBS increase, as illustrated by the increase in releases of ^{99}Tc at around 170,000 years (Figure 2.1-20(b)). The amount of activity released from the EBS by moderately soluble and weakly to moderately sorbing radionuclides in the lower natural barrier system, such as ^{237}Np , ^{242}Pu , and ^{234}U , increases after 200,000 years as well, but substantial increases are not observed until general corrosion failures of waste packages begin to dominate at about 600,000 years (as shown by the 95th percentile curves; Figure 2.1-16(b) and Figure 2.1-17(b)) and subsequent advective releases

become significant. However, these releases remain small compared to ^{99}Tc throughout the 1,000,000-year period.

The nuclear properties of ^{226}Ra explain its persistence in the nuclear waste for potentially millions of years, while its chemical properties explain its rate of migration in the EBS, unsaturated zone, and saturated zone. One of the important chemical properties of ^{226}Ra is that it exhibits moderate sorption onto waste package internal corrosion products and high sorption in the invert ballast (crushed tuff). This sorption property has the effect of slowing the rate of ^{226}Ra activity released from the EBS for several hundred years. However, a key nuclear property of ^{226}Ra is that it exhibits ingrowth from other actinide radionuclides in the uranium series decay chain. The relevant part of that decay chain consists of the following:



This decay chain is significant because it means that, even after ^{226}Ra depletes its initial inventory, it will be continuously replenished so long as there is a source of ^{230}Th and ^{234}U . While both ^{226}Ra and ^{230}Th have relatively small initial inventories in the nuclear waste, the precursor ^{234}U has a significant initial inventory. Also, the large contrast in half-lives between ^{226}Ra and ^{230}Th means that ^{226}Ra will ultimately reach a state of secular equilibrium with ^{230}Th . Similarly, after ^{230}Th depletes its initial inventory, its activity will be in secular equilibrium with its precursor ^{234}U . The net effect is that ^{226}Ra will persist in the waste form and continue to be released for potentially millions of years (SNL 2008d, Section 8.1.2.1[a]).

As discussed above, the performance of the EBS in preventing or substantially reducing the rate of radionuclide release to the Lower Natural Barrier is a function of several features and uncertain processes in the EBS. The degree of degradation of the waste package is uncertain and spatially variable, and controls the amount and rate of water that may enter the waste package and potentially allow degradation of the waste form. The thermal and chemical environment is also uncertain and spatially variable, and affects the degradation rate and characteristics of the waste forms and, more importantly, affects the thermally dependent general corrosion rate of Alloy 22 (Sections 2.3.6.2.2 and 2.4.2.3.3.6). The thermal and chemical environment also affects the solubility of the radionuclides in the aqueous phase, as well as the stability of colloids to which radionuclides may be attached. The rate of release is affected by the advective and diffusive transport pathways out of the waste package and through the invert. The transport pathways through the EBS are generally diffusive and their properties are treated as uncertain. Solubility limits significantly control the rate of radionuclide diffusion as they define the concentration gradient through which radionuclides may diffuse. Solubility limits are treated as uncertain except for those radionuclides that are not solubility limited, such as ^{99}Tc (Section 2.3.7.10). Finally, the sorption characteristics of the degraded waste package and internal structural supports are treated as uncertain, and affect the release of those radionuclides that are highly sorbed on iron substrates.

To illustrate the resulting uncertainty associated with the release of radionuclide activity from the EBS, radionuclide-specific release plots for ^{99}Tc and ^{239}Pu are presented in Figures 2.1-21 and 2.1-22 for combined nominal and early failure degradation processes and both compliance periods. Shown on each plot is the mean total inventory for that radionuclide, along with the mean release curve and 5th and 95th percentile release curves. These plots illustrate that the mean release is affected by the range of the uncertain parameters used in the analysis as summarized above. As

illustrated, the mean release is typically close to the 95th percentile of the uncertain results (SNL 2008d, Section 8.3.3.2.2[a]). The uncertainty in ^{99}Tc and ^{239}Pu releases prior to 200,000 years is dominated by uncertain parameters that determine the number of early failure waste packages and drip shields, the degradation rates of HLW glass and commercial SNF, and the diffusive transport of ^{99}Tc and ^{239}Pu from the waste form to the waste package outer barrier. In addition, uncertainty in the release of ^{239}Pu is also influenced by uncertain parameters that determine the solubility of plutonium and sorption of ^{239}Pu onto stationary corrosion products within the waste package (SNL 2008d, Section 8.3.3.2.2[a]).

Activity Releases from the EBS Due to Seismic Ground Motion Damage of Engineered Barrier System Components—Many of the aspects of EBS performance under nominal and early failure conditions summarized in the preceding discussion are relevant to the seismic ground motion modeling case. The following aspects of EBS performance that lead to additional reduction in EBS performance as modeled in the TSPA model for the seismic ground motion modeling case can be summarized as follows:

- Prior to 170,000 years, radionuclide rates and releases from the EBS are determined by processes related to vibratory ground motion-induced waste package failures (SNL 2008d, Section 8.3.3.2.2[a]). The mean release from these processes is significantly greater than the mean release from the combined nominal/early failure modeling case (Figures 2.1-23 and 2.1-20, respectively).
- Between 170,000 and 600,000 years, radionuclide releases from the EBS are determined by contributions from both nominal and vibratory ground motion induced drip shield and waste package failures (Figure 2.1-12).
- After about 600,000 years, radionuclide releases from the EBS are determined primarily by processes related to the failure of waste packages from nominal processes (Figures 2.1-16 and 2.1-17) (SNL 2008d, Section 8.3.3.2.2[a]).
- The initial breach (crack) of a commercial SNF waste packages is not likely to occur before approximately 61,000 years (Figure 2.1-13(a)), whereas the codisposal waste package is projected to experience a first breach (stress corrosion crack) much earlier (Figures 2.1-12(c) and 2.1-15(a)). For purposes of comparison, based on the 95th percentile, the initial breaches of the commercial SNF and codisposal waste packages occurred at about 170,000 years under nominal conditions. These breaches, however, were due to nominal process stress corrosion cracking in the closure-lid weld region (Figure 2.1-10) (SNL 2008d, Section 8.3.3.2.2[a]).
- Drip shield failures by combined rupture and general corrosion are largely distributed between about 40,000 and 300,000 years (Figure 2.1-11), as compared to drip shield failures by general corrosion alone (under nominal conditions), which are distributed from about 270,000 to 340,000 years (Figure 2.1-8).
- Vibratory ground motion-induced drift collapse during the post-10,000-year period causes the mean seepage fraction to increase to 70% (Table 2.1-9), as compared to the

mean value of 40% in the nominal modeling case (Table 2.1-7) (SNL 2008d, Section 8.3.3.2.2[a]).

- ^{242}Pu is a key contributor to expected dose late in the post-10,000-year period (SNL 2008d, Section 8.1.1.5[a]). Much of the mobilized plutonium sorbs onto ferrous corrosion products, and its subsequent release depends on the rates of desorption (SNL 2008d, Section 8.3.3.2.2[a]).

The potential effect of seismic events on EBS capability is shown in Figure 2.1-23 for both compliance periods. Comparison of this figure with Figure 2.1-20 does not show a significant reduction in EBS capability with respect to the sorbed radionuclides or the colloid associated radionuclides.

In the seismic ground motion modeling case, the codisposal waste packages are more likely to experience significant damage during the first 10,000 years after closure (Figure 2.1-12) because the commercial SNF waste packages are much stronger and more failure resistant. The commercial SNF waste packages will be more robust than the codisposal waste packages because the commercial SNF waste packages contain the large and tightly fitting TAD canister. The codisposal waste packages contain several smaller waste-containing canisters that do not fit as tightly, and could move more freely under the influence of ground motion (Section 2.3.4) (SNL 2008d, Section 6.1.2). In the first 10,000 years after closure, the predominant mechanism that causes damage to codisposal waste packages is stress corrosion cracks by vibratory ground motion-induced residual stresses in the waste package outer barrier (Figure 2.1-15). The drip shields remain intact for seismic events occurring in the first 10,000 years (Figure 2.1-11). As a result, dripping seepage cannot contact the waste packages. Therefore, water can enter the waste package only by vapor diffusion through the cracks in the outer barrier. As codisposal waste packages cool and the DOE SNF and HLW degrade, water films form on waste package internals, permitting the diffusive transport of radionuclides through the small cracks and into the invert. Comparing estimates of EBS release shown on Figure 2.1-20(a) with Figure 2.1-23(a) indicates a reduction in EBS capability as compared to the combined nominal and early failure scenario classes by a factor of as much as 70 for ^{99}Tc during the first 10,000 years after closure (SNL 2008d, Section 8.3.3.2.2[a]). However, the comparison still indicates substantial and similar EBS capability during 10,000 years after closure for the less mobile radionuclides.

Estimates of the EBS release shown in Figure 2.1-23(b) indicate a reduction in the EBS capability to retain ^{99}Tc by a factor of as much as 140 at 100,000 years as compared to the combined nominal/early failure modeling case (Figure 2.1-20(b)). There is also a reduction in the EBS capability by a factor between 4 and 10 for less-mobile radionuclides at 100,000 years and 1,000,000 years, including ^{226}Ra , ^{242}Pu , and ^{237}Np , which are key contributors to dose during the post-10,000-year period (SNL 2008d, Section 8.3.3.2.2[a]). Note that the activity of these radionuclides increases substantially after about 600,000 years, when failure of the waste packages by general corrosion processes dominate. The importance of general corrosion patches can be seen in Figures 2.1-16 and 2.1-17 by comparing the seismic ground motion modeling case mean results (which include general corrosion) with the nominal mean results. By 1,000,000 years, the total activity released in both the seismic ground motion modeling case and the combined nominal/early failure modeling case is approximately the same, indicating that the overall reduction in barrier

capability in each case, in terms of total activity released, is about a factor of only 10 in 1,000,000 years (SNL 2008d, Section 8.3.3.2.2[a]).

The performance of the EBS in preventing or substantially reducing the rate of radionuclide release to the Lower Natural Barrier as a result of combined seismic ground motion-induced degradation and nominal degradation processes is a function of several features and uncertain processes in the EBS. Similar to the combined nominal and early failure modeling case, the degree of degradation of the waste package controls the amount and rate of water that may enter the waste package and potentially allow degradation of the waste form. The degree of waste package degradation is highly uncertain and spatially variable, and is significantly influenced by the magnitude and timing of seismic ground motions that are also uncertain. After about 600,000 years (Figures 2.1-16 and 2.1-17), radionuclide releases from the EBS are determined primarily by processes related to the failure of waste packages from nominal processes. Again, thermal, chemical, waste-form degradation, and transport processes determine the radionuclide releases from the EBS once waste packages are breached. All of these processes contribute significant uncertainty to the projected radionuclide releases from the EBS.

To illustrate the uncertainty associated with the release of radionuclide activity from the EBS, radionuclide-specific release plots for selected radionuclides are presented in Figures 2.1-24 to 2.1-29 for combined nominal and seismic ground motion induced degradation processes:

- Figure 2.1-24: ^{99}Tc
- Figure 2.1-25: ^{237}Np
- Figure 2.1-26: ^{234}U
- Figure 2.1-27: ^{226}Ra
- Figure 2.1-28: ^{239}Pu
- Figure 2.1-29: ^{242}Pu .

The results in these figures are expected releases (averaged over the aleatory uncertainties), and thus largely reflect the influence of epistemic uncertainties. This series of plots is presented to illustrate the impact of uncertainties on the projections of the EBS radionuclide releases. As can be noted from these plots, the EBS releases for all six radionuclides corresponding to the 95th percentile are consistently close to the corresponding mean release curves, but are distant from the 5th percentile curves. This demonstrates that the mean releases are determined by expected releases for a relatively small number of epistemic sample elements for which the expected releases are comparatively large (SNL 2008d, Section 8.3.3.2.2[a]).

Summary of EBS Capability—The EBS prevents or substantially reduces the release rate of radionuclides from the waste forms, and prevents or substantially reduces the rate of movement of radionuclides from the repository to the accessible environment. The EBS performs these functions by virtue of the materials and design of the emplacement drifts, drip shields, waste packages, and waste forms and waste package internals. In addition, the EBS provides for chemical and thermal-hydrologic environments that lead to low solubilities for the radionuclides that make up the greatest fraction of the inventory activity. Finally, the EBS environments are such that radionuclide transport from the waste to the unsaturated zone is limited to a small fraction of the available inventory (less than 3×10^{-3} percent in 10,000 years, and 7% in 1,000,000 years), even in the case of seismic-induced mechanical degradation.

2.1.2.3 Lower Natural Barrier

The Lower Natural Barrier includes the unsaturated zone below the repository horizon and the saturated zone below the repository and downgradient from the repository to the accessible environment. Both the unsaturated and saturated features of the Lower Natural Barrier are ITWI (Table 2.1-1) and prevent or substantially reduce the rate of movement of radionuclides from the repository to the accessible environment due to slow advective transport combined with matrix diffusion and radionuclide sorption processes. Figure 2.1-30 is a schematic illustration of the Lower Natural Barrier.

As discussed in Section 2.1.1, the features of the Lower Natural Barrier have different processes and characteristics that influence the capability of these features to prevent or substantially reduce the rate of movement of radionuclides from the repository to the accessible environment (SNL 2008a, Section 6.2.2.3). The significant processes include hydrologic and thermal-hydrologic processes (SNL 2008a, Table 7-4) and transport processes, as identified in Table 2.1-4. Additional chemical, thermal-chemical, mechanical, and thermal-mechanical processes are generally of lesser significance in affecting the features of the Lower Natural Barrier. The processes identified in Table 2.1-4 have varying degrees of influence on the capability of the Lower Natural Barrier to perform its barrier function.

Some processes identified in Table 2.1-4 are more important contributors than others to the overall capability of the Lower Natural Barrier in preventing or substantially reducing the rate of movement of radionuclides from the repository to the accessible environment. Table 2.1-4 identifies those processes that significantly influence the ability of a particular feature to contribute to barrier capability (SNL 2008a, Table 7-4).

In the evaluation of the important processes related to the capability of the Lower Natural Barrier, consideration is given to both the beneficial as well as the potentially deleterious processes that act on each of the features of the barrier. The presence of a beneficial process generally results in preventing the movement of radionuclides or substantially reducing the rate of movement of radionuclides from the repository to the accessible environment. The evaluation of both beneficial and potentially deleterious processes that could affect the movement of radionuclides assures a more complete understanding of the barrier capability. The presence of a potentially deleterious process could result in an increase in the rate of movement of radionuclides from the repository to the accessible environment. Both beneficial and potentially deleterious processes have been identified as important contributors to the Lower Natural Barrier's capability (SNL 2008a, Section 6.2.2.3).

A few examples illustrate both beneficial and potentially deleterious processes and their effect on the Lower Natural Barrier. Sorption in the unsaturated and saturated zones has the beneficial effect of preventing the movement or substantially reducing the rate of movement of certain radionuclides that are major contributors to the activity of the radioactive waste. Climate modification, which can affect the amount of recharge in the unsaturated zone and the water table rise in the saturated zone, can significantly increase the rate of movement of radionuclides by increasing the flux. While the presence of fracture flow has a generally deleterious effect on unsaturated and saturated zone transport (depending on the degree of matrix diffusion), the absence of fracture flow has a beneficial effect of decreasing the rate of movement of radionuclides.

Unsaturated Zone below the Repository—The following processes and characteristics of the unsaturated zone below the repository are important to the capability of the Lower Natural Barrier:

- **Climate Change**—Future climate change causes several responses in the unsaturated zone beneath the repository, including changes in percolation flux and attendant radionuclide transport, water table rise, and recharge to the saturated zone. Precipitation and net infiltration into the unsaturated zone tends to increase with future climate change, causing an increase in fracture flux and, hence, a reduction in the effectiveness of matrix diffusion and an increase in recharge during the first 10,000 years after repository closure. After 10,000 years, the rate of percolation at the repository horizon is specified by proposed 10 CFR 63.342(c)(2) (70 FR 53313). In addition, based on forecast climate changes in the future, a higher water table is expected in the Yucca Mountain region for future, wetter climatic conditions. A higher water table impacts radionuclide transport in the unsaturated zone by shortening the transport distance between the repository and the water table, as presented in [Section 2.3.8](#).
- **Climate Modification Increases Recharge**—The ability of the unsaturated zone to prevent or substantially reduce the rate of movement of radionuclides is dependent on the flux of water through the unsaturated zone and the distribution of that flux within the fractured rock mass. This flux is directly dependent on the surficial recharge that, in turn, is affected by climatic change. The increase in recharge associated with the monsoon and glacial-transition climate states reduces the capability of the unsaturated zone feature below the repository to reduce the rate of radionuclide movement. This reduction is a function of (1) the increase in fracture flux and corresponding reduction in the effectiveness of matrix diffusion; and (2) the rise in the water table and the associated reduction in the unsaturated zone radionuclide travel length. The effects associated with a future climate change are included in the models presented in [Section 2.3.2](#).
- **Stratigraphy**—Stratigraphy and associated hydrologic properties have significant effects on unsaturated zone flow and transport processes due to (1) the contribution of faults in conducting flow below the repository; and (2) to the different flow characteristics of the TSw and zeolitic and vitric Calico Hills nonwelded (CHn) and Crater Flat undifferentiated (CFu) units. In particular, the low matrix permeability of the zeolitic CHn unit beneath the northern half of the repository block promotes fracture flow and/or lateral diversion towards faults. In contrast, the unaltered, vitric CHn unit beneath the southern region of the repository block has a relatively high matrix porosity and permeability, and matrix flow dominates. As a consequence, radionuclides released from the northern region of the repository tend to have much shorter transport times to the saturated zone than those released in the southern region because transport is primarily downward through fast flowing fractures and faults as opposed to much slower matrix flow. The effects of stratigraphy and hydrologic properties of the unsaturated zone are included in the flow and radionuclide transport models presented in [Sections 2.3.2](#) and [2.3.8](#), respectively.
- **Rock Properties of Host Rock and Other Units**—Percolation of water in the unsaturated zone below the repository is significantly affected by the hydrogeologic

properties of the rock units above and below the repository. Where fracture–matrix properties change abruptly, such as at the contact between welded tuffs and low-permeability units with sparse fractures, perched water zones may form, leading to lateral diversion of flow. Conversely, the presence of the PTn unit, characterized by porous flow in the matrix, attenuates and dampens the temporally and spatially variable pulses of flow moving through fractures in the welded Tiva Canyon Tuff so that the percolation of water in the unsaturated zone above and below the repository is quasi–steady state (Section 2.3.2).

- **Fractures**—Fractures below the repository conduct the majority of the percolation flux through the unsaturated zone, although (1) the low-matrix-permeability zeolitic rocks of the CHn cause increased lateral diversion toward the faults; and (2) the vitric CHn is dominated by matrix flow. The rate of flow and the extent of transport in fractures are influenced by such characteristics as orientation, aperture, asperity, spacing, fracture length, connectivity, and the nature of any linings or infills (Section 2.3.8).
- **Faults**—Faults of various sizes have been noted in the Yucca Mountain region, and specifically in the repository area. A significant fraction of percolation flux below the repository occurs through faults (SNL 2007e, Section 6.6.2.3). Faults provide fast flow and radionuclide transport pathways through the unsaturated zone, particularly below the northern region of the repository, where the low matrix permeability of the underlying zeolitic CHn unit promotes lateral flow and transport towards and down faults.
- **Fracture Flow in the Unsaturated Zone**—The rate of movement of radionuclides in the unsaturated zone is dependent on the flux of water through the fractured rock mass. This flux is distributed between faults, fractures, and the matrix of the host rock and other units in the unsaturated zone. The rate of movement of radionuclides is dependent on the degree of fracture flow, which is variable across the unsaturated zone below the repository. This rate of movement is not significantly reduced in the fractured portion of the unsaturated zone, unless matrix diffusion processes occur. The absence of fracture flow in the vitric portions of the Calico Hills below the southern half of the repository block substantially reduces the advective transport velocity, thus increasing the delay of movement of radionuclides in the unsaturated zone. The effects of fracture and matrix flow are included in the TSPA models presented in Sections 2.3.2 and 2.3.8.
- **Unsaturated Groundwater Flow in the Geosphere**—Unsaturated groundwater flow below the repository defines the redistribution of percolation flux in the unsaturated zone as a function of time, and is the primary mechanism for radionuclide transport below the repository. Although the flow rate in the unsaturated zone determines the amount of fracture flow, the fracture characteristics are also significant in determining the rate of radionuclide movement in the unsaturated zone, as discussed in Section 2.3.8.
- **Perched Water Develops**—The strongly altered CHn unit beneath the northern half of the repository is composed of zeolites and clays with low permeability and poorly developed, sparsely connected fractures. Because of low permeability, perched water may form at the contacts with CHn zeolitic tuffs below the northern half of the repository block, and a large portion of the percolating flux may be diverted laterally to the east

towards the faults, which act as main pathways for fast flow and transport in the unsaturated zone. The effects of existing perched water zones below the northern half of the repository block, and potential changes in these perched water zones caused by climate changes, are included in the site-scale unsaturated zone flow model presented in [Section 2.3.2](#).

- **Advection and Dispersion in the Unsaturated Zone**—Flow in the fractured rock system below the repository is dominated by fracture flow. Therefore, radionuclide transport is primarily advection dominated, and the influence of dispersion may be important. However, when compared to the spreading of radionuclides due to matrix diffusion effects, the impact on transport times of longitudinal dispersion is expected to be small ([Section 2.3.8.2.2.1](#)).
- **Matrix Diffusion in the Unsaturated Zone**—Matrix diffusion results in the diffusion of dissolved radionuclides from the fractures into the matrix of the rock. Because advective transport is significantly slower in the matrix, matrix diffusion is an effective retardation mechanism, especially for moderately to strongly sorbed radionuclides, due to the increase in rock surface accessible to sorption. Matrix diffusion of colloiddally transported radionuclides has been excluded from the unsaturated zone transport model presented in [Section 2.3.8](#).
- **Matrix Imbibition in the Unsaturated Zone**—Water and (dissolved and colloidal) radionuclides may be imbibed into the matrix between the flowing fractures. Matrix imbibition affects the distribution of flow between fractures and the matrix in the fractured unsaturated zone near the interface between the TSw and CHn in the Calico Hills nonwelded vitric rock beneath the southern half of the repository block, which substantially slows radionuclide transport ([Section 2.3.8](#)).
- **Sorption in the Unsaturated Zone**—Radionuclides released from the repository have varying retardation characteristics. Several radionuclides that are the dominant contributors to the total inventory are significantly retarded in the unsaturated zone when there has been significant matrix diffusion or matrix-dominated flow in the vitric Calico Hills. These include ^{90}Sr , ^{137}Cs , ^{239}Pu , ^{240}Pu , ^{241}Am , and ^{243}Am . The sorption of these radionuclides that diffuse into the matrix, or are transported in the matrix of Calico Hills, prevents the movement or significantly reduces the rate of movement of these radionuclides from the repository to the accessible environment. Sorption is included in the unsaturated zone transport models presented in [Section 2.3.8](#).

Saturated Zone—The following processes and characteristics of the saturated zone are important to the capability of the Lower Natural Barrier:

- **Climate Change**—Climate change causes two primary responses in the saturated zone: (1) water table rise, and (2) increased recharge to the saturated zone. A higher water table is expected in the Yucca Mountain region for future, wetter climatic conditions. Also, groundwater flow would tend to increase for future, wetter climates. This effect is included in the models presented in [Section 2.3.9](#).

- **Climate Modification Increases Recharge**—The increase in recharge to the saturated zone associated with the monsoon and glacial-transition climate states is expected to increase groundwater flow in the saturated zone. This effect is included in the models presented in [Section 2.3.9](#). A similar increase in groundwater flow occurs in the post-10,000-year analyses.
- **Stratigraphy**—The geometric relationships and characteristics of stratigraphic variations and faults have a pronounced effect on saturated zone flow at the site scale. The location at which groundwater flow moves from fractured volcanic rocks to alluvium is of particular significance from the perspective of barrier capability ([Section 2.3.9.2.1](#)). This volcanic/alluvium contact is important because of contrasts between the fractured volcanic units and the alluvium in terms of groundwater flow (fracture-dominated flow versus porous medium flow), and in terms of enhanced sorptive properties of the alluvium for some radionuclides relative to the volcanic rocks. Stratigraphic variations and geometry are also major factors leading to three-dimensional flow patterns in the saturated zone. These flow patterns have a significant impact on flow in the saturated zone with respect to radionuclide transport. The stratigraphic relationships are incorporated into the hydrogeologic framework model for the saturated zone site-scale flow and transport model ([Section 2.3.9.2.2](#)).
- **Rock Properties of Host Rock and Other Units**—Flow of water in the saturated zone is significantly affected by the hydrogeologic properties of the rock units, particularly where fracture–matrix properties change abruptly, such as at the contact between the volcanic and alluvium units. Rock properties also have a significant effect on the rate of radionuclide movement through their influence on the transport properties (notably, the flowing interval spacing, effective diffusion coefficient, fracture porosity, and effective porosity of the alluvium), retardation properties, and matrix porosity of the volcanic units ([Section 2.3.9](#)). Rock properties for 23 hydrostratigraphic units and 10 discrete hydrogeologic features—such as faults—are explicitly included in the saturated zone flow and transport abstraction model ([Section 2.3.9](#)).
- **Fractures**—Fracture characteristics are important to the barrier capability of the saturated zone, because groundwater flow occurs primarily within the fracture network of the volcanic tuff units. The fracture networks in the saturated zone appear to be well connected over large distances at the scales of interest (hundreds of meters to kilometers). Fracture networks, in turn, control the movement of dissolved and colloidal radionuclides below the water table. Fracture characteristics (e.g., fracture porosity, flowing interval porosity, and flowing interval spacing) are included in the saturated flow and transport abstraction model using a dual-porosity effective continuum approach ([Section 2.3.9](#)).
- **Faults**—Numerous faults of various sizes have been noted in the Yucca Mountain region, and specifically in the repository area. Faults affect the groundwater flow paths, influence the horizontal anisotropy in permeability, and can enhance dispersion by increasing permeability heterogeneities along the saturated zone flow paths. Geologic features and hydrostratigraphic units are explicitly included in the models for saturated zone flow and transport in a configuration that accounts for the effects of existing faults based on the hydrogeologic framework model ([Section 2.3.9](#)).

- **Water-Conducting Features in the Saturated Zone**—Water flow in the saturated zone occurs within either the fractured tuff units or the alluvium. The groundwater flow rates, radionuclide transport velocities, and radionuclide retardation characteristics of these different water-conducting features are significantly different. In particular, the alluvium provides a significant reduction in the movement of radionuclides to the accessible environment due to the lack of fracture flow. In addition to the differences in flow and transport characteristics of the different lithologic units in the saturated zone, the presence of discrete flowing features in the fractured tuff units affects the rate of movement of radionuclides to the accessible environment. These characteristics of the saturated zone have been included in the models presented in [Section 2.3.9](#).
- **Saturated Groundwater Flow in the Geosphere**—Groundwater flow in the saturated zone below the water table may affect long-term performance of the repository. The location, magnitude, and direction of flow under present and future conditions influence transport to the accessible environment. These effects are included in the model presented in [Section 2.3.9](#).
- **Advection and Dispersion in the Saturated Zone**—Advection is the principal transport mechanism for both dissolved and colloidal radionuclides in the saturated zone. The advective flux is dependent on the hydrogeologic characteristics of the water-conducting features in the saturated zone, as well as the groundwater flow rates through these features. Dispersive processes tend to spread transient radionuclide pulses that may be released to the saturated zone (e.g., following the water table rise associated with climate changes). These processes have been included in the models presented in [Section 2.3.9](#).
- **Matrix Diffusion in the Saturated Zone**—Matrix diffusion is the process by which radionuclides and other species transported in the saturated zone by advective flow in fractures or other pathways move into the matrix of the porous volcanic formations by diffusion. Matrix diffusion can be an effective radionuclide retardation mechanism, especially for strongly sorbed radionuclides, due to the increase in rock surface accessible to sorption. Field scale in situ tracer tests at the C-Wells demonstrated that matrix diffusion is an important transport mechanism in fractured volcanic formations in the saturated zone. Matrix diffusion is included in models presented in [Section 2.3.9](#).
- **Sorption in the Saturated Zone**—Radionuclides released from the repository have varying retardation characteristics. Several radionuclides that are the dominant contributors to the total inventory are significantly retarded in the saturated zone. These include ^{90}Sr , ^{230}Th , ^{226}Ra , ^{137}Cs , ^{239}Pu , ^{240}Pu , ^{242}Pu , ^{241}Am , and ^{243}Am . The sorption behavior of these radionuclides significantly reduces the rate of movement of these radionuclides from the repository to the accessible environment. Sorption effects are included in the models presented in [Section 2.3.9](#).

The bases for the models used in the analysis of unsaturated zone flow are described in [Section 2.3.2](#). The flow fields are generated using the three-dimensional site-scale unsaturated zone flow model with input parameters based on unsaturated zone calibrated properties. These flow fields are developed for spatially varying net-infiltration maps for the present-day, monsoon, and glacial-transition climate states and the post-10,000-year period. The processes incorporated into

the unsaturated zone transport model include sorption, fracture–matrix interaction, colloid-facilitated radionuclide transport, resuspension, and dispersion. The bases for the radionuclide transport process model used to assess the capability of the unsaturated zone component of the Lower Natural Barrier are the same as those implemented in the TSPA abstraction regarding radionuclide transport in the unsaturated zone ([Section 2.3.8.5](#)).

The flow and radionuclide transport model for the saturated zone is discussed in detail in [Sections 2.3.9.2](#) and [2.3.9.3](#), respectively. The analysis of the capability of the saturated zone component of the Lower Natural Barrier is derived from the same models used as the basis for the TSPA abstractions for flow and transport in the saturated zone. Key uncertainty parameters (i.e., groundwater flux, sorption coefficients, and matrix diffusion transport parameters) are varied, subject to uncertainty distributions based on the available data and observations, and these uncertainties are reflected in the model results.

2.1.2.3.1 Capability of the Unsaturated Zone below the Repository to Prevent or Substantially Reduce the Rate of Movement of Radionuclides to the Water Table

The unsaturated zone below the repository prevents or substantially reduces the rate of movement of radionuclides from the repository horizon to the water table. The radionuclides take time to move through the unsaturated zone. As water percolates down, sorption, and matrix diffusion cause the movement of radionuclides to be slower relative to the general movement of the percolating water. The existence of perched water bodies introduces three-dimensional lateral flow within the unsaturated zone below the repository level. Below the northern half of the repository block, low-permeability layers and perched water bodies in the CHn unit channel a large fraction of flow laterally to faults that act as conduits for water flow to the water table ([Table 2.3.2-7](#); [Section 2.3.2.2.1.4](#)). Radio nuclides are also dispersed during movement in the unsaturated zone because of variability in radionuclide transport times and in the retardation characteristics of the various volcanic units.

The data and analyses supporting models of radionuclide transport in the unsaturated zone summarized below are described in detail in [Section 2.3.8](#). [Figure 2.1-31](#) shows the sequence of hydrogeologic units comprising the unsaturated zone below the repository and a conceptualization of flow processes in these units. This figure shows that these features include the lower part of the TSw and the tuffs of the CHn and CFu units. These units together provide a feature ranging from 200 to 400 m thick (300 m thick, on average) under present-day climate conditions. The TSw unit is characterized by very low matrix permeability and well-connected, steeply dipping fracture networks. The CHn unit underlies the TSw unit. Below the southern part of the repository, the CHn unit is vitric, composed of unaltered glassy shards of volcanic ash, and characterized by relatively high matrix permeability. Fractures are rare to nonexistent in the vitric CHn unit, and flowdown through this unit is predominantly through the matrix. Below the vitric CHn unit are the devitrified and zeolitized tuffs of the Prow Pass welded tuff unit. These tuffs have low matrix permeability compared with the vitric CHn unit, and water flow through such tuffs is primarily in fractures. The fracture networks in these welded tuffs are generally bed-confined and not well connected.

The movement of radionuclides carried by water in the matrix of the TSw unit is slow because of sorption in the rock matrix. The rate of movement of radionuclides carried by water in the fractures

is more rapid than in the matrix, and sorption is weaker. Consequently, the matrix of the TSw unit more effectively retards the migration of the radionuclides than the fracture system. Matrix diffusion transfers radionuclide mass from the fracture flow into the matrix.

At the base of the TSw unit, downward-moving radionuclides encounter the CHn unit. Because of the low permeability and infrequency of connected fractures of the zeolitic CHn unit beneath the northern part of the repository block, and because the flow down from the overlying TSw unit is primarily in the fractures, perched water zones form at the TSw–CHn contact. A significant fraction of the downward-percolating flux is diverted laterally to the east in this region. The present age of the perched water ranges from several thousand years to as much as 11,000 years (Section 2.3.2.2.1.3).

Beneath the northern part of the repository, the radionuclides either enter the zeolitic CHn unit or are diverted to the east in the perched water (Figure 2.1-31). The zeolitic CHn unit is strongly altered to a mixture of minerals, including zeolites and clays. The minerals have precipitated in the pores of the rock so that the matrix permeability of the zeolitic CHn unit is low. Most of the downward flow that reaches the zeolitic CHn unit is diverted laterally through perched water zones at the TSw-CHn contact, bypassing this unit and flowing through faults or connected fractures, which leads to short radionuclide transport times to the saturated zone.

Beneath the southern part of the repository, the radionuclides are transferred into the vitric CHn unit matrix, where groundwater velocity is low relative to the velocity in the fractures and where sorption is strong. Below the vitric CHn unit, the radionuclides move predominantly in the fractures of the underlying devitrified and zeolitized tuffs. Because the fracture flow pathways are not continuous, the alternating layers of welded, nonwelded, and zeolitized tuffs delay the movement of radionuclides, which leads to long transport times to the saturated zone compared to release locations in the northern repository region (Figure 2.3.8-36).

The combination of slow water movement from the repository to the water table, and processes that retard the rate of movement of radionuclides in the unsaturated zone (Figure 2.3.8-3), results in a reduction in the activity of the radionuclides and their release to the saturated zone.

2.1.2.3.2 Capability of the Saturated Zone to Prevent or Substantially Reduce the Rate of Movement of Radionuclides to the Accessible Environment

Radionuclides that migrate through the unsaturated zone to the water table are transported through the saturated zone before they can reach the accessible environment. The data and analyses supporting models of radionuclide transport in the saturated zone that are summarized below are described in detail in Section 2.3.9.

Figure 2.1-32 shows a cross section of the units in the saturated zone. The location of this cross section is shown in Figure 2.1-33. Groundwater below Yucca Mountain is part of the Alkali Flat–Furnace Creek groundwater subbasin within the Death Valley regional groundwater system. Groundwater flow is generally to the south and east near Yucca Mountain. The southeasterly flow from the site is incorporated into the stronger southward flow in western Jackass Flats. The expected

pathway for movement of radionuclides through the saturated zone is southeast from the repository site, transitioning to southerly flow to the accessible environment in the Amargosa Desert.

The pathways for radionuclide movement in the saturated zone for the first 12 to 14 km downgradient from Yucca Mountain occur in fractured volcanic rocks. This portion of the saturated zone feature is affected by the faulting and tilting of the volcanic rocks and is represented in an equivalent continuum model in terms of two aquifers: (1) an upper volcanic aquifer associated with the Paintbrush group; (2) a lower volcanic aquifer associated with the Prow Pass, Bullfrog, and Tram Tuff units (Section 2.3.9.2.3).

The cross section shown in Figure 2.1-32 is located along the approximate pathways for radionuclide movement as the radionuclides encounter alluvial sediments approximately 12 to 14 km from Yucca Mountain. These alluvial sediments are generally represented as a single porous medium with equivalent continuum properties to represent heterogeneity in the flow and transport characteristics of these sediments.

The saturated zone feature of the Lower Natural Barrier includes the fractured volcanic rocks from below the repository to approximately 12 to 14 km southeast and south of Yucca Mountain and the saturated alluvium at the water table from the volcanic aquifer to the accessible environment. The rate of radionuclide movement in the saturated zone is quite variable, with median tracer (e.g., ^{99}Tc) transport times ranging from about 10 years to 22,000 years (SNL 2008f, Table 6-10[a]). In addition, several processes cause the rate of movement of radionuclides to be slower compared to the rate of movement of the water. The data and models for saturated zone flow and transport are discussed in Section 2.3.9.

Flow in the upper and lower volcanic aquifers is predominantly in the fractures. The matrix materials of the volcanic tuffs generally have a 2 to 6 order-of-magnitude lower hydraulic conductivity than observed in flowing fractures under natural groundwater-flow conditions. The matrix materials also have significantly greater porosity than do fractures, so there is a correspondingly greater volume of fluid stored in the matrix pore space of these saturated aquifers. The additional stored fluid and pore space is important to radionuclide transport because radionuclides can exchange between the fractures and matrix via matrix diffusion. This diffusive exchange results in a slower effective travel velocity for the bulk of the released radionuclides relative to water-flow velocities in the fractures for two reasons. First, the velocity of water in the pores of the matrix is slower than that in the fracture pores. Second, sorption onto mineral surface areas in the matrix pores will result in an even slower rate of movement of the radionuclides that diffuse into the matrix materials.

Because the alluvial materials are a porous medium, water flow and radionuclide transport occur in intergranular pores in the alluvium. The conceptual model for transport in the alluvial sediments is that of a porous continuum. The effective porosity of the alluvium is greater than the fracture porosity of the tuffs. Consequently, pore velocities in the alluvium are smaller than those in the fractures of the volcanic aquifers. Although matrix diffusion is not considered to be important in the alluvium, radionuclide rate of movement is slow because of the low water velocity. In addition, sorption onto minerals in the alluvium results in retardation of radionuclides relative to the water movement in these sediments (Section 2.3.9.3.1).

The volcanic rocks and alluvial material in the saturated zone also reduce the rate of movement of radionuclides associated with colloids. Filtration of colloids results in retardation of the movement of radionuclides embedded in the colloids or irreversibly sorbed to these colloids. Radionuclides that are sorbed reversibly to colloids are affected by matrix diffusion in the volcanic aquifers and by sorption in the alluvial sediments. Consequently, movement of these colloid-associated radionuclides is also retarded relative to the movement of water in the saturated zone.

The combination of low groundwater velocity and retardation and sorption processes prevent or substantially reduce the rate of movement of radionuclides to the accessible environment.

2.1.2.3.3 Time Period over Which the Lower Natural Barrier Functions

The Lower Natural Barrier is a durable feature of the geologic setting at Yucca Mountain, and is not expected to change in any significant way in the 10,000 years following closure of the repository. With the exception of minor effects caused by the construction of the repository, the emplacement of waste, and the increase in percolation, increase in saturated zone flux, and water table rise as a result of future climate states, the hydrogeology and physical characteristics of the Lower Natural Barrier are not expected to change in any significant way in the 10,000 years after closure. It is also assumed that, for the purposes of projecting postclosure performance after 10,000 years, but within the period of geologic stability, the intrinsic hydrologic, geologic and geochemical characteristics of the Lower Natural Barrier will not change significantly. This assumption is consistent with the requirements of proposed 10 CFR 63.342(c) (70 FR 53313) by projecting the continued effects of the 10,000-year screened-in FEPs out to the limit of geologic stability at 1,000,000 years, with the exception of those FEPs outlined in proposed 10 CFR 63.342(c) (70 FR 53313) related to the effect of seismic events, igneous events, climate change, and general corrosion beyond 10,000 years.

The unsaturated zone is largely unaffected by the local changes associated with repository construction and waste emplacement. The magnitude of changes to rock hydrologic properties attributable to coupled thermal-hydrologic-geochemical-mechanical processes is small, and does not have a significant effect on the overall behavior of unsaturated zone flow and transport. Geochemical studies have shown that minerals, such as calcite, silica, clays, and zeolites, could be dissolved and/or diagenetically altered in some areas or precipitated and altered in other areas, depending on local geochemical conditions. However, these local changes are not expected to change the overall hydraulic properties of the repository host rock that are included in the variability in performance models, because changes in fracture properties due to mineral precipitation or dissolution or thermal-mechanical stresses are on the order of natural variation (SNL 2008b, Section 6.2, FEPs 2.2.08.03.0B, Geochemical interactions and evolution in the unsaturated zone, and 2.2.10.04.0A, Thermo-mechanical stresses alter characteristics of fractures near repository) and are therefore excluded from the TSPA.

Projected climate change will raise the water table and increase the flux of percolating water through the unsaturated zone (SNL 2008b, Section 6.2, FEPs 1.3.01.00.0A, Climate change, and 1.3.07.02.0A, Water table rise affects saturated zone). The impact of these two effects on transport through the unsaturated zone is included in the TSPA. However, these factors are not expected to alter appreciably the processes that influence radionuclide transport (Section 2.3.8.4.5.5). The potential for increased percolation flux through the unsaturated zone results in increased advective transport velocities through the fractured rock mass in the unsaturated zone, which tend to decrease

the advective transport time of radionuclides to the water table. However, the properties controlling matrix diffusion and radionuclide retardation on radionuclide transport through the unsaturated zone are not expected to change with time (SNL 2008b, Section 6.2, Excluded FEPs 2.2.10.05.0A, Thermo-mechanical stresses alter characteristics of rocks above and below the repository; 2.2.10.06.0A, Thermo-chemical alteration in the unsaturated zone (solubility, speciation, phase changes, precipitation/dissolution); and 2.2.10.07.0A, Thermo-chemical alteration of the Calico Hills unit).

The volcanic tuffs and alluvium in the saturated zone are durable features of the geologic environment, and the characteristics of this feature of the Lower Natural Barrier system are not expected to change during the 10,000 year compliance period (SNL 2008a, Section 6.2.2.3.3). Processes acting during the first 10,000-year assessment are propagated to continue throughout the period of geologic stability ending at 1,000,000 years after closure (SNL 2008a, Section 6.2.2.3.3). Although the effects of these processes may change with time, the processes acting on the system are the same throughout time. The hydrologic conditions within the saturated zone may change, however, as the climate changes. At a regional scale, future climate conditions that are wetter than present-day conditions are expected to yield greater groundwater recharge, resulting in a rise in the water table and greater groundwater flux along the saturated zone flow path. This change in the water table and flux is explicitly taken into account in the model abstraction for saturated zone flow and transport.

2.1.2.3.4 Uncertainties Associated with Lower Natural Barrier Capability

The performance of the Lower Natural Barrier is subject to uncertainty that is a function of the applicability of the conceptual and numerical models used to describe flow and transport in the Lower Natural Barrier, and the degree of knowledge of the data and parameters that characterize flow and transport in the unsaturated and saturated zones beneath the repository. To accommodate both variability and uncertainty in the description of the site, many of the input parameters to the unsaturated and saturated zone flow and transport models have been defined as probabilistic distributions. This approach allows a large range of uncertainty to be directly incorporated into process and performance assessment models. The variability and uncertainty in barrier capability is reflected in the broad range of transport times and radionuclide breakthrough curves resulting from the unsaturated zone and saturated zone transport models. The treatment of data and model uncertainties associated with analyses of the Lower Natural Barrier are described in (1) [Sections 2.3.8.4.5 and 2.3.8.5.5](#) for climate and unsaturated zone flow and transport, and (2) [Sections 2.3.9.2.3 and 2.3.9.3.3](#) for the saturated zone flow and transport.

Uncertainties in the flow and transport characteristics affecting radionuclide transport in the unsaturated zone have been included in the model abstractions or have been conservatively represented, as presented in [Sections 2.3.2 and 2.3.8](#). Uncertain parameters related to unsaturated zone flow include the percolation flux and fracture–matrix interaction (which is correlated to the percolation flux), both of which affect the flux distribution in fractures. Uncertain parameters related to matrix diffusion include the matrix diffusion coefficient, and the geometric parameters that affect the effective fracture–matrix interconnection area. Uncertain parameters related to sorption include the sorption coefficients for various radionuclides in the vitric, devitrified, and zeolitic tuff rock units. Uncertain parameters used to model colloid-facilitated transport include a colloid retardation factor.

Uncertainties in the unsaturated zone flow characteristics have been addressed by evaluating four percolation flux distributions. Uncertainties in the conceptual model of matrix diffusion are larger than the impact of parameter uncertainties, and have been conservatively treated by representing matrix diffusion in the unsaturated zone transport model using a dual-permeability formulation. Other transport-related uncertainties have been addressed by sampling from the range of parameter values determined to reasonably represent the uncertainty, including sorption parameters and colloid retardation parameters.

Uncertainties in flow and transport characteristics affecting radionuclide transport in the saturated zone have been included in the model abstractions presented in [Section 2.3.9](#). Uncertain parameters related to saturated zone flow include uncertainty in the groundwater-specific discharge, flowing interval porosity, alluvium effective porosity, and horizontal anisotropy. Uncertain parameters related to matrix diffusion include flowing interval spacing, effective diffusion coefficient, and matrix porosity. Uncertain parameters related to sorption include the sorption coefficients for various radionuclides for tuff and alluvium. Uncertain parameters used to model colloid-facilitated transport include colloid retardation factors, fast fraction of colloids, groundwater concentration of colloids, and sorption coefficients onto colloids.

Uncertainties in saturated zone groundwater flow and transport have been addressed by using probabilistic representations of parameter values that are important to transport, such as hydrologic and geologic properties. For example, the uncertainty in the groundwater-specific discharge has been evaluated by considering a base case with a median specific discharge of 0.36 m/yr near the repository for the present-day climate, with a range of 0.11 to 8.9 times the base-case specific discharge. Uncertainty in groundwater flow or advection has been considered by evaluating ranges of groundwater-specific discharge, flowing interval porosity, alluvium effective porosity, and horizontal anisotropy.

There is uncertainty concerning the nature of the geology in the saturated zone along the flow path from the repository at distances of approximately 10 to 18 km downgradient from the repository. The portions of the flow path devoted to fractured volcanic rock and alluvium are important to saturated zone capability, because the movement of radionuclides through the saturated zone is affected by the contrast in the flow between these two media and because the retardation characteristics of the two media are different. Uncertainty in the location of the alluvium is represented in terms of a probability distribution for its northwestern boundary ([Section 2.3.9.3.3.4](#)). This distribution is sampled in the TSPA and in barrier capability analyses ([Section 2.4.2.3.2.1.10](#)).

2.1.2.3.5 Impact of Disruptive Events on the Lower Natural Barrier

The Lower Natural Barrier is generally unaffected by disruptive events. For seismic activity, it is expected that the general configuration of the geologic units below the repository and downgradient to the accessible environment is unchanged. The velocity of percolating water in the unsaturated zone and of groundwater in the saturated zone will not increase due to seismic activity. The characteristics of matrix and fracture flow, colloidal transport, and sorption are not expected to change due to seismic activity ([Table 2.2-5](#)) (SNL 2008b, FEPs 1.2.10.01.0A, Hydrologic response to seismic activity; 2.2.06.01.0A, Seismic activity changes porosity and permeability of rock; 2.2.06.02.0B, Seismic activity changes porosity and permeability of fractures; 2.2.06.03.0A,

Seismic activity alters perched water zones). For igneous activity, both the intrusive and eruptive cases are the results of isolated dikes of magma that rise through the Lower Natural Barrier. However, the processes and characteristics of the Lower Natural Barrier are not significantly affected (SNL 2008b, Section 6.2, FEP 1.2.04.02.0A, Igneous activity changes rock properties). Therefore, the general effectiveness of the Lower Natural Barrier to prevent or substantially reduce the rate of movement of radionuclides from the repository to the accessible environment would not significantly change following disruptive events. The summary of the effects of the disruptive events on the Lower Natural Barrier is discussed in [Section 2.2.1](#).

2.1.2.3.6 Quantification of the Lower Natural Barrier

The Lower Natural Barrier includes the unsaturated zone below the repository horizon and the saturated zone below the repository and downgradient from the repository to the accessible environment. Both the unsaturated and saturated features of the Lower Natural Barrier prevent or substantially reduce the rate of movement of radionuclides from the repository to the accessible environment due to slow advective transport combined with matrix diffusion and radionuclide sorption processes. The reduction in the rate of movement of radionuclides is examined in this section by reviewing radionuclide travel times for the unsaturated zone ([Section 2.3.8](#)) and saturated zone ([Section 2.3.9](#)), and by using the activity released from the EBS for key radionuclides described in [Section 2.1.2.2.6](#), and evaluating the release of these radionuclides from the saturated zone to the accessible environment. This approach utilizes the TSPA model that is presented in [Section 2.4](#) and in particular, the TSPA abstraction models for unsaturated zone transport and saturated zone flow and transport described in [Sections 2.3.8](#) and [2.3.9](#), respectively.

The capability of the Lower Natural Barrier to prevent the movement or substantially reduce the rate of movement of radionuclides from the repository to the accessible environment is dependent on the effects of climate change, the sorption characteristics of the radionuclides, whether the radionuclides are expected to be transported colloidally, and hydrogeologic variability within the unsaturated and saturated zones. Climate change has the effect of increasing the recharge in the unsaturated zone and raising the water table in the saturated zone. Both of these effects result in an increase in the advective transport velocity through these two features of the Lower Natural Barrier. The water table rise also causes a reduction in the transport path through the unsaturated zone. Recognizing that the rate of radionuclide of movement through the Lower Natural Barrier is a complex function with multiple processes (such as matrix diffusion, sorption, and decay), the demonstration of Lower Natural Barrier capability is presented in terms of reduction of radionuclide activity. This metric directly reflects impact of the delay and decay that occurs along the transport path from the EBS to the accessible environment.

In a seeping environment, the majority of the activity released from the EBS into the unsaturated zone enters into the fractures of the unsaturated zone as compared to the rock matrix. Drift seepage is diverted around the drip shield as it flows downward, and subsequently, through the invert carrying the radionuclide activity advectively into the fractures. The significance of fracture versus matrix releases will be discussed further below in the context of hydrogeologic variability within the unsaturated zone.

Unsaturated zone transport results presented in [Section 2.3.8.5.4](#) illustrate the importance of hydrogeologic variability within the unsaturated zone and its impact on barrier capability. This

section presents breakthrough curves for different radionuclides from specified repository release locations to the water table, assuming median values for all uncertain parameters. Underneath the northern region of the repository, transport from the EBS to the saturated zone is predominantly fracture transport, whereas underneath the southern region of the repository, transport from the EBS to the saturated zone will go through the CHn, where it will be predominantly matrix transport. The radionuclide breakthrough curves presented in [Figure 2.3.8-43](#) illustrate the impact of hydrogeologic variability for the glacial-transition 10th percentile infiltration scenario. Due to pervasive fracture transport along the entire flow path, arrival times for radionuclides are much shorter for those released from a northern location of the repository compared to those released from a southern location. The first arrival at the water table from the northern location is within a year, versus about 400 years from the southern location. Because of the longer transport time through the matrix units, cumulative arrivals at the water table are negligible for radionuclides released from the southern location, for both relatively short-lived and strongly sorbing radionuclides, including (for example) ^{137}Cs , ^{90}Sr , and ^{226}Ra ([Section 2.3.8.5.4](#)). However, significant proportions of most radionuclides released from the EBS, including short-lived and strongly sorbing radionuclides, reach the water table for releases from the northern part of the repository.

In the TSPA, radionuclides can enter the unsaturated zone transport model in either the fracture or matrix domain, depending on the nature of the hydrologic and transport conditions in the EBS ([Section 2.3.8.5.4](#)). [Figure 2.3.8-49](#) compares the normalized breakthrough curves for fracture versus matrix release for ^{99}Tc released at the northern (upper figure) or southern (lower figure) release locations. For the northern release location, nearly 50% of mass released into the fracture reaches the water table within about 20 years, compared to about 5,000 years for 50% of mass released into the matrix to reach the water table ([Section 2.3.8.5.4](#)). For the southern release location, the breakthrough curves are very similar regardless of whether the releases are in the fracture or the matrix. When radionuclide mass is released into the matrix of the TSw at the repository horizon, local matrix percolation rates are so low that, for radionuclides to escape the unsaturated zone, they must first diffuse to a nearby flowing fracture. Thus, the additional transport time is due to the slow rate of the diffusion process transporting radionuclides to the fracture. This process will be governed by the diffusion coefficient, spacing between flowing fractures, and, for sorbing species, the sorption coefficient.

Illustrations of the expected saturated zone transport are presented in [Figures 2.3.9-16](#), [2.3.9-45](#), [2.3.9-46](#), and [2.3.9-47](#). Because of matrix diffusion, radionuclide sorption and other retardation processes, many of the radionuclides released from the saturated zone will be strongly retarded. [Figure 2.3.9-16](#) shows nonsorbing radionuclides (e.g., ^{99}Tc) with median transport times in the saturated zone ranging from about 10 to 10,000 years. A significant fraction of radionuclide mass has much longer transport times in many realizations, due to the effects of matrix diffusion in fractured volcanic units. For moderately sorbing radionuclides, such as ^{237}Np ([Figure 2.3.9-45](#)), the median transport times within the saturated zone range from about 100 to more than 100,000 years. For highly sorbing radionuclides (e.g., ^{239}Pu), median transport times within the saturated zone generally exceed 10,000 years ([Figure 2.3.9-46](#)). For radionuclides irreversibly attached onto colloids, median transport times in the saturated zone range from 100 to 600,000 years ([Section 2.3.9.3.4.1.1](#) and [Figure 2.3.9-47](#)). These ranges in effective mass breakthrough times reflect the combined natural variability in transport times, as well as the effects of the uncertainties associated with the saturated zone flow and transport abstraction model ([Section 2.3.9.3](#)).

Insights into the overall effectiveness of the Lower Natural Barrier were developed via probabilistic projections. The projections were generated using the TSPA model to simulate the evolution of radionuclide releases from the repository and resultant transport through the unsaturated zone and saturated zone, extending to the accessible environment boundary. As described in [Section 2.1.2](#), two modeling cases were analyzed:

1. Combined nominal/early failure demonstration modeling case
2. Seismic ground motion modeling case.

The first modeling case provides insight into the capability of the Lower Natural Barrier to reduce radionuclide movement for conditions of early releases from a few early failed waste packages and late releases (e.g., from general corrosion patch penetrations beginning at about 600,000 years, from the 95th percentile curve) from an increased number of waste packages. The second modeling case examines the Lower Natural Barrier's capability to reduce radionuclide movement for conditions of seismic-induced releases distributed over both the 10,000-year and post-10,000-year time periods. As described in [Section 2.1.2.2.6](#), the radionuclide releases computed for the seismic ground motion modeling case occur from a variety of breach modes (e.g., seismic-induced stress corrosion cracking, rupture, puncture, and general corrosion patches).

To provide a relative metric of barrier effectiveness, the radionuclide activity released from the unsaturated zone and saturated zone was computed using the TSPA model and the balance equations (SNL 2008d, Section 8.3.3.3[a]):

$$\bar{R}_{UZ,k}(t|\mathbf{e}) = \bar{A}_{T,k}(t|\mathbf{e}) - (\bar{A}_{WP,k}(t|\mathbf{e}) + \bar{A}_{I,k}(t|\mathbf{e}) + \bar{A}_{UZ,k}(t|\mathbf{e})) \quad (\text{Eq. 2.1-2})$$

$$\bar{R}_{SZ,k}(t|\mathbf{e}) = \bar{A}_{T,k}(t|\mathbf{e}) - (\bar{A}_{WP,k}(t|\mathbf{e}) + \bar{A}_{I,k}(t|\mathbf{e}) + \bar{A}_{UZ,k}(t|\mathbf{e}) + \bar{A}_{SZ,k}(t|\mathbf{e})) \quad (\text{Eq. 2.1-3})$$

where $\bar{R}_{UZ,k}(t|\mathbf{e})$ and $\bar{R}_{SZ,k}(t|\mathbf{e})$ are the expected activities (in curies) of releases of radionuclide k from the unsaturated zone and saturated zone, respectively. The term $\bar{A}_{T,k}(t|\mathbf{e})$ is the expected total activity of radionuclide k in the inventory (initial inventory decayed through time); $\bar{A}_{WP,k}(t|\mathbf{e})$ is the expected activity of radionuclide k in a waste package (including the activity in undegraded waste forms); $\bar{A}_{I,k}(t|\mathbf{e})$ is the expected activity of radionuclide k in the invert; $\bar{A}_{UZ,k}(t|\mathbf{e})$ is the expected activity of radionuclide k in the unsaturated zone; and $\bar{A}_{SZ,k}(t|\mathbf{e})$ is the expected activity of radionuclide k in the saturated zone.

The means of the quantities $\bar{R}_{UZ,k}(t|\mathbf{e})$ and $\bar{R}_{SZ,k}(t|\mathbf{e})$ are denoted by $\bar{\bar{R}}_{UZ,k}(t)$, and $\bar{\bar{R}}_{SZ,k}(t)$, respectively, and are compared with the mean EBS releases, $\bar{\bar{R}}_{EBS,k}(t)$, to provide an indication of barrier capability. The mean percent reduction ($\bar{\bar{PR}}$) in activity achieved by the unsaturated zone

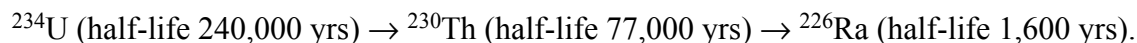
alone, and by the Lower Natural Barrier as a whole, is estimated from the equations (SNL 2008d, Section 8.3.3.3[a]):

$$\overline{\overline{PR}}_{UZ,k} = (1 - [\overline{\overline{R}}_{UZ,k} / \overline{\overline{R}}_{EBS,k}]) \times 100 \quad (\text{Eq. 2.1-4})$$

$$\overline{\overline{PR}}_{LNB,k} = (1 - [\overline{\overline{R}}_{SZ,k} / \overline{\overline{R}}_{EBS,k}]) \times 100 \quad (\text{Eq. 2.1-5})$$

where $\overline{\overline{R}}_{EBS,k}$, $\overline{\overline{R}}_{UZ,k}$, and $\overline{\overline{R}}_{SZ,k}$ are the peak values (at any time) of the mean activity release of radionuclide k within the time period under consideration (i.e., time 0 to 10,000 years and 10,000 years to 1,000,000 years).

In the special case of decay chain radionuclides, the quantities $R_{UZk}(t)$ and $R_{SZk}(t)$ typically represent in-growth instead of transport of the individual species. This is generally the case for ^{230}Th and ^{226}Ra . Their activities at any point in the Lower Natural Barrier are calculated via secular equilibrium and the simple decay chain:



Both ^{230}Th and ^{226}Ra move through the Lower Natural Barrier at significantly slower rates than their precursor ^{234}U (SNL 2008f, Table 6-10[a]). As a result, their activities are primarily determined by the chain decay process as opposed to by groundwater transport of their individual species.

Capability of Lower Natural Barrier to Prevent or Substantially Reduce the Rate of Radionuclide Movement—A demonstration of the Lower Natural Barrier capability was developed using the TSPA model to simulate radionuclide movement from the EBS through the combined unsaturated zone and saturated zone to the accessible environment. The unsaturated zone portion includes the TSw and CHn tuffs of the Crater Flat Group. These unsaturated rock layers represent a total vertical transport path of 250 to 400 m across the repository footprint, with an average of about 300 m to the water table for present-day climate conditions. For wetter climates, such as the monsoon and glacial-transition, a water table rise (Section 2.3.9.2.4.1) of about 120 m (SNL 2008d, Section 6.3.9) reduces the linear transport path (Section 2.3.9.2.4.1). The saturated zone flow path below the repository footprint, which extends 18 km to the accessible environment boundary, is composed of volcanic units and alluvium (Section 2.3.9). The projected groundwater transport pathway is southeast from the repository site, transitioning to a southerly direction towards the designated accessible environment boundary in the Amargosa Desert. The first 12 to 14 km of the saturated zone flow path is in fractured volcanic rocks; the remainder of the 18 km flow path is composed of alluvial sediments. The component models of the TSPA model account for transport in fractured-porous media, and are based on (1) a dual-continuum approach for the unsaturated zone (SNL 2008d, Section 6.3.9.2); and (2) a dual-continuum approach for the fractured volcanic units and a single-continuum approach for porous alluvium (Section 2.3.9.2.3.1).

Probabilistic projections of radionuclides releases for the 12 representative radionuclides selected in Section 2.1.2.2.6 are used to compute the curie releases (from Equations 2.1-2 and 2.1-3) and curie reductions (from Equations 2.1-4 and 2.1-5). The radionuclides considered consist of ^{137}Cs , ^{90}Sr , ^{241}Am , ^{240}Pu , ^{99}Tc , ^{239}Pu , ^{242}Pu , ^{237}Np , ^{234}U , ^{243}Am , ^{230}Th , and ^{226}Ra . Of these 12 radionuclides, 5 are transported in both dissolved and irreversible colloidal phase. These radionuclides are: ^{241}Am , ^{240}Pu , ^{239}Pu , ^{242}Pu , and ^{243}Am (SNL 2008d, Table 6.3.7-6). The calculation of radionuclide release reduction utilizes the total activity of these radionuclides, designated with superscript T. It is noteworthy to mention that the activity releases from the EBS for these five radionuclides are dominated by the dissolved-phase activities.

Barrier Capability for Nominal/Early Failure Modeling Case—The focus of this modeling case is to examine the capability of the Lower Natural Barrier for varied releases (in both time and magnitude) from the EBS. As shown in Section 2.1.2.2.6, the early failures of drip shield and waste package produce low releases, starting almost immediately at repository closure, which persist for 1,000,000 years. Added to these releases are radionuclide releases due to drip shield and waste package failure by nominal processes that mainly occur in the post-10,000-year period. These failures ultimately lead to relatively large advective radionuclide releases from an increased number of waste packages.

Projections of Barrier Capability for 10,000 Years after Closure—The projected mean activity releases from the Lower Natural Barrier, specifically $R_{SZk}(t)$, are shown in Figure 2.1-34. This figure also shows the corresponding plot for the projected releases from the EBS for 10,000 years after closure.

At 10,000 years, the mean total activity in the inventory is about 4×10^7 Ci, but the mean total activity released from the saturated zone (summed over all radionuclides) is only 6 Ci. ^{99}Tc comprises almost all of the mean total release (SNL 2008d, Section 8.3.3.3.1[a]).

In comparing the peak mean activity radionuclide releases for the large initial inventory group (SNL 2008d, Section 8.3.1[a]) (^{137}Cs (transported as a solute and reversibly sorbed on colloids), ^{90}Sr (transported as a solute), ^{241}Am (transported as a solute as reversibly and irreversibly sorbed on colloids), and ^{240}Pu (transported as a solute and reversible colloid and irreversible colloid phases)), the calculations of $PR_{LNB,k}$ (Equation 2.1-5) indicate that the Lower Natural Barrier effectively accounts for the following reductions in the activity released from EBS (SNL 2008d, Section 8.3.3.3.1[a]):

- ^{137}Cs (half-life 30.1 yrs): about 100% reduction (from about 40 μCi to about 0 μCi)
- ^{90}Sr (half-life 28.8 yrs): about 100% reduction (from about 7 μCi to about 0 μCi)
- ^{241}Am (half-life 433 yrs): about 99.9% reduction (from about 3 mCi to about 4 μCi)
- ^{240}Pu (half-life 6560 yrs): about 99.5% reduction (from about 17 mCi to about 80 μCi).

This barrier effectiveness of the unsaturated zone is supported by detailed particle tracking calculations (Section 2.3.8) that indicate mean water transport times (to the water table) from the southern part of the repository are on the order of 400 years or longer, which means that these radionuclides would experience more than 10 half-lives of decay before reaching the water table. Water transport times from northern repository locations are much shorter because of the predominance of flow through fractures. In addition, other detailed hydrologic calculations for the

saturated zone (SNL 2008f, Table 6-10[a]) indicate median radionuclide transport times ranging from 42,000 years to greater than 1,000,000 years for cesium species, and from 9,000 years to greater than 1,000,000 years for strontium species.

In the case of ^{241}Am and ^{240}Pu , reductions in radionuclide activity released are primarily the result of retardation effects arising from a combination of (1) mean seepage fractions that are less than 0.5 (Table 2.1-6), indicating that (on average) more than half of the mass released from the EBS diffuses into the matrix of the unsaturated zone; (2) sorption of dissolved phase radionuclides, reversible exchanges from dissolved to colloidal phases, and reversible colloidal filtration; and (3) radionuclide decay occurring during transport through the Lower Natural Barrier.

For ^{99}Tc (half-life 2.13×10^5 yrs), an apparent reduction in peak activity of about 62% (about 14 Ci to about 5.3 Ci) is projected to be achieved by the Lower Natural Barrier (SNL 2008d, Section 8.3.3.3.1[a]). Note, however, that a reduction of only about 20% within 10,000 years (about 7 Ci to about 5.3 Ci) is projected if the activity released from the EBS was estimated to be 7 Ci at 9,600 years (from Figure 2.1-20) to account for the rapidly changing EBS release history. This effectiveness of the Lower Natural Barrier is due to the interplay of (1) radionuclide transport by diffusion through the invert and into unsaturated zone rock matrix; (2) matrix diffusion between fractures and matrix of the unsaturated zone; (3) and matrix diffusion in the volcanic units of the saturated zone in combination with transport time in the saturated zone. However, it is important to note that this reduction is a transient condition; for instance, comparing the ^{99}Tc activities at about 1,000,000 years, the reduction is only about 5% (SNL 2008d, Section 8.3.3.3.1[a]).

Figure 2.3.9-16 shows median transport times for technetium ranging from about 10 to 10,000 years, although a significant fraction of radionuclide mass has much longer transport times in many realizations due to the effects of matrix diffusion in fractured volcanic units.

Regarding projections of $PR_{LNB,k}$ for radionuclides in the category of low to moderate solubility, low sorption, and long half-life, such as ^{239}Pu , ^{242}Pu , ^{237}Np , and ^{234}U , the reductions in peak mean activities released within the first 10,000 years are estimated to be (SNL 2008d, Section 8.3.3.3.1[a]):

- ^{239}Pu (half-life 2.41×10^4 yrs): about 99.6% reduction (from about 60 mCi to about 0.3 mCi)
- ^{242}Pu (half-life 3.75×10^5 yrs): about 99.1% reduction (from about 62 μCi to about 0.5 μCi)
- ^{237}Np (half-life 2.14×10^6 yrs): about 78% reduction (from about 0.3 mCi to about 77 μCi)
- ^{234}U (half-life 2.46×10^5 yrs): about 89% reduction (from about 0.1 mCi to about 16 μCi).

With the half-lives of these radionuclides being much greater than 10,000 years, the projected reductions in the activity are attributed to delay in the subsurface movement produced by (1) the combined processes of matrix diffusion and sorption in the unsaturated zone and (2) matrix

diffusion and sorption in the volcanic unit and sorption in the alluvium of the saturated zone. With regard to ^{239}Pu and ^{242}Pu , the percent reductions are nearly the same because they have the same sorption properties.

For ^{243}Am , ^{230}Th , and ^{226}Ra , the projected reductions in peak mean activity achieved by the Lower Natural Barrier are estimated to be (SNL 2008d, Section 8.3.3.3.1[a]):

- ^{243}Am (half-life 7,370 yrs): about 99.8% reduction (from about 2 mCi to about 4 μCi)
- ^{230}Th (half-life 7.54×10^4 yrs): about 99.4% reduction (from about 76 μCi to about 0.5 μCi)
- ^{226}Ra (half-life 1,600 yrs): about 99.9% reduction (from about 0.6 mCi to about 0.3 μCi).

These reductions occur because of very strong sorption in both the zeolitic and devitrified tuff layers of the unsaturated zone (Section 2.3.8), as well as in the volcanic units and alluvium of the saturated zone (Section 2.3.9).

Projections of Barrier Capability for the Post-10,000-Year Period—The plot for the projected mean activity released from the Lower Natural Barrier is shown on Figure 2.1-35; also shown in this figure is the corresponding projection for mean activity released from the EBS. Of the four radionuclides in the large inventory group (i.e., ^{137}Cs , ^{90}Sr , ^{241}Am , and ^{240}Pu), the inventories for ^{137}Cs and ^{90}Sr are essentially depleted by radioactive decay by 1,000 years (e.g., more than 30 half-lives of decay) after closure (Figure 2.1-18). As a result, there would be no releases of these radionuclides from the EBS or saturated zone in the post-10,000-year period. In the case of ^{241}Am and ^{240}Pu , however, their total repository inventories are still substantial at 10,000 years and are approximately 1.4×10^4 Ci for ^{241}Am and 1.6×10^7 Ci for ^{240}Pu (SNL 2008d, Section 8.3.3.3.1[a]). Consequently, releases of these radionuclides occur until about 150,000 years.

The calculations of PR_{LNBk} for the post-10,000-year period show the following reductions in the peak mean activity of ^{241}Am and ^{240}Pu (SNL 2008d, Section 8.3.3.3.1[a]):

- ^{241}Am (half-life 433 yrs): about 100% reduction (from about 0.2 mCi to about 0 mCi)
- ^{240}Pu (half-life 6,560 yrs): about 98% reduction (from about 60 mCi to about 1 mCi).

These activity reductions are similar to those projected for the 10,000 years after closure. Moreover, most of the ^{241}Am activity reduction is accounted for by the unsaturated zone. In the case of ^{240}Pu , the unsaturated zone accounts for 50% of the reduction (SNL 2008d, Section 8.3.3.3.1[a]).

For ^{99}Tc (half-life 2.13×10^5 yrs), the Lower Natural Barrier achieves a reduction in peak activity of about 5% (from about 2.8×10^4 Ci to about 2.6×10^4 Ci) at 1,000,000 years (SNL 2008d, Section 8.3.3.3.1[a]). This reduction is predominantly the result of matrix diffusion in the rock layers of the unsaturated zone and the volcanic units of the saturated zone. This activity reduction is smaller than the reductions for the 10,000-year period. However, this is due to the fact that the technetium released from the EBS in the first 10,000-year period may not have been released from the saturated zone within 10,000 years. Note that for ^{99}Tc , the travel time ranges between 10 and

22,190 years within the saturated zone, with a median travel time of 230 years (SNL 2008f Table 6-10[a]).

Regarding projections for radionuclides in the category of low to moderate solubility, low sorption in the unsaturated and saturated zones, and long half-life, such as ^{239}Pu , ^{242}Pu , ^{237}Np , and ^{234}U , the reductions in peak mean activities released are lower than those for the 10,000-year period. The projected percent reductions are (SNL 2008d, Section 8.3.3.3.1[a]):

- ^{239}Pu (half-life 2.41×10^4 yrs): about 90% reduction (from about 0.8 Ci to about 0.08 Ci)
- ^{242}Pu (half-life 3.75×10^5 yrs): about 66% reduction (from about 44 Ci to about 15 Ci)
- ^{237}Np (half-life 2.14×10^6 yrs): about 23% reduction (from about 16 Ci to about 13 Ci)
- ^{234}U (half-life 2.46×10^5 yrs): about 32% reduction (from about 1.5 Ci to about 1 Ci).

With regard to ^{239}Pu and ^{242}Pu , the percent reductions are distinct because of the effects of radioactive decay and ^{239}Pu having a small half-life compared to the 1,000,000-year time period.

In the case of ^{243}Am , ^{230}Th , and ^{226}Ra , the projected reductions in peak mean activities achieved by the Lower Natural Barrier are comparable to those for the 10,000-year period. They are estimated as follows (SNL 2008d, Section 8.3.3.3.1[a]):

- ^{243}Am (half-life 7,370 yrs): about 99.6% reduction (from about 0.2 Ci to about 0.7 mCi)
- ^{230}Th (half-life 7.54×10^4 yrs): about 85% reduction (from about 4.5 Ci to about 0.7 Ci)
- ^{226}Ra (half-life 1,600 yrs): about 97.6% reduction (from about 28 Ci to about 0.7 Ci).

Barrier Capability for Seismic Ground Motions Modeling Case—This modeling case examines the capability of the Lower Natural Barrier under conditions of EBS releases induced by vibratory ground motion events (i.e., disruptive events). The seismic ground motion modeling case is particularly relevant because it was found to be important to projections for the Individual Protection Standard (Section 2.4). In this modeling case, damage and failure of the drip shields and waste packages occur as a result of dynamic and static loadings induced by the vibratory ground motion. Moreover, the waste package breach modes are quite varied, including seismic-induced stress corrosion cracking, rupture, and puncture, as well as general corrosion penetration of the outer barrier. These breach modes ultimately lead to a broad range of slow diffusional and fast advective releases to the Lower Natural Barrier.

Projections of Barrier Capability for 10,000 Years after Closure—The projected mean activity released from the Lower Natural Barrier is shown on Figure 2.1-36. Also shown in this figure is the corresponding plot for the projected releases from the EBS for 10,000 years after closure. At 10,000 years, the mean total activity in the inventory is about 4×10^7 Ci, but the mean total activity released from the saturated zone (summed over all radionuclides) is only 540 Ci. ^{99}Tc comprises almost all of the mean total release (SNL 2008d, Section 8.3.3.3.1[a]).

In comparing the peak mean activity radionuclide releases for the large initial inventory group (Figure 2.1-18) (^{137}Cs (transported as a solute and reversible colloid), ^{90}Sr (transported solute), ^{241}Am (transported as a solute and as reversibly and irreversibly sorbed on colloids), and ^{240}Pu (transported as a solute and as reversibly and irreversibly sorbed on colloids)), the calculations of

$PR_{LNB,k}$ indicate that the Lower Natural Barrier effectively accounts for the following reductions in the peak mean activity (SNL 2008d, Section 8.3.3.3.1[a]):

- ^{137}Cs (half-life 30.1 yrs): about 100% reduction (from about 0.6 μCi to about 0 μCi)
- ^{90}Sr (half-life 28.8 yrs): about 100% reduction (from about 0.03 μCi to about 0 μCi)
- ^{241}Am (half-life 433 yrs): about 100% reduction (from about 73 μCi to about 0 μCi)
- ^{240}Pu (half-life 6560 yrs): about 99.6% reduction (from about 15 mCi to about 55 μCi).

These percent reductions are based on activity releases within the 10,000-year period only, and releases continue to increase beyond this time. These percent reductions are almost identical to those estimated for the combined nominal/early failure demonstration modeling case. Also similar is the fact that the unsaturated zone accounts for very significant reductions (e.g., 80% to 88%) of ^{137}Cs , ^{90}Sr , and ^{241}Am activities. Although the percent reductions are similar, the EBS releases for the seismic ground motion modeling case are much higher than those for the combined nominal/early failure demonstration modeling case.

The mean activity reduction projected for ^{99}Tc (half-life 2.13×10^5 yrs) is approximately 55% (from 941 Ci to 427 Ci) with more than half of the reduction provided by the unsaturated zone (SNL 2008d, Section 8.3.3.3.1[a]). This level of activity reduction for ^{99}Tc is similar to that for the combined nominal/early failure demonstration modeling case, but the number of curies released in the seismic ground motion modeling case is much higher. It is important to note that this apparent reduction is a transient condition, and the reduction of ^{99}Tc becomes small over a long time period.

The percent reductions in peak mean activity projected to be achieved by the Lower Natural Barrier for ^{239}Pu , ^{242}Pu , ^{237}Np , and ^{234}U for are as follows (SNL 2008d, Section 8.3.3.3.1[a]):

- ^{239}Pu (half-life 2.41×10^4 yrs): about 99.6% reduction (from about 48 mCi to about 0.2 mCi)
- ^{242}Pu (half-life 3.75×10^5 yrs): about 99.6% reduction (from about 49 μCi to about 0.2 μCi)
- ^{237}Np (half-life 2.14×10^6 yrs): about 81% reduction (from about 0.1 mCi to about 20 μCi)
- ^{234}U (half-life 2.46×10^5 yrs): about 93% reduction (from about 0.3 mCi to about 22 μCi).

These percent reductions are very similar to those projected for the combined nominal/early failure demonstration modeling case.

For ^{243}Am , ^{230}Th , and ^{226}Ra , the projected reductions in peak mean activity to be achieved by the Lower Natural Barrier are estimated as follows (SNL 2008d, Section 8.3.3.3.1[a]):

- ^{243}Am (half-life 7,370 yrs): about 100% reduction (from about 10 μCi to about 0 μCi)
- ^{230}Th (half-life 7.54×10^4 yrs): about 96.2% reduction (from about 11 μCi to about 0.4 μCi)
- ^{226}Ra (half-life 1,600 yrs): about 100% reduction (from about 30 mCi to about 0.6 μCi).

These percent reductions are also very similar to those projected for the combined nominal/early failure modeling case.

Projections of Barrier Capability for Post-10,000 Years after Closure—The plot for the projected mean activity released from the Lower Natural Barrier is shown in Figure 2.1-37. This figure also shows the corresponding projection for mean activity released from the EBS.

The peak mean total activity released from the saturated zone (summed over all radionuclides) is approximately 3×10^4 Ci at 800,000 years; compared to the peak mean total activity released from the EBS of about 5×10^4 Ci at 800,000 years. ^{99}Tc comprises most of the mean total release from the EBS. Figure 2.1-37 indicates an overall reduction (peak to peak) in activity releases due to the Lower Natural Barrier of about 40% (SNL 2008d, Section 8.3.3.3.1[a]).

Of the four radionuclides in the large inventory group (i.e., ^{137}Cs , ^{90}Sr , ^{241}Am , and ^{240}Pu), the inventories for ^{137}Cs and ^{90}Sr are essentially depleted by radioactive decay by 1,000 years (e.g., more than 30 half-lives of decay) after closure (Figure 2.1-18) (SNL 2008d, Section 8.3.3.3.1[a]). As a result, there would be no releases of these radionuclides from the EBS or saturated zone in the post-10,000-year period. In the case of ^{241}Am and ^{240}Pu , however, their total repository inventories are still substantial and are estimated to be approximately 1.4×10^4 Ci for ^{241}Am and 1.6×10^7 Ci for ^{240}Pu remaining in the repository at 10,000 years after closure (SNL 2008d, Section 8.3.3.3.1[a]).

For the post-10,000-year period, the calculations of PR_{LNBk} show the following reductions in the peak mean activity of ^{241}Am and ^{240}Pu (SNL 2008d, Section 8.3.3.3.1[a]):

- ^{241}Am (half-life 433 yrs): about 100% reduction (from about 3 μCi to about 0 μCi)
- ^{240}Pu (half-life 6560 yrs): about 97% reduction (from about 0.1 Ci to about 4 mCi).

These reductions are largely achieved by the unsaturated zone, and are very similar to those estimated for the combined nominal/early failure modeling case for the post-10,000-year period.

For ^{99}Tc (half-life 2.13×10^5 yrs), the Lower Natural Barrier is projected to achieve a reduction in peak mean activity of about 5% (from about 3.3×10^4 Ci to about 3.1×10^4 Ci) at 1,000,000 years (SNL 2008d, Section 8.3.3.3.1[a]). This level of reduction is similar to that estimated for the combined nominal/early failure modeling case over the post-10,000-year period.

Regarding projections for radionuclides in the category of low to moderate solubility, low sorption in the unsaturated and saturated zones, and long half-life, such as ^{239}Pu , ^{242}Pu , ^{237}Np , and ^{234}U , the reductions in peak mean activities released are lower than those for the 10,000-year period. The projected percent reductions are as follows (SNL 2008d, Section 8.3.3.3.1[a]):

- ^{239}Pu (half-life 2.41×10^4 yrs): about 88% reduction (from about 11 Ci to about 1.4 Ci)
- ^{242}Pu (half-life 3.75×10^5 yrs): about 70% reduction (from about 200 Ci to about 62 Ci)
- ^{237}Np (half-life 2.14×10^6 yrs): about 20% reduction (from about 100 Ci to about 81 Ci)
- ^{234}U (half-life 2.46×10^5 yrs): about 25% reduction (from about 14 Ci to about 10 Ci).

The unsaturated zone accounts for roughly half of the reductions in ^{239}Pu and ^{242}Pu activity; whereas, for ^{237}Np and ^{234}U , it only accounts for about one-quarter of the reductions (SNL 2008d, Section 8.3.3.3.1[a]). These reductions are consistent with those projected for the combined nominal/early failure modeling case and post-10,000-year time period.

In the case of radionuclides ^{243}Am , ^{230}Th , and ^{226}Ra , the projected peak mean activity reductions in the Lower Natural Barrier are comparable to those for the combined nominal/early failure modeling case for the post-10,000-year period. The reductions are estimated as follows (SNL 2008d, Section 8.3.3.3.1[a]):

- ^{243}Am (half-life 7,370 yrs): about 99.8% reduction (from about 3 mCi to about 8 μCi)
- ^{230}Th (half-life 7.54×10^4 yrs): about 89% reduction (from about 71 Ci to about 8 Ci)
- ^{226}Ra (half-life 1,600 yrs): about 97% reduction (from about 260 Ci to about 8 Ci).

For these three radionuclides, the unsaturated zone accounts for one-half or more of the activity reductions. Again, this reduction is consistent with those projected for the combined nominal/early failure modeling case over the post-10,000-year time period.

Uncertainty in the projections of the Lower Natural Barrier capability is influenced by uncertainties in knowledge of flow and transport processes. The TSPA model accounts for these epistemic uncertainties by using probabilistic representations of the input parameters in the component models for unsaturated zone flow, unsaturated transport model, saturated zone flow, and saturated zone transport. In the case of unsaturated zone flow and transport, the parameters of primary importance include (1) sorption coefficients for various radionuclides; (2) the matrix diffusion coefficient; and (3) the infiltration scenario (Section 2.3.8). Important parameters related to groundwater flow (or advection) in the saturated zone (Section 2.3.9) are (1) groundwater-specific discharge; (2) flowing interval porosity; (3) alluvium effective porosity; and (4) horizontal anisotropy. The process of matrix diffusion is dependent on flowing interval spacing, effective diffusion coefficient, and matrix porosity. The process of radionuclide sorption on the fractured and porous media is a function of the sorption coefficients, bulk density, and porosity for various radionuclides and geologic media.

To illustrate the uncertainty associated with the release of radionuclide activity from the Lower Natural Barrier, radionuclide-specific release plots for selected radionuclides are presented in

Figures 2.1-38 to 2.1-43 for combined nominal and seismic ground motion-induced degradation processes (SNL 2008d, Section 8.3.3.3.1[a]):

- Figure 2.1-38: ^{99}Tc
- Figure 2.1-39: ^{237}Np
- Figure 2.1-40: ^{234}U
- Figure 2.1-41: ^{226}Ra
- Figure 2.1-42: ^{239}Pu
- Figure 2.1-43: ^{242}Pu .

The results in these figures are expected releases (averaged over the aleatory uncertainties) and thus largely reflect the impact of epistemic uncertainties. These plots are presented to illustrate the impact of uncertainties on the projections of the Lower Natural Barrier radionuclide releases. As can be noted from these plots, the Lower Natural Barrier releases for all six radionuclides corresponding to the 95th percentile are consistently close to the corresponding mean release curves, but are distant from the 5th percentile curves (SNL 2008d, Section 8.3.3.3.1[a]).

Summary of Lower Natural Barrier Capability—Projections of barrier capability demonstrate that for large initial inventory, soluble, and short half-life radionuclides, such as ^{137}Cs and ^{90}Sr , the mean activity released from the EBS would be reduced by 100% (i.e., they are highly unlikely to reach the accessible environment). For radionuclides with longer half-lives, such as ^{241}Am and ^{240}Pu , the mean activity released would be reduced by 97% to 100% by the natural barrier. For radionuclides of low to moderate solubility, weak to strong sorption, and long half life—such as ^{237}Np , ^{242}Pu , and ^{239}Pu —the mean activity released from the EBS would be reduced by 80% to 100% before reaching the accessible environment during the 10,000-year period and by 20% to 88% during the post-10,000-year period. These reductions of EBS releases would be achieved by the combination of Lower Natural Barrier processes, including slow advective water transport, matrix diffusion and sorption of dissolved phase radionuclides, dispersion/dilution of dissolved and colloidal phase radionuclides, and reversible filtration of colloidal phase radionuclides, as well as radioactive decay.

2.1.3 Technical Bases for Barrier Capability

[NUREG-1804, Section 2.2.1.1.3: AC 3]

Section 2.1.1 identifies the three barriers that comprise the repository system: the Upper Natural Barrier, the EBS, and the Lower Natural Barrier. Section 2.1.2 presents a quantitative assessment of the capability of these barriers. Table 2.1-5 provides the relationship between the barriers and the TSPA models where the performance of the features of each barrier are represented. The following sections provide an overview of the technical bases for the models used to represent the performance of the barriers in the TSPA. Further details of the technical bases are provided in the relevant model abstraction sections in Section 2.3 that are identified in Table 2.1-5. Because the technical basis for the assessment of barrier capability is the same as the technical basis for the model abstractions used in the TSPA, Section 2.3 provides the technical basis for both uses of the models (i.e., for analyses of barrier capability presented in Section 2.1.2 and for analyses of individual and groundwater protection presented in Sections 2.4.2 and 2.4.4).

2.1.3.1 Upper Natural Barrier

As shown in [Table 2.1-5](#), the Upper Natural Barrier is represented in the TSPA by the infiltration, site-scale unsaturated zone flow, ambient seepage, and thermal-hydrologic seepage models. The following paragraphs provide brief summaries of the technical bases for these models.

Infiltration Model—This model was developed on the basis of geologic and hydrologic studies of soil and bedrock properties, as well as data from precipitation and temperature monitoring. For the three climate states projected for the first 10,000 years after repository closure, ranges of annual precipitation and air temperatures were forecast on the basis of analogue sites, paleoclimate data, and earth-orbital parameters. Using this information, spatial and temporal infiltration estimates were developed for use as inputs to the site-scale unsaturated zone flow model. Infiltration estimates include the range of infiltration expected under future climatic conditions. The infiltration model produces net infiltration values for use in the site-scale unsaturated zone flow model under both present-day and future climatic conditions expected during the first 10,000 years after closure. For the period from 10,000 years after permanent closure up to 1,000,000 years after closure, infiltration rates are not provided from the analysis; rather, a range of deep percolation fluxes specified by the proposed 10 CFR 63.342(c)(2) (70 FR 53313) is used in the unsaturated zone flow simulations ([Section 2.3.1.3](#)).

Site-Scale Unsaturated Zone Flow Model—This model was developed on the basis of a combination of surface- and subsurface-based field investigations and laboratory studies that have produced a conceptual understanding of flow paths in the unsaturated zone. These studies show that subsurface heterogeneities have important effects on flow paths and, together with net infiltration, control the quantity and distribution of water that comes into contact with waste emplacement drifts. Several mathematical models have been developed to simulate unsaturated zone flow under ambient conditions and in response to future climate changes. A method that could represent fracture and matrix flow under ambient and thermally perturbed conditions was selected. A dual-permeability continuum method was selected as being most consistent with available data and suitable for modeling unsaturated flow at Yucca Mountain. Mathematical models were calibrated against multiple sources of information (e.g., water potential, pneumatic, perched water, temperature, and geochemical data). The unsaturated zone flow model is used to generate flow fields that are used directly by the TSPA to predict seepage into drifts and radionuclide transport through the unsaturated zone. [Section 2.3.2.4](#) further discusses the unsaturated zone flow model.

Ambient Seepage Model—The physics that control water percolating through the unsaturated zone, combined with hydrologic properties of the rock surrounding the emplacement drifts, including the geometry of the drift opening (intact versus collapsed), provide the technical basis for this model. When percolating water encounters an opening in unsaturated rock, it tends to be diverted around the opening due to capillarity. Seepage testing in the Exploratory Studies Facility and the Enhanced Characterization of the Repository Block Cross-Drift provided the data needed to develop a seepage process model. Seepage tests were conducted for both natural percolation flux conditions and localized, high-flux conditions that could induce seepage. Results show that there is a threshold water flux, such that seepage into the drift will not occur if the local percolation flux is below the threshold. The seepage process model relies directly on seepage-rate data, and is calibrated against other seepage data not used to develop the model. This model is

abstracted for use in the TSPA. The seepage abstraction provides seepage rates and uncertainties for both intact and collapsed drifts over a range of percolation fluxes, capillary strengths, and permeabilities. [Section 2.3.3.2](#) further discusses the ambient seepage model.

Thermal-Hydrologic Seepage Model—Field testing of the thermal-hydrologic response of the host rock, particularly the Drift Scale Test in the Exploratory Studies Facility, provides the technical basis for this model. The Drift Scale Test was designed to monitor evolution of temperature and liquid saturation and to observe evidence of thermally induced liquid refluxing. Results show that heat from emplaced waste will cause pore water in the rock matrix to vaporize and move away from emplacement drift openings. In cooler rock, the vapor will condense in fractures and drain either away or back toward the emplacement drift. While temperatures are above the boiling point of water, vaporization of percolating water in the fractured rock above the emplacement drifts will prevent seepage. The thermal-hydrologic seepage model, which was developed on the basis of these results, includes the effects of capillary diversion and vaporization due to heat. In the TSPA, seepage rates and the fraction of waste package locations that experience seepage are predicted using the ambient seepage model. The technical basis provided by the thermal-hydrologic seepage model is used in the TSPA to justify the assumption that seepage cannot enter the drift if the drift wall temperature is equal to or greater than 100°C. [Section 2.3.3.3](#) further discusses the thermal-hydrologic seepage model.

2.1.3.2 Engineered Barrier System

The technical basis used to screen nuclear criticality from the postclosure performance assessment is described in [Section 2.2.1.4.1](#). As shown in [Table 2.1-5](#), the EBS is represented in the TSPA by the following models: drift degradation and rockfall, near-field chemistry, multiscale thermal-hydrologic, in-drift condensation, in-drift physical and chemical environment, drip shield degradation, waste package degradation, in-package chemistry, commercial SNF degradation, DOE SNF degradation, HLW degradation, dissolved concentration limits, colloidal radionuclide availability, and EBS flow and transport. The following paragraphs provide brief summaries of the technical bases for these models.

Drift Degradation and Rockfall—These analyses and models were developed on the basis of detailed geologic characterization of the repository host rock. Data were developed on rock mass structure and variability of rock properties. Laboratory and in situ testing provided ranges of values for mechanical and thermal properties for intact rock matrix, fractures, and large-scale properties of the lithophysal rock mass. Two- and three-dimensional numerical models, developed on the basis of these data, were used to represent the processes of degradation of drift walls and rockfall. These models provide the tools needed to assess rockfall and time-related drift degradation as a function of in situ, thermal, and seismic loading states. Results from these models are used to estimate impacts of vibratory ground motion, fault displacement, and rockfall induced by vibratory ground motion on drip shields and waste packages. [Sections 2.3.4.4](#) and [2.3.4.5](#) further discuss the drift degradation and rockfall model.

Near-Field Chemistry Model—The primary role of the near field chemistry model is to provide the near-field gas and water chemistries for use in simulating the in-drift chemical environment. Field and laboratory studies have provided the hydrologic, thermal, and mineralogical data necessary to develop this model. Measurements of pore-water and gas chemistry data in the

Exploratory Studies Facility and Enhanced Characterization of the Repository Block Cross-Drift, supplemented with kinetic and thermodynamic data from externally published sources, provide the basis for modeling the evolution of water and gas compositions in near-field host rock. Heat, gas, and liquid in the rock affect the chemical composition of host-rock pore and fracture waters and the location and type of mineral dissolution and precipitation reactions. Evaporation serves to concentrate aqueous species in solution. The TSPA uses results from this model to calculate in-drift water chemistry due to seepage evaporation ([Section 2.3.5.5](#)).

Multiscale Thermal-Hydrologic Model—Field thermal testing, modeling studies, natural analogues, and externally published data provide the technical basis for this model. The model was developed by combining the results of submodels at various scales and dimensionalities to produce a three-dimensional representation of the natural and engineered systems. This multiscale model relies on the unsaturated zone flow model for hydrologic properties and percolation flux boundary conditions and uncertainties. The multiscale model is combined with an in-drift condensation model to represent temperature and relative humidity in the emplacement drifts for the TSPA. [Section 2.3.5.4](#) further discusses the thermal-hydrologic model.

In-Drift Condensation Model—The in-drift condensation model complements the multiscale thermal-hydrologic model ([Section 2.3.5.4](#)) in terms of evaluating the in-drift thermal-hydrologic environment. Field thermal testing and modeling studies provide the technical basis for this model. The multiscale thermal-hydrologic model provides the TSPA model with the temperature and relative humidity at all waste package locations; however, the model simulations do not include axial transport of water vapor along the drifts. The in-drift condensation model was used to calculate the hydrologic effects of axial transport of water vapor, namely drift wall condensation, to be used as input to the TSPA model. The in-drift condensation model provides the TSPA model with the potential for drift wall condensation at waste package locations, and, when condensation occurs, with the magnitude of condensation, which is correlated with percolation rate. Condensation is another source of liquid water that can potentially contact the drip shield or waste package and flow through the invert in EBS flow calculations ([Section 2.3.7.12](#)) (SNL 2007d, Section 6.3.1).

In-Drift Physical and Chemical Environment—This model relies on the technical basis developed for the near-field chemistry model to establish the compositional range of waters that could contact the drip shield, the outer barrier of the waste package, and the invert. While waste package surface temperatures are high, seepage water will tend to evaporate and may form concentrated brines. The in-drift chemical environment changes with time as heat from decay decreases and geochemical processes modify in-drift conditions. Characteristics of the environment through the stages of dryout, transition, and return to a low-temperature condition are included in the range of parameters covered in this model. [Section 2.3.5.5](#) further discusses the in-drift physical and chemical environment model.

Drip Shield Degradation and Early Failure Model—Long-term corrosion tests on titanium alloys provide the technical basis for models for drip shield degradation. Literature surveys were also used to obtain data on manufacturing defects and human error probabilities to develop a drip shield early failure model. The number of potential drip shield failures is very small such that, for example, the probability of having one early failure is about 2%. Results from testing in repository-relevant environments show that creviced specimens exhibit slightly lower corrosion rates than weight-loss specimens; only the weight-loss data were used in the model. The

weight-loss sample data obtained under more extreme conditions (90°C and high fluoride concentrations) were used to represent the corrosion rate for the outer surface of the drip shield, whereas data obtained for more benign conditions were used for the underside of the drip shield. The rationale for this choice is that the outer surface would be exposed to seepage environments, whereas the inner surface would only be expected to experience water films due to condensation. Under repository conditions, the general corrosion penetration depth in the 10,000 years after closure will be extremely limited. Consequently, failures resulting from through-wall penetration will not occur until after 270,000 years, and both localized corrosion and stress corrosion cracking are not expected to significantly degrade the capability of the drip shield feature. For the case of impacts on drip shields due to seismic-induced rockfall, stress corrosion cracking is considered possible. However, this degradation mode is not included in the TSPA because cracks in the titanium are sufficiently tight that they do not allow advective flux of water, and—even if water is present—the cracks are predicted to plug from mineral precipitation and corrosion products within a few hundred years after a seismic event. [Sections 2.3.6.8](#) and [2.3.4](#) further discuss the drip shield degradation model.

Waste Package Degradation: General and Localized Corrosion, Stress Corrosion Cracking, and Early Failure—The technical basis for waste package degradation modeling was derived from the Yucca Mountain Project and externally published data. The technical basis includes data regarding general and localized corrosion, microbial processes, stress corrosion cracking, and early failure due to manufacturing defects. Data for general corrosion rates of the waste package outer barrier have been obtained from weight-loss measurements of descaled Alloy 22 samples after five years. General corrosion rates were also measured electrochemically to estimate the temperature dependence of general corrosion for Alloy 22. Localized corrosion data are available for Alloy 22 from a wide range of exposure environments. Long-term corrosion potential and short-term cyclic polarization data are available to evaluate the susceptibility of Alloy 22 to localized corrosion. Laboratory tests also provided estimates of the effects of microbial processes on general corrosion. Because penetration rate data for localized corrosion under repository conditions are limited, published crevice corrosion rates under highly aggressive conditions were also used to establish the technical basis for waste package models. Yucca Mountain Project and externally published data are available to estimate stress corrosion cracking of Alloy 22. Threshold stresses for initiation of stress corrosion cracking, crack growth rates, and stress and stress intensity factor profiles for welded regions, as well as data on weld flaws, were compiled. Literature surveys were also used to obtain data on manufacturing defects and human error probabilities to develop a waste package early failure model. [Sections 2.3.6.3](#) to [2.3.6.6](#) further discuss the waste package degradation models. [Section 2.3.4](#) discusses waste package and drip shield mechanical degradation associated with seismic ground motion.

In-Package Chemistry—This model is a reaction-path model that predicts the chemical features, such as pH and ionic strength, of in-package fluids. The technical bases for this model include degradation rates for waste package and basket materials as a function of surface area. Degradation rates for the various waste forms as a function of pH, temperature, and the surface area are also inputs to the model. A thermodynamic database has been compiled from Yucca Mountain Project and externally published data containing solubilities of radionuclides and corrosion products as a function of solution composition and temperature. Surface thermodynamic parameters for corrosion products were also obtained from the literature. The in-package water chemistry model is used to provide input to the EBS flow and transport model, which calculates

the transport of radionuclides through the degraded waste form, degraded waste package, and the invert. [Section 2.3.7.5](#) further discusses the in-package water chemistry model.

Commercial SNF Degradation—Yucca Mountain project and externally published data provide the technical basis for the commercial SNF degradation model. The rate at which the radionuclides enter solution is controlled by either the degradation rate of the waste form or by the solubility limit of the radionuclides. The commercial SNF degradation rates determine the rate at which soluble radionuclides can enter solution. The release rate of other radionuclides is determined by their solubility limits. Both Yucca Mountain Project and externally published data were used to develop thermodynamic databases for use with a geochemical modeling tool. Solubility limits, with appropriate uncertainties, are determined considering the controlling solid phases, water chemistry, temperature, and appropriate uncertainties. [Section 2.3.7.7](#) further discusses the commercial SNF degradation model.

DOE SNF Degradation—The rate at which radionuclides enter a solution is controlled either by the degradation rate of the waste form or by the solubility limit of the radionuclides. All DOE SNF types, except naval SNF, are modeled as degrading instantaneously upon waste package breach (SNL 2008a, Section 6.2.3.2). Commercial SNF degradation model results are used to represent the contribution of naval SNF in the TSPA. [Section 2.3.7.8](#) further discusses the DOE SNF degradation model.

HLW Glass Degradation—Similar to other waste forms, the rate at which radionuclides enter a solution is controlled by either the dissolution rate of the waste form or by the solubility limit of the constituent elements. Glass dissolution kinetics are known, on the basis of many experiments, to be controlled by a single dissolved species: orthosilicic acid. Both Yucca Mountain project and externally published data show that release of soluble components from glass decreases when the concentration of orthosilicic acid increases. Dissolution studies have been conducted under conditions that cover the following range of water contact modes postulated for the repository: contact with humid air, contact with dripping water, and immersion. The data were collected over a wide range of borosilicate glass compositions that meet the DOE-specified acceptance requirements for chemical durability and other specifications. [Section 2.3.7.9](#) further discusses the HLW glass degradation model.

Dissolved Concentrations Limits—This model determines the maximum dissolved concentration of radionuclides as a function of water chemistry over the range of physical and chemical conditions established in the in-package chemistry model described above. The model relies on a thermodynamic database compiled from Yucca Mountain project and externally published data. A geochemical modeling tool utilizes the database to establish solubility limits for radionuclides within the specified in-package water chemistries. Solubility limits are determined considering the controlling solid phases, water chemistry, and temperature. [Section 2.3.7.10](#) further discusses the dissolved concentrations limits model.

Colloidal Radionuclide Availability—The technical basis for the colloidal radionuclide availability model rests on both Yucca Mountain project and externally published data. Both waste form colloids resulting from waste degradation and pseudocolloids, which are colloidal particles of other materials with attached radionuclides, are evaluated. Measurements of colloid concentrations, studies of colloid stability, and experiments to determine radionuclide sorption

properties were used to develop the colloid source term abstraction used in the TSPA. Characteristics of water in the waste package from the in-package chemistry model are used to describe the stability and concentration of colloids and the distribution of radionuclides in the waste package. [Section 2.3.7.11](#) further discusses the colloidal radionuclide availability model used in the TSPA.

EBS Flow and Transport Model—The technical basis for this model is developed using the results of the seepage models, multiscale thermal-hydrologic and in-drift condensation models, in-drift chemical environment model, waste package and drip shield degradation models, in-package chemistry model, and waste form degradation and radionuclide mobilization models. The EBS flow and transport model consists of two parts: flow pathways within the EBS, and radionuclide transport along specific flow pathways. Transport out of the waste package can occur by advection when there is a liquid flux through the waste package, and by diffusion through continuous liquid pathways. These two transport processes depend on the types of penetrations through the waste package and on local seepage and condensation conditions. Diffusive transport depends on differences in concentrations, which are determined from the in-package water chemistry model and the solubility limit for each radionuclide. Concentrations in the waste package depend on radionuclide solubility limits, sorption of radionuclides onto corrosion products, sorption and desorption onto colloids, and colloid stability. Concentrations in the invert depend on radionuclide solubility limits and colloid stability in the invert, transfer of radionuclides between corrosion products and the invert, and the boundary concentrations at the invert–unsaturated zone interface. Transport at the invert–unsaturated zone interface may be advective or diffusive, and an important aspect of this model is to represent partitioning of radionuclide mass flux to the fractures and matrix consistent with the flow conditions. This partitioning is time dependent, and reflects variations in rates of radionuclide release from the EBS and changes in seepage or condensation flux in the emplacement drifts. [Section 2.3.7.12](#) further discusses the EBS flow and transport model.

2.1.3.3 Lower Natural Barrier

As shown in [Table 2.1-5](#), the Lower Natural Barrier is represented in the TSPA by the site-scale unsaturated zone flow, site-scale unsaturated zone radionuclide transport, saturated zone flow, and saturated zone radionuclide transport models. The saturated zone flow and transport abstraction model is not implemented directly in the TSPA, but is used to develop radionuclide breakthrough curves that are implemented in the TSPA using a convolution algorithm. The following paragraphs provide brief summaries of the technical bases for these models.

Site-Scale Unsaturated Zone Flow Model—[Section 2.1.3.1](#) provides an overview of this model.

Site-Scale Unsaturated Zone Radionuclide Transport Model—The technical basis for this model rests on the conceptual and numerical models developed to represent unsaturated zone flow. Advection, fracture–matrix interaction, sorption, and colloid-facilitated transport are important processes for radionuclide transport. Data sources supporting the site-scale unsaturated zone radionuclide transport model include (1) laboratory sorption and matrix diffusion measurements; (2) testing to support extension to larger scales at a test facility at Busted Butte; (3) Alcove 8–Niche 3 testing to investigate fracture–matrix interactions; (4) colloid retardation testing at the Busted Butte facility; (5) pore-water chemistry testing; and (6) isotope studies to

address the prevalence and frequency of fracture flow in the unsaturated zone. The approach used to represent unsaturated zone radionuclide transport is a dual-permeability model with distinct hydraulic and transport behavior for fractures and matrix. This approach best accounts for data from geochemical studies, field tracer tests, and modeling sensitivity studies. [Section 2.3.8](#) further discusses the site-scale unsaturated zone radionuclide transport model.

Site-Scale Saturated Zone Flow Models—The site-scale saturated zone flow model provides a three-dimensional calibrated simulation of groundwater flow paths and rates near Yucca Mountain. The technical basis for the saturated zone flow models rests on geologic field studies in the region surrounding Yucca Mountain. These studies provide the overall framework in terms of the lateral and vertical extent of aquifers and confining units, as well as locations of recharge and discharge areas. This model is calibrated using water-level data, and is supported by a variety of field data, including hydrochemical and isotopic data, and hydraulic field testing data. The site-scale model was constructed using a continuum approach. A continuum model was considered appropriate because field evidence indicates groundwater flow occurs through well-connected fractures on the order of tens to hundreds of meters apart. Use of a continuum model allows for the use of widely accepted equations describing groundwater flow through porous media. [Section 2.3.9.2](#) further discusses the site-scale saturated zone flow model.

Site-Scale Saturated Zone Transport Model—The site-scale saturated zone transport model provides a three-dimensional calibrated simulation of radionuclide transport and radionuclide concentrations in the saturated zone. The three-dimensional transport model is supplemented by a one-dimensional transport model that simulates transport of radionuclides that are daughter products resulting from ingrowth. The technical basis for this model rests on the geologic and hydrologic studies used to develop the site-scale saturated zone flow model, supplemented by additional data on chemical characteristics of dissolved or colloidal radionuclides and the characteristics of the geochemical environment along transport pathways. Transport of radionuclides as dissolved species will be affected by advection, diffusion, dispersion, and, for reactive radionuclides, sorption. Transport of radionuclides sorbed onto colloids is affected by the rate of colloid filtration, radionuclide sorption colloids, and colloid concentrations. The rate of radionuclide transport is a function of specific discharge, the porosity through which water flows, effective diffusion coefficient, dispersivity, decay constants, and radionuclide sorption coefficients. Data from hydraulic and tracer tests at a multiple-well complex provide the basis for modeling advective transport over scales relevant to radionuclide transport. These test results were used to develop values for flow and transport modeling parameters, and to confirm that the dual-porosity continuum conceptualization is appropriate for representing transport. Other field tests provide evidence supporting the predominance of fracture flow in the volcanic tuff units. Dispersivity values for the saturated zone were developed using elicitation results ([Section 2.3.9.3.3.4](#)). Sorption coefficients for the volcanic tuff and alluvium were obtained from laboratory measurements and scaled for site-scale application. [Section 2.3.9.3](#) further discusses the site-scale saturated zone transport model.

2.1.3.4 Technical Basis for Disruptive Events Potentially Affecting Barrier Capability

The capability of the barriers identified in [Section 2.1.2](#) is affected by the occurrence of disruptive events that may degrade, alter, or otherwise disrupt the features and components of the natural setting or EBS. The probability of these disruptive events is evaluated in [Section 2.2.2](#), and models

used to evaluate the effects and consequences of these events are presented in [Sections 2.3.4](#) (for mechanical degradation resulting from seismic events) and [2.3.11](#) (for disruption due to igneous events). Both of these event types are included in the scenario classes that have been retained for assessing performance of the repository system in [Section 2.4.2.1](#).

The technical basis for ground motion analysis has been formally elicited from an expert elicitation based on site-specific observations of previous seismic activity and faulting, as described in [Section 2.2.2.1](#). However, when the models developed in the probabilistic seismic hazard analysis (PSHA) were applied, low-probability ground motion values were allowed to increase without bound, eventually reaching levels that are inconsistent with the geologic setting for Yucca Mountain. Therefore, using data, analyses, and modeling results developed after the PSHA, a separate analysis was performed, using data that became available after the PSHA, to determine a reasonable bound to peak horizontal ground velocity at the waste emplacement level. A general discussion of the basis for the site specific ground motions and of the bounded hazard curve is presented in [Section 2.3.4.3](#). The effects of seismic activity on a range of possible seismic response spectra at the repository have been modeled using site-specific rock property data. The effects of seismic activity on EBS degradation have been modeled using site-specific information on rock mass response, design information on structural characteristics of the engineered features, and laboratory testing information on material properties. This information was used to evaluate the degradation of the EBS as a function of seismic PGV. The results of seismic-induced consequences are presented in [Section 2.3.4](#), and are represented in the TSPA as described in [Section 2.4](#).

The technical basis of estimates of the probability of intersection of the repository by an igneous event has been formally elicited from an expert elicitation based on observations of previous igneous activity, as described in [Sections 2.2.2.2](#) and [2.3.11.2](#). The effects of igneous activity on EBS degradation have been evaluated using analogues to similar igneous activity that have been supplemented by an independent peer review and a range of assumptions based on observations of characteristics of igneous events at analogue sites. The results of igneous-induced consequences are presented in [Section 2.3.11](#), and are represented in the TSPA as described in [Section 2.4](#).

2.1.3.5 Summary of Technical Bases for Barrier Capability

The technical bases for the assessment of the capability of the three barriers to (1) prevent or substantially reduce the rate of movement of water or radionuclides from the repository to the accessible environment; or (2) prevent or substantially reduce the rate of release of radionuclides from the waste are the same as the bases used for the compliance of the repository system with the postclosure performance assessment objectives and requirements. The barrier capability is based on the abstraction models of processes included in the performance assessment, as well as an evaluation of the processes and events that have been excluded from the performance assessment.

The identification and construction of scenario classes from the FEPs considered at Yucca Mountain are summarized in [Section 2.1.2](#), and presented in more detail in [Section 2.2](#). Those FEPs excluded from the TSPA and barrier capability analysis are summarized in [Table 2.2-5](#). Details associated with the exclusion of processes and events are presented in *Features, Events, and Processes for the Total System Performance Assessment: Analyses* (SNL 2008b) (certain processes that have been excluded from representation in the TSPA are discussed in detail in [Section 2.3](#)). Details associated

with the inclusion of processes and events acting on the features of the three barriers are presented in [Section 2.3](#), while the integration of these processes and events is summarized in [Section 2.4.1](#).

2.1.4 Summary

The Yucca Mountain repository system comprises three barriers that have the functions of (1) preventing or substantially reducing the rate of movement of water or radionuclides from the repository to the accessible environment; or (2) preventing or substantially reducing the release rate of radionuclides from the waste. These three barriers include two natural barriers and one engineered barrier system: namely, the Upper Natural Barrier, the EBS, and the Lower Natural Barrier. These barriers include multiple features that have processes and events that may act on or within the barriers to affect the capability of the performance of the barrier.

The relevant FEPs that most significantly contribute to the capability of the barriers are presented in [Tables 2.1-2](#), [2.1-3](#), and [2.1-4](#). A complete evaluation of all potential FEPs, including the technical basis for their inclusion or exclusion in the performance assessment, is presented in *Features, Events, and Processes for the Total System Performance Assessment: Analyses* (SNL 2008b).

Detailed descriptions of the models used to evaluate the barrier capability, as well as the technical basis for the treatment of uncertainties associated with the models and parameters used in the evaluation, are presented in the model abstraction descriptions in [Section 2.3](#).

The Upper Natural Barrier, by preventing or substantially reducing the amount and the rate of water seeping into the drifts, prevents or substantially reduces the rate of movement of water from the repository to the accessible environment and prevents or reduces the release rate of radionuclides from the waste. For the present-day climate, on average, more than 90% of the percolation flux would be diverted around drifts in TSw unit ([Section 2.1.2.1.6.2](#)). For the wetter climate states of the monsoonal and the glacial-transition climate states, the percentage of diverted flux would still be approximately 90% ([Section 2.1.2.1.6.2](#)). Drift collapse due to seismic events can reduce the potential for flow diversion. After several hundred thousand years, when drifts in the lithophysal units may completely fill with accumulated rubble from several seismic events, the diverted flux potentially reduces to a spatially-averaged value over lithophysal and nonlithophysal units of about 50% ([Section 2.1.2.1.6.2](#)). In the nonlithophysal units, flow diversion reduces to 0% when the threshold rockfall volume of 0.5 m³/m drift length is exceeded. In addition, during the glacial transition climate state, the Upper Natural Barrier is projected to prevent water from contacting about 60% of the waste package locations ([Section 2.1.2.1.6](#)). For collapsed drifts in the lithophysal units caused by seismic events, this percentage reduces to a spatially-averaged value over lithophysal and nonlithophysal units of about 30% ([Section 2.1.2.1.6](#)). Overall, the observed seepage percentages demonstrate the important barrier capability of the unsaturated flow processes in the fractured rock at and above the repository horizon.

The EBS prevents or substantially reduces the release rate of radionuclides from the waste, and prevents or substantially reduces the rate of movement of radionuclides from the repository to the accessible environment. It performs these functions by virtue of the materials and design of the emplacement drifts, drip shields, waste packages and waste forms, and waste package internals ([Sections 2.1.1.2](#) and [2.1.2.2](#)). In addition, the EBS provides for chemical and thermal-hydrologic

environments that lead to low solubilities for the radionuclides that make up the greatest fraction of the inventory activity. Finally, the EBS environments are such that radionuclide transport from the waste to the unsaturated zone is limited to a small fraction of the available inventory (less than $3 \times 10^{-3}\%$ in 10,000 years and 7% in 1,000,000 years), even under the wide range of likely and unlikely seismic ground motion events ([Section 2.1.2.2.6](#)).

The Lower Natural Barrier prevents or substantially reduces the rate of movement of radionuclides from the repository to the accessible environment. The key processes associated with the performance of the Lower Natural Barrier include sorption and matrix diffusion. For the radionuclides representing the dominant inventory during the first 10,000 years after closure (^{137}Cs , ^{90}Sr , ^{241}Am , ^{240}Pu and ^{239}Pu), the Lower Natural Barrier reduces activity releases from the EBS by greater than 99.5% (^{240}Pu and ^{241}Am) to 100% (^{137}Cs and ^{90}Sr). Activity releases of the solubility-limited, strongly sorbed, long half-life Pu isotopes (^{239}Pu and ^{242}Pu) are reduced by more than 99%. For radionuclides of low-to-moderate solubility, low sorption, and long half-life (e.g., ^{237}Np and ^{234}U), the Lower Natural Barrier reduces activity releases from the EBS by 78% (^{237}Np) to 89% (^{234}U). Activities associated with radionuclides important to colloid transport and decay chain in-growth (e.g., ^{243}Am , ^{230}Th , and ^{226}Ra) are reduced by the Lower Natural Barrier by more than 99%. The activity of ^{99}Tc , which is a highly soluble, nonsorbing, long half-life radionuclide, is reduced by the Lower Natural Barrier between about 20% to 62% during the first 10,000 years. However, it is important to note that this reduction is a transient condition; for instance, comparing the ^{99}Tc activities at about 20,000 years, the reduction in ^{99}Tc is effectively zero.

For the period after 10,000 years, the inventories of ^{137}Cs and ^{90}Sr are depleted by radioactive decay, and the Lower Natural Barrier reduces activity releases of ^{241}Am by 100% and ^{240}Pu by 98% ([Section 2.1.2.3.6](#)). Activities of the long half-life Pu isotopes are reduced by 90% (^{239}Pu) and 66% (^{242}Pu) respectively ([Section 2.1.2.3.6](#)). ^{243}Am , ^{230}Th , and ^{226}Ra are reduced by about 99.6%, 85%, and 97.6%, respectively ([Section 2.1.2.3.6](#)). The activities of low-to-moderate solubility, low sorption, long half-life radionuclides are reduced by approximately 23% (^{237}Np) to 32% (^{234}U) ([Section 2.1.2.3.6](#)). Release of the mobile radionuclide, ^{99}Tc , was reduced by a negligible few percent by the Lower Natural Barrier. It is important to note that only about 7% of the total available radionuclide inventory in the repository is projected to be released by the EBS to the Lower Natural Barrier. The majority of the activity released by the EBS to the Lower Natural Barrier is attributable to ^{99}Tc ([Section 2.1.2.3.6](#)). At about 200,000 years, ^{99}Tc provides about 40% of the total activity in the inventory, and at 1,000,000 years less than 10% ([Figure 2.1-19](#)). The low percentage reductions in the small amount of total mean ^{99}Tc activity released to the Lower Natural Barrier are due to its transport characteristics. The nonsorbing nature of this radionuclide causes it to be transported through the EBS and the Lower Natural Barrier at approximately the rate at which the groundwater travels.

The parameters and models used in the quantification of barrier capability are the same as those developed in [Section 2.3](#) for use in the TSPA for evaluation of performance of the natural and engineered barriers in the assessment of the individual and groundwater protection that is presented in [Section 2.4](#). Although uncertainty exists in the parameters and models of the relevant processes that affect the assessment of barrier capability and the TSPA, this uncertainty has been appropriately addressed in the assessments.

2.1.5 General References

70 FR 53313. Implementation of a Dose Standard After 10,000 Years.

BSC (Bechtel SAIC Company) 2004a. *Estimation of Mechanical Properties of Crushed Tuff for Use as Ballast Material in Emplacement Drifts*. 800-CYC-SSE0-00100-000-00A. Las Vegas, Nevada: Bechtel SAIC Company. ACC: ENG.20040309.0023.

BSC 2004b. *Conceptual Model and Numerical Approaches for Unsaturated Zone Flow and Transport*. MDL-NBS-HS-000005 REV 01. Las Vegas, Nevada: Bechtel SAIC Company. ACC: DOC.20040922.0006.

Day, W.C.; Dickerson, R.P.; Potter, C.J.; Sweetkind, D.S.; San Juan, C.A.; Drake, R.M., II; and Fridrich, C.J. 1998. *Bedrock Geologic Map of the Yucca Mountain Area, Nye County, Nevada*. Geologic Investigations Series I-2627. Denver, Colorado: U.S. Geological Survey. ACC: MOL.19981014.0301.

Helton, J.C. and Davis, F.J. 2002. *Latin Hypercube Sampling and the Propagation of Uncertainty in Analyses of Complex Systems*. SAND2001-0417. Albuquerque, New Mexico: Sandia National Laboratories. TIC: 254367.

MO0803TSPAPSAR.000. TSPA Supplemental Plots for Use in the SAR. Submittal date: 03/17/2008.

NWRPO (Nuclear Waste Repository Project Office) 2003. *Nye County Drilling, Geologic Sampling and Testing, Logging, and Well Completion Report for the Early Warning Drilling Program Phase III Boreholes*. NWRPO-2002-04. Pahrump, Nevada: Nye County, Nuclear Waste Repository Project Office. ACC: MOL.20030812.0307.

Potter, C.J.; Dickerson, R.P.; Sweetkind, D.S.; Drake, R.M., II; Taylor, E.M.; Fridrich, C.J.; San Juan, C.A.; and Day, W.C. 2002. *Geologic Map of the Yucca Mountain Region, Nye County, Nevada*. Geologic Investigations Series I-2755. Denver, Colorado: U.S. Geological Survey. TIC: 253945.

SNL (Sandia National Laboratories) 2007a. *Total System Performance Assessment Data Input Package for Requirements Analysis for Transportation Aging and Disposal Canister and Related Waste Package Physical Attributes Basis for Performance Assessment*. TDR-TDIP-ES-000006 REV 00. Las Vegas, Nevada: Sandia National Laboratories. ACC: DOC.20070918.0005.

SNL 2007b. *Stress Corrosion Cracking of Waste Package Outer Barrier and Drip Shield Materials*. ANL-EBS-MD-000005 REV 04. Las Vegas, Nevada: Sandia National Laboratories. ACC: DOC.20070913.0001.

SNL 2007c. *EBS Radionuclide Transport Abstraction*. ANL-WIS-PA-000001 REV 03. Las Vegas, Nevada: Sandia National Laboratories. ACC: DOC.20071004.0001.

SNL 2007d. *In-Drift Natural Convection and Condensation*. MDL-EBS-MD-000001 REV 00 ADD 01. Las Vegas, Nevada: Sandia National Laboratories. ACC: DOC.20050330.0001.

SNL 2007e. *UZ Flow Models and Submodels*. MDL-NBS-HS-000006 REV 03 ADD 01. Las Vegas, Nevada: Sandia National Laboratories. ACC: DOC.20080108.0003.

SNL 2008a. *Postclosure Nuclear Safety Design Bases*. ANL-WIS-MD-000024 REV 01. Las Vegas, Nevada: Sandia National Laboratories. ACC: DOC.20080226.0002;

SNL 2008b. *Features, Events, and Processes for the Total System Performance Assessment: Analyses*. ANL-WIS-MD-000027 REV 00. Las Vegas, Nevada: Sandia National Laboratories. ACC: DOC.20080307.0003.

SNL 2008c. *Simulation of Net Infiltration for Present-Day and Potential Future Climates*. MDL-NBS-HS-000023 REV 01 ADD 01. Las Vegas, Nevada: Sandia National Laboratories. ACC: DOC.20080201.0002.

SNL 2008d. *Total System Performance Assessment Model/Analysis for the License Application*. MDL-WIS-PA-000005 REV 00 ADD 01. Las Vegas, Nevada: Sandia National Laboratories. ACC: DOC.20080312.0001.

SNL 2008e. *Multiscale Thermohydrologic Model*. ANL-EBS-MD-000049 REV 03 ADD 02. Las Vegas, Nevada: Sandia National Laboratories. ACC: DOC.20080201.0003.

SNL 2008f. *Saturated Zone Flow and Transport Model Abstraction*. MDL-NBS-HS-000021 REV 03 ADD 02. Las Vegas, Nevada: Sandia National Laboratories. ACC: DOC.20080107.0006.

YMP (Yucca Mountain Site Characterization Project) 1993. *Evaluation of the Potentially Adverse Condition "Evidence of Extreme Erosion During the Quaternary Period" at Yucca Mountain, Nevada*. Topical Report YMP/92-41-TPR. Las Vegas, Nevada: Yucca Mountain Site Characterization Office. ACC: NNA.19930316.0208.

INTENTIONALLY LEFT BLANK

Table 2.1-1. ITWI Features / Components Supporting Each of the Three Barriers

Barrier	Feature^a	Barrier Function^b	Safety Classification^c
UNB	Topography and Surficial Soils	Prevents or substantially reduces the rate of movement of water	ITWI
UNB	Unsaturated Zone above the Repository	Prevents or substantially reduces the rate of movement of water	ITWI
EBS	Emplacement Drift	Prevents or substantially reduces the rate of movement of water Prevents or substantially reduces the rate of movement of radionuclides	ITWI
EBS	Emplacement Drift – Non Emplacement Openings, Closure, Ground Support, and Ventilation System	None	Non-ITWI
EBS	Drip Shield	Prevents or substantially reduces the rate of movement of water Prevents or substantially reduces the rate of movement of radionuclides	ITWI
EBS	Waste Package	Prevents or substantially reduces the rate of movement of water Prevents or substantially reduces the release rate of radionuclides from the waste Prevents or substantially reduces the rate of movement of radionuclides	ITWI
EBS	Waste Form and Waste Package Internals – TAD Canister	Prevents or substantially reduces the release rate of radionuclides from the waste Prevents or substantially reduces the rate of movement of radionuclides	ITWI
	Waste Form and Waste Package Internals – Naval Canister	Prevents or substantially reduces the release rate of radionuclides from the waste Prevents or substantially reduces the rate of movement of radionuclides Reduces the probability of criticality	ITWI
EBS	Waste Form and Waste Package Internals – DOE SNF Canister	None	Non-ITWI
EBS	Waste Form and Waste Package Internals – HLW Canister	None	Non-ITWI
EBS	Waste Form and Waste Package Internals - Naval SNF Canister System Components	Reduces the probability of criticality	ITWI

Table 2.1-1. ITWI Features / Components Supporting Each of the Three Barriers (Continued)

Barrier	Feature ^a	Barrier Function ^b	Safety Classification ^c
EBS	Waste Form and Waste Package Internals - Codisposal Waste Package Internals	None	Non-ITWI
EBS	Waste Form and Waste Package Internals – TAD Canister Internals	Reduces the probability of criticality	ITWI
EBS	Waste Form and Waste Package Internals - DOE SNF Canister Internals	Reduces the probability of criticality	ITWI
EBS	Waste Form and Waste Package Internals – Commercial Spent Nuclear Fuel and High Level Glass	Prevents or substantially reduces the release rate of radionuclides from the waste Prevents or substantially reduces the rate of movement of radionuclides	ITWI
EBS	Waste Form and Waste Package Internals – Naval Spent Nuclear Fuel	Prevents or substantially reduces the release rate of radionuclides from the waste Prevents or substantially reduces the rate of movement of radionuclides	ITWI
EBS	Waste Form and Waste Package Internals – DOE Spent Nuclear Fuel	None	Non-ITWI
EBS	Cladding – Commercial SNF / DOE SNF	None	Non-ITWI
EBS	Waste Package Emplacement Pallet	None	Non-ITWI
EBS	Invert	None	Non-ITWI
LNB	Unsaturated Zone below the Repository	Prevents or substantially reduces the rate of movement of radionuclides	ITWI
LNB	Saturated Zone	Prevents or substantially reduces the rate of movement of radionuclides	ITWI

NOTE: ^aSome features in this column are further divided into categories (signified by text after a dash) so that the feature as analyzed can be properly classified as ITWI or Non-ITWI.

^bBarrier Function defines how the identified barrier accomplishes or contributes to repository system performance.

^cITWI classification applies to barriers and features.

LNB = Lower Natural Barrier, UNB = Upper Natural Barrier.

Source: Modified from *Postclosure Nuclear Safety Design Bases* (SNL 2008a, Table 7-1).

Table 2.1-2. Summary of Features, Events, and Processes Affecting the Capability of the Upper Natural Barrier

Barrier Feature	FEP Number, FEP Name, and Screening Decision (Section 2.2, Table 2.2-5)	Processes and Characteristics that are Important to the Capability of the Barrier
Topography and Surficial Soils	1.2.02.01.0A – Fractures – Included	X
	1.2.07.01.0A – Erosion/ denudation – Excluded	
	1.2.07.02.0A – Deposition – Excluded	
	1.3.01.00.0A – Climate change – Included	X
	1.4.01.01.0A – Climate modification increases recharge – Included	X
	2.2.03.02.0A – Rock properties of host rock and other units – Included	X
	2.2.06.04.0A – Effects of subsidence – Excluded	
	2.2.07.01.0A – Locally saturated flow at bedrock/alluvium contact – Excluded	
	2.2.07.08.0A – Fracture flow in the UZ – Included	X
	2.3.01.00.0A – Topography and morphology – Included	X
	2.3.11.01.0A – Precipitation – Included	X
	2.3.11.02.0A – Surface runoff and evapotranspiration – Included	X
	2.3.11.03.0A – Infiltration and recharge – Included	X
Unsaturated Zone above the Repository	1.1.01.01.0A – Open site investigation boreholes – Excluded	
	1.1.01.01.0B – Influx through holes drilled in drift wall or crown – Excluded	
	1.2.02.01.0A – Fractures – Included	X
	1.2.02.02.0A – Faults – Included	
	1.2.04.02.0A – Igneous activity changes rock properties – Excluded	
	1.2.04.05.0A – Magma or pyroclastic base surge transports waste – Excluded	
	1.2.06.00.0A – Hydrothermal activity – Excluded	
	1.2.10.01.0A – Hydrologic response to seismic activity – Excluded	

Table 2.1-2. Summary of Features, Events, and Processes Affecting the Capability of the Upper Natural Barrier (Continued)

Barrier Feature	FEP Number, FEP Name, and Screening Decision (Section 2.2, Table 2.2-5)	Processes and Characteristics that are Important to the Capability of the Barrier
Unsaturated Zone above the Repository (Continued)	1.2.10.02.0A – Hydrologic response to igneous activity – Excluded	
	1.3.01.00.0A – Climate change – Included	X
	1.4.01.01.0A – Climate modification increases recharge – Included	X
	1.4.06.01.0A – Altered soil or surface water chemistry – Excluded	
	2.1.08.01.0A – Water influx at the repository – Included	X
	2.1.08.01.0B – Effects of rapid influx into the repository – Excluded	
	2.1.08.02.0A – Enhanced influx at the repository – Included	
	2.1.08.03.0A – Repository dryout due to waste heat – Included	
	2.1.08.11.0A – Repository resaturation due to waste cooling – Included	
	2.1.09.12.0A – Rind (chemically altered zone) forms in the near field – Excluded	
	2.2.01.01.0A – Mechanical effects of excavation and construction in the near field – Included	
	2.2.01.01.0B – Chemical effects of excavation and construction in the near field – Excluded	
	2.2.01.02.0A – Thermally-induced stress changes in the near field – Excluded	
	2.1.01.02.0B – Chemical changes in the near-field from backfill – Excluded	
	2.2.03.01.0A – Stratigraphy – Included	X
	2.2.03.02.0A – Rock properties of host rock and other units – Included	X
	2.2.06.01.0A – Seismic activity changes porosity and permeability of rock – Excluded	
	2.2.06.02.0A – Seismic activity changes porosity and permeability of faults – Excluded	

Table 2.1-2. Summary of Features, Events, and Processes Affecting the Capability of the Upper Natural Barrier (Continued)

Barrier Feature	FEP Number, FEP Name, and Screening Decision (Section 2.2, Table 2.2-5)	Processes and Characteristics that are Important to the Capability of the Barrier
Unsaturated Zone above the Repository (Continued)	2.2.06.02.0B – Seismic activity changes porosity and permeability of fractures – Excluded	
	2.2.06.03.0A – Seismic activity alters perched water zones – Excluded	
	2.2.06.04.0A – Effects of Subsidence – Excluded	
	2.2.07.01.0A – Locally saturated flow at bedrock/ alluvium contact – Excluded	
	2.2.07.02.0A – Unsaturated groundwater flow in the geosphere – Included	X
	2.2.07.04.0A – Focusing of unsaturated flow (fingers, weeps) – Included	
	2.2.07.05.0A – Flow in the UZ from episodic infiltration – Excluded	
	2.2.07.07.0A – Perched water develops – Included	
	2.2.07.08.0A – Fracture flow in the UZ – Included	X
	2.2.07.09.0A – Matrix imbibition in the UZ – Included	
	2.2.07.10.0A – Condensation zone forms around drifts – Included	
	2.2.07.11.0A – Resaturation of geosphere dryout zone – Included	
	2.2.07.18.0A – Film flow into the repository – Included	
	2.2.07.19.0A – Lateral flow from Solitario Canyon Fault enters drifts – Included	
	2.2.07.20.0A – Flow diversion around repository drifts – Included	X
	2.2.10.01.0A – Repository-induced thermal effects on flow in the UZ – Excluded	
	2.2.10.03.0B – Natural geothermal effects on flow in the UZ – Included	
	2.2.10.04.0A – Thermo-mechanical stresses alter characteristics of fractures near repository – Excluded	
2.2.10.04.0B – Thermo-mechanical stresses alter characteristics of faults near repository – Excluded		

Table 2.1-2. Summary of Features, Events, and Processes Affecting the Capability of the Upper Natural Barrier (Continued)

Barrier Feature	FEP Number, FEP Name, and Screening Decision (Section 2.2, Table 2.2-5)	Processes and Characteristics that are Important to the Capability of the Barrier
Unsaturated Zone above the Repository (Continued)	2.2.10.05.0A – Thermo-mechanical stresses alter characteristics of rocks above and below the repository – Excluded	
	2.2.10.10.0A – Two-phase buoyant flow/heat pipes – Included	
	2.2.10.11.0A – Natural air flow in the unsaturated zone – Excluded	
	2.2.10.12.0A – Geosphere dryout due to waste heat – Included	
	2.2.11.02.0A – Gas effects in the UZ – Excluded	
	2.2.12.00.0A – Undetected features in the UZ – Excluded	

Source: SNL 2008a, Table A-1.

Table 2.1-3. Summary of Features, Events, and Processes Affecting the Capability of the Engineered Barrier System

Barrier Feature	FEP Number, FEP Name, and Screening Decision (Section 2.2, Table 2.2-5)	Processes and Characteristics that are Important to the Capability of the Barrier
Emplacement Drift	1.1.01.01.0A – Open site investigation boreholes – Excluded	
	1.1.02.00.0A – Chemical effects of excavation and construction in EBS – Excluded	
	1.1.02.00.0B – Mechanical effects of excavation and construction in EBS – Excluded	
	1.1.02.01.0A – Site flooding (during construction and operation) – Excluded	
	1.1.02.02.0A – Preclosure ventilation – Included	
	1.1.02.03.0A – Undesirable materials left – Excluded	
	1.1.03.01.0A – Error in waste emplacement – Excluded	
	1.1.04.01.0A – Incomplete closure – Excluded	
	1.1.07.00.0A – Repository design – Included	
	1.1.08.00.0A – Inadequate quality control and deviations from design – Excluded	
	1.2.02.03.0A – Fault displacement damages EBS components – Included	
	1.2.03.02.0A – Seismic Ground Motion Damages EBS Components – Included	X
	1.2.03.02.0B – Seismic-induced Rockfall damages EBS Components – Excluded	X
	1.2.03.02.0C – Seismic-induced Drift Collapse Damages EBS Components – Included	X
	1.2.03.02.0D – Seismic-induced Drift Collapse Alters In-drift Thermal-Hydrology – Included	X
	1.2.03.02.0E – Seismic-induced Drift Collapse Alters In-drift Chemistry – Excluded	
	1.2.03.03.0A – Seismicity Associated with Igneous Activity – Included	
	1.2.04.03.0A – Igneous Intrusion into repository – Included	
1.2.04.04.0A – Igneous Intrusion interacts with EBS Components – Included		

Table 2.1-3. Summary of Features, Events, and Processes Affecting the Capability of the Engineered Barrier System (Continued)

Barrier Feature	FEP Number, FEP Name, and Screening Decision (Section 2.2, Table 2.2-5)	Processes and Characteristics that are Important to the Capability of the Barrier	
Emplacement Drift (Continued)	1.2.04.04.0B – Chemical Effects of Magma and Magmatic Volatiles – Included		
	1.2.04.05.0A – Magma or Pyroclastic Base Surge Transports Waste – Excluded		
	1.2.04.06.0A – Eruptive Conduit to Surface Intersects Repository – Included		
	2.1.01.04.0A – Repository-scale Spatial Heterogeneity of Emplaced Waste – Included		
	2.1.03.09.0A – Copper corrosion in EBS – Excluded		
	2.1.04.01.0A – Flow in the Backfill – Excluded		
	2.1.04.02.0A – Chemical Properties and Evolution of Backfill – Excluded		
	2.1.04.03.0A – Erosion or Dissolution of Backfill – Excluded		
	2.1.04.04.0A – Thermal-mechanical effects of backfill – Excluded		
	2.1.04.05.0A – Thermal-mechanical Properties and Evolution of Backfill – Excluded		
	2.1.05.02.0A – Radionuclide transport through seals – Excluded		
	2.1.06.01.0A – Chemical effects of rock reinforcement and cementitious materials in EBS – Excluded		
	2.1.06.02.0A – Mechanical effects of rock reinforcement materials in EBS – Excluded		
	2.1.06.04.0A – Flow through rock reinforcement materials in EBS – Excluded		
	2.1.06.07.0A – Chemical effects at EBS component interface – Excluded		
	2.1.06.07.0B – Mechanical effects at EBS component interfaces – Excluded		
		2.1.07.01.0A – Rockfall – Excluded	
		2.1.07.02.0A – Drift collapse – Excluded	
	2.1.07.06.0A – Floor buckling – Excluded		

Table 2.1-3. Summary of Features, Events, and Processes Affecting the Capability of the Engineered Barrier System (Continued)

Barrier Feature	FEP Number, FEP Name, and Screening Decision (Section 2.2, Table 2.2-5)	Processes and Characteristics that are Important to the Capability of the Barrier
Emplacement Drift (Continued)	2.1.08.01.0B – Effects of Rapid Influx into the Repository – Excluded	
	2.1.08.03.0A – Repository Dry-out Due to Waste Heat – Included	
	2.1.08.04.0A – Condensation forms on roofs of drifts (drift-scale cold traps) – Included	
	2.1.08.04.0B – Condensation forms at repository edges (repository-scale cold traps) – Included	
	2.1.08.06.0A – Capillary effects (wicking) in EBS – Included	
	2.1.08.07.0A – Unsaturated flow in the EBS – Included	X
	2.1.08.09.0A – Saturated flow in the EBS – Excluded	
	2.1.08.15.0A – Consolidation of EBS components – Excluded	
	2.1.09.01.0A – Chemical characteristics of water in drifts – Included	X
	2.1.09.02.0A – Chemical interaction with corrosion products – Included	
	2.1.09.03.0C – Volume increase of corrosion products impacts other EBS components – Excluded	
	2.1.09.09.0A – Electrochemical effects in EBS – Excluded	
	2.1.10.01.0A – Microbial activity in EBS – Excluded	
	2.1.11.01.0A – Heat generation in EBS – Included	X
	2.1.11.02.0A – Nonuniform heat distribution in EBS – Included	
	2.1.11.03.0A – Exothermic reactions in the EBS – Excluded	
	2.1.11.07.0A – Thermal expansion/stress of in-drift EBS components – Excluded	
	2.1.11.08.0A – Thermal effects on chemistry and microbial activity in the EBS – Included	X
	2.1.11.09.0A – Thermal effects on flow in the EBS – Included	
2.1.11.09.0C – Thermally-driven flow (convection) in drifts – Included		

Table 2.1-3. Summary of Features, Events, and Processes Affecting the Capability of the Engineered Barrier System (Continued)

Barrier Feature	FEP Number, FEP Name, and Screening Decision (Section 2.2, Table 2.2-5)	Processes and Characteristics that are Important to the Capability of the Barrier
Emplacement Drift (Continued)	2.1.12.01.0A – Gas generation (repository pressurization) – Excluded	
	2.1.12.03.0A – Gas generation (H ₂) from waste package corrosion – Excluded	
	2.1.12.04.0A – Gas generation (CO ₂ , CH ₄ , H ₂ S) from microbial degradation – Excluded	
	2.1.12.08.0A – Gas explosions in EBS – Excluded	
	2.1.13.01.0A – Radiolysis – Excluded	
	2.1.13.02.0A – Radiation damage in EBS – Excluded	
	2.1.13.03.0A – Radiological mutation of microbes – Excluded	
	2.2.01.01.0B – Chemical effects of excavation and construction in the near field – Excluded	
	2.2.01.02.0A – Thermally- induced stress changes in the near field – Excluded	
	2.2.01.02.0B – Chemical Changes in the Near-Field from Backfill – Excluded	
	2.2.07.06.0B – Long-Term Release of Radionuclides from the Repository – Included	
	2.2.08.03.0B – Geochemical Interactions and Evolution in the UZ – Excluded	
	2.2.08.04.0A – Re-dissolution of precipitates directs more corrosive fluids to waste packages – Excluded	
2.2.08.12.0A – Chemistry of water flowing into the drift – Included	X	
Drip Shield	1.2.02.03.0A – Fault Displacement Damages EBS Components – Included	
	1.2.03.02.0A – Seismic ground motion damages EBS components – Included	
	1.2.03.02.0B – Seismic-induced rockfall damages drip shield – Excluded	
	1.2.03.02.0C – Seismic-induced drift collapse damages EBS components – Included	X
	2.1.03.01.0B – General corrosion of drip shields – Included	X

Table 2.1-3. Summary of Features, Events, and Processes Affecting the Capability of the Engineered Barrier System (Continued)

Barrier Feature	FEP Number, FEP Name, and Screening Decision (Section 2.2, Table 2.2-5)	Processes and Characteristics that are Important to the Capability of the Barrier
Drip Shield (Continued)	2.1.03.02.0B – Stress corrosion cracking of drip shields – Excluded	X
	2.1.03.03.0B – Localized corrosion of drip shields – Excluded	X
	2.1.03.04.0B – Hydride cracking of drip shields – Excluded	
	2.1.03.05.0B – Microbially influenced corrosion (MIC) of drip shields – Excluded	
	2.1.03.07.0B – Mechanical impact on drip shield – Excluded	
	2.1.03.08.0B – Early failure of drip shields – Included	X
	2.1.03.10.0B – Advection of liquids and solids through cracks in the drip shield – Excluded	X
	2.1.03.11.0A – Physical form of waste package and drip shield – Included	X
	2.1.06.06.0A – Effects of drip shield on flow – Included	X
	2.1.06.06.0B – Oxygen embrittlement of drip shields – Excluded	
	2.1.06.07.0A – Chemical Effects at EBS Component Interface – Excluded	
	2.1.06.07.0B – Mechanical Effects at EBS Component Interfaces – Excluded	
	2.1.07.01.0A – Rockfall – Excluded	
	2.1.07.04.0B – Hydrostatic pressure on drip shield – Excluded	
	2.1.07.05.0B – Creep of metallic materials in the drip shield – Excluded	X
	2.1.08.14.0A – Condensation on underside of drip shield – Excluded	
	2.1.09.28.0B – Localized corrosion on drip shield surfaces due to deliquescence – Excluded	X
	2.1.11.06.0B – Thermal sensitization of drip shields – Excluded	
	2.1.11.07.0A – Thermal expansion/stress of in-drift EBS components – Excluded	
	2.1.13.02.0A – Radiation Damage in EBS – Excluded	

Table 2.1-3. Summary of Features, Events, and Processes Affecting the Capability of the Engineered Barrier System (Continued)

Barrier Feature	FEP Number, FEP Name, and Screening Decision (Section 2.2, Table 2.2-5)	Processes and Characteristics that are Important to the Capability of the Barrier
Waste Package	1.2.02.03.0A – Fault Displacement Damages EBS Components – Included	
	1.2.03.02.0A – Seismic ground motion damages EBS components – Included	X
	2.1.03.01.0A – General corrosion of waste packages – Included	X
	2.1.03.02.0A – Stress corrosion cracking of waste packages – Included	X
	2.1.03.03.0A – Localized corrosion of waste packages – Included	X
	2.1.03.04.0A – Hydride cracking of waste packages – Excluded	
	2.1.03.05.0A – Microbially influenced corrosion (MIC) of waste packages – Included	
	2.1.03.06.0A – Internal corrosion of waste packages prior to breach – Excluded	
	2.1.03.07.0A – Mechanical impact on waste package – Excluded	
	2.1.03.08.0A – Early failure of waste packages – Included	X
	2.1.03.10.0A – Advection of liquids and solids through cracks in the waste package – Excluded	X
	2.1.03.11.0A – Physical form of waste package and drip shield – Included	X
	2.1.06.07.0B – Mechanical Effects at EBS Component Interfaces – Excluded	

Table 2.1-3. Summary of Features, Events, and Processes Affecting the Capability of the Engineered Barrier System (Continued)

Barrier Feature	FEP Number, FEP Name, and Screening Decision (Section 2.2, Table 2.2-5)	Processes and Characteristics that are Important to the Capability of the Barrier
Waste Package (Continued)	2.1.07.01.0A – Rockfall – Excluded	
	2.1.07.04.0A – Hydrostatic pressure on waste package – Excluded	
	2.1.07.05.0A – Creep of metallic materials in the waste package – Excluded	
	2.1.08.12.0A – Induced hydrologic changes in invert – Excluded	
	2.1.08.14.0A – Condensation on underside of drip shield – Excluded	
	2.1.08.15.0A – Consolidation of EBS Components – Excluded	
	2.1.09.03.0B – Volume increase of corrosion products impacts waste package – Excluded	
	2.1.09.28.0A – Localized corrosion on waste package outer surface due to deliquescence – Excluded	X
	2.1.11.03.0A – Exothermic Reactions in the EBS – Excluded	
	2.1.11.06.0A – Thermal sensitization of waste packages – Excluded	
	2.1.11.07.0A – Thermal expansion/stress of in-drift EBS components – Excluded	
	2.1.12.03.0A – Gas generation (H ₂) from waste package corrosion – Excluded	
	2.1.13.01.0A – Radiolysis – Excluded	
	2.1.13.02.0A – Radiation damage in EBS – Excluded	

Table 2.1-3. Summary of Features, Events, and Processes Affecting the Capability of the Engineered Barrier System (Continued)

Barrier Feature	FEP Number, FEP Name, and Screening Decision (Section 2.2, Table 2.2-5)	Processes and Characteristics that are Important to the Capability of the Barrier
Cladding	1.2.02.03.0A – Fault Displacement Damages EBS Components – Included	
	1.2.03.02.0A – Seismic Ground Motion Damages EBS Components – Included	
	2.1.02.11.0A – Degradation of cladding from waterlogged rods – Excluded	
	2.1.02.12.0A – Degradation of cladding prior to disposal – Included	
	2.1.02.13.0A – General corrosion of cladding – Excluded	
	2.1.02.14.0A – Microbially influenced corrosion (MIC) of cladding – Excluded	
	2.1.02.15.0A – Localized (radiolysis enhanced) corrosion of cladding – Excluded	
	2.1.02.16.0A – Localized (pitting) corrosion of cladding – Excluded	
	2.1.02.17.0A – Localized (crevice) corrosion of cladding – Excluded	
	2.1.02.18.0A – Enhanced corrosion of cladding from dissolved silica – Excluded	
	2.1.02.19.0A – Creep rupture of cladding – Excluded	
	2.1.02.20.0A – Internal pressurization of cladding – Excluded	
	2.1.02.21.0A – Stress corrosion cracking of cladding – Excluded	
	2.1.02.22.0A – Hydride cracking of cladding – Excluded	
	2.1.02.23.0A – Cladding unzipping – Included	
	2.1.02.24.0A – Mechanical impact on cladding – Excluded	
	2.1.02.25.0A – DOE SNF cladding – Excluded	
	2.1.02.25.0B – Naval SNF cladding – Included	X
	2.1.02.26.0A – Diffusion- controlled cavity growth in cladding – Excluded	
	2.1.02.27.0A – Localized (fluoride enhanced) corrosion of cladding – Excluded	
2.1.09.03.0A – Volume increase of corrosion products impacts cladding – Excluded		

Table 2.1-3. Summary of Features, Events, and Processes Affecting the Capability of the Engineered Barrier System (Continued)

Barrier Feature	FEP Number, FEP Name, and Screening Decision (Section 2.2, Table 2.2-5)	Processes and Characteristics that are Important to the Capability of the Barrier
Waste Form and Waste Package Internals	1.2.02.03.0A – Fault Displacement Damages EBS Components – Included	
	1.2.03.02.0A – Seismic ground motion damages EBS components – Included	X
	2.1.01.01.0A – Waste inventory – Included	
	2.1.01.02.0A – Interactions between colocated waste – Excluded	
	2.1.01.02.0B – Interactions between codisposed waste – Included	
	2.1.01.03.0A – Heterogeneity of waste inventory – Included	
	2.1.01.04.0A – Repository-scale spatial heterogeneity of emplaced waste – Included	
	2.1.02.01.0A – DOE SNF degradation (alteration, dissolution, and radionuclide release) – Included	X
	2.1.02.02.0A – Commercial SNF degradation (alteration, dissolution, and radionuclide release) – Included	X
	2.1.02.03.0A – HLW glass degradation (alteration, dissolution, and radionuclide release) – Included	X
	2.1.02.04.0A – Alpha recoil enhances dissolution – Excluded	
	2.1.02.05.0A – HLW glass cracking – Included	
	2.1.02.06.0A – HLW glass recrystallization – Excluded	
	2.1.02.07.0A – Radionuclide release from gap and grain boundaries – Included	
	2.1.02.08.0A – Pyrophoricity from DOE SNF – Excluded	
	2.1.02.09.0A – Chemical effects of void space in waste package – Included	X
	2.1.02.10.0A – Organic/cellulosic materials in waste – Excluded	
	2.1.02.28.0A – Grouping of DOE SNF waste types into categories – Included	
	2.1.02.29.0A – Flammable gas generation from DOE SNF – Excluded	
	2.1.03.06.0A – Internal corrosion of waste packages prior to breach – Excluded	

Table 2.1-3. Summary of Features, Events, and Processes Affecting the Capability of the Engineered Barrier System (Continued)

Barrier Feature	FEP Number, FEP Name, and Screening Decision (Section 2.2, Table 2.2-5)	Processes and Characteristics that are Important to the Capability of the Barrier
Waste Form and Waste Package Internals (Continued)	2.1.09.01.0B – Chemical characteristics of water in waste package – Included	X
	2.1.09.02.0A – Chemical interaction with corrosion products – Included	X
	2.1.09.04.0A – Radionuclide solubility, solubility limits, and speciation in the waste form and EBS – Included	X
	2.1.09.05.0A – Sorption of dissolved radionuclides in EBS – Included	X
	2.1.09.06.0A – Reduction-oxidation potential in waste package – Included	
	2.1.09.07.0A – Reaction kinetics in waste package – Included	X
	2.1.09.08.0A – Diffusion of dissolved radionuclides in EBS – Included	X
	2.1.09.08.0B – Advection of dissolved radionuclides in EBS – Included	X
	2.1.09.10.0A – Secondary phase effects on dissolved radionuclide concentrations – Excluded	
	2.1.09.11.0A – Chemical effects of waste–rock contact – Excluded	
	2.1.09.15.0A – Formation of true (intrinsic) colloids in EBS – Excluded	
	2.1.09.16.0A – Formation of pseudocolloids (natural) in EBS – Included	
	2.1.09.17.0A – Formation of pseudocolloids (corrosion product) in EBS – Included	
	2.1.09.18.0A – Formation of microbial colloids in EBS – Excluded	
	2.1.09.19.0A – Sorption of colloids in EBS – Excluded	
	2.1.09.19.0B – Advection of colloids in EBS – Included	
	2.1.09.20.0A – Filtration of colloids in EBS – Excluded	
	2.1.09.23.0A – Stability of colloids in EBS – Included	
	2.1.09.24.0A – Diffusion of colloids in EBS – Included	
2.1.09.25.0A – Formation of colloids (waste form) by co-precipitation in EBS – Included		

Table 2.1-3. Summary of Features, Events, and Processes Affecting the Capability of the Engineered Barrier System (Continued)

Barrier Feature	FEP Number, FEP Name, and Screening Decision (Section 2.2, Table 2.2-5)	Processes and Characteristics that are Important to the Capability of the Barrier
Waste Form and Waste Package Internals (Continued)	2.1.11.05.0A – Thermal expansion/stress of in-package EBS components – Excluded	
	2.1.11.09.0B – Thermally-driven flow (convection) in waste packages – Excluded	
	2.1.12.02.0A – Gas generation (He) from waste form decay – Excluded	
	2.1.14.15.0A – In-Package Criticality (intact configuration) – Excluded	
	2.1.14.16.0A – In-Package Criticality (degraded configurations) – Excluded	
	2.1.14.18.0A – In-Package Criticality Resulting from a Seismic Event (intact configuration) – Excluded	
	2.1.14.19.0A – In-Package Criticality Resulting from a Seismic Event (degraded configurations) – Excluded	
	2.1.14.21.0A – In-Package Criticality Resulting from Rockfall (intact configuration) – Excluded	
	2.1.14.22.0A – In-Package Criticality Resulting from Rockfall (degraded configurations) – Excluded	
	2.1.14.24.0A – In-package Criticality Resulting from an Igneous Event (intact configuration) – Excluded	
	2.1.14.25.0A – In-Package Criticality Resulting from an Igneous Event (degraded configurations) – Excluded	
	2.2.08.12.0B – Chemistry of water flowing into the waste package – Included	
		3.1.01.01.0A – Radioactive decay and ingrowth – Included

Table 2.1-3. Summary of Features, Events, and Processes Affecting the Capability of the Engineered Barrier System (Continued)

Barrier Feature	FEP Number, FEP Name, and Screening Decision (Section 2.2, Table 2.2-5)	Processes and Characteristics that are Important to the Capability of the Barrier
Waste Package Pallet	1.2.02.03.0A – Fault Displacement Damages EBS Components – Included	
	1.2.03.02.0A – Seismic ground motion damages EBS components – Included	X
	2.1.06.05.0A – Mechanical degradation of emplacement pallet – Excluded	
	2.1.06.05.0C – Chemical degradation of emplacement pallet – Included	
	2.1.06.07.0A – Chemical Effects at EBS Component Interface – Excluded	
	2.1.06.07.0B – Mechanical Effects at EBS Component Interfaces – Excluded	
	2.1.11.07.0A – Thermal Expansion/ Stress of In-drift EBS Components – Excluded	

Table 2.1-3. Summary of Features, Events, and Processes Affecting the Capability of the Engineered Barrier System (Continued)

Barrier Feature	FEP Number, FEP Name, and Screening Decision (Section 2.2, Table 2.2-5)	Processes and Characteristics that are Important to the Capability of the Barrier
Invert	1.2.02.03.0A – Fault displacement damages EBS components – Included	
	1.2.03.02.0A – Seismic ground motion damages EBS components – Included	
	2.1.06.05.0B – Mechanical degradation of invert – Excluded	
	2.1.06.05.0D – Chemical degradation of invert – Excluded	
	2.1.08.05.0A – Flow through invert – Included	
	2.1.06.07.0B – Mechanical Effects at EBS Component Interfaces – Excluded	
	2.1.08.06.0A – Capillary effects (wicking) in EBS – Included	
	2.1.08.07.0A – Unsaturated flow in the EBS – Included	
	2.1.08.12.0A – Induced hydrologic changes in invert – Excluded	
	2.1.09.01.0A – Chemical characteristics of water in drifts – Included	
	2.1.09.04.0A – Radionuclide solubility, solubility limits, and speciation in the waste form and EBS – Included	
	2.1.09.05.0A – Sorption of dissolved radionuclides in EBS – Included	
	2.1.09.06.0B – Reduction- oxidation potential in drifts – Included	
	2.1.09.07.0B – Reaction kinetics in drift – Included	
	2.1.09.08.0A – Diffusion of dissolved radionuclides in EBS – Included	
	2.1.09.08.0B – Advection of dissolved radionuclides in EBS – Included	
	2.1.09.13.0A – Complexation in EBS – Excluded	
	2.1.09.19.0A – Sorption of colloids in EBS – Excluded	
	2.1.09.19.0B – Advection of colloids in EBS – Included	
	2.1.09.20.0A – Filtration of colloids in EBS – Excluded	
2.1.09.21.0A – Transport of particles larger than colloids in EBS – Excluded		

Table 2.1-3. Summary of Features, Events, and Processes Affecting the Capability of the Engineered Barrier System (Continued)

Barrier Feature	FEP Number, FEP Name, and Screening Decision (Section 2.2, Table 2.2-5)	Processes and Characteristics that are Important to the Capability of the Barrier
Invert (Continued)	2.1.09.22.0A – Sorption of colloids at air–water interface – Excluded	
	2.1.09.23.0A – Stability of colloids in EBS – Included	
	2.1.09.24.0A – Diffusion of colloids in EBS – Included	
	2.1.09.26.0A – Gravitational settling of colloids in EBS – Excluded	
	2.1.09.27.0A – Coupled effects on radionuclide transport in EBS – Excluded	
	2.1.11.07.0A – Thermal Expansion/ Stress of In-drift EBS Components – Excluded	
	2.1.11.10.0A – Thermal effects on transport in EBS – Excluded	
	2.1.12.06.0A – Gas transport in EBS – Excluded	
	2.1.12.07.0A – Effects of radioactive gases in EBS – Excluded	
	2.1.14.17.0A – Near-field criticality – Excluded	
	2.1.14.20.0A – Near-field criticality resulting from a seismic event – Excluded	
	2.1.14.23.0A – Near-field criticality resulting from rockfall – Excluded	
	2.1.14.26.0A – Near-field criticality resulting from an igneous event – Excluded	
	2.2.07.06.0A – Episodic or pulse release from repository – Excluded	
	2.2.07.06.0B – Long-term release of radionuclides from the repository – Included	
3.1.01.01.0A – Radioactive decay and ingrowth – Included		

Source: SNL 2008a, Table A-2.

Table 2.1-4. Summary of Features, Events, and Processes Affecting the Capability of the Lower Natural Barrier

Barrier Feature	FEP Number, FEP Name, and Screening Decision (Section 2.2, Table 2.2-5)	Processes and Characteristics that are Important to the Capability of the Barrier
Unsaturated Zone below the Repository	1.2.02.01.0A – Fractures – Included	X
	1.2.02.02.0A – Faults – Included	X
	1.2.04.02.0A – Igneous activity changes rock properties – Excluded	
	1.2.04.05.0A – Magma or pyroclastic base surge transports waste – Excluded	
	1.2.04.06.0A – Eruptive conduit to surface intersects repository – Included	
	1.2.06.00.0A – Hydrothermal activity – Excluded	
	1.2.10.01.0A – Hydrologic response to seismic activity – Excluded	
	1.2.10.02.0A – Hydrologic response to igneous activity – Excluded	
	1.3.01.00.0A – Climate change – Included	X
	1.3.07.02.0B – Water table rise affects UZ – Included	
	1.4.01.01.0A – Climate modification increases recharge – Included	X
	2.1.09.12.0A – Rind (chemically altered zone) forms in the near field – Excluded	
	2.1.09.21.0C – Transport of particles larger than colloids in the UZ – Excluded	
	2.2.01.03.0A – Changes in fluid saturations in the excavation disturbed zone – Excluded	
	2.2.01.04.0A – Radionuclide solubility in the excavation disturbed zone – Excluded	
	2.2.01.05.0A – Radionuclide transport in the excavation disturbed zone – Excluded	
	2.2.03.01.0A – Stratigraphy – Included	X
	2.2.03.02.0A – Rock properties of host rock and other units – Included	X
	2.2.06.01.0A – Seismic activity changes porosity and permeability of rock – Excluded	
	2.2.06.02.0A – Seismic activity changes porosity and permeability of faults – Excluded	

Table 2.1-4. Summary of Features, Events, and Processes Affecting the Capability of the Lower Natural Barrier (Continued)

Barrier Feature	FEP Number, FEP Name, and Screening Decision (Section 2.2, Table 2.2-5)	Processes and Characteristics that are Important to the Capability of the Barrier
Unsaturated Zone below the Repository (Continued)	2.2.06.02.0B – Seismic activity changes porosity and permeability of fractures – Excluded	
	2.2.06.03.0A – Seismic activity alters perched water zones – Excluded	
	2.2.07.02.0A – Unsaturated groundwater flow in the geosphere – Included	X
	2.2.07.03.0A – Capillary rise in the UZ – Included	
	2.2.07.07.0A – Perched water develops – Included	X
	2.2.07.08.0A – Fracture flow in the UZ – Included	X
	2.2.07.09.0A – Matrix imbibition in the UZ – Included	X
	2.2.07.15.0B – Advection and dispersion in the UZ – Included	X
	2.2.07.21.0A – Drift shadow forms below repository – Excluded	
	2.2.08.01.0B – Chemical characteristics of groundwater in the UZ – Included	
	2.2.08.03.0B – Geochemical interactions and evolution in the UZ – Excluded	
	2.2.08.05.0A – Diffusion in the UZ – Excluded	
	2.2.08.06.0B – Complexation in the UZ – Included	
	2.2.08.07.0B – Radionuclide solubility limits in the UZ – Excluded	
	2.2.08.08.0B – Matrix diffusion in the UZ – Included	X
	2.2.08.09.0B – Sorption in the UZ – Included	X
	2.2.08.10.0B – Colloidal transport in the UZ – Included	
	2.2.09.01.0B – Microbial activity in the UZ – Excluded	
2.2.10.04.0A – Thermo-mechanical stresses alter characteristics of fractures near repository – Excluded		

Table 2.1-4. Summary of Features, Events, and Processes Affecting the Capability of the Lower Natural Barrier (Continued)

Barrier Feature	FEP Number, FEP Name, and Screening Decision (Section 2.2, Table 2.2-5)	Processes and Characteristics that are Important to the Capability of the Barrier
Unsaturated Zone below the Repository (Continued)	2.2.10.04.0B – Thermo-mechanical stresses alter characteristics of faults near repository – Excluded	
	2.2.10.05.0A – Thermo-mechanical stresses alter characteristics of rocks above and below the repository – Excluded	
	2.2.10.06.0A – Thermo-chemical alteration in the unsaturated zone (solubility, speciation, phase changes, precipitation/dissolution) – Excluded	
	2.2.10.07.0A – Thermo-chemical alteration of the Calico Hills unit – Excluded	
	2.2.10.09.0A – Thermo-chemical alteration of the Topopah Spring basal vitrophyre – Excluded	
	2.2.10.14.0A – Mineralogic dehydration reactions – Excluded	
	2.2.11.03.0A – Gas transport in geosphere – Excluded	
	2.2.12.00.0A – Undetected features in the UZ – Excluded	
	2.2.14.09.0A – Far-field criticality – Excluded	
	2.2.14.10.0A – Far-field criticality resulting from a seismic event – Excluded	
	2.2.14.11.0A – Far-field criticality resulting from rockfall – Excluded	
	2.2.14.12.0A – Far-field criticality resulting from an igneous event – Excluded	
3.1.01.01.0A – Radioactive decay and ingrowth – Included		
Saturated Zone	1.2.02.01.0A – Fractures – Included	X
	1.2.02.02.0A – Faults – Included	X
	1.2.04.02.0A – Igneous activity changes rock properties – Excluded	
	1.2.04.07.0B – Ash redistribution in groundwater – Excluded	
	1.2.06.00.0A – Hydrothermal activity – Excluded	
	1.2.09.02.0A – Large-scale dissolution – Excluded	
	1.2.10.01.0A – Hydrologic response to seismic activity – Excluded	

Table 2.1-4. Summary of Features, Events, and Processes Affecting the Capability of the Lower Natural Barrier (Continued)

Barrier Feature	FEP Number, FEP Name, and Screening Decision (Section 2.2, Table 2.2-5)	Processes and Characteristics that are Important to the Capability of the Barrier
Saturated Zone (Continued)	1.2.10.02.0A – Hydrologic response to igneous activity – Excluded	
	1.3.01.00.0A – Climate change – Included	X
	1.3.07.01.0A – Water table decline – Excluded	
	1.3.07.02.0A – Water table rise affects SZ – Included	
	1.4.01.01.0A – Climate modification increases recharge – Included	X
	1.4.07.02.0A – Wells – Included	
	2.1.09.21.0B – Transport of particles larger than colloids in the SZ – Excluded	
	2.2.03.01.0A – Stratigraphy – Included	X
	2.2.03.02.0A – Rock properties of host rock and other units – Included	X
	2.2.06.01.0A – Seismic activity changes porosity and permeability of rock – Excluded	
	2.2.06.02.0A – Seismic activity changes porosity and permeability of faults – Excluded	
	2.2.06.02.0B – Seismic activity changes porosity and permeability of fractures – Excluded	
	2.2.07.12.0A – Saturated groundwater flow in the geosphere – Included	X
	2.2.07.13.0A – Water- conducting features in the SZ – Included	X
	2.2.07.14.0A – Chemically induced density effects on groundwater flow – Excluded	
	2.2.07.15.0A – Advection and dispersion in the SZ – Included	X
	2.2.07.16.0A – Dilution of radionuclides in groundwater – Included	
	2.2.07.17.0A – Diffusion in the SZ – Included	
	2.2.08.01.0A – Chemical characteristics of groundwater in the SZ – Included	
	2.2.08.03.0A – Geochemical interactions and evolution in the SZ – Excluded	

Table 2.1-4. Summary of Features, Events, and Processes Affecting the Capability of the Lower Natural Barrier (Continued)

Barrier Feature	FEP Number, FEP Name, and Screening Decision (Section 2.2, Table 2.2-5)	Processes and Characteristics that are Important to the Capability of the Barrier
Saturated Zone (Continued)	2.2.08.06.0A – Complexation in the SZ – Included	
	2.2.08.07.0A – Radionuclide solubility limits in the SZ – Excluded	
	2.2.08.08.0A – Matrix diffusion in the SZ – Included	X
	2.2.08.09.0A – Sorption in the SZ – Included	X
	2.2.08.10.0A – Colloidal transport in the SZ – Included	
	2.2.09.01.0A – Microbial activity in the SZ – Excluded	
	2.2.10.02.0A – Thermal convection cell develops in SZ – Excluded	
	2.2.10.03.0A – Natural geothermal effects on flow in the SZ – Included	
	2.2.10.08.0A – Thermal-chemical alteration in the SZ (solubility, speciation, phase changes, precipitation/dissolution) – Excluded	
	2.2.10.13.0A – Repository- induced thermal effects on flow in the SZ – Excluded	
	2.2.11.01.0A – Gas effects in the SZ – Excluded	
	2.2.12.00.0B – Undetected features in the SZ – Included	
	3.1.01.01.0A – Radioactive decay and ingrowth – Included	
	3.2.07.01.0A – Isotopic dilution – Excluded	

Source: SNL 2008a, Table A-3.

Table 2.1-5. Relationship between Barriers and Total System Performance Assessment Models

Barrier	Model	SAR Section
Upper Natural Barrier	Infiltration	2.3.1.3.3
	Unsaturated zone flow	2.3.2.4
	Ambient seepage	2.3.3.2.3
	Thermal-hydrologic seepage	2.3.3.3.3
Engineered Barrier System	Drift degradation and rockfall	2.3.4.4, 2.3.4.5
	Near-field chemistry	2.3.5.3.3
	Multiscale thermal-hydrologic	2.3.5.4.1
	In-drift condensation	2.3.5.4.2
	In-drift physical and chemical environment	2.3.5
	Drip shield degradation	
	Mechanical Damage	2.3.4.5
	General corrosion	2.3.6.8.1
	Early failure	2.3.6.8.4
	Waste package degradation	
	Mechanical damage	2.3.4.5
	General corrosion	2.3.6.3.3
	Localized corrosion	2.3.6.4.3
	Stress corrosion cracking	2.3.6.5.3
	Early failure	2.3.6.6.3
	In-package chemistry	2.3.7.5.3
Commercial SNF degradation	2.3.7.7.3	
DOE SNF degradation	2.3.7.8.3	
HLW glass degradation	2.3.7.9.3	
Dissolved concentration limits	2.3.7.10.3	
Colloidal radionuclide availability	2.3.7.11.3	
EBS flow and transport	2.3.7.12.3	
Lower Natural Barrier	Unsaturated zone flow	2.3.2.4
	Unsaturated zone transport	2.3.8.4
	Saturated zone flow	2.3.9.2.3
	Saturated zone transport	2.3.9.3.3

Table 2.1-6. Seepage Fractions for Codisposal and Commercial SNF Waste Packages for Combined Nominal/Early Failure Modeling Case for Glacial-Transition Climate, 2,000 to 10,000 Years

Percolation Subregion		Seepage Fraction for Codisposal Waste Packages			Seepage Fraction for Commercial SNF Waste Packages		
Subregion Index	Quantile Range	5th Percentile	Mean	95th Percentile	5th Percentile	Mean	95th Percentile
1	$p < 0.05$	0.0031	0.0881	0.2764	0.0020	0.0887	0.2823
2	$0.05 \leq p < 0.30$	0.0261	0.2292	0.5782	0.0217	0.2308	0.5780
3	$0.30 \leq p < 0.70$	0.0448	0.3306	0.7395	0.0455	0.3294	0.7439
4	$0.70 \leq p < 0.95$	0.0453	0.3846	0.7955	0.0431	0.3848	0.7998
5	$p \geq 0.95$	0.0880	0.4656	0.8447	0.0870	0.4666	0.8386
Repository Average		0.0441	0.3134	0.6898	0.0424	0.3134	0.6950

NOTE: The repository average values are based on weighted averages for each realization using the percolation subregion quantile ranges.

Source: SNL 2008d, Table 8.3-2[a].

Table 2.1-7. Seepage Fractions for Codisposal and Commercial SNF Waste Packages for Combined Nominal/Early Failure Modeling Case for Post-10,000-Year Period

Percolation Subregion		Seepage Fraction for Codisposal Waste Packages			Seepage Fraction for Commercial SNF Waste Packages		
Subregion Index	Quantile Range	5th Percentile	Mean	95th Percentile	5th Percentile	Mean	95th Percentile
1	$p < 0.05$	0.0092	0.1251	0.3166	0.0082	0.1251	0.3121
2	$0.05 \leq p < 0.30$	0.0623	0.3393	0.6525	0.0617	0.3402	0.6555
3	$0.30 \leq p < 0.70$	0.0933	0.4382	0.8072	0.0949	0.4369	0.7943
4	$0.70 \leq p < 0.95$	0.0626	0.4365	0.8464	0.0606	0.4364	0.8439
5	$p \geq 0.95$	0.0941	0.4935	0.8872	0.0934	0.4944	0.8802
Repository Average		0.0750	0.4001	0.7483	0.0784	0.3999	0.7449

NOTE: The repository average values are based on weighted averages for each realization using the percolation subregion quantile ranges.

Source: SNL 2008d, Table 8.3-3[a].

Table 2.1-8. Seepage Fractions for Codisposal and Commercial SNF Waste Packages for Seismic Ground Motion Modeling Case for Glacial-Transition Climate, 2,000 to 10,000 Years

Percolation Subregion		Seepage Fraction for Codisposal Waste Packages			Seepage Fraction for Commercial SNF Waste Packages		
Subregion Index	Quantile Range	5th Percentile	Mean	95th Percentile	5th Percentile	Mean	95th Percentile
1	$p < 0.05$	0.0031	0.0881	0.2764	0.002	0.0887	0.2823
2	$0.05 \leq p < 0.30$	0.0261	0.2292	0.5782	0.0217	0.2308	0.578
3	$0.30 \leq p < 0.70$	0.0448	0.3306	0.7395	0.0455	0.3294	0.7439
4	$0.70 \leq p < 0.95$	0.0453	0.3846	0.7955	0.0431	0.3848	0.7998
5	$p \geq 0.95$	0.088	0.4656	0.8447	0.087	0.4666	0.8386
Repository Average		0.0441	0.3134	0.6898	0.0424	0.3134	0.6950

NOTE: The repository average values are based on weighted averages for each realization using the percolation subregion quantile ranges.

Source: SNL 2008d, Table 8.3-4[a].

Table 2.1-9. Seepage Fractions for Codisposal and Commercial SNF Waste Packages for Seismic Ground Motion Modeling Case for Post-10,000-year Period

Percolation Subregion		Seepage Fraction for Codisposal Waste Packages			Seepage Fraction for Commercial SNF Waste Packages		
Subregion Index	Quantile Range	5th Percentile	Mean	95th Percentile	5th Percentile	Mean	95th Percentile
1	$p < 0.05$	0.3252	0.4666	0.6965	0.3231	0.4673	0.6923
2	$0.05 \leq p < 0.30$	0.3077	0.6484	0.9164	0.3089	0.6491	0.9173
3	$0.30 \leq p < 0.70$	0.309	0.7196	0.9725	0.3114	0.7193	0.975
4	$0.70 \leq p < 0.95$	0.231	0.7051	0.9793	0.226	0.7041	0.9803
5	$p \geq 0.95$	0.3076	0.7525	0.9878	0.3107	0.7518	0.9869
Repository Average		0.2909	0.6871	0.9450	0.2912	0.6870	0.9465

NOTE: The repository average values are based on weighted averages for each realization using the percolation subregion quantile ranges.

Source: SNL 2008d, Table 8.3-5[a].

Table 2.1-10. Drift Wall Condensation for Commercial SNF Waste Packages for Stage 2 and Stage 3 Condensation

Percolation Subregion	Commercial SNF Waste Packages							
	Stage 2				Stage 3			
	Probability	Mean Waste Package Fraction	Mean Rate (m ³ /yr)	Mean Duration	Probability at 1,500 years	Mean Waste Package Fraction	Mean Rate (m ³ /yr) at 1,500 years	Mean Duration
1	0	0	0	NA	0.020	0.020	7.50×10^{-5}	750 to 2,000 years
2	0	0	0	NA	0.023	0.023	6.74×10^{-5}	750 to 2,000 years
3	0	0	0	NA	0.020	0.020	7.94×10^{-5}	750 to 2,000 years
4	0	0	0	NA	0.0067	0.0067	6.95×10^{-6}	750 to 2,000 years
5	0	0	0	NA	0.010	0.010	4.78×10^{-5}	750 to 2,000 years

NOTE: Drift wall condensation fraction and flux is the same for both the Nominal/Early Failure and Seismic Ground Motion Modeling Cases.
NA = not applicable

Source: SNL 2008d, Table 8.3-6[a].

Table 2.1-11. Drift Wall Condensation for Codisposal Waste Packages for Stage 2 and Stage 3 Condensation

Percolation Subregion	Codisposal Waste Packages							
	Stage 2				Stage 3			
	Probability	Mean Waste Package Fraction	Mean Rate (m ³ /yr)	Mean Duration	Probability at 1,500 years	Mean Waste Package Fraction	Mean Rate (m ³ /yr) at 1,500 years	Mean Duration
1	1	1	0.54	0 to 1,000 years	0.020	0.020	6.78×10^{-5}	750 to 2,000 years
2	1	1	0.54	0 to 1,000 years	0.017	0.017	5.97×10^{-5}	750 to 2,000 years
3	1	1	0.54	0 to 1,000 years	0.017	0.017	7.16×10^{-5}	750 to 2,000 years
4	1	1	0.54	0 to 1,000 years	0.0033	0.0033	6.00×10^{-5}	750 to 2,000 years
5	1	1	0.54	0 to 1,000 years	0.010	0.010	4.32×10^{-5}	750 to 2,000 years

NOTE: Drift wall condensation fraction and flux is the same for both the Nominal/Early Failure and Seismic Ground Motion Modeling Cases.

Source: SNL 2008d, Table 8.3-7[a].

Table 2.1-12. Mean Seepage Rates for Waste Packages during Stage 2 and Stage 3 Condensation

Percolation Subregion	Mean Seepage Rates (m ³ /yr) 0 to 2,000 Years (Seepage at 1,500 years)	
	Commercial SNF Waste Packages	Codisposal Waste Packages
1	0.0112	0.0111
2	0.0517	0.0517
3	0.0736	0.0733
4	0.0803	0.0798
5	0.112	0.110

NOTE: Mean seepage rate is the same for both the Nominal/Early Failure and Seismic Ground Motion Modeling Cases over the first 2,000 years.

Source: SNL 2008d, Table 8.3-8[a].

Table 2.1-13. Decay of Total Curie Inventory as a Function of Time and Dominant Contributors to Total Curie Inventory

Time After Closure (years)	Percent of Total Initial Curie Inventory	Major Contributors to Total Inventory at Time after Closure
0	100.00	¹³⁷ Cs (46%), ⁹⁰ Sr (29%), ²⁴¹ Am (10%)
10	81.20	¹³⁷ Cs (45%), ⁹⁰ Sr (28%), ²⁴¹ Am (12%)
100	20.75	²⁴¹ Am (41%), ¹³⁷ Cs (22%), ⁹⁰ Sr (13%), ²³⁸ Pu (11%)
1,000	4.20	²⁴¹ Am (48%), ²⁴⁰ Pu (29%), ²³⁹ Pu (19%)
10,000	1.18	²³⁹ Pu (52%), ²⁴⁰ Pu (40%)
100,000	0.10	²³⁹ Pu (46%), ⁹⁹ Tc (27%)
500,000	0.03	⁹⁹ Tc (26%), ²²⁹ Th (9%), ²³⁰ Th (9%), ²²⁶ Ra (9%), ²³³ U (9%), ²³⁷ Np (9%), ²⁴² Pu (8%), ²³⁴ U (7%)
1,000,000	0.02	²³³ U (15%), ²²⁹ Th (15%), ²³⁷ Np (14%), ⁹⁹ Tc (9%), ²³⁰ Th (7%), ²²⁶ Ra (7%), ¹³⁵ Cs (7%), ²³⁶ U (6%), ²⁴² Pu (6%)

Source: SNL 2008d, Table 8.3-1.

INTENTIONALLY LEFT BLANK

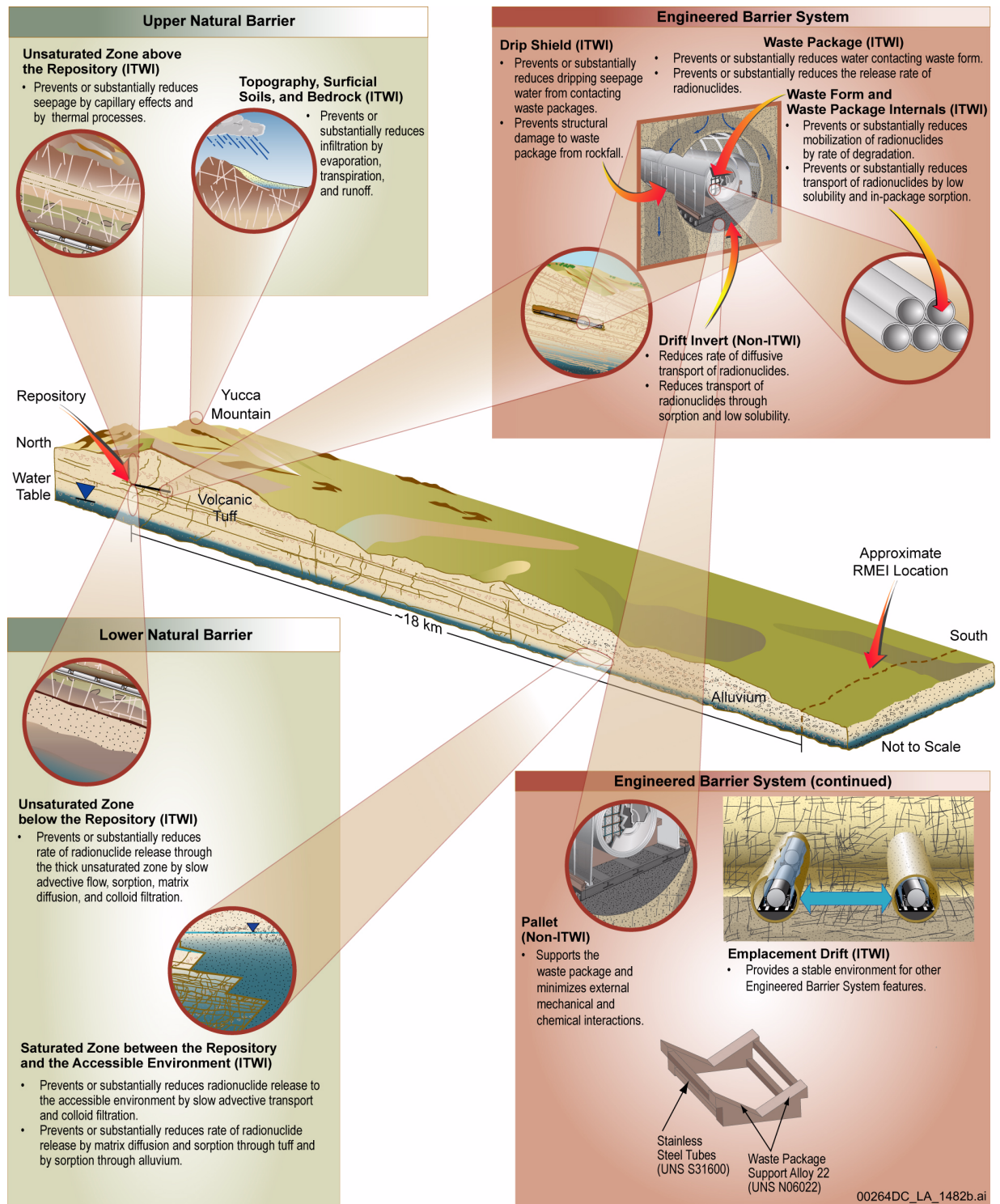


Figure 2.1-1. Schematic Illustration of the Multiple Barrier Repository System

NOTE: Some of the features/components shown are not important to barrier capability, but are illustrated here for completeness. The approximate RMEI location is the southern-most edge of the controlled area at 36°40'13.6661" North latitude. This is approximately 18 km south of the repository along the predominant direction of groundwater flow.

ITWI = important to waste isolation; Non-ITWI = not important to waste isolation.

INTENTIONALLY LEFT BLANK

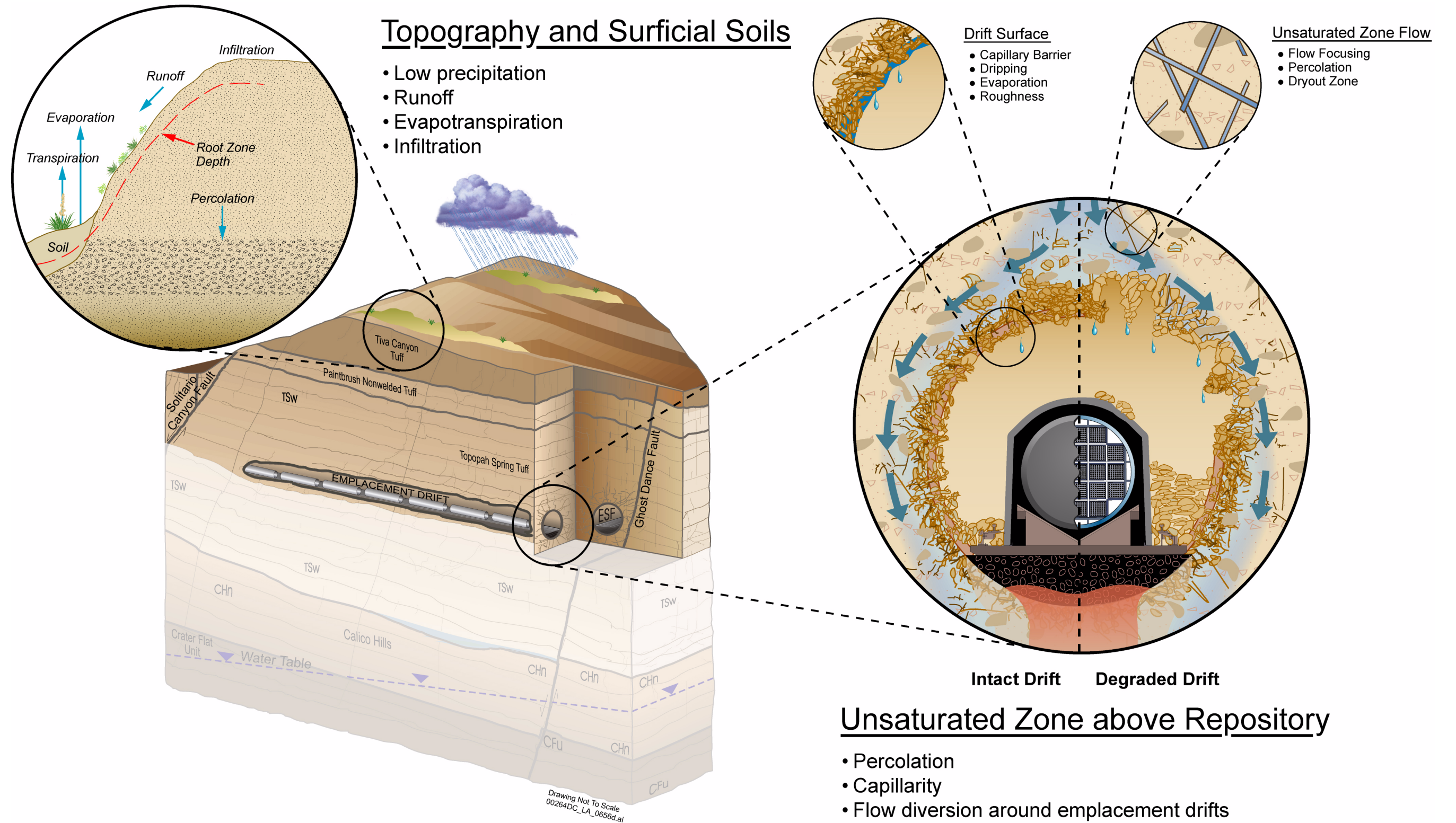
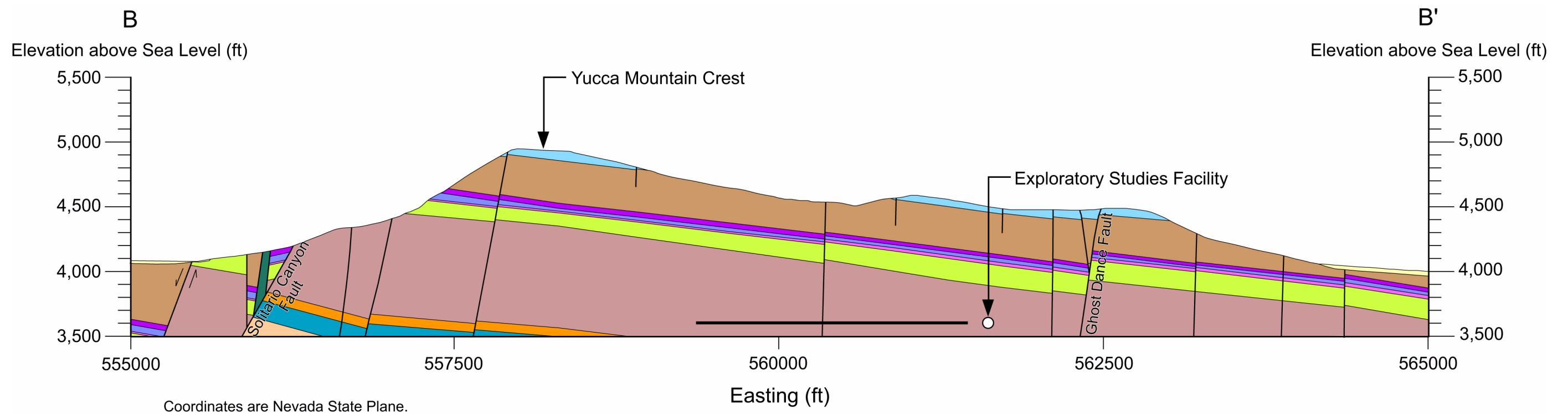
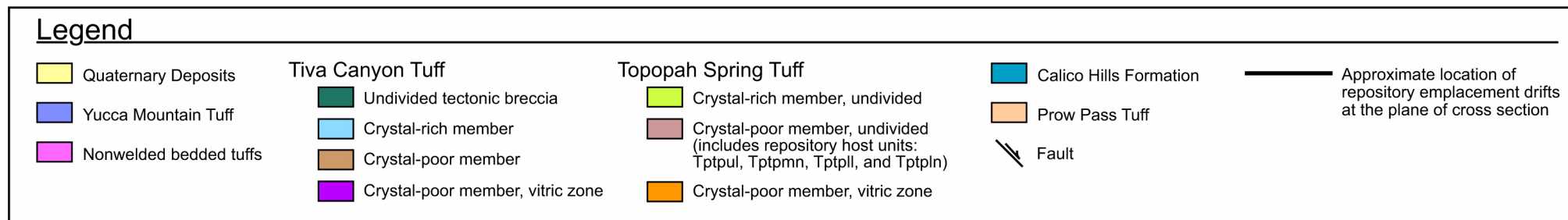


Figure 2.1-2. Schematic of the Upper Natural Barrier

INTENTIONALLY LEFT BLANK



Coordinates are Nevada State Plane.



00264DC_LA_0538d.eps

NOTE: The location of the cross section is shown in Figure 2.1-4. The portion of the repository shown is only the portion that intersects this plane. The PTn includes the nonwelded bedded tuffs and the Yucca Mountain Tuff.

Source: Day et al. 1998.

Figure 2.1-3. Cross Section of Unsaturated Zone from Surface to Repository Horizon

INTENTIONALLY LEFT BLANK

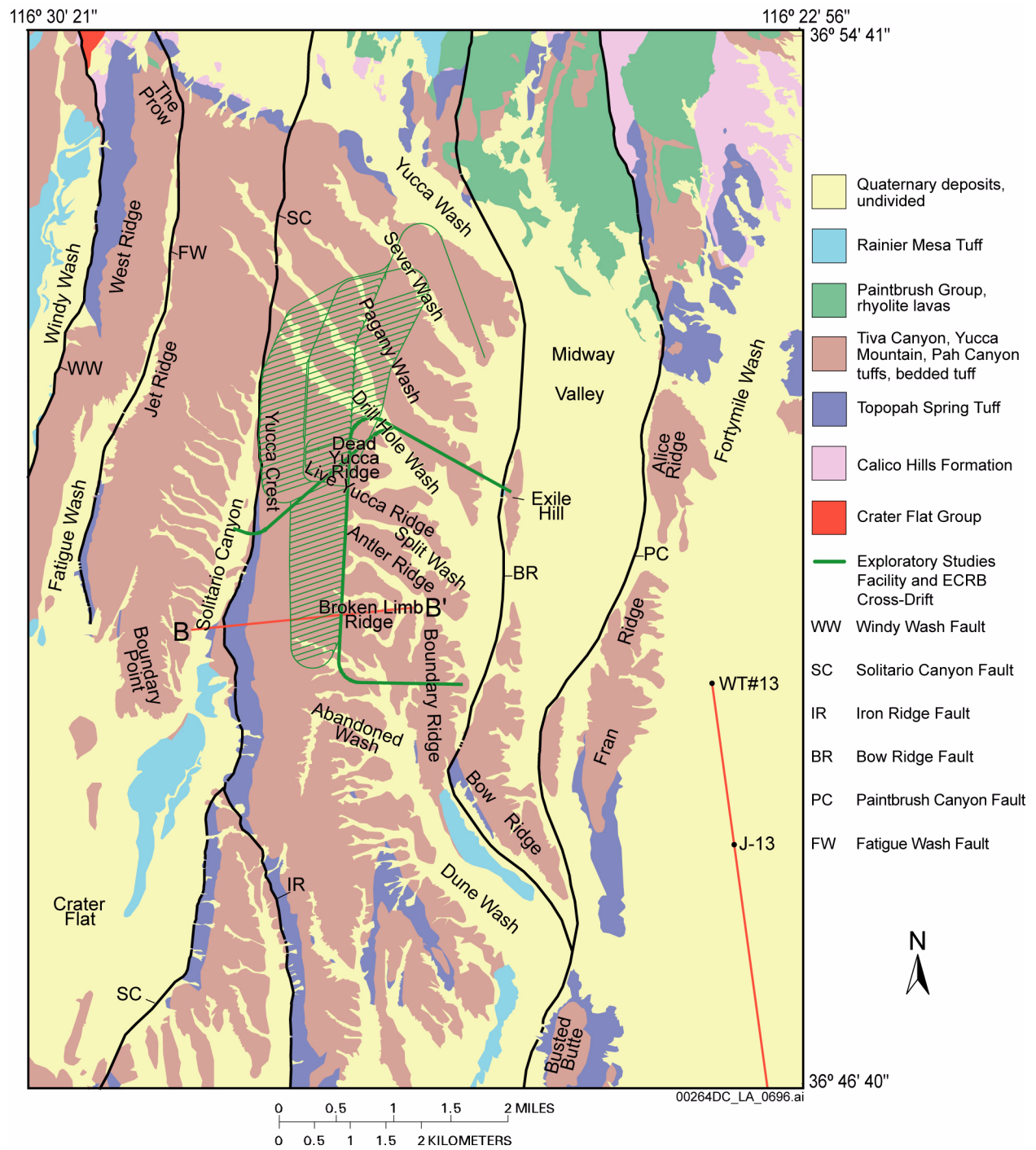


Figure 2.1-4. Simplified Geologic Map Showing Major Lithostratigraphic Units in the Yucca Mountain Site Area

NOTE: The location of the cross sections shown in Figures 2.1-3 and 2.1-30 is indicated by the line crossing the southern part of the repository. The line crossing through WT#13 and J-13 indicates the beginning portion of the cross section shown in Figure 2.1-32. Repository footprint is shown for illustrative purposes only.

Source: Potter et al. 2002.

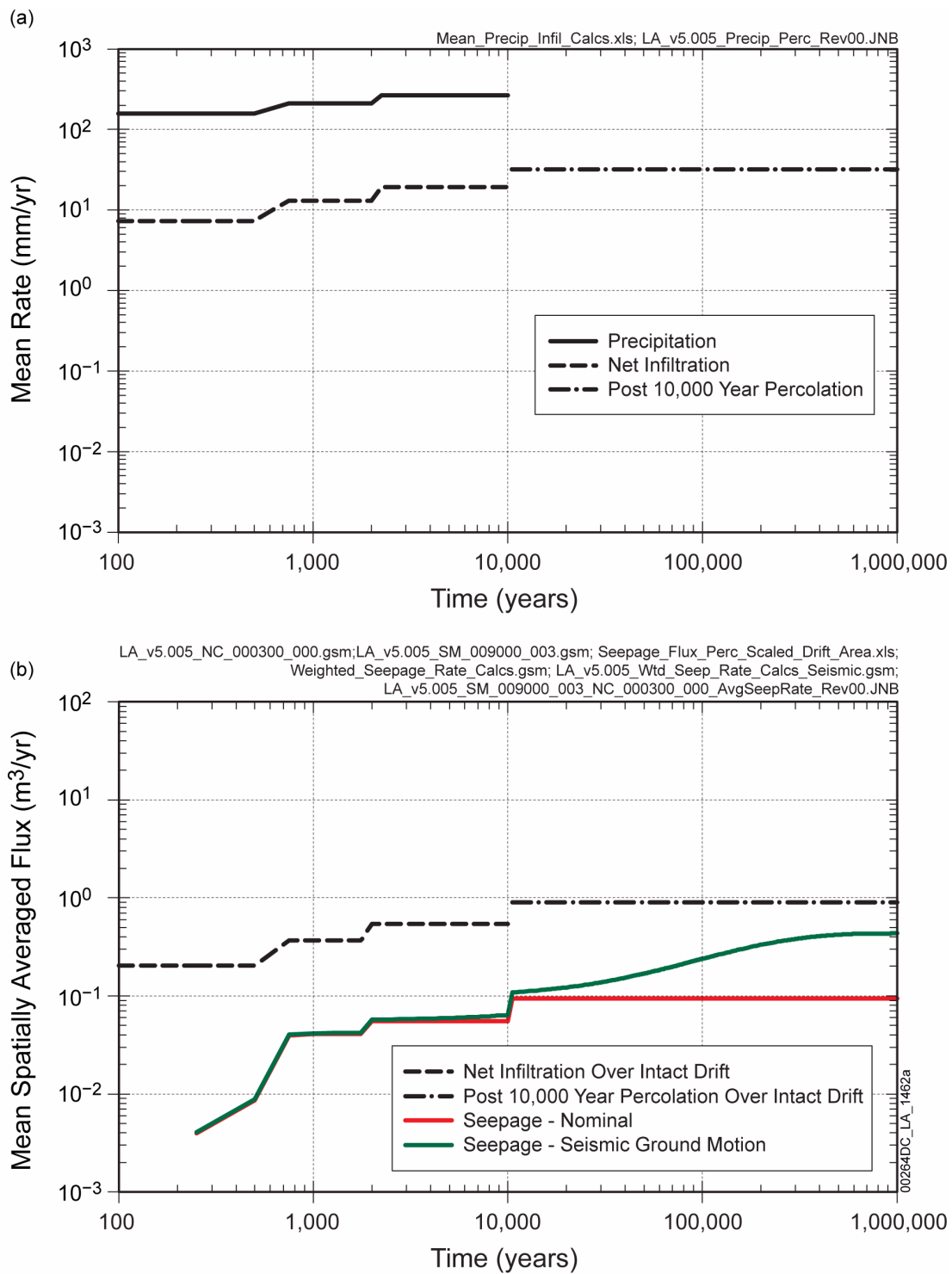


Figure 2.1-5. Upper Natural Barrier Capability to Prevent or Substantially Reduce the Rate of Water Movement to the Waste for the Mean Spatially-Averaged (a) Annual Precipitation, Net Infiltration, and Post-10,000-Year Percolation and (b) Drift Seepage Fluxes for the Combined Nominal/Early Failure Modeling Case and Seismic Ground Motion Modeling Case—1,000,000 Year Period

Source: SNL 2008d, Figure 8.3-3[a].

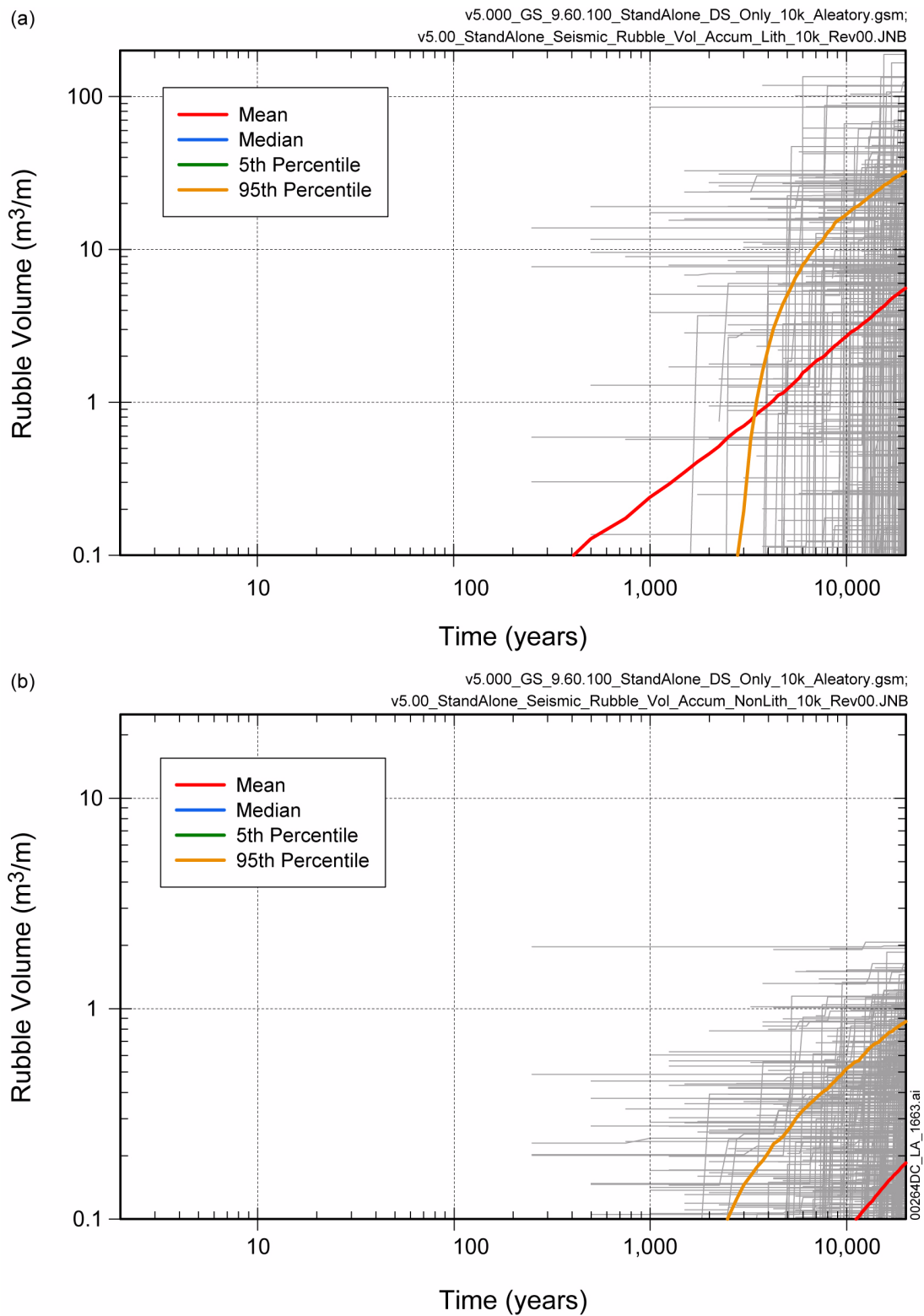


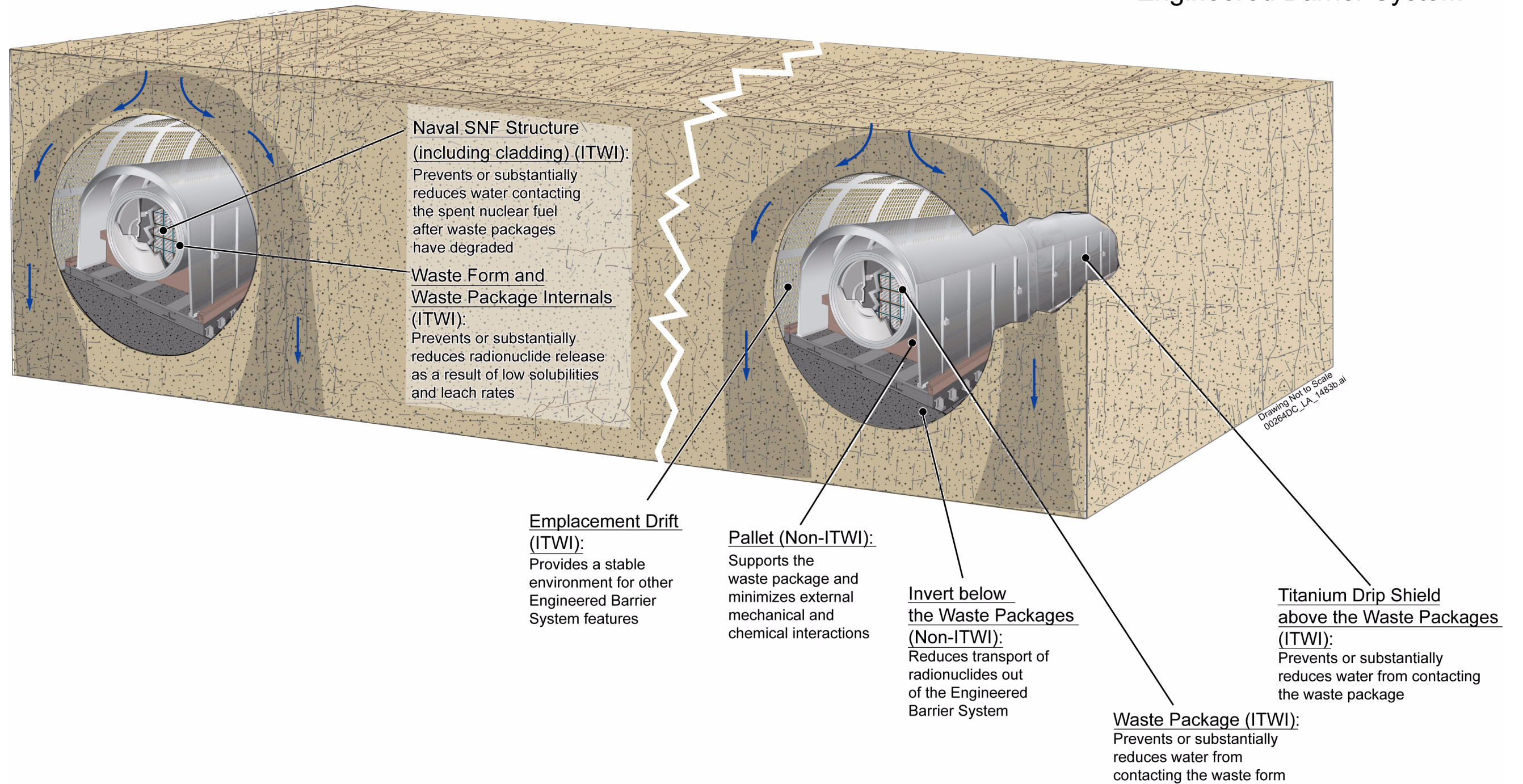
Figure 2.1-6. Volume of (a) Lithophysal and (b) Nonlithophysal Rockfall Over 20,000 Years

NOTE Median and 5th percentile are below the plotted range.

Source: SNL 2008d, Figure 7.3.2-19.

INTENTIONALLY LEFT BLANK

Engineered Barrier System



NOTE: ITWI = Important to waste isolation, Non-ITWI = Not important to waste isolation.

Figure 2.1-7. Schematic of the Engineered Barrier System

INTENTIONALLY LEFT BLANK

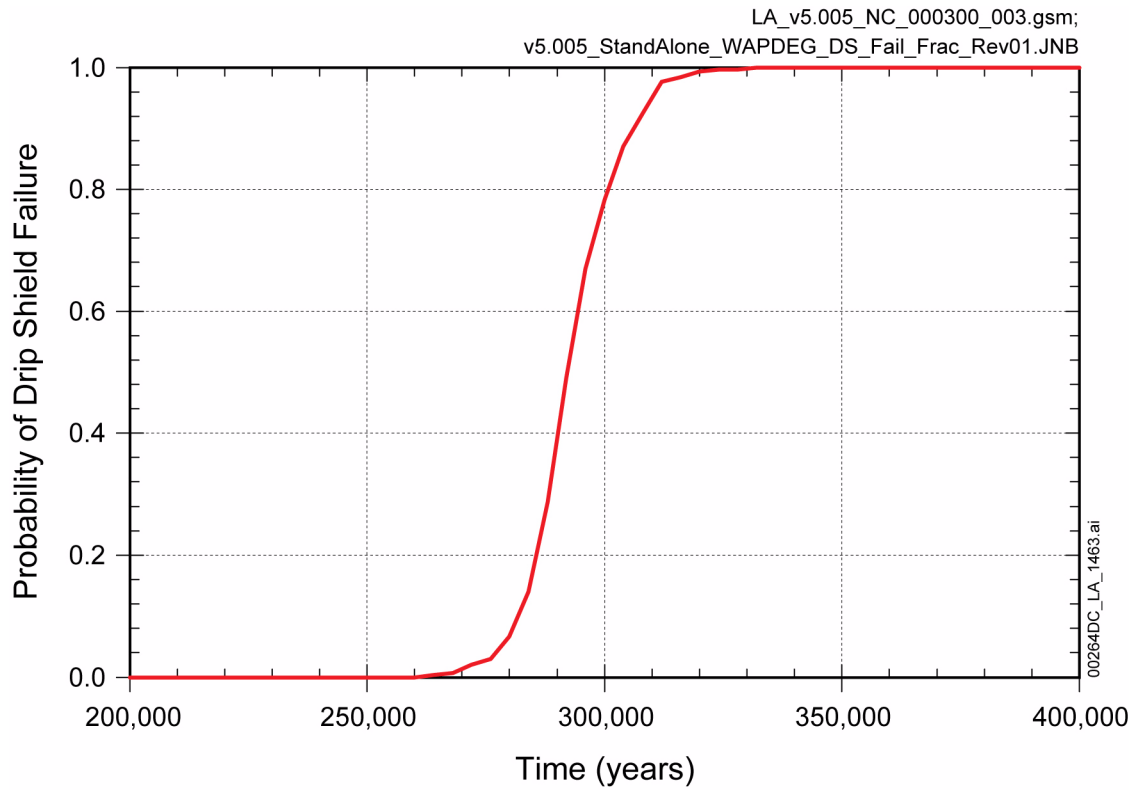


Figure 2.1-8. Probability of Drip Shield Failure by General Corrosion for the Nominal Modeling Case Based on 300 Epistemic Realizations of Drip Shield General Corrosion Rates

Source: SNL 2008d, Figure 8.3-4[a].

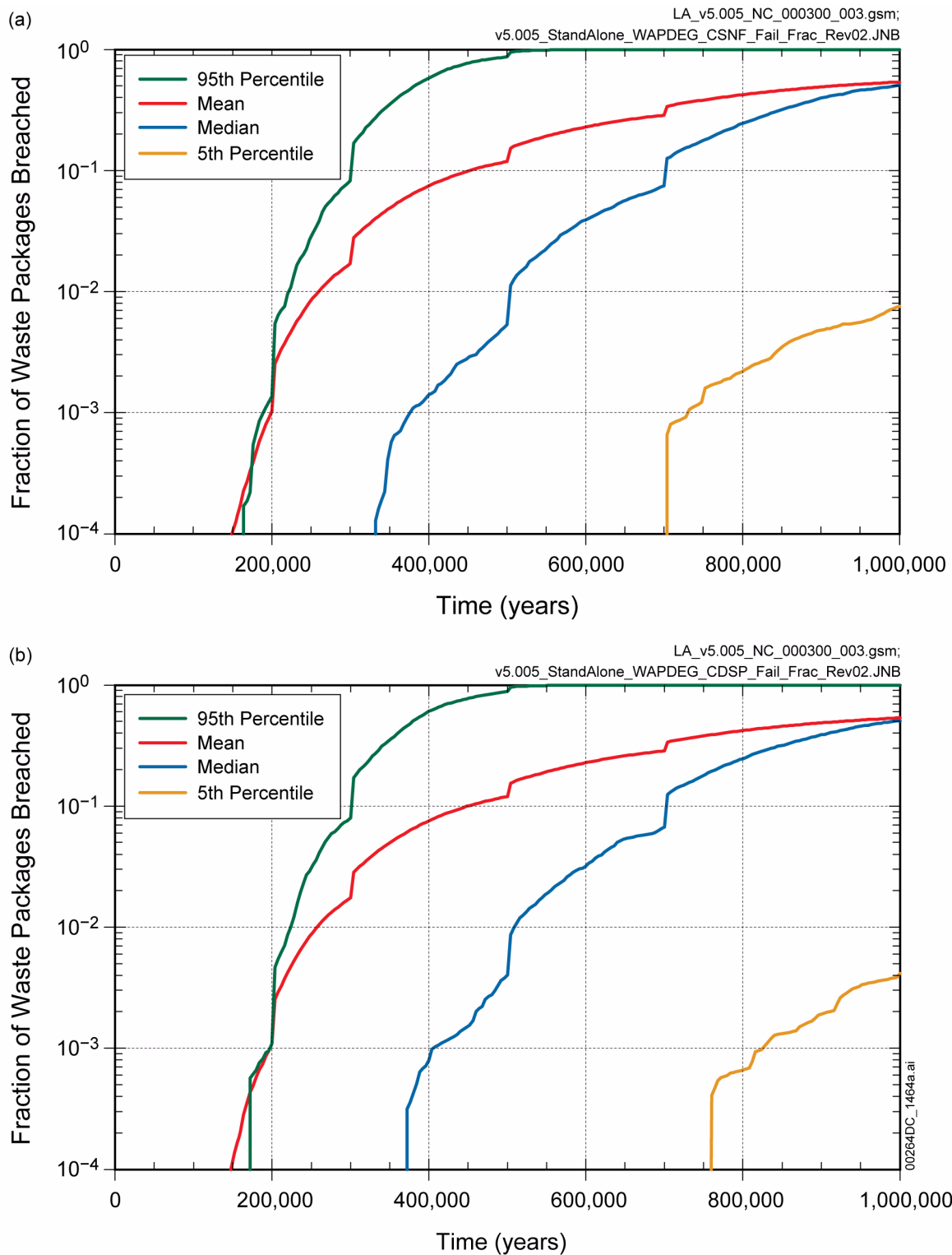


Figure 2.1-9. Summary Statistics for Fraction of Waste Packages Breached for (a) Commercial SNF Waste Packages and (b) Codisposal Waste Packages for the Nominal Modeling Case as a Function of Time

Source: SNL 2008d, Figure 8.3-5[a].